Energy Efficiency in Next Generation Cellular Networks

Attai Ibrahim Abubakar

Submitted in fulfilment of the requirements for the
Degree of Doctor of Philosophy

James Watt School of Engineering
College of Science and Engineering
University of Glasgow

July 2022

Abstract

There is an exponential growth in the energy consumption of cellular networks due to the surge in data traffic, explosion of handheld and Internet-of-Things (IoT) devices, development of data-hungry mobile applications, increasing support for new and emerging use cases, the introduction of ultra-dense networks, and aerial base stations (BSs). This will create the challenge of increased energy consumption for next-generation cellular networks that is bound to escalate, if not properly managed. This thesis seeks to address this challenge and make future cellular networks more energy- and cost-efficient, and environmentally sustainable. To achieve this, analytical methods, conventional approaches, and machine learning solutions are utilized to develop novel optimization frameworks that can minimize the energy consumption in heterogeneous cellular networks (HetNets) while satisfying quality of service (QoS) constraints.

First, energy optimization in ultra-dense heterogeneous networks (UDHNs) through cell switching and traffic offloading is studied. Though dynamic cell switching is a common technique for reducing energy consumption in UDHNs, most current methods are computationally demanding, making them unsuitable for practical applications in UDHNs with a large number of BSs. As a result, scalable and computationally efficient cell switching and traffic offloading frameworks using Q-learning, a reinforcement learning algorithm, and artificial neural networks (ANN), a supervised learning algorithm, is initially developed. However, these solutions are effective only in small- to medium-sized networks. Subsequently, a lightweight cell switching scheme called Threshold-based Hybrid cEll SwItching Scheme (THESIS), which combines the benefits of multi-level clustering (MLC) and exhaustive search (ES) algorithms is proposed. In addition, the two components of the THESIS algorithm, k-means and ES, are used for benchmarking. The performance evalaution reveals that THESIS algorithm is able to find a good trade-off between optimal energy saving performance and computational complexity. Hence, it is suitable for cell switching purposes in real networks with large dimension.

Second, the cell switching solution is extended to include spectrum leasing.

Spectrum leasing involves leasing out unused spectrum for a fee (in this case, those originally occupied by switched off BSs). A solution to enable mobile network operators (MNOs) gain additional revenue from leasing dormant spectrum, in addition to reducing energy consumption (electricity bills) via cell switching, is proposed. In this direction, a network scenario comprising primary network (PN) operators, who hold the spectrum license, and secondary network (SN) operators, who need to lease the spectrum is considered. Moreover, both non-delay-tolerant (NDT), and delay-tolerant (DT) spectrum demand scenarios are also considered. A cell switching and spectrum leasing framework based on the simulated annealing (SA) algorithm is developed to maximize the revenue of the PN while satisfying the QoS constraints. The simulation results reveal that the DT spectrum demand is more beneficial to both PN and SN operators as it results in 19% increase in the revenue generated by the PN, while leading to a 21% surge in the amount of spectrum that can be accessed by the SN.

Third, energy consumption has been identified as one of the major factors limiting the adoption of unmanned ariel vehicles (UAVs) in cellular networks (e.g., for providing additional offloading capacity during cell switching, and spectrum leasing operations), hence, the quest for green UAV-based cellular communications. To this end, a comprehensive survey on energy optimization techniques in UAV-based cellular networks is conducted, which revealed that it is energy-inefficient to continuously make UAV-BSs hover or fly to provide wireless coverage. Thus, an alternative deployment scheme where UAV-BSs land on designated locations, known as landing stations (LSs), is considered, and the appropriate separation distances (Δ) between LSs and the optimal hovering position (OHP) are evaluated. Mathematical frameworks using stochastic geometry are developed to model the relationship between power consumption, coverage probability, throughput, and Δ. Numerical results reveal about 95% reduction in energy consumption, which results in more than 20 times increase in the service time of UAV-BS when the LSs are exploited compared to OHP. However, this energy reduction is obtained at the expense of some degradation in coverage probability and throughput, which can be compensated for by increasing the transmit power of the UAV-BS as Δ increases. This leads to a slight increase in the energy consumption of UAV at LS which is significantly lesser than that of the UAV at OHP.

In summary, this thesis presents scalable and computationally efficient energy and revenue optimization frameworks for terrestrial and aerial cellular networks that can be applied to large-scale networks, which are typical in next generation of cellular networks. The proposed solutions would lead to a reduction in operating cost, increased profitability, and the achievement of net-zero emission target.

University of Glasgow

College of Science & Engineering

Statement of Originality

Name: Attai Ibrahim Abubakar

Registration Number:

I certify that the thesis presented here for examination for a PhD degree of the University of Glasgow is solely my own work other than where I have clearly indicated that it is the work of others (in which case the extent of any work carried out jointly by me and any other person is clearly identified in it) and that the thesis has not been edited by a third party beyond what is permitted by the University's PGR Code of Practice.

The copyright of this thesis rests with the author. No quotation from it is permitted without full acknowledgement.

I declare that the thesis does not include work forming part of a thesis presented successfully for another degree.

I declare that this thesis has been produced in accordance with the University of Glasgow's Code of Good Practice in Research.

I acknowledge that if any issues are raised regarding good research practice based on review of the thesis, the examination may be postponed pending the outcome of any investigation of the issues.

Signature: .....

Date: .....

List of Publications

Journals

1. Omeke K., **Abubakar A. I.**, Zhang L., Abbasi Q. H., Hussain S. and Imran M. A.,(2022), "How Reinforcement Learning is Powering the Smart Ocean," IEEE Internet of Things Magazine (Under review)

2. **Abubakar A. I.**, Ahmad I., Omeke K., Ozturk M., Ozturk C., Ali Makine Abdel-Salam, Mollel, M. S., Abbasi Q. H., Hussain S. and Imran M. A.,(2022), "A Survey on Energy Optimization Techniques in UAV-Based Cellular Networks: From Conventional to Machine Learning Techniques," IEEE Open Journal of Communication Society (Under review)

3. **Abubakar A. I.**, Mollel, M. S., Onireti O., Ozturk M., Ahmad I., Asad S. M., Sambo Y., Hussain S., and Imran M. A. (2022), "Are UAVs Feasible for Green Wireless Communications?", IEEE Transactions in Vehicular Technology (Under review)

4. **Abubakar A. I.**, Ozturk C., Ozturk M., Mollel, M. S., Asad S. M., Hassan N. U., Hussain S. and Imran M. A. (2022), "Revenue Maximization through Cell Switching and Spectrum Leasing in 5G HetNets," in IEEE Access, vol. 10, pp. 48301-48317, 2022, doi: 10.1109/ACCESS.2022.3172280. IEEE Access (Accepted for Publication)

5. **Abubakar A. I.**, Mollel, M. S., Ozturk M., Hussain S., and Imran M. A. (2022), "A Lightweight Cell Switching and Traffic Offloading Scheme for Energy Optimization in Heterogeneous Ultra-Dense Networks", Physical Communication, https://doi.org/10.1016/j.phycom.2022.101643.

6. Ozturk, M., **Abubakar, A. I.**, Rais, R. N. B., Jaber, M., Hussain, S. and Imran, M. A. (2022), "Context-Aware Wireless Connectivity and Processing Unit Optimization for IoT Networks", IEEE Internet of Things Journal, doi: 10.1109/JIOT.2022.3152381.

7. Asad S., Tahir A., Rais R., Ansari S., **Abubakar A. I.**, Hussain S., Abbasi Q., and Imran M. (2021) Edge Intelligence in Private Mobile Networks for Next-Generation Railway Systems. Front. Comms. Net 2:769299. doi: 10.3389/frcmn.2021.769299

8. Mollel, M. S., **Abubakar, A. I.**, Ozturk, M., Kaijage, S. F., Kisangiri, M., Hussain, S., Imran M. A, Abbasi, Q. H. (2021). A Survey of Machine Learning Applications to Handover Management in 5G and Beyond. IEEE Access, 9, 45770-45802.

9. Ozturk, M., **Abubakar, A. I.**, Nadas, J. P. B., Rais, R. N. B., Hussain, S. and Imran, M. A. (2021). Energy Optimization in Ultra-Dense Radio Access Networks via Traffic-Aware Cell Switchingn IEEE Transactions on Green Communications and Networking. doi: 10.1109/ TGCN.2021.3056235.

10. **Abubakar, A. I.**, Ozturk, M., Omeke, K., Hussain, S. and Imran, M. A. (2020). The Role of Artificial Intelligence Driven 5G Networks in COVID-19 Outbreaks: Opportunities, Challenges, and Future Outlook. Frontiers in Communication and Networks, Front.1:575065. doi: 10.3389/frcmn.2020.575065.

11. Mollel, M. S., **Abubakar, A. I.**, Ozturk, M., Kaijage, S., Kisangiri, M., Zoha, A., Imran, M. A. and Abbasi, Q. H., 2020. Intelligent handover decision scheme using double deep reinforcement learning. Physical Communication, p.101133.

Conference Proceedings

1. **Abubakar, A. I.**, Ozturk, M., Rais, R. N. B., Hussain, S. and Imran, M. A., 2020, August. Load-Aware cell switching in Ultra-Dense Networks: An Artificial Neural Networks Approach. In 2020 International Conference on UK-China Emerging Technologies (UCET) (pp. 1-4). IEEE.

2. **Abubakar, A. I.**, Ozturk, M., Hussain, S. and Imran, M. A., 2019, September. Q-learning assisted energy-aware traffic offloading and cell switching in heterogeneous networks. In 2019 IEEE 24th International Workshop on Computer Aided Modeli Design of Communication Links and Networks (CAMAD) (pp. 1-6). IEEE.

3. Ozturk, M., **Abubakar, A. I.**, Hassan, N. U., Hussain, S., Imran, M. A. and Yuen, C., 2019, August. Spectrum Cost Optimization for Cognitive Radio Transmission over TV White Spaces using Artificial Neural Networks. In 2019 UK/China Emerging Technologies (UCET) (pp. 1-4). IEEE.

Book chapters

1. Ozturk, M., **Abubakar, A. I.**, Hussain, S. and Abbasi, Q. H., and Imran, M. A. (2020) Cognitive Radio Spectrum Sensing: From Conventional Approaches to Machine Learning-based Predictive Techniques. In Basar E. and Abbasi Q. H., P.(eds.) IET: Flexible and Cognitive Radio Access Technologies for 5G and Beyond.

2. Imran, M., Ozturk, M., **Abubakar, A. I.**, Klaine, P. V., Hussain, S. and Abbasi, Q. H., 2019. Mobility Prediction Based Resource Management. Wiley 5G Ref: The Essential 5G Reference Online, pp.1-18.

Contents

List of Tables

List of Figures

List of Acronyms

3D	Three Dimensional
1G	First Generation
2G	Second Generation
3G	Third Generation
4G	Fourth Generation
5G	Fifth Generation
6G	Sixth Generation
AAO	All-Always-On
ADC	Analog to Digital Converter
ADMM	Alternating Direction Method of Multiplier
ANN	Artificial Neural Networks
ARIMA	Auto-Regressive Integrated Moving Average
ASE	Area Spectral Efficiency
BCA	Block Coordinate Ascent
BB	Base Band
BCD	Block Coordinate Descent
BS	Base Station
BRETS	Bayesian Response Estimation and Threshold Search
CAPEX	Capital Expenditure
CBS	Control Base Station
CCF	Coalition Formation Game
CCP	Concave Convex Procedure
CDR	Call Detail Record
CDSA	Control Data Separated Architecture
C-RAN	Centralized Radio Access Network
CRN	Cognitive Radio Network
CNN	Convolution Neural Networks
D2D	Device-to-Device Communication
DBS	Data Base Station

DC	Direct Current
DDPG	Deep Deterministic Policy Gradient
D-RRH	Drone Mounted Remote Radio Head
DRL	Deep Reinforcement Learning
DT	Delay-Tolerant
EARTH	Energy-Aware Network Technologies
EE	Energy Efficiency
eMBB	Enhanced Mobile Broadband
ES	Exhaustive Search
FL	Federated Learning
FSO	Free Space Optics
GA	Genetic algorithm
GMM	Gaussian Mixture Model
GS-STN	Geographic and Semantic Spatial-Temporal Network
HetNet	Heterogeneous Networks
HL	Hidden layer
ICT	Information and Communication Technology
IoT	Internet of Things
IP	Internet Protocol
kNN	k-nearest neighbour
LiPo	Lithium Polymer
LoS	Line-of-Sight
LS	Landing Station
LSTM	Long and Short Term Memory
MBS	Macro Base Station
MC	Macro Cell
MCP	Multilevel Circle Parking
MDP	Markov Decision Process
MEC	Mobile Edge Computing
MFG	Mean Field Game
MIMO	Multiple Input and Multiple Output
ML	Machine Learning
MLC	Multi-Level Clustering
mMTC	Massive Machine-Type Communication
MNO	Mobile Network Operator
MSE	Mean Square Error
MVNO	Mobile Virtual Network Operator
NBG	Nash Bargain Theory

NDT	Non-Delay-Tolerant
NFV	Network Function Virtualization
NLP	Natural Language Processing
NOMA	Non-Orthogonal Multiple Access
OfCom	Office of Communications
OFDMA	Orthogonal Frequency Multiple Access
OHP	Optimal Hovering Position
OL	Output layer
OPEX	Operating Expenses
OTOcell	Offline-Trained-Online-Cell
PAPR	Peak-Average-Power-Ratio
PN	Primary Network
PSO	Particle Swarm Optimization
PU	primary User
PV	Photo Voltaic
QoS	Quality of Service
RAN	Radio Access Network
RAT	Radio Access Technology
RB	Resource Block
ReLU	Rectified Linear Unit
RF	Radio Frequency
RRH	Remote Radio Head
RL	Reinforcement Learning
RMSE	Root Mean Square Error
RNN	Recurrent Neural Network
SA	Simulated Annealing
SARSA	State-Action-Reward-State-Action
SBS	Small Base Station
SCA	Successive Convex Approximation
SNR	Signal-To-Noise-Ratio
SPMS	Solar Power Management System
SSE	Sum of Square Errors
SN	Secondary Network
SNR	Signal to Noise Ratio
SU	Secondary User
SVM	Support Vector Machine
TACT	Transfer Actor-Critic
THESIS	Threshold-based Hybrid cEll SwItching Scheme

TSP	Travelling Salesman Problem
UAV	Unmanned Aerial Vehicle
UDN	Ultra-Dense Networks
UDHN	Ultra-Dense Heterogeneous Network
UE	User Equipment
URLLC	Ultra-Reliable and Low Latency Communications
VAR	Virtual and Augmented Reality
VNS	variable Neighbourhood solution
WEM	Weighted Expectation Maximization
WPCN	Wireless Powered Communication System
WPT	Wireless Power Transfer
XGBOOST	Extreme Gradient Boosting

List of Symbols

S	Set of all possible solutions
E_s	Energy saving obtained from each solution
s^*	The optimal solution
E_t	Total energy saving of the optimal solution
s_o	Initial solution
s	Current solution
s'	Neighbour solution
t	Time slot
Δ	Difference between current and neighbour solution
u	Random number generated from uniform distribution
φ	The number of local search iterations for each temperature
$\mathcal{K}$	Boltzmann's constant
ϑ	Difference between a feasible solution (s') and a neighbor solution (s)
ϱ	Temperature change counter
h_i	Transfer function of a neuron
$\iota(\cdot)$	The activation
M_{L}	Number of layers
x_i	Input
w_i	Weight vector
b_i	Bias
σ_i	Set of data points in a dataset
γ_j	Centroid of the cluster
k	Number of clusters
Λ	Mean of a cluster
D_k	Euclidean distance between data points and centroids
$Q(s_t, a_t)$	State-action value function
s_t	Current state
s_{t+1}	Next state
a_t	Current action

a	Set of all possible actions
R_{t+1}	Expected reward
$\Re$	Penalty
ε	Discount factor
ζ	Learning rate
χ	Window size
P_o	Constant power consumption component
η	Slope of load dependent power consumption component
P_{tx}	Instantaneous transmit power
P_{max}	Maximum transmit power
P_s	Sleep mode power consumption
M_F	Total number of RBs
M_o	Number of RBs occupied per time
τ	Instantaneous traffic load of a BS
Ω	Set of all possible switching strategies
ω	Any given switching strategy
M_m	Total number of MCs in the network
M_b	Total number of BSs in an MC
M_T	Total number of time slots
Υ^i	Total traffic demand served by the network before cell switching
$\hat{T}^i$	Total traffic demand served by the network after cell switching
C_{opt}	Optimum cluster to switch off
$\mathrm{E}_{s_{\min}}$	Minimum energy saved
X	represents data points in a cluster
B_{th}	Threshold value of the number of SBSs in a cluster
BS_{cal}	Best combination of SBSs to switch off per cluster
BS_{opt}	Optimal combination of SBSs to switch off in each MC
$E_{BS_{\text{opt}}}$	Energy savings of the optimum combination of BSs
ξ	CO_2 Conversion factor
$C_{\text{RB},F}$	Fixed spectrum price
$C_{\text{RB},t}$	Dynamic spectrum price
d	Duration of each time slot
M_T	Total number of time slots
$C_{\text{e},t}$	Cost of electricity per time slot
$\Psi_{\text{s},t}$	Amount of spectrum supplied by the PN
$\Psi_{\text{D},t}$	Amount of spectrum demanded by the SN
υ_p	Temperature reduction parameter
$\mathcal{T}$	Initial Temperature

$\mathcal{T}_F$	Final Temperature
$\mathcal{N}$	Utility function for making BS switch off decision
h	UAV-BS altitude
R	coverage radius
ϕ_u	Density of user distribution
Δ	Separation distance between OHP and LS
H_i	Channel gain
μ	Noise power spectral density
α	Path loss exponent
D_o	Path loss at reference distance
R_i	Distance between LS and UE
$\mathcal{R}$	Average spectral efficiency
δ_c	Profile drag coefficient
ρ	Air density
r_s	Rotor solidity
A	Rotor disc area
B_v	Blade angular velocity
R_r	Rotor radius
κ	Incremental correction factor
W	Aircraft Weight
λ	SNR threshold
N	System noise
v	Distance between O$'$ and UE
θ	Angle formed by the projection of LS to the 2D plane and the UE

Acknowledgements

My most profound gratitude goes to the Almighty God for sustaining my life and keeping me in health all through this PhD. For the wisdom, inspiration, strength, and His favour that enabled me to secure this scholarship, I am eternally grateful to Him.

My special appreciation goes to my first supervisor, Prof. Muhammad Ali Imran, for his constant guidance, support, encouragement, and motivation that enabled me to complete this research. He was always available and responsive whenever I encountered difficulties and challenges in the course of my research. Thank you for creating the enabling environment within the CSI group that enabled me to excel in my research and also collaborate with fellow researchers. I am deeply grateful to my second supervisor, Dr. Sajjad Hussain, for believing in me, for giving me the needed push to perform better and improve on myself, and for dedicating time every week to discuss and guide me in every step of this research.

To Dr. Metin Ozturk, Dr. Michael S. Mollel and Kenechi Omeke, you guys have really been of immense help in discussing my ideas, reviewing and proof reading my manuscripts as well as providing the needed motivation to continue my research work. I acknowledge the contributions of Cihat Ozturk, Asad Muhammad, Iftikhar Ahmad, Aysenur Turkmen, Ali Makine Abdel-Salam, Dr. OluwaKayode Onireti, Dr. Yusuf Sambo, Dr. Naveed Ul Hassan, Dr. Naveed Bin Rais, Dr. Ahmed Zoha, and Dr. Qammer H, Abbasi towards the success of my PhD.

I appreciate the Tertiary Education Trust Fund (TETFund) of the Federal Republic of Nigeria for granting me the sponsorship that enabled me to undertake this PhD research and the Federal University of Agriculture, Makurdi for granting me the training leave I needed to pursue my PhD.

I sincerely appreciate my lovely wife, Linda I yefu Attai, for her patience, love, and support and for making me a father, through the birthing of our beautiful daughter, Glory Ojochegbe Aanuoluwaposimi Attai, who is the crowning joy of my PhD journey. To my parents, siblings and in-laws, thank you for your prayers, support and encouragement. I really appreciate you.

I would not be able to mention the names of everyone that assisted me during my research, but for all those who contributed in one way or the other towards the completion of my PhD, I appreciate you all.

Chapter 1

Introduction

1.1 Research Overview

Cellular networks have been undergoing series of evolution from first generation (1G) to the present fifth generation (5G) networks. This is due to constant increase in the number and type of connected devices, mobile subscribers as well as the development of data-hungry applications, such as real-time video streaming, online gaming, social networking, etc. [1]. As a result, there is a continuous surge in data traffic. Moreover, with the inclusion and support for technologies such Internet-of-Things (IoT) and machine-type communication, there is going to be a significant escalation in traffic demands [2]. In addition, the need to support new and emerging uses cases in industrial verticals, such as virtual and augmented reality (VAR), vehicular communications, smart cities, etc. [3], it is expected that further explosion in the traffic demands on cellular networks will be witnessed. Accommodating this surge in data traffic and massive connectivity of devices is beyond the capacity of legacy fourth generation (4G) networks, hence the evolution in cellular communications to the current 5G networks [4]. There are also ongoing research works towards the development of sixth generation (6G) networks as 5G may not be able to meet the stringent requirements of some of the services that would be supported by cellular networks, including tactile internet, remote surgery, industrial automation, self-driving cars, etc. These requirements include ultra high data rates in terabits per second, latency in the order of hundreds of microseconds, massive connections of billions of devices per square kilometer, etc. [5–7].

Three major services have been proposed in 5G networks including enhanced mobile broadband (eMBB), ultra-reliable and low-latency communications (uRLLC) and massive machine type communications (mMTC) [1]. Of these three services, the eMBB has been saddled with the responsibility of handling capacity

enhancement and high data rate requirements of the network. To achieve enhanced capacity for eMBB, three techniques have been employed in 5G networks. These techniques include: i) spectrum extension by exploiting the millimeter wave (mm-wave) frequency band; ii) spectral efficiency using multiple-input-and-multiple-output (MIMO) antennas and cognitive radio; and iii) network densification through the deployment of a large number of base stations (BSs) [8, 9]. Network densification, which involves the massive deployment of small base stations (SBSs) alongside few macro base stations (MBSs) based on frequency reuse, is the most common and effective approach for capacity enhancement. Moreover, spectrum extension using mm-wave frequency depends on network densification to achieve its full potential, as the transmission range at high frequencies is greatly attenuated, thereby resulting in a small coverage footprint, while spectral efficiency techniques are limited by the amount of spectrum available [1, 10, 11]. Network densification has the advantage of bringing the BSs closer to the users thereby reducing the transmit power of user devices. It can also lead to a better channel condition and a higher data rate transmission [12]. However, if not properly managed, the dense deployment of BSs would result in increasing the overall energy consumption of the network [13]. Hence, since 5G networks are designed to meet a thousand-fold capacity increase, a thousand-fold increase in energy efficiency (EE) needs to be achieved in order to match its energy consumption with that of legacy networks [14].

The increase in energy consumption of cellular networks results in more greenhouse gas emission and operating expenditure (OPEX) for mobile network operators (MNOs). The information and communication technology (ICT) sector contributes about 2% to the global CO_2 emission worldwide with the cellular networks contributing about 15% - 20% of this percentage. This value is expected to further increase with the escalation in data traffic demands [14, 15]. In addition, the energy bills of MNOs account for about 30% of their OPEX in developed countries and up to 50% in developing countries [15,16]. Hence, reducing the energy consumption of cellular networks would result not only in reduced CO_2 emission but also less OPEX [17, 18]. The radio access network (RAN), which is mainly made up of BSs, has been identified as the main source of energy consumption in cellular networks with the BSs contributing about 80% [14, 17]. In addition, it has also been discovered that the BS still consumes about 50%-60% of its full load energy consumption even when in idle state (i.e., zero traffic load) [15]. Therefore, a paradigm shift in BS operation is needed to achieve a significant reduction in the energy consumption of cellular networks.

From EE perspective, the traditional approach of keeping the BSs always on is

not suitable for ultra-dense networks (UDNs) as many BSs would remain dormant when not serving any user requests. Detailed studies [19–21] on cellular data traffic pattern show that traffic demands exhibit spatial and temporal variation across BSs at different times of the day due to user mobility and traffic usage pattern. This makes the traffic load at various locations of the network vary from no-load to full-load, thereby resulting in energy wastage during period of no or low traffic demand [14, 17].

Therefore, adapting network operation to variation in traffic load such that BSs are only active when needed, rather than been always active, will result in considerable energy savings. This can be achieved by cell switching where the BSs with low or no traffic are switched off in other to conserve energy. Cell switching operation is a cost-effective way of saving energy in cellular networks because it is easy to implement and involves minimal infrastructural changes in networks [18]. The goal of cell switching operation is to ensure that the total energy consumed by the network is proportional to the traffic demand. Moreover, the quality of service (QoS), such as the throughput of users, must also be guaranteed through various techniques, such as traffic offloading, user association, etc. Hence, a trade-off between energy consumption and QoS requirements is often the main focus of most energy optimisation objectives [22].

Even though from the EE perspective, cell switching is a very effective method because it leads to energy conservation, however, from the spectral efficiency perspective, it is ineffective as it results in spectrum under-utilisation. This is because the spectrum that was originally occupied by the BSs that were turned off during cell switching operation remain dormant during the periods of inactivity. This dormant spectrum can be leased by major network operators who hold the spectrum license to smaller network operators who require small amount of spectrum and cannot afford to purchase the spectrum license for their data transmission. This would not only lead to enhanced spectrum utilisation but also generate additional revenue for the major network operators thereby enhancing their profitability. Hence, cell switching can be combined with spectrum leasing to provide enhanced benefit to MNOs in terms of reduced energy bills, additional revenue generation, and environmental sustainability.

Another area where energy optimisation is greatly needed is unmanned aerial vehicles (UAVs)-assisted wireless communication networks where BSs are mounted on UAVs (also known as UAV-BSs) to provide connectivity. UAV-BSs are being envisioned as one of the technologies in 6G that enable ubiquitous three Dimensional (3D) network coverage combined with terrestrial BSs due to their flexibility, adaptability and ease of deployment. For this to be achieved, there

is a need to carefully consider their energy consumption, as it poses a higher challenge compared to that of terrestrial BSs [6, 7, 23]. This is to ensure that their application in cellular networks does not further heighten the total energy consumption of the network as the energy consumption due the mobility of the UAV-BS is very significant compared to that of data transmission. Although various techniques have been devised to recharge the UAV-BS battery [24, 25], the frequent movement of the UAV-BS to and from the charging stations might result in service disruptions which could negatively impact the QoS of the network [26]. In addition, most of the energy optimisation techniques that have been devised to reduce the energy consumption of the UAV-BS, including trajectory design, optimal positioning, transmission scheduling, and power allocation, do not result in significant reduction in energy consumption [24, 25]. Hence, there is a need to develop more innovative energy-efficient deployment strategies that would result in more significant energy reduction in the UAV-BS, to enhance the battery lifetime and maximise the service time of the UAV-BSs.

Moreover, the implementation of cell switching and spectrum leasing mechanisms as well as energy-efficient UAV deployment strategies in 5G and beyond networks could be quite challenging. This is because the high density of BS deployment and the dynamically changing environment increase the network complexity, and the number of performance metrics that need to be considered in the optimisation process. Hence, scalable and computationally efficient optimisation frameworks comprising analytical, conventional and machine learning (ML) algorithms need to be developed to handle the demands of these networks. This would prevent service delays, minimise computational overhead, and other service degradation, which could undermine the potentials of next generation cellular networks.

1.2 Research Motivation

The constant expansion of cellular networks to accommodate the ever-increasing service demands by the deployment of more BSs means that there would be more demand for energy. The adoption of UAV-BSs in 6G networks for 3D ubiquitous network coverage means higher energy consumption is also anticipated [27]. This is accompanied by i) financial challenges in the form of increased OPEX, capital expenditure (CAPEX) and reduced profit generations from increased energy bills; ii) environmental challenges such as global warming and climate change and iii) network challenges in the form of reduced QoS due to network congestion and sudden network failures [14]. Hence, this research seeks to ensure i) business sus-

tainability; ii) environmental sustainability; and iii) improved QoS during periods of network congestion or sudden network failure. To achieve this, the motivations of this research are discussed under the following headings.

1.2.1 Reduction in OPEX and CAPEX

For MNOs to continue providing network services to users, their business must be profitable. The business can increase profit by serving more customers and reducing both CAPEX and OPEX. However, with the rising demand for data services and enhanced QoS, the MNOs are constantly forced to improve their networks services by upgrading existing software and hardware infrastructures, adopting newer technologies, deploying more BSs, purchasing more spectrum bands, etc., which are very capital intensive. In addition, with the rising energy prices, and energy consumption of cellular networks already accounting for up to 30% and 50% of OPEX in developed and developing or under-developed countries [15], there is a need for more energy saving strategies to be developed in order to reduce the OPEX. Furthermore, energy optimisation would help prolong the battery lifetime of UAV-BSs thereby enabling them to serve ground users for a longer duration. This would lead to a reduction in the number of UAV-BSs that needs to be deployed, thus resulting in reduced OPEX and CAPEX.

1.2.2 Environmental Sustainability

There is great a focus on environmental conservation from both the government and cooperate organisation because of the adverse effects that greenhouse gas emission is having on the environment, such as global warming and climate change. The increase in greenhouse gas emission is because most of the energy that is utilised in various sectors comprising the cellular communications industry is generated from non-renewable energy sources, such as coal, gas, crude oil, etc. The carbon footprint of the ICT industry is currently estimated to contribute about 2%-5% to global CO_2 emission [16], and is projected to reach about 14% in 2040 [28], with the cellular networks accounting for about 15% - 20% of the CO_2 emission in the ICT industry [17]. The emission is anticipated to increase further if appropriate measures are not taken. Hence, reducing the energy consumption of cellular networks would result in lesser energy demands, which translates to reduce carbon emission to the environment. This would enable MNOs to meet the net zero[1] emission targets. In addition, it would also lead to a reduction in

[1]This is the timeline agreed by the several nations at the climate change conference in Glasgow, COP26 to decarbonise all the sectors of their economy by 2050.

the carbon footprint of other sectors that are related to the cellular networks, such as transportation, commerce, etc.

1.2.3 Revenue Maximisation

Apart from the fact that minimising energy consumption in cellular networks results in lesser OPEX, it can also serve as a means of generating additional revenue for MNOs. This additional revenue can be obtained by exploiting the dormant or under-utilised spectrum that results from the cell switching operation, via spectrum leasing. Spectrum leasing provides the mechanism whereby dormant spectrum can be leased to third party network providers, such as IoT service providers or small network operators for a fee [29], thereby enabling the MNOs to generate monetary gains or additional profit. In addition, spectrum leasing enables these small network operators who cannot afford to purchase the spectrum license to access the spectral resources that they need for data transmission. This is because the price of spectrum license could be as high as 37.8 million according to the UK spectrum auction in 2018[2] which can only be afforded by a few large MNOs. Hence, there is a need for cell switching to be accompanied by spectrum leasing to enable small operators to access the little chunks of spectrum for their data transmission which would result in enhanced spectrum utilisation, and revenue generation for MNOs.

1.2.4 Improvement in QoS

Cellular networks are often prone to sudden surge in traffic demands due to events involving large gathering of people, such as football matches, concerts, etc., which makes the BSs in such area to be overburdened, thereby resulting in poor QoS in the form of low data rate, call drops, etc. In addition, during periods of sudden BS failure, users in that area would experience service denials or degradation in their QoS as the surrounding BSs may not be able to cater for the demands of users of the failed BS. These scenarios require quick deployment of additional BSs to enhance the capacity of existing BS and also to take over the service of the faulty BS. UAV-BSs are quite handy in such scenarios as they can be easily deployed to provide back-up services required to enhance user throughput and coverage. However, because UAV-BSs are battery powered and the amount of energy that can be stored in their batteries is very limited, they can only operate for a short duration before their battery depletes [25, 30]. Therefore, energy

[2]https://www.ofcom.org.uk/data/assets/pdffile/0021/130737/Annexes-5-18-supporting-information.pdf [accessed 27th January 2022].

optimisation is needed in UAV-BSs to enable them provide cellular coverage for longer periods, and thereby enhancing the QoS of ground users. Moreover, since the UAV-BSs utilise more energy for hovering and flying compared to fixed BSs, alternative energy-efficient deployment approaches need to be developed to significantly reduce the energy consumption of UAV-BSs.

1.3 Research Objectives

The main objective of this research is to minimise the energy consumption of the RAN of next generation cellular networks without violating the QoS (coverage loss, throughput, and coverage probability) constraints. However, in the pursuit of this primary objectives, the following research objectives are considered in this thesis:

- Develop a scalable and computationally efficient cell switching and traffic offloading framework, using both ML and meta-heuristic algorithms, for energy optimisation in ultra-dense heterogeneous networks (UDHNs).
- Develop a revenue maximisation model to generate additional revenue for MNOs, by taking advantage of the dormant spectrum resulting from the implementation of cell switching operation in 5G heterogeneous networks (HetNets), and leasing it to other smaller network operators. In addition to the monetary savings that is obtained from the cell switching operation due to reduced electricity bills.
- Investigate an alternative energy-efficient deployment technique for UAV-BSs using the landing station (LS) concept, and develop mathematical frameworks for determining suitable positions for the UAV LSs. This is to ensure that additional offloading capacity can be provided by UAV-BSs during cell switching, and spectrum leasing operations, in order to enhance energy savings and revenue generation.

1.4 Research Contributions

The major contributions of this thesis are summarized and itemized below:

1. A lightweight cell switching scheme, also known as Threshold-based Hybrid cEll swItching Scheme (THESIS), is proposed for energy optimisation in UDHNs. The proposed method is computationally efficient and produces results that are close to the optimal solution. It is scalable, that is, it can be

applied to large scale networks where many SBSs are deployed without any significant surge in the computational complexity. In addition, a benchmark algorithm, known as multilevel clustering (MLC) purely based on k-means algorithm, is developed for comparison with the proposed method.

2. A cell switching and spectrum leasing framework based on simulated annealing (SA) algorithm is developed to determine the optimal policy that maximises the revenue in 5G HetNets while respecting QoS constraints.

3. The feasibility of an alternative energy-efficient deployment scheme is examined where UAVs can be made to land on designated locations, also known as LSs, is considered. Then, the impact of the separation distances between these LSs and the optimal hovering position (OHP) on the network performance is evaluated. Specifically, mathematical frameworks are developed using stochastic geometry tools to model the relationship between UAV power consumption, coverage probability, throughput, and separation distance.

1.5 Thesis Organisation

The remaining part of this thesis is organised as follows:

In Chapter 2, the various types of BS deployments within the RAN are discussed, followed by the presentation of power consumption models for fixed BSs and UAV-BSs. Then, an overview of the various energy optimisation algorithms are briefly discussed. Finally, energy optimisation in fixed cellular networks, revenue Maximisation in cellular networks, and energy optimisation in UAV-based cellular networks were briefly discussed while highlighting the state-of-the-art, and research gap analysis. Chapter 3 focuses on the development of a scalable and computationally efficient cell switching algorithm to minimise the energy consumption of a UDHN. In pursuit of this objective, two initial solutions are developed using Q-learning and artificial neural networks (ANN), followed by a hybrid cell switching framework comprising a combination of k-means clustering algorithm and exhaustive search (ES) algorithm that is scalable and computationally efficient.

The main theme of Chapter 4 is on maximising the revenue of MNOs by ensuring that the dormant spectrum resulting from cell switching operation are utilised to generate additional revenue by leasing them to smaller network providers. A system model comprising both primary network (PN) and secondary network (SN) is considered. Then, a cell switching and spectrum leasing framework

based on simulated annealing (SA) algorithm is developed to determine the maximum revenue that can be obtained by the PN. Afterwards, the results obtained are presented and discussed. The need to develop an alternative energy-efficient approach for UAV-BS deployment using the LS concept is first identified in Chapter 5 with the aim of determining the optimal separation distance between the LS and OHP that would not significantly degrade the QoS of the network. To achieve this, the system model showing the UAV deployed in the OHP and a possible LS position where the UAV can land to provide network service at a much-reduced energy consumption is presented. Then, employing the tool of stochastic geometry, various mathematical expressions are derived to model the relationship between the separation distance, power consumption, coverage probability, and throughput of the UAV-BS. Finally, the derived models are evaluated numerically and validated using Monte Carlo simulations. This thesis is concluded in Chapter 6 with a summary of the key contributions alongside recommendations for future work.

Chapter 2

Literature Review

In this chapter, brief discussions on the various types of BS deployment within the RAN is first presented. Then, the power consumption components and power models for a BSs and UAV are presented. Afterwards, an overview of analytical, conventional, and ML algorithms that are applied for energy optimisation in cellular networks are presented with more detailed discussions on the specific algorithms applied in this thesis. Finally, the major themes of this thesis including energy optimisation in fixed cellular networks, revenue maximisation in cellular networks, and energy optimisation in UAV-based cellular network are discussed with a brief review of the state-of-the-art and research gap analysis in each area.

2.1 Types of Base Station Deployments

The RAN is the part of the cellular network that serves as an interface between the various devices and the core network. Its core function is to provide radio link between the mobile devices and the core network using BSs and backhaul connections. The BS is the major component of the RAN. As previously stated in Chapter 1, the RAN is the most energy consuming part of cellular networks, contributing about 80% of the total energy consumption with the BSs accounting for about 50% to 60% of the energy consumed in the RAN [15]. Therefore, since the BS is the major contributor to the energy consumption of the RAN, most of the energy optimisation techniques are mainly focused on reducing the energy consumption of the BSs. As a result, the energy consumption of the BS is also the main focus of this thesis. However, before going into discussions on the energy consumption of the BS, the various kinds of BS deployments in the RAN are considered.

There are various strategies for deploying BSs in the RAN which have evolved from the homogeneous scenario, where only one type and a few number of BSs are

deployed, through heterogeneous scenario to UDN scenario, where a large number of different types of BS are deployed [9]. In addition, there is also a UAV-based network deployment where the BSs are mounted on UAVs (also known as UAV-BSs) to provide aerial network coverage and is one of the prospective technologies for achieving 3D ubiquitous coverage in 6G networks [5,27]. A brief discussion on each type of BS deployment in the RAN is presented in the following paragraphs.

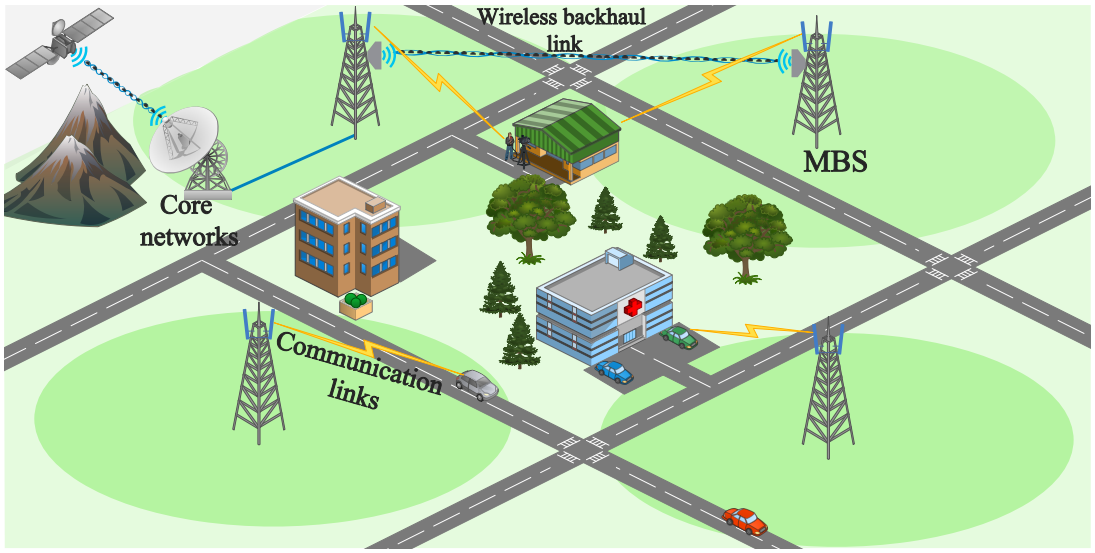

Figure 2.1: A homogeneous network comprising only MBSs.

2.1.1 Homogeneous Networks

This type of cellular network deployment comprises only one type of BS, usually MBSs, meaning that all BSs have similar characteristics, including transmission power, coverage area, antenna radiation pattern, etc. They are normally deployed in a uniform hexagonal grid within the network area. MBSs have a high transmission power of between 5W and 40W and a very large transmission range of up to 35 kilometers [31]. As a result, only a few of them are needed to provide coverage in an urban or rural area. However, this deployment strategy has low area spectral efficiency which leads to low data rate and is only suitable for voice calls and low data rate services as was prevalent in 2G networks [32]. With the advent of broadband services from 3G networks onward, and the increasing demand for higher data rate and connection speed, improved capacity and coverage, as well as for enhanced indoor coverage, it became clear that the homogeneous deployment was no longer capable of meeting these requirements, hence the shift to heterogeneous networks [33]. Fig. 2.1 illustrates a homogeneous network comprising only one type of BS, the MBS.

2.1.2 Heterogeneous Networks

This type of network deployment comprises different types of BSs that are distinguished by their unique characteristics, including transmission power, range, size, and varying applications in terms of outdoor or indoor usage. A heterogeneous network (HetNet) comprising a few MBSs and different types of small BSs (SBSs) is depicted in Fig. 2.2. The various types of BSs that make up a HetNet and their various characteristics include [34–36]:

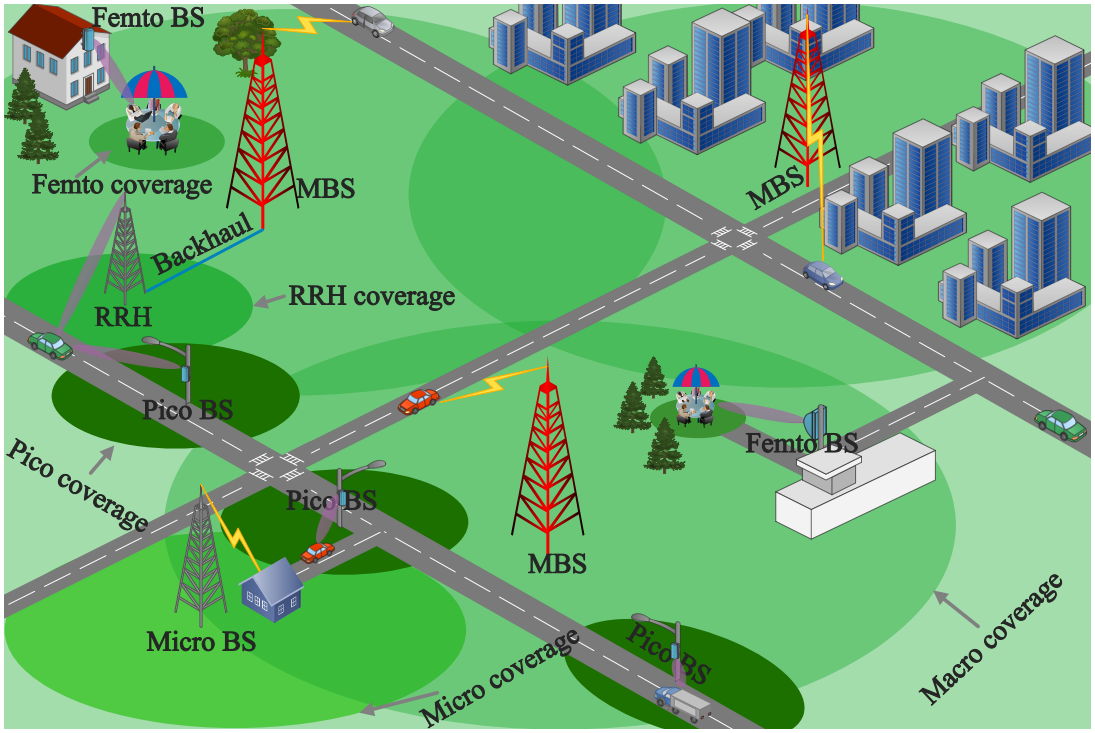

Figure 2.2: A heterogeneous network comprising MBS and small BSs including remote RRH, micro, pico and femto BSs.

- **Macro BS:** This type of BSs have high transmit power ranging from 5W to 40W, are very large in physical size and are usually deployed to provide large coverage in urban or rural areas. The antennas of this type of BSs are usually located on very high masts or on the roof top of very tall buildings. They also help to provide umbrella coverage while the smaller BSs are deployed to specific areas of the network such as hot spot zones or cell edges for capacity enhancement.

- **Remote radio head (RRH):** This type of BS is deployed to achieve coverage extension from a central BS, usually a MBS, to a remote location. Fibre cables are used to establish connection between the RRH and MBS in order to ensure proper coordination between both BSs. They are used

for centralised network densification as opposed to the use of other types of BSs such as pico and femto BSs that are used for distributed network densification.

- **Micro BS:** These are medium range BSs that are deployed mainly at the roof top. They usually have lesser transmission power compared to the MBS typically in the range of 5W to 10W. They are deployed outdoors by the network operators in a planned manner to provide coverage in hot spot areas. They can be equipped with either omni-directional or directional antennas. They can also be connected to the MBS to achieve inter-site coordination.

- **Pico BS:** This type of BSs can be installed by mobile operators either indoors or outdoors to provide coverage enhancement at hot spot areas by offloading traffic from MBSs. The typical transmission power for pico BSs is between 250mW and 2W for outdoors while that for indoor deployment is 100mW. The coverage range of pico BS is about 100m and they are usually equipped with omni-directional antennas. They can also be connected to MBS to achieve inter-site coordination.

- **Femto BS:** This type of BSs are deployed and installed by the users to provide indoor coverage at homes, offices, etc., and also assist in offloading traffic from MBSs. Their typical transmission power and range is about 100mW and 10m to 30m and they are also equipped with omni-directional antennas. The can be connected to the network via any broadband connection available at the user premises such as coaxial cable or fibre. The can also be interfaced with the MBS to ensure inter-site coordination.

2.1.3 Ultra-Dense Networks

Ultra-densification is a major theme of 5G and beyond networks because of the explosive growth in traffic demands and the stringent QoS requirements resulting from the diverse use cases employing cellular communications [1]. This would enable the achievement of the high magnitude of capacity enhancement target in 5G and beyond networks. According to [37], UDNs have three main features: 1) massive deployment of small BSs of equal or greater number than the number of users in an area which would help improve spectral efficiency through enhanced frequency reuse. These large number of small BSs are mostly deployed under the MBS coverage to enhance network capacity and balance the network load via traffic offloading from MBSs; 2) dense and multi-tier BS deployments that are

interconnected to each other which might result in increased network complexity; and 3) quick access and flexible handovers. The dense deployment and small BS footprint would mean that the UE would have to switch connections regularly from one BS to another for improved QoS. Hence, efficient handover mechanisms must be put in place to ensure seamless connection during the handover. Despite

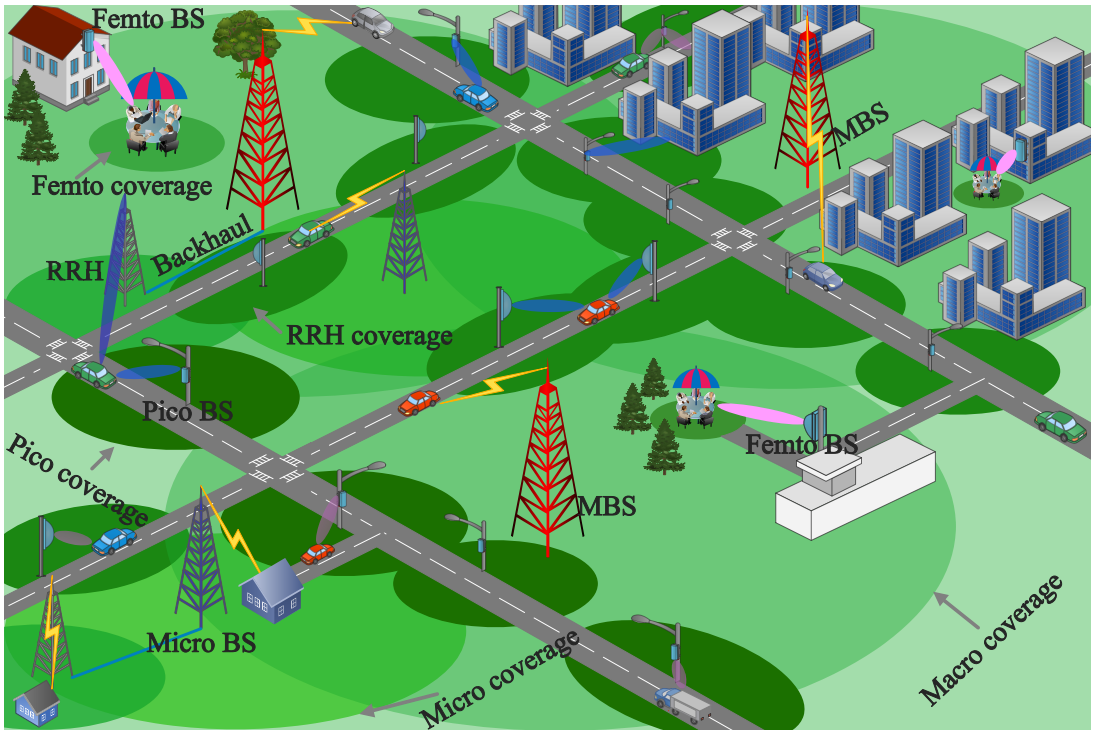

Figure 2.3: An ultra-dense network comprising a few MBSs and many SBSs (RRH, micro, pico and femto BSs).

the numerous advantages of UDNs including capacity and coverage enhancement, load balancing, and improved data rate and connection speed, there is also the problem of increased energy consumption due to the increased deployment of small BSs as well as energy wastage due to continuous operation of the BS even when it is not serving any user request, which if not properly managed, would be a major challenge in 5G and beyond networks [14]. An ultra-dense network that is made up of a few MBSs and several SBSs is depicted in Fig. 2.3.

2.1.4 UAV-Based Networks

This is also known as aerial networks and comprises UAV-BSs. It is a very promising BS deployment approach for next generation cellular networks as it brings a lot of flexibility, adaptability, and robustness to the wireless communication networks. The UAV-BSs can be deployed: i) to provide emergency services during partial or total network failure; ii) for coverage and capacity enhancement in

already existing networks. In the following paragraphs, the main types of UAVs and the two major categories of UAV-BS deployments for wireless communications are discussed.

Types of UAVs

UAVs, also known as drones, are of three main categories: i) fixed-wing; ii) rotary-wing; and iii) hybrid UAVs [24].

i. **Rotary-wing UAVs:** They are designed to perform vertical take-offs and landings. One of the main design features of rotary-wing UAVs is that they can hover on a fixed and specified location, making them perfect candidates to perform tasks like continuous cellular coverage and sensing [24]. However, the power consumption of rotary-wing UAVs is higher, as they operate at a low altitude with little mobility and their constant fight against gravity results in more power consumption [24].

ii. **Fixed-wing UAVs:** These are another type of UAV that can glide through the air and operate at higher altitude, making them more energy efficient and capable of carrying heavier payloads [25]. However, fixed-wing UAVs require a runway for landing and take-off and are more expensive than rotary-wing UAVs [38].

iii. **Hybrid UAVs:** The limitations of both rotary- and fixed-wing UAVs led to the emergence of this new type of UAV in terms of shape and aerodynamics [39]. The fundamental design strategy behind the hybrid ones is to combine the features of both rotary-, and fixed-wing UAVs for various maneuvers and flights dynamics. These UAVs can perform vertical take-off and landing (VTOL) in copter mode and shift to high-speed forward flight in aeroplane mode [40].

Types of UAV-BSs Deployments

There is an ever-increasing application of UAVs in different aspects of wireless communications. In each of these applications, wireless networks can comprise standalone UAV-BSs, where only single or multiple UAV-BSs are deployed to provide cellular coverage [41, 42], or UAV-assisted cellular networks, where both UAV-BSs and fixed or terrestrial BSs are deployed together for enhanced network coverage [43]. The two major types of UAV-BS deployments are illustrated in Fig. 2.4, while brief discussions on each deployment type are presented in the following paragraphs.

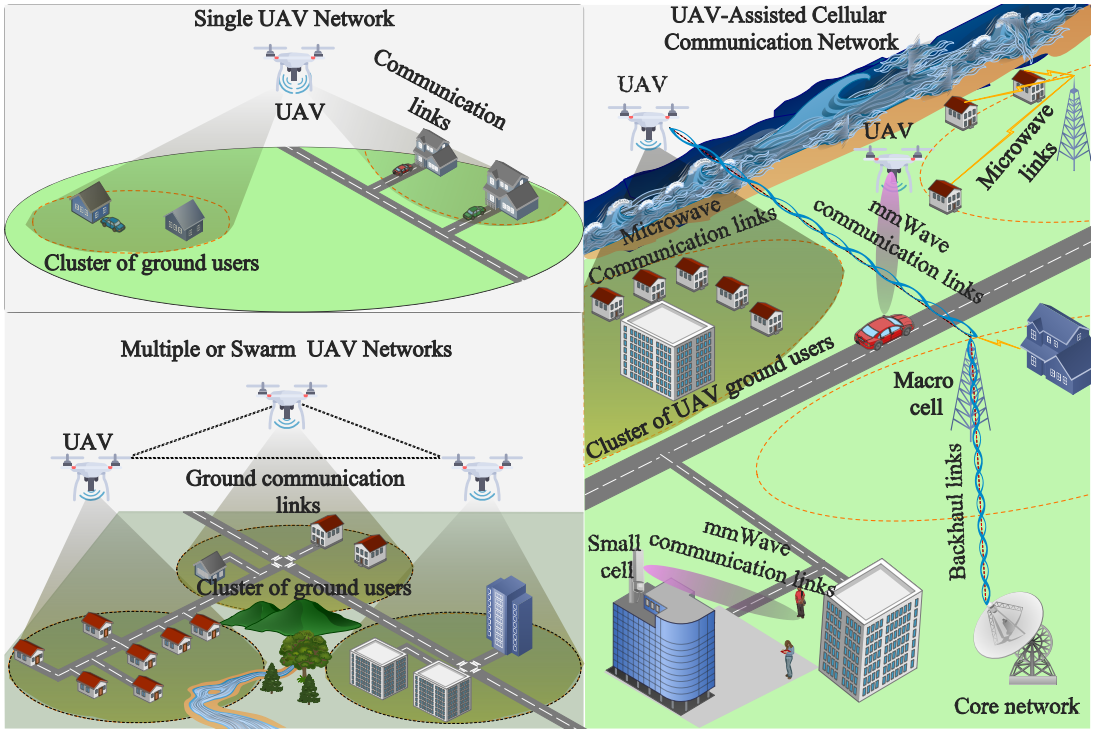

Figure 2.4: Illustration of the two major types of UAV deployments: UAV stand-alone deployment comprising single and multiple UAV networks, and UAV-assisted cellular networks comprising both UAV-BSs and terrestrial BSs.

Standalone UAV-BS Deployments: Standalone UAV deployment involves the deployment of single or multiple UAV-BS to provide network service in an area without fixed cellular network coverage. Two major deployment scenarios exists in this approach. The first scenario involves the deployment of a single UAV-BS to provide a wireless network service in an area including harvesting data from IoT networks, act as a relay to provide wireless service to users that have been separated by large obstacles such as mountains and hills, etc. [44]. In the second scenario, multiple UAV-BSs are deployed in the form of a swarm network to provide a complete wireless network service to a particular area, which could be a dedicated network for an organisation, to provide wireless service in rural areas without prior cellular network infrastructure, etc [45].

The major challenge with single UAV deployment is that when a fault occurs in the UAV-BS, it could result in complete network failure. On the other hand, in a multi-UAV-BS system, when a single UAV-BS fails, the system can be reconfigured to provide a sub-optimal solution. However, this does not mean that the use of multiple UAV-BSs does not have disadvantages, as the problem of proper coordination among the multiple UAV-BSs deployed exists [46]. In summary, choosing between a single UAV-BS or multiple UAV-BSs deployment depends on the nature of the communication system that is being developed and the problem

that the network would address.

UAV-BS Deployment with Fixed BSs (UAV-Assisted Cellular Networks): This involves the deployment of either single or multiple UAV-BSs on top of existing fixed cellular network infrastructure (terrestrial BSs) to provide enhanced capacity and coverage in different scenarios [47]. For example, during major events, such as football matches and concerts, involving a large gathering of people, the networks in such areas would be very congested, which could lead to poor QoS. In such scenarios, UAV-BSs can be deployed to provide additional capacity in order to reduce network congestion, and to enhance the data rate of the users in hotspot regions and at the cell edges [43]. In addition, UAV-BSs can help to provide communications with highly mobile user equipment (UE), thereby preventing frequent handovers, which can negatively affect their QoS [48]. One of the main advantages of deploying UAVs in existing cellular networks is that they can change their locations depending on the network conditions, which helps in increasing the QoS, restoring network at failed BS sites, achieving load balancing, offloading traffic from MBSs, and extending the coverage. Hence, UAV-BS deployment in cellular networks is a key design consideration in future heterogeneous wireless networks that can enable various applications such as smart cities, mobile computing, and autonomous vehicle networks, etc. [49].

The Role of UAVs in Wireless Networks

UAVs have been employed for various operations in both military and civilian domains including object detection, location tracking, goods delivery, and information dissemination. Recently, they have also found several applications in wireless communications because of their flexibility, adaptability, and easy deployment. Some of these applications include: i) emergency services (pop-up networks) [50, 51]; ii) data harvesting [52, 53]; iii) content caching and computation offloading [54, 55]; iv) load balancing [56, 57]; v) coverage extension or relaying [58, 59]; vi) Capacity/throughput enhancement [60, 61]; vii) backhauling [62, 63]; and viii) EE [47, 64].

2.2 Power Consumption Models

Power consumption models are used to estimate the power consumed in a terrestrial or aerial BS by quantifying the amount of power consumption in each of the components that make up the BS. Therefore, in this section, brief discussions on the various power consumption components of both types of BSs are presented.

2.2.1 Power Consumption of a Fixed BS

In this section, the components responsible for power consumption in a fixed BS are briefly highlighted, after which the power consumption model for a fixed BS is presented and discussed.

Base Station Components

A BS is made up of several transceivers each serving one transmit/receive antenna element. A transceiver comprises various components including power amplifier (PA), radio frequency (RF) unit, baseband (BB) unit, main power supply unit, cooling system, and antenna interface. Each of these components are briefly discussed in the following [65, 66]:

- **Power amplifier (PA):** The PA accounts for most of the power consumption in a BS, and its function is to improve the power level of the RF signals received or transmitted from and through the antenna. However, power amplifiers suffer from non-linearity and distortion, which tends to reduce the amplifier's efficiency, and hence, more advanced amplifier design using techniques such as clipping and pre-distortion can be used to enhance the efficiency and achieve linearity.

- **Radio frequency (RF) unit:** This unit is made up of a transmitter and a receiver for signal transmission and reception. The architecture of the RF unit varies depending on the type of BS. For macro and micro BSs, low-intermediate frequency architectures are used while in pico and femto BSs, zero-intermediate frequency architectures are utilised. The power consumption of the RF unit is mostly affected by the bandwidth, signal-to-noise-and-distortion ratio as well as the analog-to-digital conversion resolution.

- **Baseband (BB) unit:** This unit is responsible for digital signal processing functionalities including modulation/demodulation, channel estimation and equalization, filtering, etc., with each of this process contributing to the power consumption in this unit.

- **Power supply unit:** The unit comprises the main supply unit which provides the alternating current (AC) needed to power the BS, which must be converted to direct current (DC) as most BSs use DC to power their components. In addition, there are also converters whose function is to convert the DC to the levels required to power the different components of the BS. These conversion process are usually associated with some losses which reduces the EE of the BS.

- **Cooling system:** The BS, particularly the MBS, requires an active cooling system to keep the temperature under certain thresholds that is needed to ensure the proper functionality of the certain components in the BS and to prevent their breakdown due to excessive heating during their operation. Smaller BSs, such as pico and femto BSs, do not require cooling system due to their low energy consumption. The cooling system has been found to contribute about 30% to the total power consumption of the BS [67], hence significant energy saving can be achieved by reducing the energy consumption due to cooling. However, the use of RRH with MBS obliterates the need for an active cooling system as the power amplifiers can be cooled by atmospheric air.

- **Antenna interface:** The antenna is a passive device whose function is to convert electrical signals into electromagnetic signals and vice versa. The antenna interface which is the connecting point between the antenna and the PA introduces certain losses such as the feeder loss which also reduces the power efficiency of the BS. This was more significant in traditional MBSs were the antenna was in a different location from the PA, but with RRH, where the PA is situated in the same location as the antenna, the feeder loss is greatly reduced. For small BS, the feeder loss is considered to be negligible.

Base Station Power Consumption Model

In order to quantify the power consumption of the mobile cellular networks, power consumption models that can estimate the amount of energy consumed by the various components and subsystems of the network are required. Since the BS is the major power consumption component in the cellular network, most research activities have been focused on developing accurate power consumption models for the BS. Different BS power consumption models have been proposed in [65, 66, 68–72].

The Energy-Aware Radio Technologies (EARTH) power consumption model is the most widely applied one and it is able to capture the power consumption of different BS types and sizes under different network scenarios. It is expressed as [65]:

$$P_{\text{in}} = N_{\text{TRX}} \cdot \frac{\frac{P_{\text{out}}}{\mu_{\text{PA}} \cdot (1-\rho_{\text{feed}})} + P_{\text{RF}} + P_{\text{BB}}}{(1-\rho_{\text{DC}})(1-\rho_{\text{MS}})(1-\rho_{\text{cool}})} \tag{2.1}$$

where P_{in} is the power supplied to the BS, N_{TRX} is the number of transmit/receive antennas, P_{out} is the output power from each antenna, μ_{PA} is the power amplifier

efficiency, P_{RF} is the power consumption due to radio transmission, P_{BB} is the power consumption of the base band unit, ρ_{feed}, ρ_{DC}, ρ_{MS} and ρ_{cool} are the feeder, DC-DC power supply, main supply, and cooling losses, respectively.

However, the BS power consumption is usually approximated by linear models [65, 68, 69] because they are easy to apply and provide a near-accurate approximation of the actual power consumption of the BS [65]. The linear power consumption model consists of two parts: the static (or load independent part) and the dynamic (or load dependent part). The static power consumption does not vary with traffic load and it comprises power consumption of the cooling system, processing units, power supply unit while the dynamic power consumption varies with traffic load and it comprises power consumed in the PA and RF unit.

The linear approximation of the EARTH's BS power consumption model [65] can be expressed as:

$$P_{\mathrm{BS}} = N_{\mathrm{TRX}}. \begin{cases} P_{\mathrm{o}} + \eta P_{\mathrm{tx}}, & \text{if } 0 < P_{\mathrm{tx}} < P_{\mathrm{max}} \\ P_{\mathrm{s}}, & \text{if } P_{\mathrm{tx}} = 0, \end{cases} \tag{2.2}$$

where P_{BS} is the total power consumption of a BS, η, is the slope of the load dependent power consumption, P_{o} denotes the constant power consumption component of the BS when in operation, P_{s} is the power consumed by the BS when in sleep mode. P_{tx} and P_{max} are the instantaneous and maximum transmit power of the BS, respectively. Although, various BS power consumption models have been proposed in the literature [70–72], the EARTH's linear BS power consumption model [65] is the most commonly applied because of its simplicity and easy adaptation to all types of BSs. As a result, it is adopted in this thesis for modelling the power consumption of the BS.

2.2.2 Power Consumption of a UAV-BS

The power consumption of UAV-BS comprises two components: communication or BS power consumption and Propulsion or UAV power consumption. The power consumption model of the BS mounted on the UAV is the same as that of the fixed BS. Therefore, since it has been considered in the previous section, this section is dedicated to the discussions on the UAV power consumption. In this regard, the basic components of the UAV are first highlighted, followed by the presentation of the power consumption model of the UAV. Finally, a brief discussion on the various power supply and charging mechanisms used to power the UAVs during the course of their operation.

UAV Components

UAV comprises of the following units or subsystems: the propulsion unit, monitoring and control unit, power supply unit, and the payload [26, 73].

- **Propulsion unit:** This unit constitutes a major portion of the weight of the UAV and is also the most energy consuming part of the UAV, comprising the motor and propellers. It is responsible for ensuring the mobility of the UAV by converting the electrical energy supplied by the UAV batteries into mechanical energy. The most common type of motor used in miniature UAVs is the brush-less DC motor because of its high efficiency, reliability, and good torque [74].

- **Monitoring and control unit:** This unit comprises on-board flight control and mission-oriented sensors and processors that are responsible for collecting and analysing of flight data, communicating with ground station, executing navigation and control algorithms, and planning the missions of the UAV. The communication modules that enable the UAV to communicate with the ground control unit is also part of this unit. The major source of energy consumption in this unit is due to the processing of the data received from the various sensors in order to make informed decision regarding the UAV flight [73].

- **Power supply unit:** This unit consists of the power source responsible for supplying electrical energy for powering the UAV and the payload, by means of battery, grid power (for tethered drones), renewable energy (e.g., solar, wind, etc.) and fuel cells. In addition, there are also omni- and uni-directional converters, which are responsible for controlling the flow of power during the process of charging and utilisation of the UAV battery.

- **Payload:** The payload is the part of the UAV that is used to carry various equipment and accessories, such as cameras and sensors for monitoring and surveillance purposes. They are also used to carry BS in other to provide cellular services. The size of the payload varies depending on the type of the UAV and contributes to the total weight and how long each UAV can fly. Hence, they are normally designed with maximum take off weight which specifies the maximum weight that can be supported by the UAV for a given flight duration [24].

UAV Power Model

Various power consumption models have been proposed for both fixed-wing and rotary-wing UAVs in the literature [75–79]. However, in this thesis, a rotary-wing UAV is considered because of its ability to hover in a fixed position above the ground. The power consumption model for rotary-wing UAVs proposed in [76] is adopted.

The power consumption of the rotary-wing UAV due to propulsion can be expressed as [76]:

$$P(V) = P_c\left(1 + \frac{3V^2}{U_{\text{tip}}^2}\right) + P_i\left(\sqrt{1 + \frac{V^4}{4v_0^4}} - \frac{V^2}{2v_0^2}\right)^{+} \frac{1}{2} d_0 \rho r_s A V^3 \tag{2.3}$$

where P_c and P_i represent the blade profile and induced power, respectively. U_{tip}, v_o, d_0, r_s, ρ, A and V represent the tip speed of the the rotor blade, mean motor induced velocity during hovering, fuselage drag ratio, rotor solidity, air density, rotor disc area and propulsion velocity, respectively.

To obtain the power consumption due to hovering, which is the case where the UAV is stationary in the air, $V = 0$ is substituted into (2.3) which gives:

$$P_{\text{hov}} = P_c + P_i, \tag{2.4}$$

and then substituting the respective expressions for P_c and P_i from [76] into (2.4), the full expression for power consumption due to hovering can be obtained as follows:

$$P_{\text{hov}} = \frac{\delta_{\text{c}}}{8} \rho r_s A B_v^3 R_r^3 + (1 + \kappa) \frac{W^{2/3}}{\sqrt{2\rho A}}. \tag{2.5}$$

where δ_c, R_r, B_v, k , $W$is the profile drag coefficient, rotor radius, blade angular velocity, incremental correction factor for induced power, and aircraft weight, respectively.

UAV Power Supply and Charging Mechanisms

Even though UAVs have found increasing application in wireless communications because of their flexible deployment, easy adaptation, and cost-effectiveness [25], there are some challenges that limit their full exploitation in wireless networks. The most important of these challenges is power and energy consumption limitation [24]. Miniature UAVs are usually powered with rechargeable batteries for operations, while large UAVs are powered by using non-renewable resources, such as fuel and gas, to provide more energy to the UAV for longer flight time.

To maximise the flight duration and the service time of UAVs, various alternative sources of power supply and charging mechanisms have been developed and tested. Some of the UAV sources of power supplies are battery [80,81], grid (tethering) [82, 83], fuel cells [84, 85], renewable/energy harvesting sources including solar, wind, RF, etc. [86, 87], and hybrid sources such as solar, battery and fuel cell-battery [88–91]. As battery-powered UAVs are the most common means of powering miniature UAVs, different battery charging/recharging mechanisms have been developed including swapping [92, 93], laser beam charging [94] and wireless powered charging systems [95, 96].

2.3 Energy Optimisation Approaches

In this section, energy optimisation techniques for both fixed and UAV-based cellular networks are broadly categorised under analytical, conventional and ML techniques. Then, the specific methods under each category such stochastic geometry (analytical method), ES and SA (conventional methods), artificial neural networks (ANN), k-means, and Q-learning (ML techniques) are discussed in more detail.

2.3.1 Analytical Approaches

These methods employ mathematical tools to describe network entities, the interactions among various network entities, and to the model network performance. Normally, closed-form expressions are derived which describe the average performance of the network from which certain design parameters of the network can be optimised. One of the common analytical methods that are employed for energy optimisation in wireless communication networks is stochastic geometry. In the following paragraphs, discussions on stochastic geometry are presented as it is one of the methods employed in this thesis for energy optimisation.

Stochastic geometry

Stochastic geometry enables a generalized model to be developed which approximates the average performance of the network over all realizations [97]. It employs a particular kind of random distribution, known as point process (PP) to model the distribution of network elements in a given location. After that, expressions are derived which relates the network performance metrics such coverage probability, ergodic capacity, EE, etc. to the network parameters that needs to be optimised. These expressions enable network behaviour to be understood as

well as their relationship with certain design variables or parameters. As a result of this information, network engineers would be able to analyse the various trade-offs that can be accommodated within the network and make informed decisions based on the different scenarios that would be encountered in practical networks [98]. The most common PP employed in stochastic geometric for analyzing wireless network performance is the Poisson PP (PPP) because of its flexibility and tractability and can be defined as:

Definition 1. *A PP* $\Phi = \{x_i; i = 1, 2, 3, ...\} \in \mathbb{R}^d$ *is a PPP if and only if the number of points inside any compact set* $\mathcal{B} \subset \mathbb{R}^d$ *is a Poisson random variable, and the numbers of points in disjoint sets are independent [98].*

2.3.2 Conventional Approaches

Several conventional optimisation methods have been applied for energy optimisation in fixed and UAV-based cellular networks in the literature. Therefore, in this thesis, the conventional methods are grouped into three major categories, namely: exact, heuristic, and meta-heuristic methods. In addition, the meta-heuristic methods are further divided in three categories: Evolutionary-based, swarm intelligence-based, and trajectory-based algorithms.

In the following paragraphs, the common conventional algorithms will be briefly discussed. However, the specific methods that are applied for energy optimisation in this thesis including ES and SA algorithms are discussed in more details.

Exact Methods

Exact methods are guaranteed to always find the optimal solution to an optimisation problem. However, these methods are inefficient, especially in operational decision processes, due to the unacceptable solution times and their inability to reach solutions in large-size problems in a reasonable time [99]. An example of the exact method is the ES algorithm, and is briefly discussed in the following paragraph because it is one of the methods applied for energy optimisation in this thesis.

Exhaustive search algorithm: This algorithm tries all the possible combinations of the solution in order to find to optimal solution [100]. As far as the optimal solution concerned, the ES is always guaranteed to find the optimal solution because it searches sequentially through all the possible combinations to select the best solution. However, the main challenge with ES is the problem

of combinatorial explosion, which results when the number of candidates in the search space becomes very large. As such, ES becomes computationally burdensome and infeasible to implement in realistic networks with a large dimension. Hence, ES algorithm should be combined with other heuristic or ML algorithms that can help reduce the search space in order to increase the speed of execution and reduce the complexity of finding a near optimal solution. The pseudo-code for ES algorithm is presented in Algorithm 1, where S is the set of all possible solutions, s_o is the initial solution, s^* is the solution that gives the maximum energy saving, E_t is the energy saving of the optimal solution, M_b is the number of BSs in the network, and *total_row* represents the total number of data samples in a dataset.

Algorithm 1: Exhaustive search (ES)

```
Initialize number of BSs, M_b;
Function compute energy saving from action (S), E_s ← f(S);
for row = 1, total_row do
    Initialize action s_o;
    Output s* ← s_o, as action with Max energy saving;
    for t = 1, 2^{M_b} do
        compute E_t ← f(t) ;
        if E_t ≥ E_s then
            s* ← t ;
        end
    end
    output: s*
end
```

Heuristic Algorithms

Exact algorithms are developed in such a way that the optimal solution can be achieved in a limited time. However, for some very difficult optimisation problems (e.g., NP-hard or global optimisation), this limited amount of time may expand exponentially in relation to the problem sizes. Heuristics lack this guarantee and, as a result, often provide solutions that are less than optimum or approximate solutions. Heuristic algorithms, on the other hand, frequently find acceptable solutions in a reasonable amount of time. In addition, they are often problem-dependent, that is, they are designed for a specific problem as energy optimisation in cellular networks, UAV routing problems, etc. There are two main heuristic approaches to solving hard optimisation problems. One of such approaches is the constructive heuristics which develops solutions via iterations.

It is called a constructive heuristic because it begins with an empty solution and continues to expand on it until a complete solution is discovered [101]. The other heuristic method is called improvement or local search heuristics. Improvement heuristics start with a complete solution and then strives to improve on the existing solution further by local searches. Examples of heuristic algorithms are block coordinate descent (BCD), Dinkelbacks method, and successive convex approximation (SCA), etc.

Meta-heuristic algorithms

A meta-heuristic, on the other hand, is a high-level problem-independent algorithmic framework that offers a set of principles or techniques for the development of heuristic optimisation algorithms. However, a specific definition is quite tricky, and many scholars and practitioners use the terms heuristics and meta-heuristics interchangeably. As a result, the word meta-heuristic may also refer to a problem-specific implementation of a heuristic optimisation algorithm based on the rules given in such a framework. Different from heuristic methods, a meta-heuristic knows nothing about the problem it will be applied to as it can treat functions as black boxes. For more information on meta-heuristic algorithms, the studies in [102] can be examined. In the following paragraphs, meta-heuristic algorithms will be examined in three categories.

i. **Evolutionary-based algorithms:** These are population based algorithms that tries to mimic the concept of natural evolution. The mode of operation of these algorithms is to first create a population of all possible solutions and assign scores to each solution, depending on how good they are, using a fitness function. Then, over time, the population evolves and better solutions are identified [103, 104]. A common example of evolutionary-based algorithms that is used for energy optimisation in cellular communications network is the genetic algorithm (GA) [105–107].

ii. **Swarm intelligence-based algorithms:** These are algorithms that are inspired from nature, based on the relationship between living organisms, such as ants, birds, bees, etc [108]. In the algorithm implementation process, a swarm is created comprising several entities that have limited intelligence. These entities interact with each other using a specified principle, with no central entity coordinating them, and overtime, a holistic intelligence in achieved [109]. Common examples of swarm intelligence-based algorithms that have been applied for energy optimisation in cellular networks includes particle swarm optimisation (PSO) [110–112] and ant colony

optimisation (ACO) [113, 114].

iii. **Trajectory-Based Algorithms:** These are algorithms that employ a single agent that traces a trajectory while moving through the search space in order to determine the global optimal solution. In the process, a better solution is accepted while a solution that is not so good may be accepted with a specific probability. Examples of trajectory-based algorithms that have been applied for energy optimisation in cellular networks include SA and variable neighbourhood search algorithm. However, SA algorithm would be detailed in the following paragraphs because it is one of the methods applied in this thesis. SA algorithm is considered in this thesis because it has an inbuilt mechanism that makes it not to be easily trapped in the local minimum like most heuristic algorithms [115]. In addition, its performance closely approximates the optimal solution but with a significantly lesser computational overhead. Moreover, it can be easily applied to the cell switching and spectrum leasing problem that is considered in this thesis.

Simulated annealing algorithm (SA): This is a meta-heuristic algorithm developed by Kirkpatrick et al. in 1983 to solve optimisation problems. The SA method is based on the analogy between the annealing process in physical systems that minimises the energy state of the solids and is applied to find the solution to many combinatorial optimisation problems [115]. The SA algorithm is a probability-based heuristic that deals with the annealing process in solid materials with an analogical approach [116]. The working principle of annealing simulation is based on the process during which a heated solid material cools down. It is applied to optimisation problems by simulating the cooling process with the algorithm. It is used in the optimisation of difficult problems such as scheduling, inventory control and routing in the literature [117–120].

In addition, SA algorithm is one of the algorithms that has proven its success in cellular and mobile network applications [117]. In this context, it can be easily integrated into many problems has increased the popularity of the algorithm. One of the most important features of the SA algorithm is that it ensures that results which degrades the objective function values are included in the solution process under certain conditions in order not to be stuck at a local optimum. In other words, an improved objective function value is always accepted, whereas moves that worsen the objective values are accepted on a probabilistic basis. In basic SA algorithm, the

criteria used to accept a worse objective function are the random number generated between 0 and 1, the improvement in the objective function, and the current temperature values. In the operation steps of the algorithm, as the temperature of the system decreases, the possibility of accepting worse results decreases. The probability of increase in the amplitude of the energy, δE at temperature, $\mathcal{T}$ is presented in (2.6):

$$p(\delta) = \exp(-\frac{\delta E}{\mathcal{K}\mathcal{T}}), \tag{2.6}$$

where $\mathcal{K}$ is Boltzman constant.

Therefore, the starting temperature of the system must be high enough to allow any feasible solution to be accepted. However, if the initial temperature is set too high, the search process will be random until the temperature decreases to a certain level. Also, a stop criterion is required for the algorithm. A certain ϱ value is determined as a stopping criterion in order not to prolong the search process excessively. During the search process the algorithm attempts to transform the current solution s into one of its neighbors s' selected at random. However, in the proposed algorithm, instead of randomly selecting a neighborhood structure, each neighborhood is applied in order. A similar approach is available in sequential variable neighborhood search (VNS) algorithm [121]. The search area is expanded in each iteration due to the small number of neighborhood types. The pseudo code of the SA algorithm is shown in Algorithm 2, where s_0 denotes the initial solution, S is the set of possible solutions, $\mathcal{T}$ denotes temperature, φ is the number of local search iterations for each temperature, u is a random variable between 0 and 1, ϑ is the difference between a neighbor solution (s') and the current solution (s), s^* is the optimal solution to the problem, and ϱ is the temperature change counter.

2.3.3 Machine Learning Approaches

ML are a class of algorithms that have the ability to learn from datasets without being explicitly programmed like conventional or heuristics algorithms [122]. They have been applied in various fields such as natural language processing and computer vision and is now gaining wide acceptance in the field of wireless communications for the following reasons [123–125]: Firstly, they are able to learn hidden user behaviours or network characteristics form historical data that cannot be analytically modelled. Secondly, unlike heuristic algorithms, they are able

Algorithm 2: SA algorithm

```
Identify initial solution: s_0 ∈ S;
Calculate objective function s_0;
Define an initial temperature 𝒯 > 0;
Set to zero temperature change counter ϱ = 0 ;
s = s_0,   f(s) = f(s_0);
s* = s_0,   f(s*) = f(s_0);
define local search iteration number for each temperature (k);
repeat
    n = φ;
    repeat
        generate neighbor solution s';
        ϑ = f(s') − f(s);
        if (ϑ ≤ 0) then
            s = s';
        else
            generate a random number from uniform distribution in the
             0-1 range (u);
            if (u < exp(−ϑ/𝒯)) then
                s = s';
            end
            if (f(s') < f(s*)) then
                s* = s';
            end
        end
        n = n − 1;
    until n = 0;
    ϱ = ϱ + 1;
    𝒯 = 𝒯 (t);
until (to the stop if condition is meet);
s* is the heuristic solution of the problem
```

to adapt to changing network conditions in order to optimise the performance of the network. Finally, they require very little or no human involvement in the implementation process hence are a catalyst for achieving network automation or self-organising networks. Generally, they can be classified according to the amount and type of supervision they get during their training period. There are six major categories of ML algorithms: supervised learning (ML), unsupervised learning (UL), semi-supervised learning, deep learning (DL), reinforcement learning (RL), and federated learning (FL). However, only supervised, unsupervised and RL methods are discussed in the following paragraphs because they are the methods applied in this thesis for energy optimisation in cellular networks.

Supervised Learning (SL)

In SL, the training set comprises both the input dataset and the desired output, also referred to as labels. SL learns a function (a match between the input data and the result data) by extracting information from the input data and the labels that are fed into the machine [126]. SL problems are divided into two main categories, which are regression and classification [127]. In regression problems, a continuous output is predicted; that is, the input variables are mapped to a continuous output. Examples of regression SL methods are linear regression, ridge regression, step-wise regression, etc [128]. Regression is applied in wireless networks for traffic prediction to enable proactive load balancing, and resource allocation. It is also used for user location prediction to enable proactive handover optimisation [129]. In classification problems, a categorical output is predicted, that is, the input variables are mapped to different output classes, which could be a binary class (comprising two classes) or multi-class (comprising many classes). Logistic regression, naïve bayes classifier, k-nearest neighbor, ANN and support vector machine are examples of SL classification methods [127]. Multi-classification finds application in wireless networks with regards to selecting the optimal sets of BSs to switch off in energy optimisation problems, and in the identification of various kinds of attacks on the network [130].

In this thesis, ANN is the SL technique adopted because of its unique qualities such as non-linearity, versatility and advanced learning capabilities [131, 132], hence, it is briefly described in the following paragraphs.

Artificial neural networks (ANN): is a biologically inspired learning algorithm that attempts to mimic the functioning of the neurons in the brain. A typical structure of an ANN model is presented in Fig. 2.5. It consists of three major layers including the input layer, hidden layer, and output layer [122,131,133]. Each layer comprises neurons which are connected to previous and subsequent layer neurons. The neurons contains activating units which are triggered depending on the input from the preceding layer neurons. The basic mathematical expression for the neuron is given as:

$$h_i = \iota\left(\sum_{i=1}^{M_{\mathrm{L}}} x_i w_i + b_i\right), \tag{2.7}$$

where $\iota(\cdot)$ is the activation, x_i is the input, w_i is the weight vector, and b_i is the value of the bias associated with the layer and M_{L} is the number of layers. The essence of the activation function is to regulate the output from a neuron while

the bias is meant to regulate the input to the activation function. There are various kinds of activation functions that have been employed in the literature including sigmoid, tanh, rectified linear unit (ReLU), softmax, etc [131, 134].

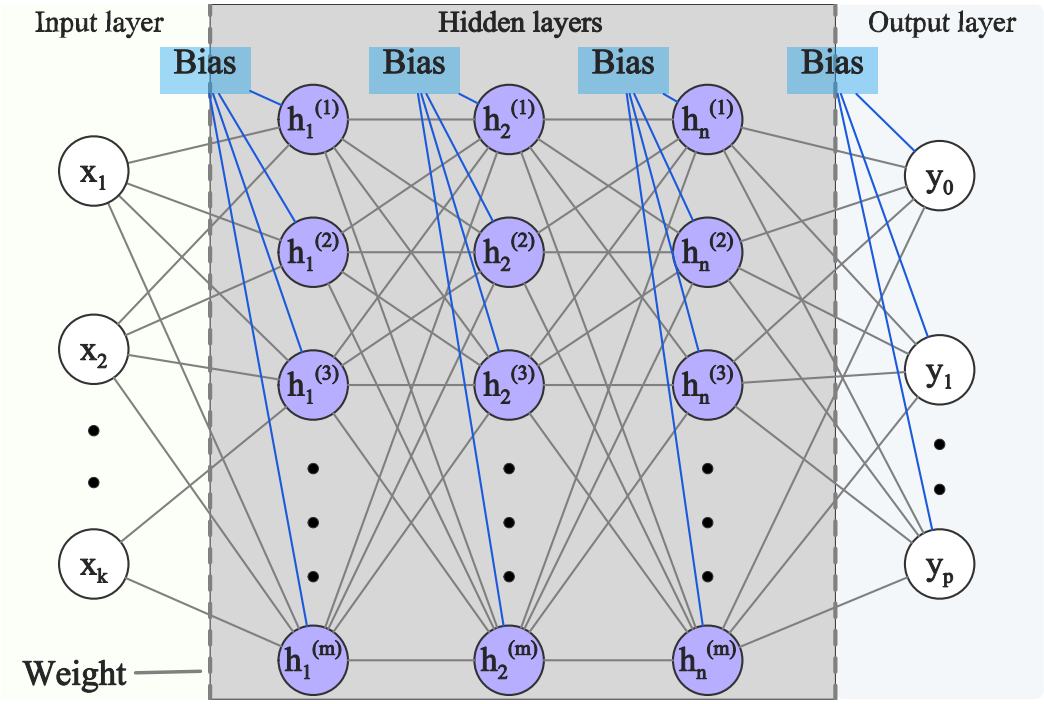

Figure 2.5: A typical ANN model structure

The process of training the ANN involves both forward propagation and backward propagation. In the former, the input data is exposed to different layers of the ANN in sequential manner from input to output layer while in the latter, the data passes from output to the input layers and is the process where the various parameters of the network are learnt. During the forward pass, the discrepancy between the real output value and the predicted value, which is often referred to as the cost, is estimated using a utility function such as mean square error (MSE), root MSE (RMSE), or cross entropy. The error obtained when the utility function is estimated is propagated backwards to update the weights and bias of each layer of the network using an optimisation algorithm such as gradient descent. The number of hidden layers, neurons, utility function, activation function, and optimisation algorithm are collectively referred to as hyper-parameters and determine the performance of the network [122, 131, 133].

Unsupervised Learning (UL)

UL algorithms work with a set of inputs. The input dataset for training does not have a labeled output. For this reason, in UL, clustering, association, and pattern discovery are performed over existing data. It has a working mechanism that is

different from SL. The purpose of UL is to enable the identification of patterns within the training datasets and categorize the input objects according to the patterns defined by the system [135]. These algorithms are expected to develop specific outputs from unstructured inputs by looking for unexplored relationships between each instance or input object. UL algorithms can be classified into three main groups: clustering, association analysis, and dimensionality reduction. k-means, k-median, hierarchical clustering, and expectation maximisation are the most common examples of clustering category [136, 137]. Apriori, Eclat and FP-Growth are examples of association analysis models [138], while principal component analysis (PCA) and linear discriminant analysis (LDA) are examples of dimensionality reduction category [139].

The k-means algorithm is one of the most popular algorithms that is used for clustering or partition dataset in the literature and is employed in the thesis for clustering the traffic load of BSs. Therefore, the k-means algorithm is briefly discussed in the following paragraph.

k-means: It is one of the most commonly used clustering algorithms because it is simple to apply and guarantees convergence in such a way that all the input samples fall into a specific cluster [140]. k-means is used in segmenting unlabelled dataset into k clusters, where the number of clusters, k, also coincides with the number of cluster centroids. k-means follows an iterative process when assigning data points into different clusters [141]. Normally, a centroid is defined for each cluster and the data points that are nearest to each cluster are associated with it. Then, the centroids positions are updated by averaging the values of the data points associated with them. By way of illustration, given a set of M_{dt} data points in a dataset, $\sigma_i = \{\sigma_1, \sigma_2, \ldots, \sigma_{M_{\mathrm{dt}}}\}$, where σ_i represents the whole dataset and $\sigma_1, \sigma_2, \ldots$ represents the individual data points in the dataset. The process of applying k-means algorithm to partition the dataset into clusters and determine the number of data points, $M_{\mathrm{dt},j}$ in each cluster, γ_j, where γ_j denotes the centroid of cluster j and $j \in \{1, 2, \ldots, k\}$ can be determined using the pseudo-code in Algorithm 3 [132, 140]. The error in k-means clustering is evaluated by computing the Euclidean distance between the data points and their associated centroids according to [141]:

$$D_{k-means}(\gamma_j) = \sum_{\sigma_i \in \gamma_j} \|\sigma_i - \Lambda\|^2, \tag{2.8}$$

where the mean of cluster j is denoted by Λ.

One of the most critical aspects of clustering is determining the optimal num-

Algorithm 3: k-means Algorithm

Data: k, data points $\{\sigma_1, \sigma_2, \ldots, \sigma_{M_{\mathrm{dt}}}\}$
Result: Number of clusters

Initialize by randomly selecting the centroids $(\gamma_1, \gamma_2, ..., \gamma_k)$;
while *cluster assignments change* **do**
  for *each data point* (σ_i) **do**
    find the closest centroid, γ_j using:

$$\arg\min_j D(\sigma_i, \gamma_j) \tag{2.9}$$

  end
  for *each cluster* $(j \in \{1, 2, \ldots, k\})$ **do**
    let centroid γ_j be the mean of data points associated with γ_j

$$\gamma_j = \frac{1}{M_{\mathrm{dt},j}} \sum_l \sigma_l \quad | \quad \{l = i \iff \sigma_i \in \gamma_j\} \tag{2.10}$$

    Go back to step 3
  end
end

ber of clusters to split the dataset to. One of the popular methods for finding the optimal number of clusters from a given dataset is the elbow method [142]. In the elbow method, the optimal number of clusters is obtained by evaluating the sum of the squares errors (SSE) between the data points in each cluster and the centroid. The SSE values obtained are plotted against the k values. Then the point of inflection of the curve is selected as the optimal number of clusters.

Reinforcement Learning (RL)

Although it is not completely different from SL and UL methods, RL imitates human's learning process. It shows how a system can perceive its environment and learn to make the right decisions in order to reach its goal. It differs from both SL and UL in that the agent is not given any prior knowledge of the environment, such as input data and output data, but gathers information about the environment by interacting with the environment and learning to take the right action in any given situation (for example, by repeated trial and error over a period). This method is frequently used in fields such as robotics, game programming, disease diagnosis, and factory automation [143, 144]. There are a few concepts associated with RL such as environment, agent, state, action and reward function, policy, value function, and model, which are briefly discussed in the following paragraphs [132, 145, 146].

- **Environment:** The environment is anything within the agents surrounding that can be observed. For example, in a cellular communication networks, the environment constitutes the BSs, UEs, traffic load, channel condition, etc.

- **Agent:** This is the main actor in the environment that takes actions. Considering a cellular network, the agent could be the MBS that tries to optimise the switching off/on pattern of the SBS to minimise its energy consumption.

- **Action:** An action is normally selected and performed by the agent out of a set of possible actions within the environment to maximise the reward function. In a cellular network where it is assumed that the agent is the BS, the action set could be all the possible combinations of BSs to switch off in order minimise the energy consumption of the network. Hence, different combinations of BSs are selected and the result reward function is evaluated.

- **State:** This describes the agents condition with respect to the action taken. Still using the example of minimizing the energy consumption of network, the state of the agent could be either sufficient or insufficient offloading capacity, depending on the action taken.

- **Reward function:** This is the function that needs to be maximised by the agents actions. From the point of view of optimisation, this is known as the objective function. Depending on the kind of problem, the reward function could also be converted to penalty function. In such instances, the objective is to minimise instead of maximizing the reward function such as in the case of energy minimisation.

- **Policy:** The policy determines the behaviour of the agent or how the agent would act within an environment, i.e., it maps the agents states to the required actions [130, 146]

- **Value function:** Two kinds of values functions exists: the state value function which evaluates the expected value when a state is visited while the action value function evaluates the expected value of the action taken by the agent in a given state.

- **Model:** It is used to depict the environment as well as study the effects of agent's actions on the environment. It must be noted that not all RL algorithms require the model of the environment, some have model-free execution mechanism.

The basic structure of an RL model is illustrated in Fig. 2.6 [146].

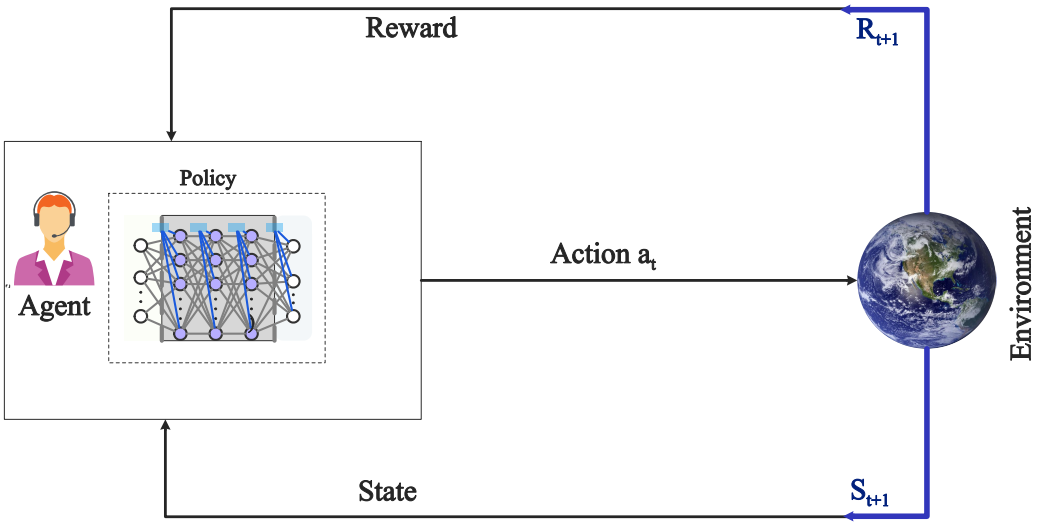

Figure 2.6: Basic structure of RL

Common examples of RL algorithms include: Q-learning, state-action-reward-state-action (SARSA), multi-armed bandit, actor-critic, etc [147]. However, Q-learning is the RL algorithm that is applied in this thesis because it is model-free and exhibits quick convergence compared to other RL algorithms [148]. Hence, it is briefly discussed in the following paragraph.

Q-learning: Q-learning is one of the most popular RL algorithms, and has a proven capability of working in dynamic environments [146, 149]. It is a model-free RL algorithm, which means that the model of the environment is not required before hand. Rather, it learns by a trial and error method through repeated interaction with the environment to gain experience needed to improve performance. In addition, it is an off-policy algorithm, which means that the policy employed during the model training process is different from that used in updating the action value function. This property enables quick convergence to be achieved in Q-learning [148]. The pseudo-code of Q-learning algorithm is presented in Algorithm 4 [146].

The action value table is updated using the Q-learning equation:

$$Q(s_t, a_t) := Q(s_t, a_t) + \zeta\Big[R_{t+1} + \varepsilon \underset{a}{max}(Q(s_{t+1}, a)) - Q(s_t, a_t)\Big], \tag{2.11}$$

where $Q(s_t, a_t)$ is the state-action value function, s_t and s_{t+1} are the current and next states, respectively. R_{t+1} is the expected reward for the next step and a_t is the taken action, where a is the set of all possible actions. ζ is a learning rate and ε is a discount factor. Note that the max function in (2.11) should be

Algorithm 4: Q-Learning pseudo-code

```
Input  : Input
Output: Output
Initialize Q(s_t, a_t) := 0;
for every episode do
    for each iteration do
        Estimate the current state s_t;
        Take an action a_t;
        Evaluate reward R_{t+1};
        Update Q(s_t, a_t) using (2.11);
        move to the next state s_{t+1}.
    end
end
```

converted to *min* function to make the update policy suitable for a penalty-based framework.

2.4 Energy Optimisation in Fixed Cellular Networks

In this section, various methods of energy saving in fixed cellular networks are briefly presented. Afterwards, the cell switching approach is discussed with the state-of-the-art and research gap analysis.

2.4.1 Energy Saving Techniques

Four major techniques have been proposed for energy saving in fixed or terrestrial BSs including hardware design, planning and deployment strategies, and energy harvesting techniques, network operation and managements [14]. Hence, in this section, each of these techniques is briefly discussed, then the cell switching approach is considered in more details involving a brief review of the state-of-the-art, and research gap analysis.

- **Hardware Design:** Energy saving based on hardware solutions includes energy efficient designing of RF chain, and transmitter and receiver [150, 151]. More emphasis is placed on the redesign of the PA since it is the most energy consuming part of the BS [152], thus a PA with high efficiency would greatly enhance the EE of the network [153, 154].

- **Energy Harvesting:** Energy harvesting for powering cellular networks involves harnessing energy from the environment sources, such as solar,

wind, etc. [155], and radio waves, that is, energy gotten from radio signals transmitted in the air [156]. However, the use of renewable energy source to power cellular network faces the challenge of the erratic or uncertainty in the availability of these energy sources at every time of the day. Hence, these energy sources have to use energy storage components such as batteries or capacitors as a back up during periods they are not available [14].

- **Network Planning and Deployment:** This energy saving technique involves planning the BS deployment in order to ensure that optimal number of BSs, types of BSs, and type of antennas needed to provide the required QoS are deployed. In this regard, two energy efficient network deployments approaches have been proposed including heterogeneous BSs, which involves the deployment of different types of BSs, and massive multiple-input-multiple-output (mMIMO), which involves the use of a large number of antenna arrays in a BS.

- **Network Operation and Management:** These methods rely on the spatio-temporal variation in the network traffic load to adjust certain network parameters such as transmit power, bandwidth, etc., or switch of certain network components such as antennas, sectors, or the whole BS, in order to save energy. In this regard, antenna muting [157], cell zooming [158], adaptive sectorization [159], and cell switching techniques [17, 22, 160] have been proposed.

Energy Saving Enablers

Several technologies and techniques have been designed to enhance the energy saving potentials in cellular networks. For fixed cellular network, these energy saving enablers include: cloud radio access network (C-RAN) [18, 161], control data separated architecture (CDSA) [162–164], caching [165–167], re-configurable intelligent surfaces (RIS) [168–171] , device-to-device (D2D) communications [172–175], and traffic offloading [176–180].

CDSA offers some inherent energy saving potentials because it enables underutilised SBSs to be easily switched off to save energy while their traffic load is taken over by the MBS, thereby preventing coverage holes in the network [162, 163]. Hence, it is adopted as the HetNet architecture in this thesis and detailed in the following paragraphs, followed by a discussion on cell switching, which is a major approach that is applied for energy optimisation in this thesis.

Control Data Separated Architecture (CDSA)

Energy saving technique based on cell switching in conventional cellular architecture was challenging because it results in coverage holes because the area that was originally covered by the switched off BS cannot be fully covered by neighbouring BSs thereby leading to QoS degradation. In addition, it is not possible to completely turn off the BS because certain parts of the BS must be on to quickly respond to changes in network traffic thereby limiting the amount of energy saving that can be achieved. This led to the introduction of CDSA [162].

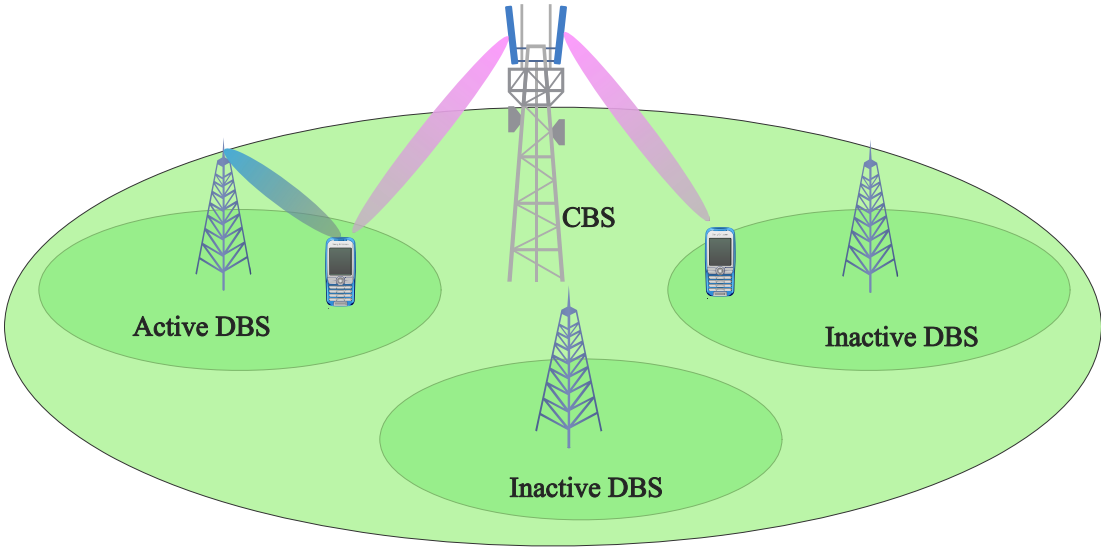

Figure 2.7: CDSA showing CBS as well as active DBS serving user requests while inactive DBSs are switched off to save energy.

In CDSA, the control plane is separated from the data plane. The function of the control plane is for the provision of ubiquitous coverage, signalling between users and network which is needed for data transmission to take place such as radio resource control (RRC) connection establishment, scheduling information, etc. This enables the provision of wide coverage at a low frequency to ensure flexibility in connection and mobility. The data plane is responsible for high capacity and data rate, and exploits high frequency. In addition, in this architecture, all the users are connected to the control BS (CBS) which in most cases is the MBS while active users are simultaneously connected to both CBS and the data BS (DBS). Hence, the DBS can be turned off when it is not connected to any user. When the users become ready to start data transmission, the CBS then chooses the best DBS and establishes connection between the DBS and the users. Since the control plane provides continuous coverage with the help of a few

CBSs while the data plane provides data plane through the DBS, the DBSs can be adapted to the traffic load of the network without affecting the basic coverage provided by the CBSs [162–164]. Fig. 2.7 illustrates the CDSA with an active DBS and a CBS serving user requests while inactive DBSs are switched off to save energy.

2.4.2 Cell Switching

This can also be referred to as BS sleeping or BS off/on approach. This energy saving approach takes advantage of the spatio-temporal variations in the traffic load of the network to dynamically switch off under-utilised BSs when they are not serving any user or serving very few user requests [22,160,181]. It is normally accompanied with traffic offloading which is the process where the traffic demand of users originally provided by the BSs that are to be turned off are transferred to the neighbouring BSs in the same or higher tier in order to maintain the QoS of the users that were originally associated with the sleeping BSs [177]. The cell switching implementation enables the BSs to be operated in an on-demand manner rather than always on which enables the energy consumption of the BSs to scale with the traffic load, thus enhancing its EE and preventing energy wastage during periods of inactivity or very low usage [182]. The cell switching approach is a very effective approach as it results in significant reduction in energy consumption compared to other approaches such as antenna muting, sectorization, and cell zooming. In addition, it requires minimal changes to the network configuration and it is also cost effective to implement [14,183].

2.4.3 State-of-the-art on Cell Switching

Dynamic cell switching techniques are the most commonly employed methods for optimising energy consumption in cellular networks because they are the cheapest to implement and require minimal changes to the network architecture [14, 22, 183]. There are various approaches in the literature for the implementation of cell switching in UDHN in order to minimise its energy optimisation. Here, a brief review of the state-of-the-art for energy optimisation in cellular networks is presented.

The authors in [184] proposed a load-aware SBS switching off/on mechanism the power consumption in UDNs. The proposed approach considered the following:

- the effect of the neighbouring SBSs load on the switching process,

- the switching energy cost involved in changing the user connection from sleeping to active SBSs.

To solve these problems, two heuristic algorithms were proposed. First, a centralized user association algorithm was developed to minimise the switching energy cost by ensuring that more users are connected to SBSs that have lower likelihood of being turned off. Then, a heuristic SBS switching algorithm that considers the effect of the neighbouring cell load was developed to determine the optimal SBSs switching strategy that would minimise the total power consumption of the network. The results obtained showed that the proposed approach leads to more energy savings compared to other heuristic approaches that do not consider the above two factors.

A neural network approach to cell switching was proposed in [185] to determine the optimal cell switching strategy that would result in minimal energy consumption in a HetNet. To achieve this objective, two factors were considered: i) how to determine the specific periods when the SBSs is to be turned off; and ii) the optimal combinations of SBSs that need to be turned off during these periods. Hence, two solution procedures were developed using two neural network architectures; i) dense neural network (DNN); and ii) recurrent neural networks (RNN). The first consists of a two-step solution where the DNN is used to predict the short-term traffic loads of the SBSs to determine when some SBSs can be turned off, after which the optimal switching pattern is analytically derived. The second solution employs RNN and performs both traffic predictions and determination of the optimal switching strategy at the same time. Numerical results reveal excellent performance in terms of energy savings and QoS.

The work in [186] investigated the problem of energy-delay trade-off in 5G HetNets with multilevel BS sleeping. They considered a scenario where there is a constraint on the maximum sleeping duration of the BSs due to periodic transmission of synchronization signals (SS). As a result, different levels of sleep mode were considered while satisfying the QoS constraints. In addition, the effect of co-channel interference was taken into consideration during the BSs sleep mode operation. A distributed Q-learning algorithm was developed to adapt the sleep mode level to the level of activity in the BSs. Performance evaluation reveals that more energy saving can be obtained when delay-tolerant users are considered.

A more comprehensive review of the state-of-the-art on cell switching is found in Section 3.2.

2.4.4 Research Gap Analysis

The major challenge with cell switching is that it involves a combinatorial problem which requires the selection of the optimal set of BSs to switch off out of a possible combination of BSs; it is NP hard, that is, it is difficult to solve, it takes a reasonable amount of time to solve, and cannot easily be solved using standard methods. In addition, the complexity of this problem increases exponentially with the number of BSs deployed in the network [22]. Even though various state-of-art cell switching techniques have been proposed in literature including conventional and ML approaches, however, most of these approaches have their own challenges and limitations.

Conventional approaches such as heuristic algorithms have the advantage of providing a sub-optimal cell switching solution with less computational overhead. However, the challenge with heuristic algorithms is that they are hard-coded, have poor generalization ability and as such are not able adapt to the dynamically changing network environment envisioned in 5G and beyond UDNs. Moreover, since the network conditions change dynamically, there is a need for repeated application of the solution each time there is a change in the condition of the network, thereby resulting in huge time and computational overhead. Most times, before these computations are completed and the decision implemented, the network condition would have changed, thereby leading to sub-optimal results which would negatively affect the QoS of the network [123, 124]. Hence, they are not suitable for energy optimisation in 5G UDHNs as they could result in poor network performance.

ML approaches have the advantage of being able to learn hidden user behaviours or network characteristics from historical data that cannot be analytically modelled. Unlike heuristic algorithms, they are able to adapt to changing network conditions in order to optimise the performance of the network [123–125]. However, they also have their own challenges. For example, RL-based cell switching approaches, such as Q-learning, usually use tables (Q-tables) to store the learnt state-action values (Q-values). Hence, there is a Q-table entry for every action taken by the agent in the network environment. This approach is only feasible when the network dimension is small or medium. However, when the network dimension becomes very large, as obtained in 5G UDNs, it would become computationally burdensome to learn the Q-table, as the number of states or actions would greatly increase. In addition, a large memory would also be required to store the learnt Q values. As a result, it is not feasible to use Q-learning for cell switching operation in UDNs [146]. Moreover, the training process of cell switching methods that employ ANN and DRL algorithms involve a very large

computation overhead, which makes them unsuitable for real-time network operation.

Considering the various challenges of the diverse set of methods proposed in literature as well as the increase in size and complexity of next generation cellular networks, there is a need for more research work to be carried out in order to develop scalable and computationally efficient cell switching algorithms that are suitable for 5G and beyond UDN. Therefore, in Chapter 3 of this thesis, a contribution to this research direction is made by developing a hybrid algorithm for energy optimisation.

2.5 Revenue Maximisation in Cellular Networks

In this section, an approach for generating additional revenue for MNOs by exploiting the vacant spectrum that is made available from the cell switching process and leasing it to other network operator for IoT applications, smart grid, etc. is discussed. The state-of-the art on cell switching and spectrum leasing alongside research gap analysis are also presented.

2.5.1 Limitations of Cell Switching

Although cell switching is a very effective method for minimizing the energy consumption of cellular networks, it also results in spectrum under-utilisation as the spectrum that was originally occupied by the BSs that are turned off remains dormant during periods of their inactivity. This dormant spectrum can be exploited to serve other applications through spectrum leasing and by doing so the spectrum can be properly utilised while generating additional revenue to the MNOs [187].

2.5.2 Spectrum Leasing

Spectrum leasing is the process where spectrum licensed holders and users (also known as primary network (PNs) or primary users (PUs)) lease their spectrum to unlicensed networks or users (also known as secondary networks (SNs) or secondary users (SUs)) for certain benefits which could be: i) for monetary gains; 2) for enhanced throughput; and 3) to minimise the power consumption of the PUs [29]. The first case is of interest in this thesis. By spectrum leasing, the dormant spectrum from cell switching operation can be exploited by SN operators who require a smaller amount of spectrum for their data transmission and

cannot afford to purchase a spectrum license like the PN operators. This is because spectrum is normally auctioned by the telecommunication regulatory body in each country (e.g., Office of Communications (Ofcom) in the UK) at a very expensive rate. Hence, spectrum leasing results in enhanced spectrum utilisation and additional revenue to the PN operators, since it has been observed that the licensed spectrum is not always fully utilised most of the time [188]. The spectrum purchased by the SN from the PN can be used to provide data services which are delay tolerant (DT) such as meter readings, health information from wearables, etc., and do not require real-time data transmission. It can also be used to provide non-delay tolerant (NDT) services such as location and traffic update services, voice calls, etc., which require real-time data transmission for quick decision making. Therefore, the PN operator can gain revenue both from energy cost savings due to dynamic cell switching and from leasing the dormant spectrum of the BSs that are turned off to the SN.

2.5.3 State-of-the-art on Cell Switching and Spectrum Leasing

Various approaches to spectrum leasing have been proposed in the literature [189]. A few of these techniques are briefly discussed in the following paragraphs. The authors in [190] considered the problem of the spectrum leasing and spectrum allocation to obtain the best leasing price and PU-SU pair while improving the spectral efficiency of both users. To achieve this objective, the problem was broken down into three parts:

- How to pair the PUs with the SUs?
- How to determine the best spectrum leasing price?
- How to properly allocate the spectrum to the SUs?

The pairing problem was modelled as a marriage between PUs and SUs and solved using matching theory while Stackelberg game was applied to find the best spectrum leasing price as well as the spectrum allocation policy. The results obtained reveal that the best spectrum leasing price, spectrum allocation strategy and paring between PUs and SUs was achieved, while enhancing the spectral efficiency of the network.

The work in [191] investigated the possibility of leasing certain parts of TV white spaces know as high priority channel (HPC) to small cognitive radio wireless network operator for IoT applications. Their goal was to reduce the HPC leasing

cost while satisfying varying QoS requirements of IoT applications. The following steps were considered: i) queuing data packets of delay tolerant IoT applications until when there is free TV white space; ii) compressing the size of data packets thereby transmitting data with reduced quality; and iii) how to determine the minimum spectrum leasing cost for NDT IoT applications. To solve this problem, an ANN-based online solution was proposed to determine the optimal HPC cost while respecting QoS constraint which closely approximates the offline solution proposed in [192].

Regarding cell switching and spectrum leasing, the authors in [193] considered a cognitive cellular network architecture comprising both PNs and SNs. On one hand, the PN wants to reduce its energy consumption by turning off some BSs while ensuring that its QoS is maintained by offloading affected users to the SN and paying a roaming fee. On the other hand, the SN on its part, wants to maximise its throughput by leasing the spectrum of the PN for a price. Their objective was to ensure the collaboration of both networks while optimising the utilities function of both networks. The utility for the PN is its outage probability and profit while that of the SN is maximizing its user sum-rate and profit. A heuristic algorithm was developed to determine the optimal set of BSs to switch off, as well as the optimal resource allocated to the SN while respecting the constraints of both networks. The work in [194] is similar to that in [193] except that in addition to energy saving, reduction of CO_2 emission was also considered.

2.5.4 Research Gap Analysis

Although there are many works in literature on spectrum leasing, very few consider the combination of cell switching and spectrum leasing [193, 194]. The few that consider cell switching and spectrum leasing fail to consider certain network deployment scenarios and pricing policies which makes their work simplistic and not suitable for next generation cellular networks. Specifically, a homogeneous network deployment was considered whereas next generation networks are mainly HetNets and UDNs. By considering HetNets deployment scenario, the PN can avoid roaming charges by offloading the traffic of switched off SBSs to the MBS rather than the SN BSs as considered in previous works. As such, the PN does not need to depend on the SN for energy saving during the cell switching process as this would lead to additional charges, which would limit the amount of revenue that can be generated from spectrum leasing. Also, a more realistic pricing policy that considers the effects on spectrum and electricity demand on the spectrum and electricity prices needs to be considered in the pricing policy as it is a better representation of what is obtainable in real systems.

All these factors necessitate the extension of existing works using more realistic network deployment scenarios, and pricing models that are more realistic, and relevant to next generation networks. The consideration of these factors also introduces new complexities to the cell switching and spectrum leasing problem. Moreover, by considering a HetNet with vertical traffic offloading to the MBS instead of a homogeneous networks with horizontal traffic offloading to the SN BS as in [193,194], the decision of which set of SBSs to switch off and lease their spectrum to the SN becomes more complex. This is because, in CDSA, only one MBS provides umbrella coverage for a group of SBSs, and they must offload their traffic to it before they can be turned off. However, in the homogeneous network with horizontal traffic offloading that was considered in previous works, the BSs individually decides the SN to offload their traffic load and lease or share their spectrum with before going into sleep mode. Hence, the decision regarding which set of SBSs to switch off before leasing their spectrum to the SN is more challenging in the HetNet with CDSA scenario compared to that considered considered in previous work. Therefore, a new solutions needs to be developed to address this challenge, and the new solution is presented in Chapter 4 of this thesis.

2.6 Energy Optimisation in UAV-based Cellular Networks

In this section, various methods of energy saving in UAV-based cellular networks are briefly highlighted. Then, the UAV positioning approach alongside the state-of-the-art and research gap analysis are discussed.

2.6.1 Energy Saving Techniques

Similar to fixed cellular networks, four major techniques for energy saving in UAV-based cellular networks also exist [24, 25]. Thus, in this section, each of these techniques are highlighted, then energy efficient UAV positioning including the state-of-the-art and research gap analysis are discussed since it is one of the methods considered in this thesis.

- **Hardware Design:** Energy saving based on hardware solutions involves energy efficient design of UAV motors [26, 74, 77] and more efficient design of the body of the UAV to enable it to easily overcome air resistance [195].

- **Energy Harvesting:** Even though energy harvesting does not directly translate to energy savings in UAVs, it would enable the UAVs to operate for a longer period of time when combined with other energy sources such as battery. For example, solar PVs can be mounted on the UAVs to enable them to harvest the energy needed to sustain their flight from the sun during periods of high solar radiation, and then switch to battery during periods of no sunlight because of the fluctuations in renewable energy sources [90]. Moreover, these type of energy sources are environmentally friendly as they do produce greenhouse gas emissions.

- **Network Operation and Management:** One of the ways of minimizing energy consumption via network operation is through transmission scheduling [196, 197]. Another approach is through power allocation and control where the the total transmit power of the UAV-BS is minimised while ensuring the QoS of users are maintained [198].

- **Network Planning and Deployment:** This involves planning the paths or designing the trajectories that the UAVs would fly in order to minimise energy consumption while serving ground user requests within a given region [48, 75, 76]. It also involves finding the optimal position that the UAVs need to hover, for the case where the UAV is to be stationed in a particular location, to serve ground users with minimal energy consumption [199, 200].

Energy Saving Enablers

For UAV-based cellular networks, the energy saving enabling technologies include: RIS [201–206], mobile edge computing (MEC) [207–210], network slicing/network function virtualization [211–213], cooperative communications [214–217], and energy harvesting technologies [216, 218–220].

Since energy efficient UAV positioning is one of the methods considered in this thesis, it is discussed in more details in the following paragraphs.

2.6.2 UAV Positioning

This involves the determination of the optimal position and altitude that the UAV-BSs need to be placed for the case where the UAV-BSs is deployed in a stationary position in order to serve ground users with the minimal energy consumption. For the case where the UAV-BS has to fly but stop at certain points along it routes to provide coverage, optimal positioning entails finding the optimal hovering locations along the UAV-BS path that would result in minimum

energy consumption. In this regards, a few works have considered different UAV placement techniques by varying the altitude, coverage radius, tilt angle, etc., of the UAV-BSs for enhanced EE [199, 200, 221].

2.6.3 State-of-the-art on Energy Efficient UAV Positioning

There are many works in the literature related to energy optimisation in the UAV-based cellular networks [24, 222]. As regarding UAV positioning for minimizing energy consumption in UAV-based cellular networks, a brief review of the state-of-the-art is presented in the following paragraphs with the goal of highlighting the various categories of existing works.

The authors in [221] proposed an energy-efficient 3D positioning strategy for UAV-BSs to minimise the UAV-BS's energy consumption. The following factors were considered:

- both communication energy (energy required for data processing and transmission) and propulsion energy (energy required for hovering the UAV-BS).
- directional antennas whose tilt angle can be adjusted.

The gradient descent algorithm was applied to determine the tilt angle and minimum altitude that would optimise the total energy consumption of the network while improving the coverage and the throughput. The results obtained revealed that a significant amount of energy savings can be obtained compared to other methods that did not consider antenna tilting.

The work in [223] considered the problem of determining the optimal UAV-BS hovering locations along the UAV-BS flight path that would maximise the EE such that the UAV battery life can be extended while enhancing network throughput. To achieve this objective, the UAV was made to fly through a defined path with designated hovering points. At each designated hovering point, the distance between each UAV-BS and ground user was obtained in order to calculate the SNRs, which were then applied to determine the power allocation for each ground user and the UAV-BS. Then, the power allocation and UAV-BS locations are used to derive the maximum EE metric. The above procedure is applied to all designated hovering points and the hovering point that gives the maximum EE value is selected as the optimal. The performance evaluation of the proposed method reveals that a considerable enhancement in EE is achieved with a reduction in the throughput.

Recently, an alternative deployment approach where the UAV can be made to land in some designated locations, known as landing stations (LSs), such as surrounding tall buildings, lamp stands or specially designed platform has been proposed in [224], wherein the authors utilised the LSs to maximise the service time of a UAV-BS and sum-rate of the network. The authors in [225] performed a capacity comparison between hovering and landed mm-wave UAV-BSs in order to enable the selection of the preferred deployment option.

A more detailed review of the state-of-the-art on energy efficient UAV positioning can be found in section 5.2 while a comprehensive review of the energy optimisation techniques in UAV-based cellular networks from conventional to ML approaches along with energy saving enablers and open research challenges has been provided in [226], as part of the research outputs of this thesis.

2.6.4 Research Gap Analysis

Although the use of UAVs for wireless communications has attracted much research attention, most applications of UAVs for wireless communication provisioning are not feasible as researchers fail to consider some vital aspects of their deployment, especially the energy requirements of both the UAV and communication system. This is because the huge energy consumption overhead involved in flying or hovering UAVs makes them less appealing for green wireless communications [24]. Moreover, the various approaches proposed to reduce the energy consumption of the UAV including optimal placement, trajectory optimisation, transmission scheduling and resource allocation do not result in significant energy reduction, as most of these works consider the UAV to be flying or hovering while serving user demands.

Even though the LS concept was introduced in [224], certain aspects of its deployments have not been considered yet. For example, an in-depth analysis of the suitable locations within the network where these LSs can be located as well as its impact on the various network performances metrics such as energy consumption, coverage probability, and throughput is yet to be investigated in the literature. The LS has a huge energy saving potential because it eliminates the energy consumption due to constant hovering or flying the UAV-BS over the service area. Hence, in Chapter 5 of this thesis, an in-depth evaluation of the LS concept with respect to energy consumption, coverage probability and throughput is carried in order to ascertain its viability for green wireless communications.

2.7 Summary

In this chapter, various types of BS deployment within the RAN including homogeneous, heterogeneous, ultra-dense, and UAV-based networks were first discussed because of the major contribution of BSs to the energy consumption cellular networks. Then, the power consumption components of fixed and UAV-BS as well as the power models for quantifying the power consumption of both types of BSs were presented. Afterwards, three main categories of energy optimisation algorithms including analytical, conventional approaches and ML approaches were briefly discussed. Finally, energy optimisation in both fixed and UAV-based cellular networks, and revenue Maximisation in cellular networks were discussed including a review of the state-of-the-art on cell switching, cell switching and spectrum leasing and energy efficient UAV positioning approaches alongside research gap analysis.

Chapter 3

Cell Switching in UDHNs

3.1 Introduction

The proliferation of mobile phones, increasing use-cases of IoT devices, and the development of advanced mobile applications which are demanding in terms of bandwidth and latency, have led to increase in the demand for mobile services. This has made MNOs to continually increase their capacity through the deployment of more BSs, thereby resulting in increased energy consumption [227]. In addition, the introduction of network densification to cater for the expected 1000 times increase in capacity of 5G network compared to legacy networks would further heighten the energy consumption of the network [183, 228, 229]. From an economic and environmental perspective, the aforementioned surge in capacity of 5G and beyond networks must not be done at the expense of huge energy consumption overhead. This is because increased energy consumption would result in more operational expenditure in the form of increased electricity bills as well as environmental degradation due to increased CO_2 emission, as the energy used to power the BSs is mainly obtained from fossil fuels [14, 230]. Even though cell switching has been identified as a major approach to energy savings in UDN, the development of suitable optimisation frameworks that has been quite challenging. This is because the scale and complexity of the next generation networks requires that scalable and computationally efficient solution to be developed.

The pursuit of the development of a scalable and computationally efficient cell switching solution began with the use of RL algorithm, which is very effective in making decisions out of a wide range of options and have been successfully applied in other fields, such as robotics, games, etc [231, 232]. This is because they can adapt to changing environments through learning and then decide the action that would yield the best desired performance. In this regard, the few related works that have employed RL for cell switching in HetNets were first

considered. The authors in [177, 233] had proposed the use of Q-learning for cell switching and traffic offloading in HetNets. It was observed that these works did not consider CDSA but rather adopted the conventional architecture. In addition, they only considered horizontal traffic offloading; which is the case where the SBS transfers its traffic to neighboring SBSs before switching off. Furthermore, they did not consider the increase in the transmission power of the SBSs due to traffic offloading when estimating the power consumption of the network. The challenge with horizontal traffic offloading[1] is that the neighbouring BSs may not be close enough or have sufficient capacity to accommodate the traffic of the BSs that are switched off, thereby resulting in QoS degradation. Also, since the neighbouring BSs have to increase their transmit power to accommodate the traffic of switched off BSs, this leads to increased energy consumption in the network.

Hence, improving on their work, an RL-based cell switching scheme using Q-learning is proposed that employs vertical traffic offloading, which is the case where the traffic load of the BSs to be turned off are transferred to the MBS, a higher tier BS, in a HetNet with CDSA during periods of low traffic load before turning them off in order to maintain QoS of the network. In addition, the increase in energy consumption of the MBS due to offloaded traffic as well as the amount of radio resources in the MBS is considered in order to develop an efficient switching mechanism. This is to ensure that the MBS can accommodate all the traffic load of the SBSs that are to be turned off before switching them off. However, Q-learning use tables to store the learnt state-action values which becomes extremely difficult to learn and requires a very large memory to store the learnt table when the state or action becomes very large [146]. Hence, it is only suitable for small to medium sizes networks but is not feasible for UDNs with massive number of SBSs.

Afterwards, an ANN-based cell switching framework was developed. ANN are known as universal approximators because they are able to find the relationships between complex non-linear functions and are also known for their excellent generalization ability [234], hence they have found numerous applications in the field of wireless communications [123]. In addition, ANN models can be trained offline and then plugged into the network in order to enhance real-time decision making

[1]By adopting HetNet with CDSA and vertical traffic offloading in this work rather the conventional HetNet and horizontal traffic offloading, the decision of which set of SBSs to switch off is more challenging. This is because in vertical traffic offloading, the MBS has to decide which combination of SBSs, out of all the possible combination of SBSs, to switch off in order to save energy while considering its ability to accommodate the traffic of the switched off SBSs. However, for horizontal traffic offloading, considered in previous works, each SBS can decide which neighbouring SBS to offload its traffic load to, which makes the cell switching decision easier to arrive at.

by reducing the network delays [123]. A few research works have been carried out regarding the application of ANN for cell switching purposes [185, 235, 236]. However, these previous works only consider simplistic network scenarios where very few SBSs are deployed, hence, such solutions may not be suitable when network dimension becomes very large and complexity increases. In addition, only one type of SBS was considered in the aforementioned works which is not the case in a real network where different types of SBS (RRH, micro, pico, and femto cell) are deployed, thus making their considered scenarios unrealistic.

Therefore, ANN is exploited to determine the optimal cell switching strategy in a UDN. Specifically, an ANN-based cell switching framework is developed, which is referred to as offline-trained online cell switching (OTOcell), to learn the optimal switching strategy for the SBSs in a UDN. The developed model is computationally efficient since the training is done offline, after which the trained model is implemented in the network for real-time decision making. This is particularly important for UDNs, where the MBSs are already over-burdened with signalling and computational operations, in which case, adding a cell switching algorithm on top of these would make their workload more severe. Various types and numbers of SBSs are considered to validate the robustness and scalability of the proposed solution. However, the proposed ANN-based cell switching framework depends on a heuristic algorithm to determine the optimal switching pattern which it utilises as dataset to train the ANN model. Hence, any error in the training dataset would propagate through the ANN model, thereby resulting in a more sub-optimal result. Although the model can be trained online before applying for real-time cell switching, as the network size increases, the model training becomes increasingly difficult and would require more time and computation resources. Since the model has to be updated frequently for enhanced cell switching, the ANN-based cell switching would not be suitable for cell switching in large scale networks such as UDNs. Therefore, there is a need for a scalable and computationally efficient solution to be developed, that can be applied to both small and large scale networks.

As far as optimal cell switching solutions are concerned, the ES, also known as the brute-force algorithm always guarantees to find the optimal result because it sequentially searches all the possible combination of SBSs and selects the best combination to switch off [237]. However, the computational complexity of the algorithm increases exponentially as the numbers of SBSs increases, although it is computationally efficient and generates the optimal results very fast when the number of SBSs are few. An alternative approach could be obtained by compromising slightly on the optimality of ES while achieving a solution that is

both scalable and of reduced complexity by first clustering the SBSs into smaller groups to reduce the search space by clustering using k-means algorithm, and then applying ES to each cluster separately in order to determine the set of SBSs to switch off per time.

Finally, a cell switching framework known as Threshold-based Hybrid cEll swItching Scheme (THESIS) that combines unsupervised ML scheme and ES algorithm for energy optimisation in UDHN is proposed. The proposed method combines the advantages of unsupervised learning in terms of scalability and low complexity and ES algorithm in terms of optimality, to produce a cell switching strategy that is more computationally efficient but sub-optimal to the ES solution. In other words, the proposed approach tries to find a good trade-off between the performance and computational complexity, such that the computational complexity is significantly reduced without compromising much on the performance. In addition, the proposed framework can be applied even when the number of SBSs deployed in the network becomes very large, making it scalable and eliminating the limit of network size while applying the algorithm. This makes THESIS more applicable and feasible for the next generations of cellular communication networks, where the number of BSs are expected to be a lot higher than the legacy networks through the concept of network densification.

3.2 Related Works

There are various approaches in the literature for the implementation of cell switching in UDHN to minimise its energy optimisation. They can broadly be classified into analytical, heuristic and ML approaches.

As regards analytical approaches for cell switching, the authors in [238] proposed an analytical model to determine the number of SBSs that can be switched off with vertical traffic offloading was proposed using two sleeping schemes (random and repulsive scheme). In the random scheme, the SBSs have equal probability of being turned off while in the repulsive scheme, only the SBSs closest to the MBS are turned off. The authors in [239] proposed a SBS switching scheme to minimise the energy consumption in a HetNet based on stochastic geometry.

For heuristic methods, the work in [240] considered the joint optimisation of the area spectral efficiency (ASE) and EE of a two-tier UDHN. A firefly algorithm was developed to determine the optimal system parameters that would jointly optimise the ASE and EE of the network. The authors in [241] proposed an energy efficient traffic offloading framework for a HetNet based on queuing theory. A heuristic based traffic offloading algorithm was developed to maximise the EE

of the network while ensuring that the stability of the queues is maintained. Three heuristic algorithms were proposed in [242] for the Maximisation of the EE of a dense HetNet without compromising the QoS of users. In [243] the authors considered the problem of SBS power control and user association in HetNets and proposed a heuristic algorithm to determine the switching pattern of redundant SBSs during periods of low traffic. In [244], the authors proposed an SBS switching mechanism based on particle swarm optimisation to minimise the energy consumption of a HetNet without violating QoS constraints. An SBS switching mechanism for EE optimisation in HetNet using genetic algorithm was proposed in [245] while respecting QoS constraints. A novel SBS wake up scheme was developed in [246], where the SBSs offload their traffic to MBS before entering into sleep mode while an optimal number of SBSs are woken up to accommodate the increase in traffic load during peak traffic periods.

The authors in [184] considered the problem of user association and dynamic SBSs switching in order to minimise the energy consumption in UDNs while considering the switching energy cost. Two heuristic algorithms were proposed: the first is a centralized user association algorithm for minimizing the switching cost while the second is an enhanced heuristic for further reduction in the energy consumption of the network. A cooperative energy optimisation scheme for 5G UDNs using graph theory was proposed in [247]. The network was first represented as a graph after which the graph theory is employed to determine the switching off/on pattern of the SBSs in the network. The work in [248] proposed an EE optimisation scheme for a two-tier HetNet via BS switching and traffic offloading. A distributed algorithm based on message-passing was developed to minimise the over-all power consumption of the network while maximizing the sum rate. In [249], the problem of power minimisation in cached-enabled BSs was investigated while considering the limitation in radio resources and BS storage capacity. Three heuristic algorithms were developed to determine the sub-optimal bandwidth and user association strategy as well as to minimise the power consumption of the network.

Regarding Q-learning methods, the work in [250] considered the problem of energy consumption and CO_2 emission of a HetNet deployment in a smart city context. A Q-learning-based cell switching framework was proposed to reduce the energy consumption and CO_2 emission levels of the network. In [251], a mobility management based energy optimisation framework for HetNets was proposed using both supervised and Q-learning algorithms. The proposed framework uses supervised learning alongside historical dataset of bus passengers passing through the HetNet to predict the traffic loads of the BSs while Q-learning was used to

determine the cell switching and traffic offloading strategy that would minimise both the energy consumption and CO_2 emission level. The work in [186] investigated the trade-off between energy consumption and delay in a HetNet where the sleep mode of the SBSs can be adjusted to different levels for the purpose of energy saving while ensuring that the QoS is maintained. A distributed Q-learning algorithm was developed to adapt the sleep level of the SBSs to their activity level while considering co-channel interference. The author in [252, 253] apply Q-learning algorithm for adaptive sleep mode management in order to optimise energy consumption of BSs in 5G homogeneous network deployment. In [177], centralized and decentralized Q-learning algorithm was developed to optimise the traffic offloading and SBS switch off process. A transfer actor-critic (TACT) model to optimise the dynamic switching off/on of SBSs in order to match traffic load with energy consumption in a HetNet was developed in [233].

A location-aware BS sleeping strategy that jointly optimises the trade-off between energy consumption and delay in a 5G HetNet was introduced in [254]. A Q-learning algorithm which considers the location and velocity of the users in determining the sleep mode level of the BS was developed to maximise the energy delay trade-off of the network. In [255], the authors proposed a cell switching mechanism using fuzzy Q-learning in order to maximise the EE of a HetNet without compromising the QoS. In addition, to avoid coverage holes when some BSs are switched off, a D2D communication mechanism was also incorporated into the sleeping mechanism. The authors in [256] proposed a dynamic framework for adjusting the load and energy consumption of the SBSs in a HetNet. The framework uses Q-learning to learn the optimal offloading policy required to turn off the redundant SBSs in the HetNet while balancing the load of the remaining SBSs. A wake-up strategy for BSs with hybrid energy supplies was proposed in [257]. A fuzzy-logic algorithm which considers the solar energy of the BS as well as the traffic demand of the network was developed to determine the optimal wake-up strategy.

In [258], an online learning framework was proposed to jointly optimise the energy consumption and interference of a HetNet. The problem was first modelled as a contextual bandit problem and than a Bayesian response estimation and threshold search (BRETS) algorithm was developed to control the off/on status of the SBSs while maintaining the QoS. The authors in [259] introduced a learning policy for EE optimisation in HetNets by dynamically turning off/on the SBSs in order to adapt them to the traffic demand at different times of the day. The first modelled the network traffic as a Markov decision process (MDP) and developed modified upper confidence bound algorithm using restless multi-armed

bandit for learning the optimal switching policy. The authors in [237] developed a RL based cell switching framework using SARSA algorithm with value function approximation to determine the optimal switching policy that would minimise the energy consumption in an ultra dense network while ensuring that the QoS of the network is maintained.

Considering ANN and deep RL methods, the authors in [235], proposed an ANN algorithm to determine the switching pattern that maximises the EE of the network while ensuring that the minimum bit rate requirements of the users is satisfied. The authors in [185] applied ANN for traffic prediction and cell switching decision with two different ANN architectures. The authors in in [260] proposed an ANN based cell switching framework for energy optimisation in UDN was proposed. The proposed framework is able to determine the optimal switching strategy that would result in minimum energy consumption without violating the QoS of the network. The authors in [261] proposed an online context-aware power optimisation scheme for SBSs in a cache-enabled HetNet. The energy minimisation problem was first modelled as a multi-armed bandit problem then a Bayesian neural network was used to determine the optimal switching pattern that would optimise the energy consumption of the network. A deep RL and traffic prediction framework was designed in [262] for determining the sleeping strategy in a RAN. Their approach uses geographic and semantic spatial-temporal network (GS-STN) for traffic forecasting while the BS sleeping problem was formulated as an MDP and solved using actor-critic RL.

The authors in [263] proposed an energy-aware traffic offloading scheme for EE optimisation in HetNets. In the proposed scheme, the traffic demand of the network was first predicted using deep neural networks after which the traffic offloading strategy was obtained using deep Q-networks. The work in [264] developed a deep RL framework for energy optimisation in a RAN using the dynamic cell switching approach. A double deep Q-learning network was developed to determine the optimal sleeping strategy that will minimise the energy consumption of the network while ensuring that the QoS of the network is maintained. The authors in [265], developed a dynamic BS sleeping strategy, known as DeepNap. The proposed method employs deep Q-networks to learn the optimal sleeping policies of the BSs.

For clustering-based cell switching approaches, a cluster-based femto BSs switching scheme to maximise the EE of a HetNet was developed in [266], wherein semi-definite programming based correlation clustering algorithm was used to determine the cluster with minimum EE as well as the number of femto BSs to switch off within the cluster while considering load balancing and probability of

outage. Similarly, in [267], a cluster-based cell switching scheme for EE optimisation in ultra dense SBS network was proposed while considering the user QoS and inter-cell interference. The EE problem was first formulated using stochastic geometry, then k-means algorithm was used to partition the dense SBSs into clusters. In addition, a sorting algorithm based heuristic, was developed to determine the number of SBSs to switch off in each cluster. The authors in [268] proposed cluster-based sleeping strategy to minimise the power consumption and interference in dense HetNets using clustering algorithm. In their proposed method, the SBSs are clustered based on their interference level, after which the clusters with large interference values are selected. Then, a binary particle swarm optimisation algorithm is applied to each of the selected clusters to determine the sleeping strategy.

Despite the fact that various approaches for cell switching have been proposed in the literature as discussed in the preceding paragraphs, these approaches have their own challenges that necessitates the development of novel cell switching solutions. Though heuristic approaches to cell switching have less computation cost, the often produce sub-optimal results. Moreover, they have poor generalization ability which makes them unable to adapt to dynamically changing network environment. ML approaches have the advantage of been able to learn the hidden patterns in the network from historical data and are also able to adapt to dynamically changing network conditions unlike heuristic algorithms. However, ML approaches such as Q-learning use tables to store the learnt state-action values, which limits their application when the network dimension becomes very large. This is because the size of the state-action value table increases as the network dimension increases, which makes it computationally burdensome to learn and would also require a large memory to store the learnt table. Other ML methods such as ANN and DRL are very computationally demanding to train and as such would not be suitable for application in UDNs. In addition, those that are based on clustering, though computationally efficient, produce very sub-optimal results which could limit the performance of the network.

To tackle these challenges, a lightweight cell switching scheme also known as THESIS for energy optimisation in UDHNs is proposed. The developed approach combines the benefits of MLC and ES algorithm to produce a solution whose optimality is close to that of the ES (which is guaranteed to be optimal), but is computationally more efficient than ES. As a result, it can be applied for cell switching in real networks even when their dimension is large. The performance evaluation shows that THESIS significantly reduces the energy consumption of the UDHN and can reduce the complexity of finding a near-optimal solution from

exponential to polynomial complexity.

3.3 Contributions

1. Development of a Q-learning framework for cell switching and traffic offloading in HetNets with CDSA while considering the amount of resources in the MBS and incremental power consumption on the MBS due to traffic offloading from sleeping SBSs.

2. Development of an ANN-based cell switching framework, which is referred to as offline-trained online cell switching (OTOcell), to learn the optimal switching strategy for the SBSs in a UDN while considering different types of SBSs.

3. Development of a hybrid cell switching framework to minimise the power consumption of a UDHN with the following objectives:

   - THESIS, a scalable cell switching approach based on an unsupervised ML algorithm (k-means) and ES algorithms is developed for energy optimisation in UDHN. The proposed method is computationally efficient and produces results that are close to the optimal solution. It can also be applied to large scale networks where many SBSs are deployed.
   - A benchmark algorithm purely based on k-means algorithm is developed for comparison with the proposed method.
   - The quantity of CO_2 savings that can be obtained when the proposed cell switching approach is implemented is also evaluated.
   - A complexity comparison of the proposed algorithms with the benchmark algorithm is carried out in order to ascertain the computational efficiency of the proposed method.
   - Finally, in order to capture the real life dynamics of the network, the performance of the proposed method is evaluated through extensive simulations using traffic data obtained from a real network and compared with other benchmark methods.

In the remaining parts of this chapter, each of the proposed cell switching optimisation frameworks is detailed from the system model, problem formulation, performance evaluation, results and discussions starting from the Q-learning framework, followed by ANN-based framework and finally THESIS.

3.4 Q-learning Assisted Energy-Aware Cell Switching and Traffic Offloading in HetNets

3.4.1 System Model

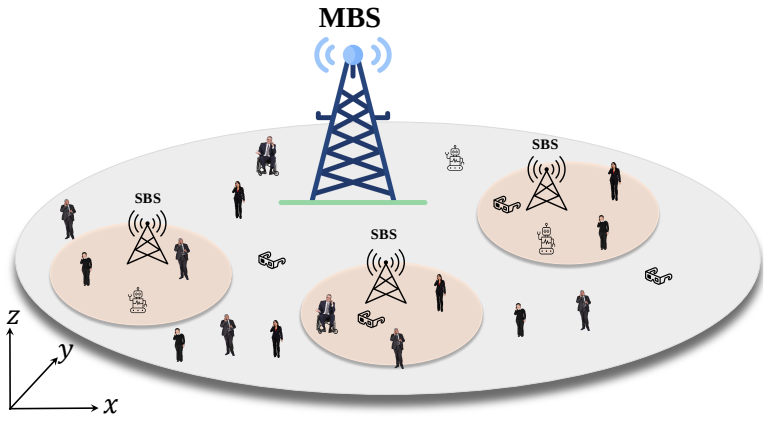

Figure 3.1: Network model comprising a MBS and three SBSs in HetNet deployment with CDSA (Note that this is a simplified system model of the HetNet with CDSA. other details of the CDSA are captured in the simulations).

A two-tier HetNet consisting of a MBS and three SBSs as shown in Fig. 3.1, with CDSA where the MBSs and SBSs operate in dedicated frequency bands is considered. The MBS is responsible for providing coverage, signalling as well as low data rate services while the SBSs provide high capacity in hotspot locations and are linked to the MBS using the backhaul. SBSs are switched off during low traffic load periods and their traffic offloaded to their associated MBS provided there is enough radio resources in the MBS to accommodate the offloaded traffic load.

Power Consumption Model of HetNet

The Earth model [65] for determining the total power consumption of a BS as expressed in (2.2) is adopted.

A network consisting of BSs (both MBS and SBSs) is assumed with each having limited number of resource blocks (RBs). Both MBS and SBSs have the same number of RBs. The load profile of each BS considered to be the proportion of RBs occupied per minute over a 24 hour period. Hence, for a BS having (M_{F}) total number of RBs with (M_{o}) number of RBs occupied per minute, the load (τ_i) of the BS per minute as well as the relation between τ_i, P_{tx} and P_{max} can be expressed as [65, 269]:

$$\tau_i = \frac{M_{\mathrm{o}}}{M_{\mathrm{F}}} = \frac{P_{\mathrm{tx}}}{P_{\mathrm{max}}}. \tag{3.1}$$

$$P_{\mathrm{tx}} = \tau_i . P_{\mathrm{max}}, \tag{3.2}$$

where $i = \{1, 2, 3, ..., \mathrm{T}\}$, and i is in minutes.

Combining (2.2) and (3.2) and assuming that P_{s} is zero when the BS is in sleep mode, the total power consumption of a MBS can be expressed as:

$$P_{\mathrm{m}} = P_{\mathrm{o}}^{\mathrm{m}} + \eta_{\mathrm{m}} \tau_i^{\mathrm{m}} P_{\mathrm{max}}^{\mathrm{m}}, \tag{3.3}$$

where P_{m} denotes the total power consumption of a MBS, $P_{\mathrm{o}}^{\mathrm{m}}$ denotes the constant power consumption component of the BS when the BS is in operation, η_{m} is the load dependent component of power consumption of the MBS, τ_i^{m} is the load of the MBS per minute.

The total power consumption of a SBS is given as:

$$P_{\mathrm{s}}^{j} = P_{\mathrm{o}}^{\mathrm{s}} + \eta_{\mathrm{s}} \tau_i^{s} P_{\mathrm{max}}^{\mathrm{s}}, \tag{3.4}$$

where P_{s}^{j} denotes the total power consumption of a SBSs, $j = \{1, 2, 3, ...\mathrm{M}_b\}$, is the number of SBSs, $P_{\mathrm{o}}^{\mathrm{s}}$ denotes the constant power consumption component of SBS in active mode, η_{s} is the load dependent component of power consumption of the SBS, τ_i^{s} is the load of the a SBS at every minute.

The total power consumption of the HetNet is the sum of the power consumption of the MBS and all the SBSs under its coverage. It can be written as:

$$P_{\mathrm{HetNet}} = P_{\mathrm{m}} + \sum_{j=1}^{M_b} P_{\mathrm{s}}^{j}, \tag{3.5}$$

where P_{HetNet}, P_{m} and P_{s}^{j} is the total power consumption of the HetNet, the power consumption of the MBS as well as that of the j-th SBS respectively.

3.4.2 Problem Formulation

The aim is to determine the optimal strategy to switch off lightly loaded SBSs during low traffic periods that will minimise the total power consumption of the HetNet while considering the availability of radio resources and increase in transmit power of the MBS due to traffic offloading as constraints. Therefore,

the optimisation problem can be formulated as:

$$\begin{aligned} \min_{\omega\in\Omega} \quad & \mathrm{P}\Big(\omega\Big) \\ \text{s.t.} \quad & \sum N_{\mathrm{s}}^{\mathrm{off}} < \Big(N_{\mathrm{m}}^{\mathrm{T}} - N_{\mathrm{m}}^{\mathrm{U}}\Big), \\ & \sum P_{\text{s-off}}^{j} > \Delta P_{\mathrm{m}}, \end{aligned} \tag{3.6}$$

where Ω is the set of all possible SBS switching strategies. $\mathrm{P}\Big(\omega\Big)$ is the expected power consumption of the HetNet using any switching strategy ω. The first constraint is the radio resource constraint[2], which implies that the number of RBs required to offload the traffic of sleeping SBSs, $\sum N_{\mathrm{s}}^{\mathrm{off}}$ must be less than the available number of RBs in the MBS, where N_{m}^{T} and N_{m}^{U} are the total number of RBs and utilised RBs in the MBS respectively. The second constraint is the dynamic power (power consumption due to transmission) constraint which implies that the power consumption gain $\sum P_{\text{s-off}}^{j}$ obtained by switching off SBSs must be greater than the increase in power consumption in the MBS, ΔP_{m} as a result of additional load from sleeping SBSs. A RL-based SBS switching and traffic offloading mechanism is developed in the next session to optimise energy consumption in the HetNet.

3.4.3 Proposed Q-learning Based Cell Switching Framework

A RL-based cell switching framework is proposed to implement the SBS switching operation. RL is a risk and reward kind of learning whereby the agent (or MBS) gets information from the environment and then tries to take action and is rewarded or penalized depending on whether the action taken is right or wrong. RL is applied in this work due to its suitability to handle this kind of tasks that involve making decisions out of a wide-range of options [270]. As an illustration in our study, the MBS interacts with the network environment, obtains information about the traffic loads levels of the SBSs through its backhaul connection with them and then decides which combination of SBSs to switch off per time. Hence, RL is able to cope with the requirement for solving this kind of problem because it can adapt to changing environment through learning and then decide the action that would yield the best desired performance.

In this work, Q-learning algorithm [146] is adopted. Q-learning is one of the

[2]In this work, it is assumed that once there is sufficient RBs at the MBS for traffic offloading, the QoS requirements of the users would be satisfied. However, in real networks, other factors such as the user distance from the MBS as well as the channel condition must also be considered.

most popular reinforcement algorithms, and has a proven capability of working in dynamic environments [149]. There are six main components in Q-learning: (i) agent, (ii) environment, (iii) action, (iv) state, (v) reward/penalty, and (vi) action-value table. Agent takes actions by interacting with a given environment in order to maximise the reward or minimise the penalty. After each action that the agent takes, resulting state and reward/penalty are evaluated. Then, the action-value table, which stores the rewards/penalties for all the possible actions and states, are updated according to (2.11).

Q-learning is an off-policy method, meaning that it follows different policies in determining the next action and updating the action-value table. The policy guides the agent in deciding the next action to take and also helps in updating action-value table. In addition, the policy can be stochastic, i.e., based on a given distribution (e.g., ϵ-greedy) or deterministic, i.e., based on some predefined or fixed values (e.g., μ policy). Although ϵ-greedy[3] is the base policy, π policy, where $\epsilon > 0$, is followed in selecting the next action, while μ policy, where $\epsilon = 0$, is followed in updating the action-value table. Moreover, Q-learning is a model-free approach, where the agent does not have a prior knowledge about the environment; instead it interacts with the environment by taking actions.

The motivation for using Q-learning in this work stems from the fact that as a model free learning algorithm [146], it is suitable for application in dynamic environments whose statistics continually change, such as the traffic loads of BSs in a HetNet, and it has low computational overhead compared to other cell switching heuristic algorithms which mainly employ ES techniques. Hence, it can lead to a more robust and scalable implementation of BS switching even when the network size is large. It has also been proven to converge to the optimal solution most of the time [271].

In designing the SBS switching mechanism, the goal is to find the best switching strategy i.e., select the best set of SBSs to switch off out of all possible set of SBSs. This is known as the optimal policy in RL. A simple HetNet deployment scenario is assumed as a representative case comprising 1 MBS and 3 SBSs which can later be generalized with more BSs. The environment is the traffic loads levels of the SBSs. The state is related to the optimisation constraint which is the availability of the radio resources in the MBS for traffic offloading. Two states,

[3] ϵ-greedy is one of the policies that can be used by a Q-learning agent to learn the optimal decision during the training phase. This policy selects the action having the highest state-action value with a probability $1 - \epsilon \in [0, 1]$ and a random action with probability ϵ.

δ_1 and δ_2, are then described as follows:

$$\begin{cases} \delta_1, & C_m < C_{ol}, \\ \delta_2, & C_m \geqslant C_{ol}, \end{cases} \tag{3.7}$$

where C_m is the maximum amount of radio resources available at the MBS and C_{ol} is the amount of radio resources required for the traffic load of the sleeping SBSs to be offloaded to the MBS. The first state is when the radio resource constraint is not satisfied and the second state is when the radio resource constraint is satisfied. The penalty function[4], $\Re$, is designed to be the total power consumption of the network as in (3.5):

$$\Re(a) = P_{\text{HetNet}}(P_{\text{m}}, P_{\text{s}}^{\text{j}}). \tag{3.8}$$

The penalty function guides the agent (in this case the MBS) in deciding the set of SBSs to switch per time. It takes as inputs the power consumption of the MBS and that of all active SBSs and outputs the total power consumption of the HetNet. So, essentially, the penalty is the total power consumption of the HetNet. The goal of the agent is to take actions with lesser penalty, in order to achieve the aim of this work which is energy minimisation. So actions that encourage lesser power consumption (lower value of the penalty function) are encouraged, while those that lead to more power consumption (higher value of the penalty function) are discouraged. There are eight possible action sets that the agent can take. These actions correspond to each policy, that is, the set of SBSs that can be switched off at a given time instant.

The proposed Q-learning framework is deployed at the local controller, located at the MBS, since the MBS is saddled with the responsibility of controlling the off/on status of the SBSs under its coverage in the CDSA. The SBSs communicate their traffic load information periodically to the MBS via dedicated control channel, then the Q-learning algorithm takes the traffic load information of the SBSs and MBS, alongside the power consumption parameters of the BSs, and decides which set of SBSs to turn off. The Q-learning algorithm is provided in Algorithm 5, where χ is the window size for resetting the action-value table.

[4]The penalty function in the proposed Q-learning framework is the total power consumption of the HetNet. It comprises the power consumption of the MBS and that of all the SBSs under it coverage. It is related to the RBs in Table 3.1 because the amount of RBs occupied in the BS constitutes the load of the BS which ultimately affects the total power consumption of the BS.

Algorithm 5: Proposed Q-Learning Algorithm

Input : Traffic loads of MBS and SBSs
Output: SBSs to be switched off

```
Initialize Q(s, a) := 0;
for every episode do
    if episode ≡ 0 (mod χ) then
        Initialize Q(s, a) := 0;
    end
    for iterations do
        Determine the current state using (3.7);
        Take an action;
        Calculate penalties through (3.8);
        Go to the next state;
        Update the action-value table with (2.11).
    end
end
```

3.4.4 Performance Evaluation

In this section, the performance of the proposed Q-learning based cell switching algorithm is evaluated. The network parameters used for the simulation were obtained from [65] and are listed in Table 3.1. The learning rate, ζ, is set to

Table 3.1: Simulation parameters for Q-learning based cell switching

Parameter	**Value**
Bandwidth	20MHz
Number of RBs per MBS	100
Number of RBs per SBS	100
$P^m_{\max}$, $P^s_{\max}$	20 W, 6.3 W
P^m_c, P^s_c	130 W, 6.3 W
η_m, η_s	4.7, 2.6
Number of iterations	100

0.1 while the discount factor, ε, is set to 0.9 [149]. The simulation environment comprises a MBS and three SBSs. A scenario where horizontal offloading among the SBSs is not possible as their footprints do not overlap is considered. As such, vertical offloading from SBSs to MBS is considered in this work. Also the MBS controls the switching off/on operation of the SBSs under its coverage. The network is monitored over a 24 hour period with 1 minute resolution, meaning that the switching operation is performed every minute. A comparison of energy consumption of the HetNet with and without Q-learning at different BSs traffic load is carried out. With no Q-learning, no switching mechanism is implemented,

hence all the BSs are active irrespective of their traffic load level. Then, the energy consumption gain achieved by implementing the proposed Q-learning based cell switching algorithm is quantified.

The load of the SBSs, τ_{s}, are generated using a uniform random distribution and can be depicted as $\tau_{\mathrm{s}} \in [0, m_{\mathrm{s}}]$, where m_{s} is the normalized maximum load level of the SBSs. Similarly, a uniformly distributed[5] random traffic load of the MBS, τ_{m}, is also generated using $\tau_{\mathrm{m}} \in [0, m_{\mathrm{m}}]$, where m_{m} is the normalized maximum load level of the MBS. For each simulation, m_{m} is specified while the load of the SBSs are continually varied. The energy consumption of the HetNet

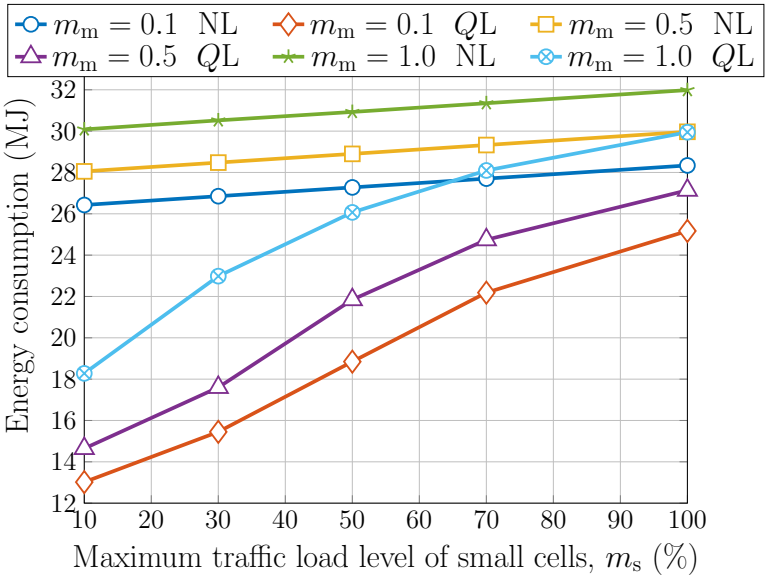

Figure 3.2: Total HetNet energy consumption with and without Q-learning where NL represents energy consumption without Q-learning while QL represents energy consumption with Q-learning and m_{m} is the normalized maximum load of the MBS. $\zeta = 0.1$ and $\chi = 50$.

with and without learning is depicted in Fig. 3.2. It can be be observed that there is a significant reduction in the total power consumption of the HetNet with the application of the developed Q-learning-based cell switching algorithm. This is because Q-learning is able to select the optimal set of SBSs to be switched off per time thereby enabling the HetNet to operate with minimal energy consumption.

Fig. 3.2 also shows that the energy consumption of the HetNet increases as the traffic load of the SBSs increases. With increasing the traffic load on the SBSs, the opportunity for offloading the traffic to the MBS reduces due to availability of limited resources, therefore more SBSs have to be left in active mode in order to

[5]This is a simplified traffic model that is used in this preliminary work to show the varying nature of the traffic load of the network. However, the traffic load of real networks follow a trend that is similar to a normal distribution over a whole day, as the network traffic is lowest at the morning and night periods, while it peaks towards the afternoon period [20].

sustain the increased network traffic load. As a result, the HetNet has to operate at a higher energy consumption rate when the traffic load increases. Also from Fig. 3.2, the lower the value of m_{m}, the lesser the energy consumption since there will be provision to switch off more SBSs but higher m_{m} values results in higher energy consumption. Please note that m_{m} and m_{s} are the maximum values that the traffic loads of the MBS and SBSs can get to. However, during simulations, the values of the traffic load of the MBS and SBSs are continually varied. For example, $m_{\mathrm{m}} = 1$ and $m_{\mathrm{s}} = 100\%$, means that the normalized traffic load of the MBS can vary from 0 to 1 and that of the SBS can vary from 10% to 100% respectively, during the simulation. It does not mean that the value of m_{m} is fixed at 1 or that of m_{s} is fixed at 100% throughout the simulation. This explains the discrepancy between the value of the energy consumption with NL and QL when $m_{\mathrm{m}} = 1$ and $m_{\mathrm{s}} = 100\%$, as the Q-learning algorithm still has opportunity to switch off some SBSs, since the traffic loads of the MBS and SBSs still fluctuates at these values of m_{m} and m_{s}.

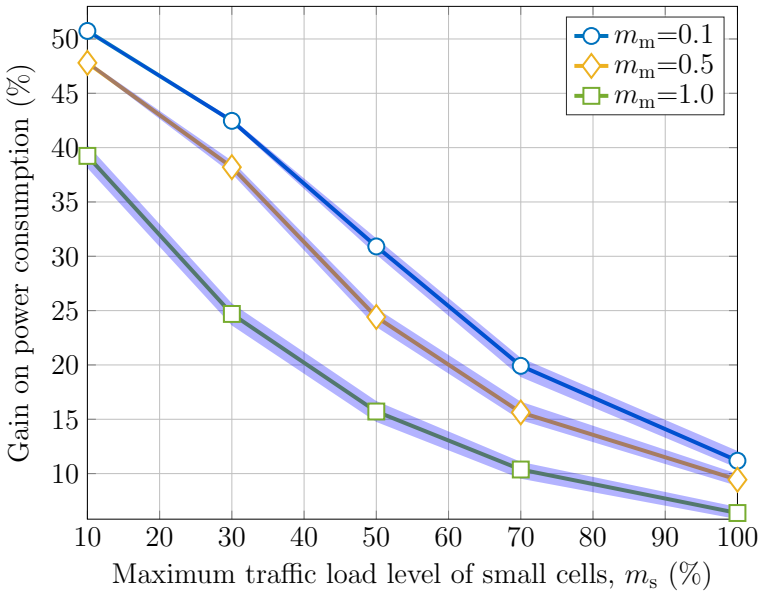

Figure 3.3: Energy consumption gain with Q-learning (i.e. percentage reduction in HetNet energy consumption with Q-learning). $\zeta = 0.1$ and $\chi = 50$. Note that while the shaded areas in the figure show the confidence levels (minimums and maximums of 100 runs) of the findings, the straight lines with markers represent the averages of the runs.

Fig. 3.3 presents the gain in energy consumption as well as the confidence levels of the results obtained when Q-learning is implemented. Since the findings in Fig. 3.3 are obtained using the results of Fig. 3.2, the confidence levels are only presented in Fig. 3.3 for the sake of simplicity of the presentation. The energy consumption gain is the percentage reduction in energy consumption of

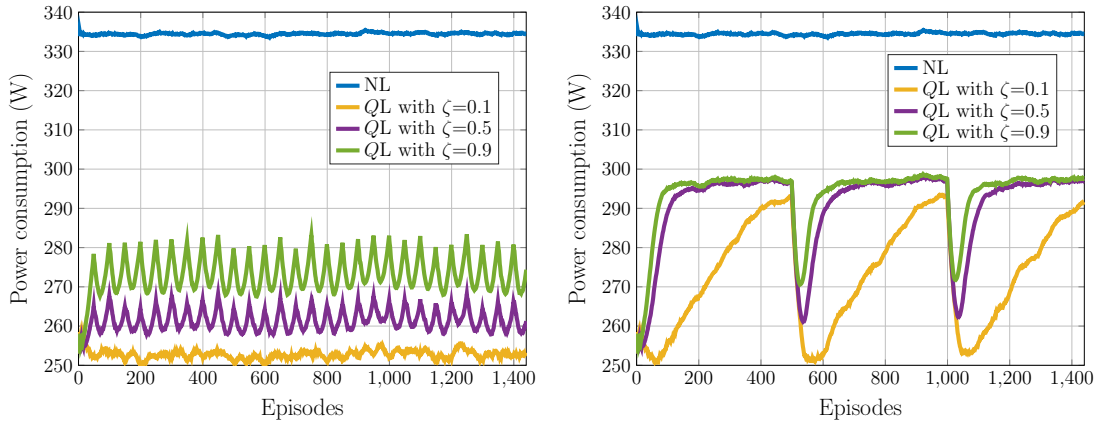

(a) Window size of $\chi = 50$ (b) Window size of $\chi = 500$

Figure 3.4: Performance impacts of learning rate, ζ and the window size for resetting the action-value table, χ, on Q-learning convergence. The maximum traffic loads for both MBS and SBSs (m_{m} and m_{s}) are set to 0.5. The results are the averages of 100 runs.

the HetNet due to the application of the proposed framework. Similar to the observation in Fig. 3.2, the power consumption gain reduces with increasing the SBS load, as the probability of switching off SBSs reduces with increasing traffic load. Fig. 3.3 also shows that higher energy consumption gain is obtained with lesser m_{m} values but the gain decreases as the value of m_{m} increases because more switching opportunities exits when the maximum load of the MBS is low. The simulation results reveals that an energy consumption gain of up to 50% can be achieved with the proposed Q-learning framework.

The experimental proof of convergence of the proposed Q-learning algorithm and the impact of ζ, and χ, for initializing the action-value table are shown in Fig. 3.4. The main idea of initializing the action-value table with w is to decrease the computational expense of Q-learning implementation. Ideally, the action-value table should be initialized once at the beginning of the implementation, and kept the same until the end in order to reduce the computational cost. When building the action-value table, environment learning takes some time in the beginning; however, once the environment is learnt, minor changes in the built action-value table would be enough for Q-learning to adapt itself to new conditions. Nonetheless, this is only the case for gradually changing environments, where Q-learning adapts itself easily. Since the traffic loads of the MBS and SBSs are determined in a random manner, it results in abrupt changes in the environment of interest, making the built action-value table no more valid, as the experienced environment might be significantly different from the learnt one.

Initializing the action-value table at every episode could be an approach for

this kind of abruptly changing environments; however, it comes with the expense of computational burden, since it makes Q-learning learn the environment at each episode. Thus, instead of initializing the action value-table at each episode, it could be initialized at every χ episodes in order to save from the computational cost. However, there is a trade-off between the performance of Q-learning and the computational cost, making the selection of proper ζ and χ quite critical.

There are two main takeaways that can be inferred from Fig. 3.4: 1) Comparing Fig. 3.4a and Fig. 3.4b, smaller χ values give better results in terms of the performance of Q-learning, as the action-value table learnt just after the initialization is not valid for upcoming episodes due to abrupt changes in the environment, resulting in performance degradation. 2) Fig. 3.4a reveals that having smaller ζ value is better given that Q-learning starts focusing on the new observations more with decreasing ζ. Therefore, in this work, χ and ζ are selected as 50 and 0.1, respectively.

3.4.5 Limitations

Q-learning algorithm can be used for real-time cell switching as it has the ability to adapt to changing network traffic condition to learn the optimal cell switching strategy that will lead to minimum energy consumption in the network. However, its implementation involves learning a Q-table entries for every state-action pair. For large networks involving many BSs, the number of actions for any given state becomes very large and very computationally demanding as a huge Q-table has to be learnt. In addition, a very large memory is needed to store the learnt Q-table [146]. As a result, this solution can only be applied to small or medium size networks. Another attempt to develop a solution that can be applied to large scale networks by handling the challenges associated with Q-learning-based cell switching scheme is considered. In this regard, an ANN-based cell switching framework is developed because of the capability of ANN algorithm to serve as a universal approximator and its ability to be trained offline and implemented online.

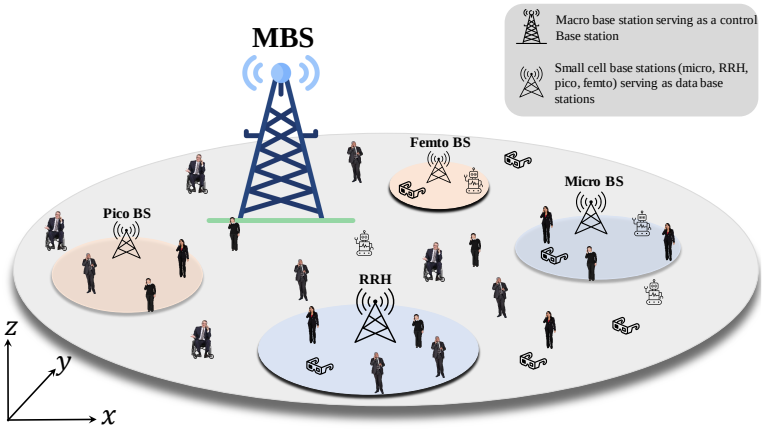

Figure 3.5: A UDN comprising a MBS and different types of SBSs

3.5 Load-Aware Cell Switching in Ultra-Dense Networks: An Artificial Neural Network Approach

3.5.1 System Model

A heterogeneous UDN, with CDSA, comprising both MBS and SBSs is considered. Four types of SBSs (RRH, micro, pico, and femto cell) are considered in the work. The MBS—which encompasses the footprints of the SBSs—is constantly kept on, and also orchestrates the switching operation of the SBSs via its backhaul connection to them. The SBSs, on the other hand, can be turned off/on based on their traffic load and are responsible for handling high data traffic demands. Vertical traffic offloading is considered, such that the traffic load of the SBSs that are switched OFF are offloaded to the MBS to ensure that the QoS of the offloaded users are maintained.

Power Consumption Model

The power consumption model of a BS proposed in [65] and previously defined in (2.2) is adopted.

The total power consumption of the UDN comprises the power consumption of the MBS and that of all the SBSs deployed under its coverage. This can be expressed as:

$$P_{\text{tot}} = P_{\text{m}} + \sum_{j=1}^{M_b} P_{\text{s},j}, \tag{3.9}$$

where P_{tot}, P_{m} and $P_{\text{s},j}$ are UDN's total, MBS's, and j-th SBS's power consump-

tion, respectively.

3.5.2 Problem Formulation

The aim of this research is to select the optimal combination of SBSs to switch off, during periods of low or no traffic in order to minimise the total power consumption of a UDN while ensuring that the QoS of the users originally connected to the switched off SBSs are maintained by the MBS.

Hence, the optimisation objective[6] can be defined as:

$$\begin{aligned} \min_{\omega \in \Omega} \quad & P_{\text{tot}}(\omega) \\ \text{s.t.} \quad & \hat{\tau}_{\text{m}} \leq 1. \end{aligned} \tag{3.10}$$

where ω is the selected SBS switching policy, while Ω is the set of all the possible SBS switching combinations. $P_{\text{T}}(\omega)$ is the expected power consumption of the network with ω switching policy. $\hat{\tau}_{\text{m}}$ is the traffic load of MBS after the offloading is complete, and is given as

$$\hat{\tau}_{\text{m}} = \tau_{\text{m}} + \sum_{j=1}^{M_b} \tau_{\text{s},j} \Gamma_j, \tag{3.11}$$

where τ_{m} and $\tau_{\text{s},n}$ are the original traffic demands (i.e., before offloading) of MBS and j-th SBS, respectively, and M_b is the total number of SBSs in the network. Γ_j is a control parameter, which is responsible for offloading the traffic load of only the switched OFF SBSs, such that

$$\Gamma_j = \begin{cases} 1, & \text{if SBS}_j \textit{ is OFF} \\ 0, & \text{if SBS}_j \textit{ is ON}, \end{cases} \tag{3.12}$$

where SBS_j is the j-th SBS.

The constraint in (3.10) is to ensure that there must be sufficient capacity in the MBS to accommodate both the original traffic demand of the MBS, τ_{MBS}, and the total traffic demand of all the SBSs that are switched OFF in order to maintain the QoS.

[6]Please note that only the most important constraint, which is the availability of offloading capacity at the MBS, has be included in (3.10) to avoid repetition. However, all the other constraints in (3.6) also apply here. All these constraints alongside the need to select the optimal combination of SBSs to switch off per time out of all the possible combinations, necessitates the use of ML in this work.

3.5.3 Proposed ANN-Based Cell Switching Framework

Most of the cell switching solutions developed using heuristic approaches, such as ES or genetic algorithm, are not suitable for real-time implementation, particularly in networks with large dimensions because they are usually computationally demanding. As a result, before these algorithms decide which set of SBSs to switch off/on and execute the decision, the network state would have changed[7], thereby leading to sub-optimal switching decision and delays.

However, these heuristic approaches can be combined with ANN to accelerate the computation of the optimal cell switching strategy. The proposed framework is built upon two basic observations: 1) cell switching can be considered to be a problem of deciding the mapping between the traffic demand and optimal switching pattern; 2) ANN are popularly referred as universal function approximators, implying that they can learn the mapping between almost any input and output [234].

Based on these observations, an offline-trained online cell switching (OTOcell) framework is proposed to determine the optimal switching strategy that maps the traffic demand of the BSs to the optimal cell switching pattern. The proposed OTOcell framework is summarized in Fig. 3.6. The traffic loads of the MBS and all the SBSs associated with it are collected and stored in the *Traffic Load Database*. The traffic loads are then passed to the *Training Dataset Generator* which consists of the ES algorithm, and Input/Output Mapper. The ES algorithm uses the optimisation function in (3.10) to decide the optimal set of SBSs to switch off/on per time while the Input/Output Mapper prepares the training dataset—which includes the traffic loads, and optimal switching combinations. The training dataset is then transferred to the *Offline Model Generator* for ANN model training, validation and testing.

The justification for using the proposed framework is twofold: 1) once the ANN model is fully trained[8], the optimal cell switching pattern can be obtained in real-time, that is, whenever the network status changes, without resorting to

[7]In this work, the dynamics of the network environment is captured by the traffic model and the distribution of the SBSs employed. However, since this is this a preliminary work, a random traffic and a few SBSs are considered. The main work in 3.6 considers many SBSs and a real network traffic model [272].

[8]The mechanism behind the training process of the proposed ANN model is that it has to be exposed to sufficient data from the network over a long period, such that the environmental dynamics of the network would have been fully learnt by the model. Hence, even though it is trained offline, and implemented online, it would still be able to perform effectively well in the real network due to the periodic and repetitive nature of network traffic [20]. However, there is also room for model update, a situation where a copy of the model is retrained and parameters fine tuned periodically with new data generated by the network in order to enable it to be able to capture recent occurring network conditions that was not previously captured in the original dataset it was trained with.

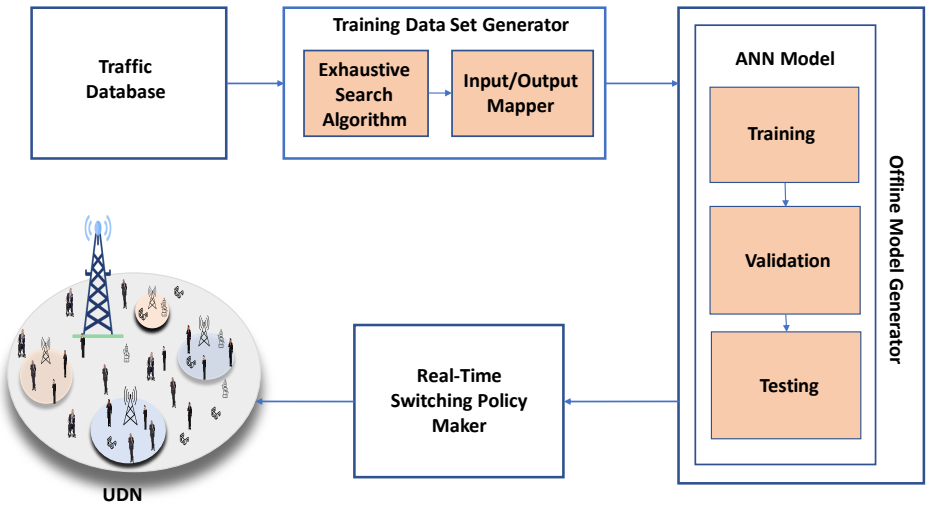

Figure 3.6: Overview of the proposed OTOcell framework.

computing the optimisation objective afresh; 2) both training dataset generation and the ANN training stage, which are the computationally intensive processes, can be done offline, thus enabling the trained model to be implemented for real-time cell switching without additional computational overhead and delays to the network.

The ANN model utilised is a feed-forward architecture comprising one input layer, three hidden layers (HLs), and one output layer (OL). The number of neurons in the input layer is determined by the input features of the training dataset (number of SBSs and MBS), the number of neurons in the HL are selected empirically by trying different combinations, and the OL neurons is given by 2_b^M, where M_b is the number of SBSs. The activation function for the HL neurons is rectified linear unit (ReLU) while that of the output neurons is softmax. The activation function is a set of rules that determines whether a neuron would be activated or not when it receives an input. ReLU activation function can receive any real value as input, but is activated only when the value of the input is greater than 0. Its superior training performance makes it a preferred choice over other activation functions at the HL neurons. Softmax activation function maps input to a set of probabilities, as such they are used in multi-classification problems consisting of more than one output classes [273].

The function of the ANN is to learn the mapping between the SBS traffic demands and the optimal switching pattern through training. The training process involves adjusting the ANN parameters, using gradient-descent algorithms, such

Table 3.2: Parameters for the developed ANN model

Parameter	**Scenario 1**	**Scenario 2**
HLs, Neuron size	3, 128 X 128 X 128	3, 128 X 128 X128
OL neuron size	16	4096
Learning rate	0.0001	0.001
Batch size	30	50
Epochs	1000	1000
HL activation function	ReLU	
OL activation function	Softmax	
Loss function	Categorical-crossentropy	
optimiser	Adam	

that the difference (error) between the expected output (i.e., predicted output) and the actual output (label) is as close to zero as possible. This error is usually estimated using a loss function and in this case, the categorical cross-entropy function is employed. The trained cell switching model is then transferred to the *Real-time Switching Policy Maker* for real-time SBS switching.

3.5.4 Performance Evaluation

Simulation Scenario and Data-Set Generation

Two simulation scenarios, Scenario-A and Scenario-B, with different number of SBSs are considered to test the performance of the proposed model on varying network sizes. Both scenarios consists of 1 MBS, but Scenario-A has 4 SBSs (1 of each type of SBBS), while Scenario-B has 12 SBSs (2 RRH, 3 micro, 4 pico, and 3 femto cells)[9]. The traffic load of both MBS and SBSs are generated using uniform random distribution model, such that $\tau_{\mathrm{m}} \in [0, m_{\mathrm{m}}]$ and $\tau_{\mathrm{s}} \in [0, m_{\mathrm{s}}]$ where $m_{\mathrm{m}}, m_{\mathrm{s}}$ are the maximum normalized loads of the MBS and SBSs, respectively. In Scenario-A, BS switching pattern were generated for 7 days with one-minute resolution using ES amounting to about 10,000 observations, while Scenario-B was for 35 days[10] resulting in about 50,000 observations. For the remaining simulation parameters, the values in [65] are adopted.

ANN Training and Testing

For Scenario-A, two datasets—each comprising about 10,000 traffic load samples of the BSs and their corresponding optimal switching patterns—were used for

[9]The number of each type of SBS was selected randomly.

[10]More dataset is generated in Scenario-B because the increase in network dimension and complexity makes the training process more difficult.

training and testing the proposed model. For Scenario-B, one dataset comprising about 50,000 traffic load samples and their corresponding optimal switching patterns was utilised, out of which 80% was used for training and 20% for testing. The training of the model in both scenarios is carried out using the Adam optimisation algorithm [274]. Table 3.2 summarizes the parameters of both models. Upon successful training of both models in each scenario, the trained models are then applied to the test dataset in order to evaluate the performance of the trained models.

Results and Discussions

Figs. 3.7a and 3.7b present a comparison of the total power consumption of the UDN, for both scenarios of OTOcell versus two benchmark approaches: 1) All-ON, which is the conventional approach where no switching is implemented, that is, all the SBSs and MBS are constantly kept on; and 2) ES approach, which tries to find the best switching policy by considering all the possible switching combinations and selecting the one that results in the least power consumption while the constraint in (3.10) is satisfied. The ES approach is guaranteed to always return the optimal policy, and hence the goal of any switching technique is to produce the closest approximation of this approach.

In Fig. 3.7a, it can be observed that the performance of the proposed OTOcell is the same as that of ES most of the time but shows slight variations at some time instances due to wrong cell switching prediction from the OTOcell. Compared to the All-ON, it can be observed that the OTOcell shows a reduction in power consumption, however, it was observed that due to the few number of SBSs[11] the reduction in power consumption is not significant most of the time as the SBSs have fewer opportunities to sleep.

In Fig. 3.7b, where the number of SBSs is increased from 4 to 12, the OTOcell shows a slightly lesser performance compared to that of Fig. 3.7a as the deviation from the optimal ES is more pronounced. This can be traced to the fact that the network dimensions and complexity is increased in Scenario-B compared to Scenario-A, and as a result the OTOcell is prone to more prediction errors. However, compared to the All-ON method, the proposed method shows a significant reduction in power consumption at all time instances owing to the fact the number of SBSs has tripled, hence there are more opportunities to switch OFF more SBSs.

[11]The results presented here are the preliminary work that led to the main work in section 3.6. That is why a few number of SBSs and a random traffic model was considered. In the main work, up to 120 SBSs and a real traffic model are considered.

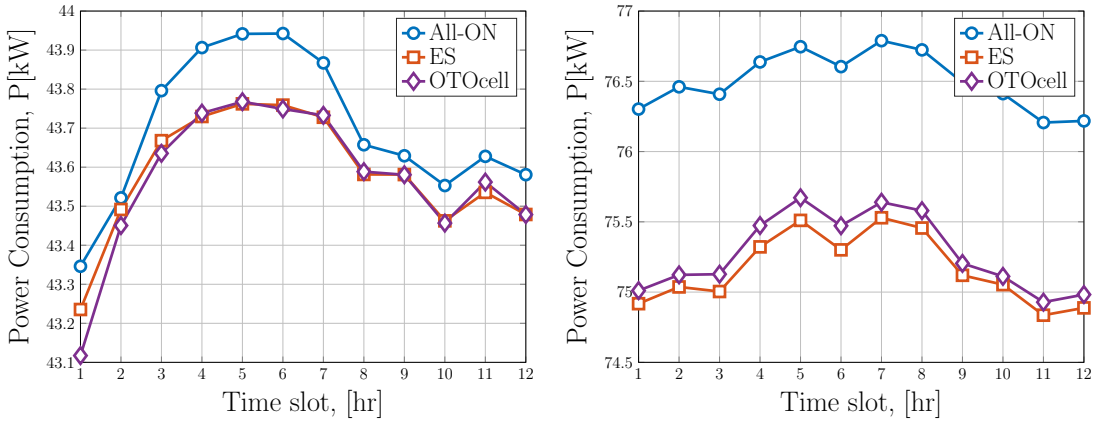

(a) $M_b = 4$ (b) $M_b = 12$

Figure 3.7: Power consumption comparison between OTOcell and benchmarks when $M_b = 4$ and $M_b = 12$.

The QoS metric considered in this work is the coverage loss ($\mathcal{C}_L$). It is defined as the measure of the percentage of available traffic load that is lost due to the cell switching operation [185]. It is evaluated by finding the difference between the total traffic load supported by the network before and after cell switching and traffic offloading. The target is for $\mathcal{C}_L = 0\%$, which implies that there is no traffic loss and as such, the QoS of the network is not violated. However, due to prediction errors, the value of $\mathcal{C}_L$ may be slightly higher than 0%. Hence, the evaluation of the proposed framework is also carried out using the coverage loss metric to ascertain the impact of the OTOcell framework on the QoS of the network.

When both the proposed and benchmark methods are evaluated using the coverage loss metric for 4 SBSs, the value of $\mathcal{C}_L = 0\%$, which means that the QoS of the network is not violated by the proposed method. However, when the numbers of SBSs increases to 12, the value of $\mathcal{C}_L$ is about 0.3%. This can be traced to inappropriate switch off/on decisions due to wrong predictions from the proposed framework occasioned by the increase in network dimension and complexity which makes it more difficult to accurately train the ANN model. Hence, the QoS of the network is slightly reduced when the network dimension increases, but the overall effect on the network is very minimal.

3.5.5 Limitations

The proposed ANN-based cell switching approach is computationally efficient because it can be trained offline before online implementation, thereby reducing the computational burden of the MBS which serves as the CBS, that is already been

saddled with signalling functionalities. However, as the network size increases, the computational overhead required for offline training becomes very high. Also, since the model requires periodic update in order to enhance its prediction accuracy, a huge computational complexity, which increases with the size of the network, is involved in implementing this method. There is also the problem of error propagation as the training dataset is normally obtained from a heuristic algorithm whose output may not be optimal. As a result, this method would only be suitable for small to medium size networks with few BS deployments. Therefore, as next generation cellular networks involves network densification and ultra-densification comprising large deployment of BSs, there is a need to develop a cell switching framework that can be implemented online, is scalable, has lesser computational complexity and does not depend on training dataset from a heuristic algorithm. This led to the development of THESIS which is presented in the following section.

3.6 A Lightweight Cell Switching and Traffic Offloading Scheme for Energy Optimisation in Ultra-Dense Heterogeneous Networks

3.6.1 System Model

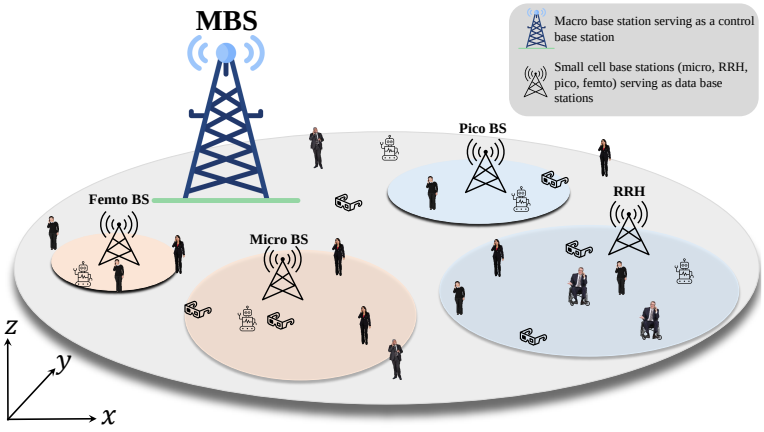

Figure 3.8: A UDHN with one MC comprising a MBS and different types of SBSs (RRH, micro, pico and femto BS).

A UDHN comprising multiple macro cells (MCs) is considered. Each MC consists of a MBS, and a large number of SBSs each have different capacities and power consumption profiles. The UDHN employs CDSA such that the MBSs

serve as the control BSs and are responsible for signalling, low data rate transmission and de (activation) of SBSs under their coverage. The SBSs, on the other hand, serve as data BSs, are deployed in areas with high traffic intensity for capacity enhancement and high data rate transmission. In addition, vertical traffic offloading is considered such that the SBSs with little or no traffic load can be turned off, and the traffic originally associated with them is transferred to the MBSs. This is to ensure that the QoS of the network is not violated. In this work, it is assumed that before cell switching is implemented, all the traffic demands from the users are supported by the network, meaning that the UDHN always has sufficient radio resources[12] for the users. In other words, because the UDHN is designed in terms of radio resources, when all the SBSs are on, all the users are guaranteed sufficient resources, but this cannot be guaranteed with cell switching. The QoS metric considered in this work is the $\mathcal{C}_L$, which is a measure of the percentage of traffic load that is lost due to the implementation of cell switching. Hence, for the QoS of the network to be maintained, $\mathcal{C}_L$ must be equal to 0%, and this occurs when the total traffic load supported by the network before and after cell switching is implemented is the same. The network model is presented in Fig. 3.8.

Power Consumption of the UDHN

The total power consumption of the UDHN consists of the power consumption of the MBSs and that of the SBSs. The power consumption of the j^{th} BS in the i^{th} MC at time t, $P_t^{i,j}$, is given as [65, 72]:

$$P_t^{i,j}(\tau_t^{i,j}) = P_{\text{o}} + \tau_t^{i,j}\eta P_{\text{tx}}, \tag{3.13}$$

where P_{o} is the constant circuit power consumption, $\tau_t^{i,j}$ represents the instantaneous traffic load of the j^{th} BS in the i^{th} MC, η is the load dependent power consumption component and P_{tx} is the transmission power of the BS. The value of P_{o}, η, and P_{tx} depends on the type of BS (i.e., MBS, RRH, micro, pico and femto BS).

Therefore, considering a UDHN with multiple MCs, where the MCs are indexed by i, the total power consumption of the UDHN at time t, $P_{\text{tot},t}$, can be

[12]In this work, it is assumed that the availability of sufficient resources or bandwidth at the MBS is enough to ensure that all offloaded users from switched off SBSs are adequately accommodated. However, in real networks, this might not be the case as other factors such as the channel condition, and user location or mobility must also be considered. This is one of the limitations of this current work that should be properly investigated in future works.

expressed as:

$$P_{\text{tot},t}\ (\tau_t^{i,j}) = \sum_{i=1}^{M_m} \sum_{j=1}^{M_b} P_t^{i,j}(\tau_t^{i,j}), \tag{3.14}$$

where $P_t^{i,1}$ denotes the power consumption of the MBS in the i^{th} MC. M_m and M_b denote the number of MCs within the UDHN and the number of BSs (including an MBS and SBSs) within an MC, respectively.

3.6.2 Problem Formulation

A certain duration of time (T) is considered such that T is partitioned into different time slots (in mins) of equal duration d (in mins). Then, an index vector t is defined which stores the time slots in sequential order and can be expressed as $t = [1, 2, ..., M_T]$, where M_T is the number of time slots and is written as $M_T = T/d$. The BSs in each MC are represented by $B^{i,j}$ with $B^{i,1}$ denoting the MBS. A scenario where the UDHN can decide to switch off/on some SBSs during periods of low traffic in order to minimise the energy consumption of the network is also considered. The goal is to determine the optimal switching strategy (i.e., the optimal set of SBSs to turn off/on) in each time slot that would result in minimal energy consumption in the UDHN.

Therefore, the total power consumption of the UDHN (accumulated over all the time slots) when cell switch off/on is considered can be expressed as:

$$P_{\text{tot}}\ (\tau_t^{i,j}, \Gamma_t^{i,j}) = \sum_{t=1}^{M_T} \sum_{i=1}^{M_m} \sum_{j=0}^{M_b} [\Gamma_t^{i,j} P_t^{i,j}(\tau_t^{i,j}) + (1 - \Gamma_t^{i,j}) P_s^{i,j}], \tag{3.15}$$

where $P_s^{i,j}$ denotes the sleep mode power consumption of the BS (i.e., power consumption when switched off) and $\Gamma_t^{i,j}$ represents the off/on state of the j^{th} BS in the i^{th} MC at time t i,e.,

$$\Gamma_t^{i,j} = \begin{cases} 1, & \text{if } B^{i,j} \text{ is ON} \\ 0, & \text{if } B^{i,j} \text{ is OFF} \end{cases} \tag{3.16}$$

Since the MBS is constantly active, $\Gamma_t^{i,1} = 1$, $\forall t$.

The optimisation objective is to minimise the total power consumption of the UDHN while ensuring that the QoS[13] of the network is maintained. Therefore,

[13]The QoS is evaluated using the coverage loss metric, which is defined as the measure of the percentage of traffic load that is lost due to cell switching operation. Hence, for the QoS of the network to be maintained, the total traffic demand supported by network before and after cell switching must be the same, that is the first constraint (3.18). For that to happen, there must be sufficient radio resources or bandwidth at the MBS to accommodate the offloaded traffic of

the power minimisation objective function can be expressed as:

$$\min_{\Gamma_t^{i,j}} \quad \mathrm{P}_{\mathrm{tot}}(\tau_t^{i,j}, \Gamma_t^{i,j}), \tag{3.17}$$

$$\text{s.t.} \quad \Upsilon^i = \hat{T}^i, \quad \forall i, j, \tag{3.18}$$

$$\hat{\tau}_t^{i,1} \leq \tau_{\mathrm{m}}^{i,1}, \tag{3.19}$$

$$\Gamma_t^{i,j} \in \{0, 1\}. \tag{3.20}$$

The constraint (3.18) is to ensure that the traffic demand that is supported by the UDHN before and after cell switching and traffic offloading is the same, where Υ^i is the total traffic demand that was served by the UDHN before cell switching (i.e., when no traffic offloading was implemented) and $\hat{T}^i$ is the total traffic demand that is served by the UDHN after cell switching and traffic offloading. The second constraint given in (3.19) is to ensure that the maximum traffic demand that the MBS can support is not exceeded when offloading the traffic of the SBSs that would be switched off to the MBS, where $\tau_{\mathrm{m}}^{i,1}$ is the maximum traffic demand that the MBS can serve. The third constraint (3.20) denotes the off/on status of j^{th} SBS in i^{th} MC as defined in (3.16).

3.6.3 Proposed Hybrid Cell Switching Framework (THESIS)

The aim of this work is to determine the optimal online policy for switching off/on the SBSs of the UDHN without compromising the QoS of the network. Popular heuristic approaches such as the ES algorithm, even though always finds the optimal policy, due to huge computational complexity when the number of SBSs deployed becomes very large, are not suitable for this kind of problem. It is only suitable for application in networks with a few SBSs as the optimal results in such cases are quicker to compute with the ES algorithm. Considering the limitation of applying the ES algorithm, particularly when the network size is very large, a lightweight cell switching scheme known as THESIS is proposed, which combines k-means clustering and ES algorithms for energy optimisation in UDHN. Before going into details about the proposed approach, for the sake of keeping the discussion easy to follow, the developed benchmark scheme known as multi-level clustering (MLC) is first introduced, which is purely based on the k-means clustering algorithm. Therefore, in the following subsections, discussions on the foundations of cell clustering is first carried out, followed by the benchmark

the sleeping SBSs, that is the second constraint (3.19).

MLC and the proposed approach, respectively.

Cell Clustering

The basis for developing both the benchmark and proposed cell switching algorithm is to cluster the SBSs with similar traffic loads and decide which cluster(s) or set of SBSs within a cluster can be switched off to minimise the total energy consumption of the UDHN. To cluster the SBSs, an unsupervised learning algorithm known as the k-means algorithm is applied. However, the number of clusters must be determined in advance, before finding the members of each cluster. Thus, the number of clusters becomes a hyper-parameter for the k-means algorithm. One approach to choosing the optimal number of clusters is to use the elbow method[14] [142]. Hence, in the following subsection, a brief discussion on k-means algorithm followed by the elbow method is presented.

k-means Algorithm

The k-means algorithm is one of the clustering algorithms that is used to split an unlabelled dataset into k clusters, $C = \{C_1, C_2, \ldots, C_k\}$, where the optimal number of clusters, k, also represents the number of cluster centroids and C_k denotes the k^{th} cluster. The number of clusters is usually determined before hand using the elbow method (which would be elaborated in the following paragraphs). Hence, given the traffic loads of the SBSs in each MC of the UDHN, $\tau_t^{i,j}$, and the optimal number of clusters, k to partition $\tau_t^{i,j}$, the task of the k-means algorithm is to minimise the intra-cluster distance between similar traffic loads and the centroid (mean) of each cluster. The objective function of k-means algorithm, $J(k, \tau_t^{i,j}, \Lambda)$, can be expressed as [275, 276]:

$$\min_{\Lambda} J(k, \tau_t^{i,j}, \Lambda) = \sum_{m=1}^{k} \sum_{\tau_t^{i,j} \in C_{\text{k}}} \left\| \tau_{i,j} - \Lambda \right\|^2, \tag{3.21}$$

where Λ is the mean or center of the cluster C_{k}.

Selection of Optimal Number of Clusters (Elbow Method)

One of the most critical aspects of clustering is determining the optimal number of clusters to split the dataset. This is because the performance of the cluster-based cell switching algorithm depends on selecting the optimal number of clusters

[14] In order to partition a given dataset into clusters, the optimal number of clusters must first be determined. Hence, elbow method is a common algorithm that is used to determine the optimal number of clusters that should be used by the k-means algorithm to partition any given dataset.

to group the SBSs in the UDHN. The elbow method provides a suitable way of finding the optimal number of clusters from a given dataset. In the elbow method, the optimal number of clusters can be obtained by first evaluating the sum of the squares errors (SSE) between the data points in each cluster and the centroid to obtain k values. The SSE can be expressed as [142]:

$$\text{SSE} = \sum_{g=1}^{k} (X - c_k)^2 , \tag{3.22}$$

where k is the number of clusters, X is the data points in a certain cluster, and c_k is the centroid of that cluster. Then the SSE is plotted against the k values. The value of k where the SSE curve forms an elbow before flattening out is selected as the optimal number of clusters to partition the data points in the dataset.

Multi-level Clustering Based Cell Switching scheme

The MLC algorithm performs repeated clustering, and re-clustering[15] of the SBSs deployed within the coverage area of the MBS according to their traffic loads and attempts to offload the traffic load of the SBSs in the lightly loaded cluster to the MBS. Then the total power consumption of the UDHN after offloading the traffic of the cluster(s) to the MBS is determined. Finally, the cluster(s) which results in the least power consumption in the UDHN is selected as the optimal cluster(s). The pseudo-code of the MLC algorithm is presented in Algorithm 6, where C_{opt} is the optimal number of clusters(s) to switch, $\text{E}_{s_{\min}}$ is the minimum energy by switching off cluster(s), ν is a table containing all clusters, E_x is the energy saved a cluster is switched off, $\tau_t^{i,x}$ and $\tau_t^{i,1}$ are the traffic load of any given cluster, and that of the MBS respectively. The description of the algorithm is described as follows.

The elbow method is used to determine the optimum number of clusters. Based on the optimal number of clusters, the k-means algorithm is applied to perform the first level of SBS clustering according to their traffic loads. After that, the aggregate traffic load of each cluster ($\tau_t^{i,x}$) is computed and compared to the available radio resources at the MBS in order to determine the number of clusters that can be switched off. Then, the energy-saving of the network is computed after offloading the traffic of each of the selected cluster(s) to the MBS. The remaining clusters whose aggregated traffic load exceeds the maximum

[15]The process of clustering and re-clustering is part of the internal working mechanism of the algorithm, and this occurs repeatedly until the optimal number of cluster(s) that should be switched off is determined. However, the actual implementation of the decision of the algorithm on the network takes places every 10 minutes.

Algorithm 6: MLC

input : Traffic loads of MBS and SBSs
Initialize optimum number of cluster(s) to switch off, $C_{opt} \leftarrow$ None;
Initialize minimum energy saved by switching off cluster(s) x, $E_{s_{min}} = 0$;
Perform optimised k-means clustering with elbow-method to determine the optimal number of clusters, k;
Initialize the table, ν, containing the clusters and the traffic loads of the SBSs;
for $x \in k$ **do**
  if $\tau_t^{i,x} + \tau_t^{i,1} \leq 1$ **then**
    E_x = Energy saved by switching off cluster x;
    Remove cluster x from ν;
    if $E_x \geq E_{s_{min}}$ **then**
      $C_{opt} \leftarrow x$;
      $E_{s_{min}} \leftarrow E_x$
    end
  end
end
if *there is any cluster left in* ν **then**
  Recursively return to step 3 by re-clustering each cluster left in ν;
else
  output: C_{opt}
end

traffic demand that can be served by the MBS ($\tau_m^{i,1} = 1$ (normalized)) are further divided into smaller clusters by repeating the preceding steps until only a single SBS is left whose traffic demand exceeds that of the MBS or all the SBSs have been exhausted and there are no more SBSs left. Finally, the energy-saving of the UDHN is computed after the various levels of clustering and traffic offloading have been carried out. The energy-saving values obtained are then ranked in descending order, and the one with the highest energy saving is selected as the optimal cluster/sub-cluster, and all the SBSs in that cluster are switched off.

Threshold-based Hybrid Cell Switching Scheme

Even though the MLC method can be applied for cell switching when the network dimension is very large, however, it produces results that are very sub-optimal compared to the ES algorithm. It should be noted that the goal of any sub-optimal algorithm is to produce a result that closely approximates the ES solution. As a result, the optimality of the MLC method is improved by developing the THESIS algorithm, which combines the advantages of MLC in terms of scalability (i.e., its applicability when the number of SBSs in the network becomes very

large) and that of the ES algorithm in terms of optimality, to produce a solution that is close to the optimal result. In addition, the proposed THESIS is scalable and very computationally efficient compared to the ES method. The pseudo-code of the THESIS is presented in Algorithm 7, where B_{th} is the maximum number of BSs that can be in a cluster, BS_{cal} is the best combination of SBSs to switch off in each cluster, BS_{opt} is the optimal SBS combination to switch off, $E_{BS_{opt}}$ is the energy saved in of the network when the optimal set of BS is switched off. The procedure for the implementation of the algorithm is illustrated in Fig. 3.9, and described as follows.

Algorithm 7: THESIS

input : Traffic loads of MBS and SBSs
Initialize B_{th} as the maximum number of BSs in the cluster.;
Initialize optimal SBS combination to switch off, $BS_{opt} \leftarrow$ None;
Initialize minimum energy saved by switching off SBSs, $E_{s_{min}} = 0$;
Perform optimised k-means clustering with elbow-method to search optimal k-cluster.;
Initialize the table, ν, containing the clusters and the traffic load of the SBSs;
for $x \in k$ **do**
    if $|k_x| \leq B_{th}$ **then**
        Run ES search and obtain the best combination of SBSs to switch off (BS_{cal}) and their respective power consumption $E_{BS_{opt}}$;
        if $E_{s_{min}} \leq E_{BS_{opt}}$ **then**
            $BS_{opt} \leftarrow BS_{cal}$;
            $E_{s_{min}} \leftarrow E_{BS_{opt}}$;
            Remove cluster k_x from ν;
        end
    end
end
if *there is any cluster left in* ν **then**
    Recursively return to step 3 by re-clustering individual cluster left in ν;
else
    output: BS_{opt}
end

The proposed cell switching and traffic offloading procedure can be divided in three phases:

- **Initialization phase:** In this phase, the SBSs and the MBS send their traffic load information to the local controller. Then, based on their traffic load information, the local controller does the initial partitioning of the

SBSs in the MC into different clusters using both elbow method (3.22) and k-means clustering (3.21).

- **Decision phase:** The decision phase is where the local controller decides which set of SBSs to switch off per time. It does this by evaluating each cluster and comparing the number of SBSs in them to the threshold value (B_{th}[16]). For the clusters where the number of SBSs is less than B_{th}, ES algorithm is applied to them in order to obtain the set of SBSs to switch off that would result in maximum energy saving in the network while respecting the QoS constraints. The clusters with number of SBSs greater than B_{th} are further partitioned to smaller clusters with number of SBSs is less than or equal to B_{th}, then ES is applied to each of the clusters. Then, the sets of SBSs that can be switched off in each cluster that would result in maximum energy saving in the network while satisfying QoS constraints are obtained. Finally, the maximum energy saving values obtained from the different sets of SBSs are ranked in descending order, and the one with the highest energy saving is selected as the optimal set of SBSs to switch off.

- **Execution phase:** This is the phase where the decision taken regarding the optimal set of SBSs to switch off[17] is implemented. Before the switching off operation is executed, the local controlled first ensures that all the concerned SBSs offload their traffic to the MBS, after which they are then switched off.

The difference between the proposed THESIS and MLC is that MLC repeatedly clusters the SBSs and tries to find the cluster(s) to switch off based on the one that satisfies the constraints and yields the maximum energy saving. On the other hand, THESIS goes a step further by searching within the clusters to select the set of SBSs that meet the constraints and give a maximum energy saving. This ability of THESIS to search within the clusters enables it to discriminate between the different types of SBSs (in terms of capacity and power consumption profile) when selecting the set of SBSs to switch off within the clusters while the MLC does not have this capability. Thus giving THESIS an advantage over the MLC.

[16]The value of B_{th} was determined experimentally by trying different values and selecting the one that results in least computation or simulation time.

[17]The power consumption due to switching off and on has not been taken into consideration in this work, as the emphasis of this work is on developing a computationally efficient and scalable algorithm for cell switching in UDHNs. Future work would consider the effect of the power consumption due switching off and on of the BSs on the amount of energy savings that can be obtained in the network.

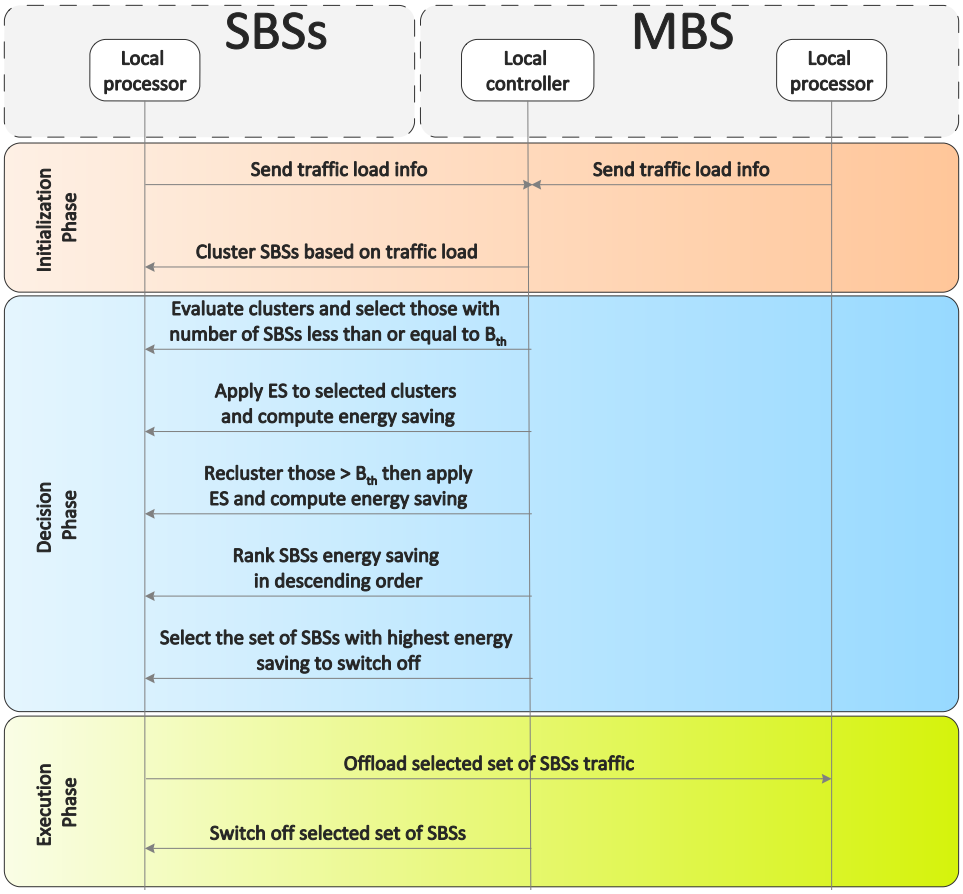

Figure 3.9: Proposed Cell switching and traffic offloading implementation procedure.

3.6.4 Performance Evaluation

In this Section, the performance of the proposed scheme is evaluated using various metrics and compared with other benchmark algorithms. In addition, the complexity comparison of the proposed and benchmark methods is also carried out. The proposed THESIS can be applied to any network irrespective of the network dimension in terms of number of MCs involved. It should be noted that since the UDHN comprises many MCs, each consisting of one MBS and several SBSs, the proposed framework is implemented at the MBS of each MC as it is responsible for controlling the operations of the SBSs within the MCs. Hence, only one MC in the UDHN[18] is considered since the results obtained can be applied to all other MCS in the network. The hardware used for this simulation is a DELL XPS 7590 laptop computer, with the following specifications: Intel core i7-9750H processor @ 2.6 GHz(12 CPUs), ~ 2.6GHz, 32GB of RAM, Windows 10 64bit OS and 1

[18]Please not that the heterogeneity in this work arises from the use of different types of BSs, MBS, RRH, micro, pico and femto cells, each having different power consumption parameters as can be seen in Table 3.3.

TB SSD of disk space. Spyder version 4.0.1, which runs Python version 3.7, is used as a software. To work with Spyder, the development environment chosen was Anaconda, which is a free complete suite popular for Python development as well as development of other languages. The parameters used for the simulations are presented in Table 1.

Traffic Data and Simulation Parameters

To compute the total power consumption of the UDHN using (3.15), the traffic load of the MBS and SBSs are required. The call detail record (CDR) of the city of Milan that was made available by Telecom Italia [272] is used as the dataset for this simulation. The dataset has the city of Milan divided into 10000 square grids, with each grid having an area of 235 $\times$ 235 square meters. The call, text message and internet activities performed in each grid were recorded with a 10 minutes resolution for two months (November-December 2013). Even though the activity levels of the dataset are unit-less and no information regarding how the dataset was processed was provided, it was assumed that the CDR of each grid is their traffic load as they represent the amount of network resources utilised by the users within each grid for each time slot. However, in the course of data processing, only the internet activity level was considered as the traffic load for the BSs since the 5G networks being investigated are mainly internet protocol based. The combination of the internet activity level of two randomly selected grids was used to denote the traffic load of the MBS, while that of a single grid was considered for each of the SBSs. The traffic loads were then normalized with respect to the amount of radio resources of each of the SBSs in the UDHN (i.e. RRH, micro, pico and femto SBSs).

Performance Metrics

- **Power Consumption:** This is the instantaneous power consumption of the UDHN during the simulation time for each method based on (3.15). This metric enables us to carefully evaluate the performance of each approach as it reflects the instantaneous changes in power consumption of the network at different times of the day.

- **Energy Saved:** This metric is used to quantify the total amount of energy (in Joules) that is saved over the whole simulation time (24 hours). The energy saved for the proposed and benchmark approaches are obtained by comparing the presented methods with the case where all the BSs (both MBS and SBSs) are always on (it will be referred to as all-always-on(AAO)

Table 3.3: Simulation parameters for THESIS

Parameter	**Value**
Bandwidth of MBS	20MHz
Bandwidth of SBSs	15MHz, 10MHz, 5MHz, 3MHz
Number of RBs per MBS	100
Number of RBs per SBSs	75, 50, 25, 15
P_{tx} (MBS) (W)	20
P_{tx} (RRH, micro, pico, femto) (W)	20, 6.3, 0.13, 0.05
P_{o} (MBS) (W)	130
P_{o} (RRH, micro, pico, femto) (W)	84, 56, 6.8, 4.8
η (MBS, RRH, micro, pico, femto)	4.7, 2.8, 2.6, 4.0, 8.0
$P^{\text{s}}_{\text{BS}_{i,j}}$ (RRH, micro, pico, femto)(W)	56, 39, 4.3, 2.9
B_{th}	12
ξ	0.2556

hereafter), such that the energy consumption of the presented methods and AAO are determined, and the difference between the presented method and AAO are individually calculated as their energy saved.

- **Carbon Emission:** One of the benefits of energy optimisation is that it ensures the reduction of the carbon foot print of the network. The carbon emission level of the network can be obtained from the total energy consumption with the help of the CO_2 conversion factor (ξ). The CO_2 emission ($\mathcal{E}_{CO_2}$) associated with the energy consumption of the UDHN (E_{u}) can be expressed as [250]:

$$\mathcal{E}_{CO_2} = \xi \sum_{t=1}^{T} E_{\text{u},t}. \tag{3.23}$$

- **Coverage Loss ($\mathcal{C}_L$):** The effect that both the proposed and benchmark methods have on the QoS of the network after their implementation is evaluated using this metric. The coverage loss is defined as a measure of the total traffic load of the network that is lost due to the implementation of cell switching [185]. In calculating $\mathcal{C}_L$, the percentage difference in the total traffic load of the network before and after cell switching is obtained. This can be expressed as:

$$\mathcal{C}_L = \frac{\Upsilon^i - \hat{T}^i}{\Upsilon^i} \times 100\%, \tag{3.24}$$

where Υ^i is the total traffic load of the UDHN before cell switching and

traffic offloading while $\hat{T}^i$ is the total traffic load of the UDHN after cell switching and traffic offloading.

Benchmarks

1. **ES:** This method yields optimum results and is always guaranteed to find the best switching pattern from all possible combinations of SBSs switching patterns. It also considers the amount of radio resources at the MBs when determining the best switching option such that the maximum traffic demand that the network can serve is not exceeded. Hence, the QoS of the network is always guaranteed when this method is applied. The goal of any cell switching algorithm is to closely approximate this approach.

2. **MLC:** This scheme has been described in detail in Section 3.6.3. It employs only k-means algorithm to determine the optimal number of clusters to switch off per time in order to minimise the total power consumption of the UDHN. This method involves much lesser computation overhead compared to ES, respects the QoS constraints as ES, and can be applied even when the network dimension is very large. However, Its performance is sub-optimal compared to the ES approach.

3. **AAO:** In this approach, no cell switching is implemented, and as such, all the SBSs are continuously left on. There is also no need for traffic offloading in this method because none of the SBSs are turned off. This method ensures that the QoS of the network is always maintained, but there is no energy saving in this approach since the SBSs are always kept on.

Since the goal of this paper is to find a suitable trade-off between optimality and computational complexity, ES and MLC algorithms have been selected as benchmarks[19] in this work. ES algorithm is selected as one of the benchmarks as a representative of an optimal algorithm because it has been proven in various aspects of wireless communications [19,277,278] to always find the optimal solution. Although it is optimal and accurate, its complexity is very high and increases exponentially as the network size increases. On the other hand, MLC algorithm is selected as another benchmark, which is a representative for low-complexity solutions and have been applied in many wireless network research areas [266–268] to find computationally efficient and scalable solutions. However, the performance of these solutions are usually far from optimal. Moreover, AAO is also used as a

[19]These two benchmarks have been chosen in this work because other closely related solutions existing in the literature fall under one of these category. Moreover, they can also be easily applied to the problem at hand, without encountering many complications.

benchmark because it helps to quantify the amount of energy and CO_2 savings that can be obtained when the cell switching methods are implemented.

It should be noted that tabular RL approaches such as Q-learning, multi-armed bandit, and deep RL approaches such as deep and double-deep Q-networks that are known for intelligent decision making have not been considered as benchmarks in this work. This is because, as pointed out in Sections I and II, it is computationally demanding to learn the state-action table, and a large memory is required to store the learned state-action table when the network dimension is very large, as considered in this work. It is also very computationally demanding to train deep RL models [123, 146] as such, they cannot be applied for online cell switching operation considered in this work. The goal of this work is to develop a solution that closely approximates the optimal solution. Therefore, since ES is always guaranteed to produce the optimal result, it is selected as the principal benchmark in this work. The MLC algorithm which is used as a benchmark was inspired by one of the closely related works in the literature [268]. However, most times, it is very challenging use closely related works as benchmarks because even though the problems may look similar, each has their own peculiarities and would entail going through a rigorous process before one can apply them to the problem at hand.

Results and Discussions

Fig. 3.10a presents a comparison of the instantaneous power consumption of the proposed and benchmark methods over a 24 hour-period for 20 SBSs. The first thing that can be observed from Fig. 3.10a is that the pattern of power consumption of both the proposed and benchmark methods follow that of the traffic load of the network throughout the day, such that it is low when the traffic load is low and high when the traffic load is high. The reason for this is that there are more opportunities to switch off many SBSs when the traffic load is low than when it is high, hence the discrepancies in power consumption values at different times of the day. Second, the power consumption of AAO is higher than both the proposed THESIS and benchmark methods because no BS switching is performed in this method which means that all the SBSs are constantly kept on. Third, the power consumption of the ES method is the lowest of all the methods, including the proposed method, because it searches sequentially through all the possible SBS switching combinations to select the option that leads to least energy consumption in the network at each time slot. However, this approach usually involves a huge computation overhead, making it only applicable to networks where the number of SBSs are few.

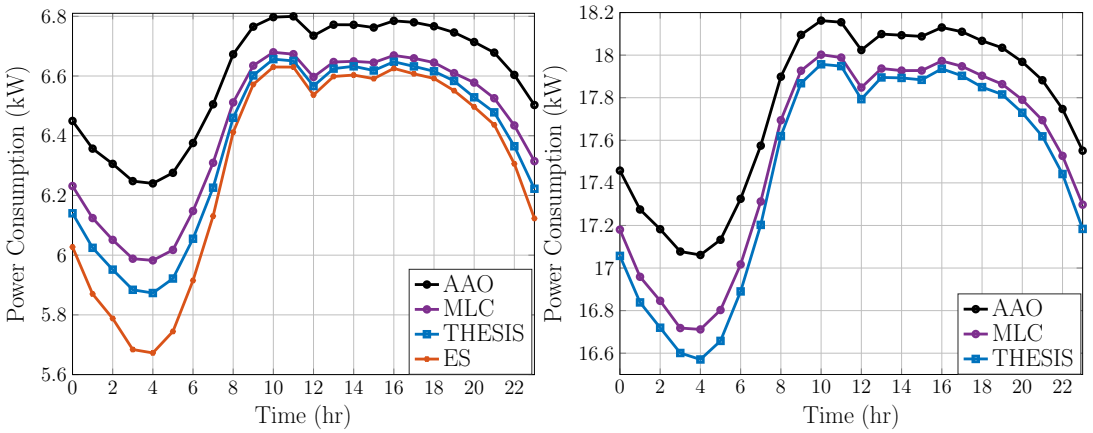

(a) $N = 20$ (b) $N = 60$

Figure 3.10: Instantaneous power consumption over a 24 hrs period for 20 and 60 SBSs.

Fourth, it can be observed that the performance of the proposed THESIS method is very close (with 0.4% difference) to that of the ES method when the network traffic is high, but the margin becomes wider (with 3.5% difference) when the network traffic is low. The reason for the higher performance difference when the network traffic load is low than when it is high is because during the periods of low traffic, even though there are more opportunities to switch off more SBSs, because the THESIS first partitions the SBSs into clusters before applying the ES to each cluster, the size of the search space is reduced. Hence, it has lesser opportunity to explore in order to determine the best switching combination that would result in lower power consumption in the network. On the other hand, during periods of high traffic load, the performance of the proposed method and the ES are much closer because there are very few opportunities to switch off the SBSs, therefore the higher search space of the ES does not give it much advantage over the proposed method. However, the time complexity of the proposed method and ES is analyzed in Section 3.6.4, it will be clear that the compromise in performance is greatly compensated with the complexity and scalability.

Fifth, it can be observed that apart from AAO, where no SBS is switched off, the performance of other methods exceeds that of MLC. This can be traced to the fact that MLC considers only the traffic loads of the SBSs when clustering and offloading the traffic of sleeping SBSs to the MBS, without considering that there are different types of SBSs (with different capacity and power consumption profiles), and as such it might just be preferable to switch off a few SBSs with higher power consumption than many SBSs with low power consumption. It can also be observed that the performance of the MLC closely follows that of the proposed THESIS, particularly during periods of high network traffic, however, THESIS

is able to outperform MLC more during periods of low traffic load because, in addition to clustering the SBSs according to their traffic load, ES is also applied to each cluster which enables it to discriminate among the different types of SBSs in order to select the best combinations of SBSs that would result in lesser power consumption in the network compared to the MLC approach. However, during periods of high traffic load in the network, the difference in power consumption between both methods is not significant because there are very few opportunities to switch off SBSs and lesser opportunities to search within the clusters. Hence, their performance becomes very close during such periods.

Fig. 3.10b shows the power consumption of the UDHN when 60 SBSs are deployed. It should be noted that ES algorithm is not considered in this scenario due to the huge computation overhead involved as well as limitations in the computing capacity of the device that was utilised. It can be observed that the trend of the power consumption when the proposed THESIS and benchmark methods are applied in Fig. 3.10b follows the traffic load of the network as obtained in Fig. 3.10a except that the magnitude of power consumption of the network is much higher in Fig. 3.10b because more SBSs are deployed in this scenario compared to the previous one. This finding is also quite intuitive since the total power consumption of the network (P_{tot}) is the cumulative sum of the power consumption of all the BSs involved in the networks, as seen in (3.14), and thus once the network dimension rises, the total power consumption also increases. The power consumption of AAO is also higher in this scenario compared to all other methods because no SBSs is turned off but are all left on to serve user demands. The performance of MLC also follows that of the proposed THESIS in this scenario, with THESIS performing much better than MLC during periods of low traffic. This is due to the superior ability of THESIS to determine the best set of SBSs from the various clusters to switch off that would result in lesser power consumption in the network rather than trying to switch off a whole cluster without considering the types of SBSs in the cluster as this affects the magnitude of power consumption that can be obtained.

Fig. 3.11 presents the total energy saved over a 24-hour period when the proposed and benchmark methods are applied for different number of SBS deployment. The first thing that can be observed from Fig. 3.11 is that the total energy saved in the network increases as the number of SBSs deployed increases. This is due to the fact that with more SBS deployment, there are more opportunities to switch off many SBSs, which leads to more energy saving. It can also be observed that the ES method gives the highest energy saving of all of the methods applied. However, it is accompanied by a very high computation overhead, and

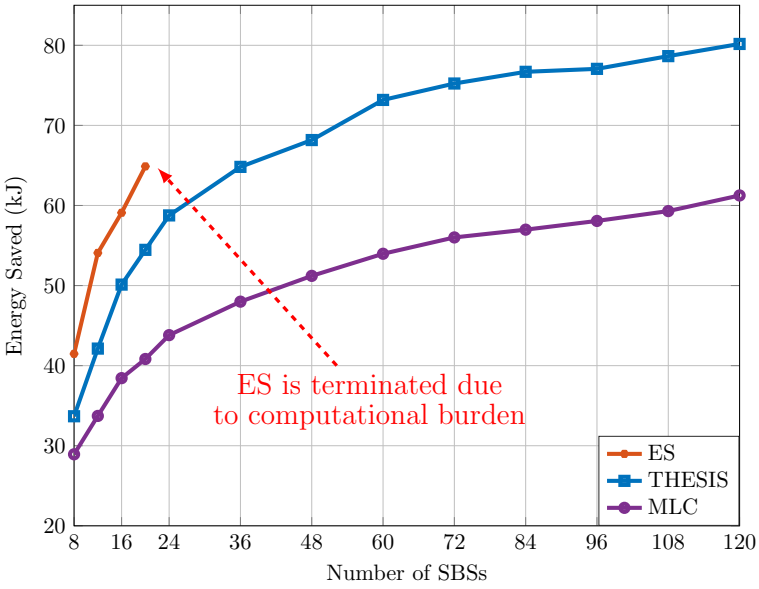

Figure 3.11: Energy saved in the UDHN for different number of SBSs over a 24 hrs period.

hence it cannot be applied in real networks with very large dimensions. As a result, the simulation had to be stopped at 20 SBSs due to the limitations of the device that was utilised to handle such computation complexity.

The magnitude of the energy saved in the network when the proposed THESIS is applied also increases as the number of SBSs deployed increases. It can also be observed that the energy saved increases with high magnitude as the number of SBSs increases until when the number of SBSs reaches 60, afterwards the difference in energy saving between successive SBS deployments becomes smaller and almost constant. The rationale behind this is that even though there are more opportunities to switch off more SBSs as the number of SBSs increases, due to limited amount of radio resources at the MBS, the difference in the amount of SBSs that can be switched off is not much after 60 SBSs. The energy saving performance of THESIS is quite lesser than that of ES because of the wider search space that is available for searching for the optimal solution in ES compared to THESIS, however, the much lesser computation overhead involved in former compared to the latter makes it a more preferable for practical network deployment comprising many SBSs.

The energy saving of MLC method also increases with the number of SBS deployment, however, its energy saving seems to flatten out faster than THESIS approach. The inability of MLC to discriminate between the different types of SBSs when clustering the SBSs accounts for its lesser performance compared to the proposed method while the limitation in the amount of radio resources

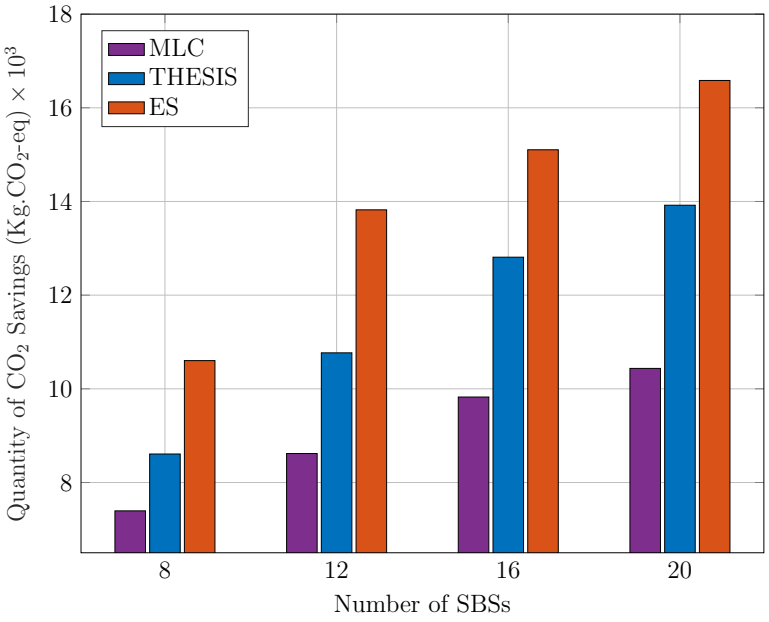

Figure 3.12: Quantity of CO_2 saved for different number of SBSs over a 24 hour period.

needed for offloading the traffic of the SBSs at the MBS accounts for the lesser difference in energy saving in MLC method after 60 SBSs similar to what is observed in THESIS method. Finally, it can be observed that the difference in the energy saving between the THESIS and MLC also increases with higher magnitude as the number of SBSs increases until about 60 SBSs when it becomes almost constant. The reason is that there are more opportunities to switch off more SBSs as the number of SBSs increases which accounts for more energy saving in both THESIS and MLC while THESIS is able to discriminate among the different types of SBSs when making a cell switching decision thus making it produce higher energy saving compared to MLC. However, the almost constant energy saving difference observed after about 60 SBS is due to insufficient radio resources at the MBS to accommodate more traffic from the SBSs before turning them off.

Fig. 3.12 presents the quantity of CO_2 saving that is obtained when the proposed and benchmark methods are applied to the UDHN with different number of SBSs. Note that the CO_2 saving up to 20 SBSs is shown here so as to study the relative performance of the all the algorithms since the ES approach cannot be applied beyond this number of SBSs due to computation complexity. It is important for us to quantify the amount of CO_2 savings because one of the goals of the proposed cell switching algorithm is to ensure that the carbon foot print or quantity of CO_2 emission associated with the UDHN is greatly reduced by reducing the amount of energy consumption of the network as most of the

energy used to power the BSs are obtained from fossil fuels. Thus, a reduction in the energy consumption of the network leads to a reduction in amount of energy demanded which translates in lesser CO_2 emission thereby resulting in environmental conservation and prevention of global warming [14, 279].

From Fig. 3.12, it can be observed that the quantity of CO_2 saving increases as the number of SBSs increases because there are more opportunities to switch off more SBSs, which translates to greater CO_2 saving. The ES algorithm gives the highest CO_2 saving but as already observed previously, it computational complexity limits its application in large scale networks such as UDHN. The CO_2 saving of the proposed THESIS algorithm is about 18% lesser than that of ES due to the better switching ability of ES, however its computation efficiency makes it more suitable for application in real network even when their dimension is very large. The MLC approach produces the least CO_2 savings because of its sub-optimal performance compared to the proposed method even though it is most computationally efficient, its very sub-optimal performance does not make it suitable for application in large networks.

The $\mathcal{C}_L$ metric has been considered as a measure of the QoS of the network in order to ensure that the constraint in (3.18) and (3.19) are maintained. The QoS of the network is maintained by ensuring that the total traffic demand that is served by the network before and after cell switching is performed remains constant by offloading the traffic of the SBSs that are to be switched off to the MBS and ensuring that the maximum traffic demand that can be served by the MBS is not exceeded during traffic offloading. A coverage loss of 0% is obtained when both the proposed THESIS and the benchmark methods applied. This means that THESIS and the benchmark methods are able to ensure that the QoS of the UDHN is not violated. THESIS is carefully designed such that it checks whether a given combination of SBSs in each cluster can be offloaded to the MBS before proceeding to switch them off. A similar approach is also employed in the ES approach in order to ensure that the capacity of the MBS is not exceeded. For the MLC approach, the aggregate traffic of each cluster is also compared with the available radio resources at the MBS to see whether it can accommodate it before turning off the cluster(s).

Complexity

One of the ways of evaluating the complexity of an algorithm is to determine its time complexity, that is, the simulation run time or time taken for the simulation to be complete [280]. Fig. 3.13 presents the time complexity comparison between the proposed THESIS approach and the benchmark methods. From Fig. 3.13, it

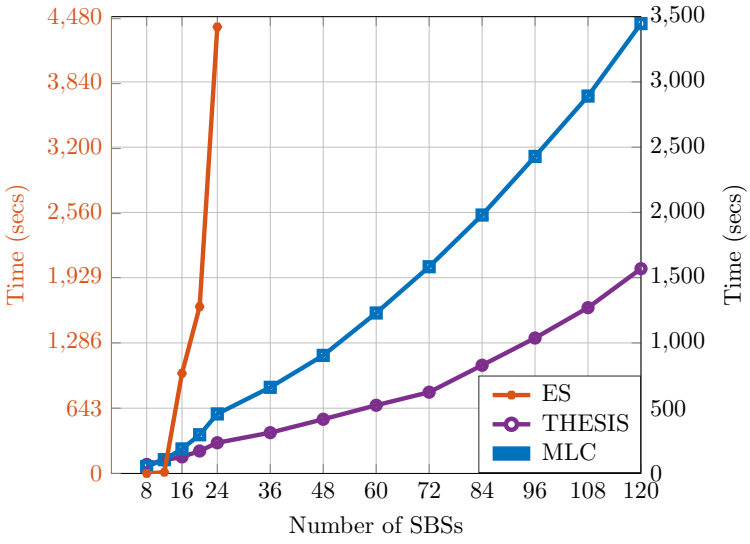

Figure 3.13: Time complexity: total time taken to complete the simulation for different number of SBSs. Note: Two time axis are used in this figure for the purpose of clarity, else both times mean the same thing.

can be observed that with ES algorithm, when the number of SBSs are few (i.e., less than 16), the time complexity is very low, but from 16 SBSs and above, there is an exponential rise in the computational complexity. This is because the number of search spaces increases exponentially with every increment in the number of SBSs. Therefore, even though ES is always guaranteed to give the optimal switching strategy, due to its huge computational overhead, it is not feasible to apply it for cell switching in UDHN comprising large number of SBSs.

The time complexity of the MLC algorithm can be observed to increase gradually and almost linearly. The complexity of MLC is very low because the number of clusters formed do not greatly increase as the number of SBSs increases, hence lesser time is required to select which cluster to switch off. Though the MLC is the most computationally efficient method, it is the least optimal approach and may not lead to much energy saving in the UDHN when applied. The time complexity of THESIS is also quite low when the number of SBSs are less than 20, but afterwards, its time complexity begins to increase with a higher magnitude compared to the MLC. Overall, THESIS exhibits a polynomial time complexity which is because in addition to clustering, it also involves searching for the optimal combination of SBSs to switch off in each cluster. However, with the introduction of B_{th}, which limits the number of SBSs in the clusters where ES would be applied, the number of search spaces is reduced. The time complexity of THESIS is much lesser than that of ES and slightly higher than that of MLC but its energy saving performance is much closer to the optimal solution than the MLC.

In Summary, comparing the energy saving performance of the algorithms in Fig. 3.11 and the complexity in Fig. 3.13, it can be observed that the energy and CO2 saving performance of THESIS is 31% higher but 95%[20] more computationally complex than MLC while on the other hand, it is 30% less optimal but has a computation complexity that is significantly lesser than that of ES[21]. These values prove that the developed algorithm does not compromise on the performance much while reducing the complexity, making it more applicable and feasible for the next generations of cellular communication networks, where the number of BSs are expected to be a lot higher than the legacy networks through the concept of network densification.

3.7 Conclusion

In this chapter, the need for the development of a scalable and computationally efficient cell switching framework for next generation cellular networks was emphasized because of the increasing size and complex of these networks. Then attempts at developing computationally efficient and scalable models using Q-learning and ANN were first discussed followed by discussions on THESIS, the hybrid cell switching model which enabled the actualization of this objective. THESIS is scalable and is able to—without much loss in optimality—produce a solution that has much lesser computation complexity compared to optimal ES algorithm and can be applied to a network where a large number of SBSs are deployed. A benchmark cell switching scheme using MLC was also developed which though is more computationally efficient than the proposed method, has a poorer performance with respect to energy and CO_2 savings compared to THESIS. Overall, the performance of THESIS algorithm shows that it is able to find a good trade-off between optimality in terms of the amount of energy and CO_2 reduction that can be achieved and complexity in terms of the computation overhead required to find the optimal solution. This is very important because with the massive deployment of SBSs in next generation networks, achieving energy efficient communication via real-time cell switching decision would be very

[20]Even though the complexity of THESIS seems significant compared to that of MLC, it can be seen from Fig. 3.11 that MLC produces a very sub-optimal result compared to ES, which makes it inapplicable for cell switching in UDHNs. The increase in the complexity of THESIS, is the trade-off that is incurred for having a performance that is close to that of the optimal ES algorithm, though with significantly lesser complexity. Hence, the suitability of THESIS for cell switching in UDHNs. However, since the complexity of the proposed solution increases with the number of SBSs deployed in each MC, the size of the network that it can be applied to would depend on the latency requirements of the network.

[21]These values are the averages of the values for different number of SBSs, and obtained from Fig. 3.11 and Fig. 3.13.

challenging for both heuristic and ML algorithms because of the dynamic network condition and the huge computational complexity involved. Although many works in the literature have tackled the cell switching problem, the main issue is always scalability, which will be more severe with the next generations of cellular communications networks. Therefore, with the implementation of the proposed solution (THESIS), the cell switching concept will be able to play its role in making wireless networks more energy efficient—considering the stringent EE requirements of 5G and beyond networks, it would become more obvious how this is crucial in such networks.

Chapter 4

Revenue Maximisation in 5G HetNets

4.1 Introduction

The demand for capacity improvement in order to achieve enhanced data transmission is a constant challenge facing MNOs. This is due to increase in the number of connected devices, increasing use of data hungry applications, such as online gaming and multimedia services, as well as other emerging use cases including virtual and augmented reality, driver-less cars, etc [281]. In addition, with the proliferation of IoT devices where virtually everything is connected to the Internet, the demand for more capacity would further escalate [282]. One of the ways of achieving capacity improvement is to opportunistically exploit the dormant spectrum resulting from the cell switching operation through spectrum leasing, in order to generate additional revenue for the MNOs while ensuring efficient spectrum utilisation. By so doing, both energy saving and revenue generation can be achieved in one goal. This would result in a joint optimisation problem involving energy consumption minimisation and revenue maximisation. Hence, the goal of this work is to obtain both energy saving and additional revenue via cell switching and spectrum leasing.

Various techniques for implementing dynamic cell switching in cellular networks have been proposed in the literature [237,239,243–245,248,250,260]. These methods comprise analytical, heuristic and ML-based approaches. Similar optimisation techniques have also been proposed for spectrum leasing [191,265,283–286]. However, very few research works have considered both cell switching and spectrum leasing for maximizing the revenue of the PN [193,194], even though only a homogeneous network deployment scenario as well as a fixed electricity and spectrum pricing policy were considered, thereby making their work quite simplistic.

In order to fill in the above-mentioned gaps in the literature, two different perspectives should be taken into consideration. First, the cell switching and spectrum leasing problems should be considered together in order to have a holistic view. Therefore, in this work, the cell switching and spectrum leasing concepts are combined to produce a joint optimisation problem. To do this, the energy saving via cell switching is converted to its monetary representative, that is, the reduction in the energy bills, such that the energy saving, and revenue can be combined. This enables us to model the joint optimisation problem in a way that a single objective function can be designed, since the outputs of both energy saving and spectrum leasing are monetary. Second, such holistic view should be tested in a more realistic and complex scenario to verify its applicability and feasibility. For this purpose, a HetNet scenario with different types of SBSs is considered. Moreover, in addition to classical fixed pricing policy, a dynamic pricing policy for both electricity and spectrum is also adopted. These two components of the considered scenario (i.e., diverse set of SBSs and dynamic pricing policy) make it not only more realistic but also more challenging, given that each type of SBS has different characteristics and the overall system becomes quite dynamic (e.g., the loads of BSs and the prices of electricity and spectrum change at each time slot).

The solution to this problem is non-trivial as it involves trying different options out of a large set of possibilities. The optimal solution is the ES approach because it tries all the possible options before selecting the best one; however, it results in a huge computational overhead especially when the number of SBSs deployed in the network becomes very large.

4.2 Related Works

Dynamic cell switching techniques are the most commonly employed methods for optimising energy consumption in cellular networks because they are the cheapest to implement and require minimal changes to network architecture [14]. These techniques result in significant energy savings compared to other methods such as cell zooming, bandwidth adaptation, sectorization, etc [22, 183]. For the sake of completeness, a few cell switching approaches are presented here since a more comprehensive state-of-the-art has been presented in section 3.2.

The authors in [239] proposed a SBS switching scheme to minimise the energy consumption in a HetNet based on stochastic geometry. In [243] the authors considered the problem of SBS power control and user association in HetNets and proposed a heuristic algorithm to determine the switching pattern of redundant

SBSs during periods of low traffic. In [248], a user association and cell switching algorithm based on belief propagation was developed to maximise the EE of a HetNet by switching off BSs with few users while transferring serving users to neighbouring BSs. In [244], the authors proposed an SBS switching mechanism based on particle swarm optimisation to minimise the energy consumption of a HetNet without violating QoS constraints. An SBS switching mechanism for EE optimisation in HetNet using genetic algorithm was proposed in [245] while respecting QoS constraints.

The authors in [250] proposed a RL-based cell switching approach to optimise the EE as well as the CO_2 emission in a HetNet. A cell switching and traffic offloading scheme for energy optimisation in ultra-dense network using artificial neural network was proposed in [260]. The authors in [237] developed a scalable RL based cell switching framework using SARSA algorithm with value function approximation to determine the optimal switching policy that would minimise the energy consumption in an ultra dense network while ensuring that the QoS of the network is maintained.

Even though dynamic cell switching results in significant energy savings, it also results in spectrum under-utilisation as the spectrum that was originally allocated to the SBSs that are switched off remain dormant when they are inactive. These dormant spectrum can be exploited via spectrum leasing operations.

There are three major reasons for performing spectrum leasing [29]: i) For monetary gains, ii) to maximise transmission rates, and iii) to reduce the energy consumption of PUs. In the first case, the PN leases some of its spectrum to the SN at a cost in order to generate additional revenue. In the second case, the PN shares some of its spectrum to the SN in exchange for assistance in data transmission, thereby enhancing the data rates of the PUs. In the third case, the SUs act as a relay to the PUs thereby reducing the transmission distance between the PUs and the BSs which leads to energy savings in the PUs. In this thesis, the first case where spectrum leasing is employed for monetary gains in order to maximise the revenue of the MNOs is the focus.

In this regard, various research works using techniques such as game theory, matching theory, and ML techniques, etc., have been proposed [191, 265, 283–288]. The authors in [283] proposed a traffic-adaptive spectrum leasing scheme whereby the SUs are able to negotiate the duration of channel leasing with the PUs in order to ensure their continual utilisation of the leased channel for the complete transmission of the data in their buffer. To achieve this objective, the average utilities of both the PN and SN were first formulated, after which a spectrum leasing agreement that is beneficial to both parties was developed using

Stackelberg game model.

The work in [265] proposed a joint optimisation scheme for spectrum leasing and spectrum allocation using both Stackelberg game and matching theory. The proposed approach is able to determine the best price for leasing the spectrum as well as the best PU-SU pair while enhancing the spectral efficiency of the PUs and SUs. In [284], the authors considered a spectrum leasing problem between MNOs and mobile virtual network operators (MVNOs) using matching theory in order to maximise the utilities of both parties in terms of spectrum leasing cost and bandwidth allocation. Their goal is to find a suitable pairing between the MNOs and MVNOs that would maximise the revenue of the MNOs as well as the bandwidth allocated to the MVNOs. The work in [191] considered the problem of spectrum leasing optimisation for CRN transmission over TV white spaces. A neural network based solution was proposed to determine the optimal transmission policy that would result in minimal spectrum leasing cost while considering the QoS of the CRN. The authors in [287] considered the spectrum leasing problem involving two sellers (PNs) with the aim of determining the optimal spectrum to lease to the SNs that would result in maximum revenue to both sellers. The problem was modelled as a non-cooperative game then a closed form expression of the Nash equilibrium that would maximise the spectrum leasing revenue of both sellers was derived.

In [288], the authors proposed a pricing-based spectrum leasing scheme in order to optimise the performance of both PUs and SUs while providing monetary profit to the PU. The problem was formulated as a non-cooperative game and some learning schemes were proposed to determine the optimal action of the SUs that would optimise the utilities of both parties. The works in [285] and [286] considered the problem of resource allocation and spectrum leasing in CRNs where the PUs lease part of their spectrum to the SUs in exchange for data transmission assistance from the SUs as well energy saving for the PUs. A resource optimisation model for the CRN to minimise the power consumption of the PUs, while considering the uncertainty of the communication environment was proposed. In addition, a distributed resource allocation algorithm was developed to determine the optimal resource allocation to the SUs that would result in energy saving for the PUs while guaranteeing the QoS of both PU and SUs. In [289], an adaptive spectrum leasing with channel aggregation for CRN was considered where the amount of spectrum that the PUs can lease to SUs varies with the number of active transmissions as well as the amount of buffered data. In addition, SUs with spectrum priority are allowed to utilise multiple channels for data transmission. A leasing algorithm was developed to adjust the amount

of spectrum to be leased while satisfying the requirement of both PUs and SUs.

Joint cell switching and spectrum leasing has been considered in [193] and [194] to maximise the profit of both PN and SN as well as to minimise the energy consumption of PN. The authors in [193] considered a CRN comprising both PN and SN where the PN aims to reduce its energy consumption by turning off some BSs and transferring the users to the SN to maintain their QoS. In addition, the PN obtains revenue by leasing the free spectrum to the SN while the SN also gains revenue from the PN by charging a roaming price. A sub-optimal heuristic algorithm was developed to optimise the energy consumption of the PN by determining the set of BSs to switch off. The work in [194] is similar to [193], however, its aim is to maximise the profit of both the PN and SN while considering the CO_2 emission and QoS.

In this paper, a cell switching and spectrum leasing framework is developed for revenue Maximisation in a HetNet. Different from previous works in [193] and [194] where a homogeneous network was considered for the PN, a HetNet with different types of SBSs is considered for the PN, which makes this work more realistic. In addition, traffic offloading from the PN SBSs that are switched off to the SN SBSs was not considered as in previous works, since this would lead to additional expenses on the part of the PN in the form of roaming charges. Rather, vertical traffic offloading where the traffic load of PN SBSs that are switched off are offloaded to the MBS to maintain their QoS is considered, in order to maximise the profit of the PN. Furthermore, a fixed pricing policy was considered in the previous works while in this work, both fixed and dynamic electricity and spectrum pricing policies as well as DT and NDT spectrum demand scenarios are considered. This is because both pricing policies and spectrum demand scenarios are a better representation of what is obtainable in real systems.

4.2.1 Contributions

In this work, a cell switching and spectrum leasing framework is proposed to maximise the revenue of the PN. The proposed algorithm can learn the optimal cell switching and spectrum leasing policy that would result in maximum revenue for the PN while ensuring that the QoS of the PN is maintained. The proposed framework is implemented locally at each MBS since they are responsible for controlling the SBSs under their coverage. The following are the contributions of this work:

- The energy saving due to cell switching is first converted to the monetary domain (e.g., the reduction in the electricity bills) in order to produce a joint

optimisation problem with a single optimisation objective, where both the energy saving and revenue from spectrum leasing are in the same domain (e.g., monetary domain), which makes it possible for them to be combined.

- The problem is formulated as a binary integer programming problem and a cell switching and spectrum leasing framework is developed using the SA algorithm to determine the optimal policy that maximises the revenue of the PN while ensuring that the QoS is maintained.

- A HetNet comprising four different types of SBSs is considered, which makes the network scenario more complex and realistic compared to the previous works that considered only homogeneous scenario.

- Two electricity and spectrum pricing policies: 1) fixed and 2) dynamic policy are considered, in order to study the effects of constant and varying electricity and spectrum prices on the maximum revenue of the PN, as both could be the cases faced in real systems. For the dynamic pricing policy, both DT and NDT spectrum demand scenarios are also investigated.

- Roaming charges incurred in previous works are avoided by ensuring that only vertical traffic offloading between SBSs that are switched off and the MBS of the PN is considered, in order to minimise additional expenses and maintain the QoS of the network.

- In addition to the ES algorithm, two benchmark solutions are also developed for comparison with the proposed framework.

- A complexity comparison of the proposed method with that of the ES is carried out to highlight the advantage of the proposed framework.

- Finally, in order to capture the realistic behaviour of the network, the performance of the proposed framework is evaluated using real data comprising call detail records (CDR) of Milan city via extensive simulations, and the result obtained is compared with benchmarks.

4.3 System Model

Two types of networks are considered: First, the PN is a HetNet with CDSA [162] comprising multiple MCs. Each MC consists of one MBS and several SBSs. The MBSs serve as control BSs, provide constant coverage and low data rate transmission. The SBSs are deployed within the coverage of the MBSs and serve

as data BSs to provide high data rate transmissions in hot spot zones. The communication between MBS and SBSs are carried out in the control channels, which are separated from the data channels. Four types of SBSs—RRH, micro, pico and femto—are considered. Second, a SN is also assumed to operate in the same coverage area and the HetNet allows this SN to lease some unused spectrum whenever PN SBSs are put to sleep.

In this context, the SN BSs periodically communicates their spectrum demand information to the MBS through a dedicated control channel. Similarly, the traffic load information of the SBSs is also periodically communication to the MBS through a dedicated control channel. The MBS then decides which set of SBSs to switch off in order to maximise the revenue of the PN based on the available radio resources in the MBS, the traffic loads of the SBSs, and the spectrum demanded by the SN's BSs without violating the QoS of the PN. This can be maintained by ensuring that the traffic load of the SBSs that are switched off are transferred to the MBS.

In this work, it is assumed that the traffic load of all users can be sustained by the network before cell switching and spectrum leasing is implemented, which means that the network has enough radio resources to support all user traffic demands. However, when cell switching and spectrum leasing is implemented, there is no guarantee that the network would always have sufficient resources to handle the traffic load of all users any more. Hence, the QoS is defined as the capacity of the network to sustain the traffic load of all the users after cell switching and spectrum leasing operation. This is referred to as coverage loss in [185].

Due to the CDSA employed, all the MCs are assumed to have similar deployment characteristics except for the number and composition of SBSs. In addition, they also function in a decentralized manner, with the MBS responsible for controlling the operations of all the SBSs in each MC. Hence, in this work, only one MC comprising 12 SBSs is considered, four of each type of SBSs, as a representation of other MCs within the network. Each PN SBS, has a SN BS associated with it, bringing the total number of SN BSs considered to 12. The network model is presented in Fig. 4.1.

4.3.1 Power Consumption of HetNet

The BS power consumption model in [65, 72] is adopted for estimating the power consumption of the BSs in the HetNet[1] The total power consumption of the

[1]Please not that the heterogeneity in this work arises from the use of different types of BSs, MBS, RRH, micro, pico and femto cells, each having different power consumption parameters

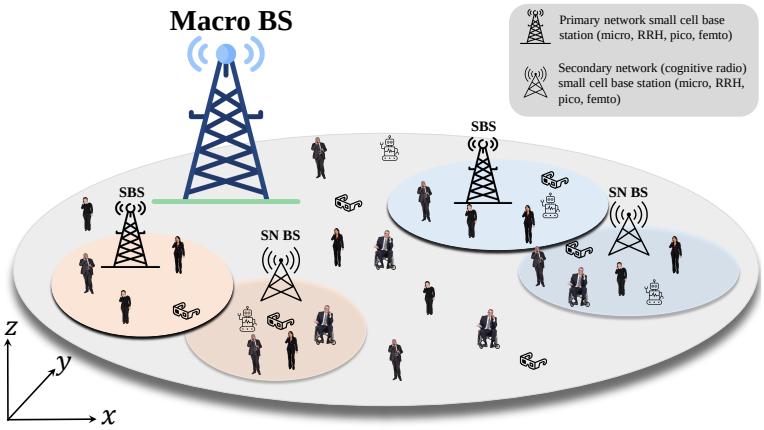

Figure 4.1: The PN comprises a HetNet deployment of MBS and various types of SBSs and the SN comprises SN BSs.

HetNet comprises sum of the power consumption of the MBS and that of all the SBSs under its coverage. The instantaneous power consumption of a BS, $P_{\mathrm{BS},t}$, at time t can be expressed as:

$$P_{\mathrm{BS},t}\ (\tau_t) = P_{\mathrm{o}} + \tau_t \eta P_{\mathrm{tx}}, \tag{4.1}$$

where P_{o} is the constant circuit power consumption, τ_t is the instantaneous traffic load of any BS at time t, η is the load dependent power consumption component and P_{tx} is the transmission power of the BS. It should be noted that the value of P_{o}, η, and P_{tx} is different for each type of BS (i.e., MBS, RRH, micro, pico, and femto).

As such, the instantaneous total power consumption of the HetNet, $P_{\mathrm{HN},t}$, at time t can be expressed as:

$$P_{\mathrm{HN},t}\ (\tau_t^{i,j}) = \sum_{i=1}^{M_m} \sum_{j=1}^{M_b} P_{\mathrm{BS},t}^{i,j}(\tau_t^{i,j}), \tag{4.2}$$

where $P_{\mathrm{BS},}^{i,j}$ and $\tau_t^{i,j}$ denotes the power consumption and traffic load of the j^{th} BS in the i^{th} MC respectively, and $P_{\mathrm{BS}^{i,1}}$ represents power consumption of the MBS in the i^{th} MC. M_m and M_b are the number of MCs within the HetNet and the number of BSs (including an MBS and SBSs) within an MC, respectively.

4.3.2 Pricing Policy:

Two kinds of pricing policies are considered for both the electricity and spectrum:

as can be seen in Table 4.1.

Fixed Pricing Policy: The unit cost of electricity as well as that of the spectrum remains constant throughout the day, irrespective of the fluctuations in energy or spectrum demand.

Dynamic Pricing Policy: The electricity and spectrum price varies according to the amount of electricity and spectrum demanded at different times of the day. The dynamic pricing model for electricity was adapted from [290], where the instantaneous electricity prices were obtained by multiplying the fixed price by a variable factor to indicate changes in the prices at different times of the day. For the dynamic spectrum price, it is assumed that the spectrum prices follow the traffic demand pattern of the PN. However, these values are scaled with the fixed spectrum price such that: $C_{\mathrm{RB},t} = m \,.\, C_{\mathrm{RB,F}}$, where m is a time variable function that changes with the instantaneous traffic load, τ_t, i.e., $m = f(\tau_t)$, $C_{\mathrm{RB},t}$ and $C_{\mathrm{RB,F}}$ are the dynamic and fixed spectrum price (i.e., cost per RB), respectively. According to 3GPP [291], a RB is equivalent to 12 successive subcarriers, thus taking one subcarrier to be 15kHz, one RB is considered to be 180kHz. The dynamic electricity and spectrum pricing policies are presented in Fig. 4.2.

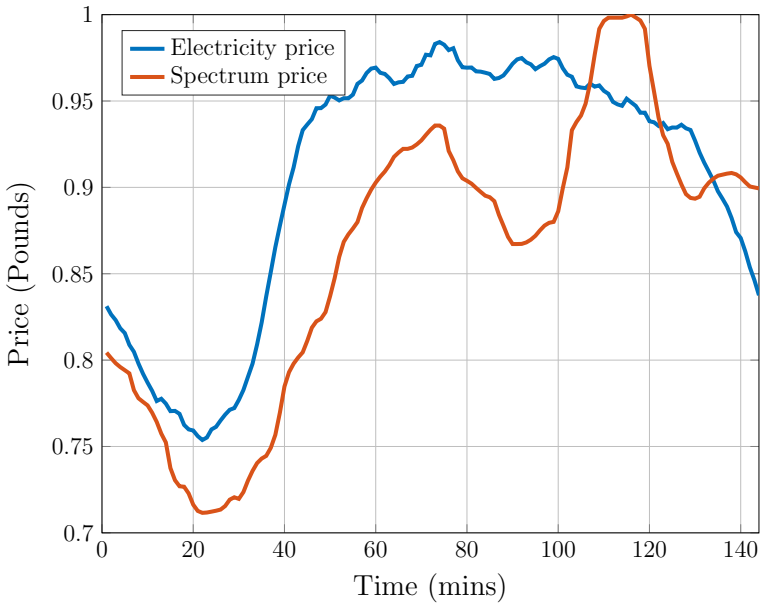

Figure 4.2: Dynamic electricity and spectrum pricing policy (normalized) for every 10 minutes over a 24 hours period.

Under the dynamic spectrum pricing policy, two types of spectrum demand scenarios are considered:

- **Non-Delay Tolerant (NDT):** This scenario deals with applications such as location updates, voice calls, etc., that require real-time data transmission and cannot tolerate delay because of the sensitivity of the information

and its requirement for quick decision making. For such applications, the SN has to demand for the spectrum as soon as the need for data transmission arises, irrespective of the spectrum price.

- **Delay Tolerant (DT):** There are some other applications such as meter readings, feedback from wearables, etc., whose information may not be needed for real-time decision making and hence can tolerate some level of delay in data transmission. In these scenarios, the SN can decide to accumulate their service demands until the periods of the day where the spectrum price is cheapest, before transmission to save cost. In this work, the cheapest period is statistically decided only once and then the traffic is adjusted accordingly.

4.4 Problem Formulation

A specific time period T (in mins) is considered and it is then divided into equal time slots (in mins) with a duration of d (in mins). Then, an index vector t is defined that stores the time slots in an order, such that $t = [1, 2, ..., M_T]$, where M_T is the number of time slots and is given by $M_T = T/d$. The BSs of the PN are represented by $B_{\mathrm{P}}^{i,j}$ while that of the SN by $B_{\mathrm{S}}^{i,j}$. The problem is viewed from the PN perspective and formulate the revenue Maximisation problem by considering the revenue obtained from the combination of cell switching and spectrum leasing. Since the PN obtains its power supply from the grid, it can decide to turn off some SBSs during periods of low traffic to reduce their energy cost (i.e., gain some revenue from energy saving) and also lease the dormant spectrum to the SN in order to gain additional revenue.

Revenue from Cell Switching

The overall power consumption—the summation of the power consumption of all the BSs over all the time slots—when no cell switching is implemented (i.e., when all the BSs are on), P_{on}, can be expressed as:

$$\mathrm{P}_{\mathrm{on}} = \sum_{t=1}^{M_T} \sum_{i=1}^{M_m} \sum_{j=1}^{M_b} P_{\mathrm{BS},t}^{i,j}(\tau_t^{i,j}). \tag{4.3}$$

The overall power consumption—the summation of the power consumption of all the BSs over all the time slots—when cell switching is implemented (i.e., when

some BSs are turned off), $\mathrm{P_{cs}}$, is given by:

$$\mathrm{P_{cs}} = \sum_{t=1}^{M_T} \sum_{i=1}^{M_m} \sum_{j=1}^{M_b} [\Gamma_t^{i,j} P_{\mathrm{BS},t}^{i,j}(\tau_t^{i,j}) + (1 - \Gamma_t^{i,j}) P_{\mathrm{BS,s}}^{i,j}], \tag{4.4}$$

where $P_{\mathrm{BS,s}}^{i,j}$ is the power consumption of the BS when it is switched off (i.e., sleep mode power consumption of the BSs) $\Gamma_t^{i,j}$ denotes the off/on status of the $(i,j)^{\mathrm{th}}$ BS at time t, i,e.,

$$\Gamma_t^{i,j} = \begin{cases} 1, & \text{if } B_{\mathrm{P}}^{i,j} \text{ is on} \\ 0, & \text{if } B_{\mathrm{P}}^{i,j} \text{ is off,} \end{cases} \tag{4.5}$$

Since the MBS is always on, $\Gamma_t^{i,1} = 1$, $\forall t$.
Please note that the switch off period in this work lasts for 10 mins, as this period coincides with the regularity with which the network traffic data [272] that is used for this simulation was collected.

Then, the overall power saving due to cell switching, P_{sv} can be expressed as:

$$P_{\mathrm{sv}} = P_{\mathrm{on}} - P_{\mathrm{cs}}. \tag{4.6}$$

Therefore, the revenue due to energy saving, R_{E}, can be expressed as:

$$R_{\mathrm{E}} = \sum_{t=1}^{M_T} P_{\mathrm{sv},t} \frac{T}{M_T} \mathrm{C_{e,}}_t, \tag{4.7}$$

where $\mathrm{C_{e,}}_t$ is the cost of electricity at time t, and $P_{\mathrm{sv},t}$ is the energy saving at time t.

Revenue from Spectrum Leasing

The revenue due to spectrum leasing, (R_{l}), can be expressed as:

$$R_{\mathrm{l}} = \sum_{t=1}^{M_T} \sum_{i=1}^{M_m} \sum_{j=1}^{M_b} (1 - \Gamma_t^{i,j}) \min(\Psi_{\mathrm{S},t}^{i,j}, \Psi_{\mathrm{D},t}^{i,j}) \mathrm{C_{RB,}}_t \tag{4.8}$$

where $\Psi_{\mathrm{S},t}^{i,j}$ denotes the amount of spectrum (number of RBs) supplied by $B_{\mathrm{P}}^{i,j}$, $\Psi_{\mathrm{D},t}^{i,j}$ denotes the amount of spectrum demanded by $\Psi_{\mathrm{S},t}^{i,j}$ from $B_{\mathrm{P}}^{i,j}$ and $\mathrm{C_{RB,}}_t$ is the unit cost of spectrum (i.e., price per RB) at time t.

$B_{\mathrm{P}}^{i,j}$ and $B_{\mathrm{S}}^{i,j}$ are assumed to have the same capacity, which implies that $\Psi_{\mathrm{D},t}^{i,j} \leq$

$\Psi_{\mathrm{S},t}^{i,j}$. Therefore, (4.8) can be simplified as:

$$R_{\mathrm{l}} = \sum_{t=1}^{M_T} \sum_{i=1}^{M_m} \sum_{j=1}^{M_b} (1 - \Gamma_t^{i,j}) \Psi_{\mathrm{D},t}^{i,j} \mathrm{C}_{\mathrm{RB},t}. \tag{4.9}$$

Total Revenue

The total revenue of the PN, R_{T} can be expressed as:

$$R_{\mathrm{T}} = R_{\mathrm{E}} + R_{\mathrm{l}}, \tag{4.10}$$

and substituting (4.7) and (4.9) in (4.10), R_{T} becomes:

$$\begin{aligned} R_{\mathrm{T}} &= \sum_{t=1}^{M_T} P_{\mathrm{sv},t} \frac{T}{M_T} \mathrm{C}_{\mathrm{e},t} + \sum_{t=1}^{M_T} \sum_{i=1}^{M_m} \sum_{j=1}^{M_b} (1 - \Gamma_t^{i,j}) \Psi_{\mathrm{D},t}^{i,j} \mathrm{C}_{\mathrm{RB},t} \\ &= \sum_{t=1}^{M_T} \sum_{i=1}^{M_m} \sum_{j=1}^{M_b} (1 - \Gamma_t^{i,j}) \Psi_{\mathrm{D},t}^{i,j} \mathrm{C}_{\mathrm{RB},t} + P_{\mathrm{sv},t} \frac{T}{M_T} \mathrm{C}_{\mathrm{e},t}. \end{aligned} \tag{4.11}$$

Replacing (4.7) with (4.3) and (4.4) and simplifying (4.11), the closed form expression for the total revenue is obtained and can be expressed as:

$$\begin{aligned} R_{\mathrm{T}} = &\sum_{t=1}^{M_T} \sum_{i=1}^{M_m} \sum_{j=1}^{M_b} (1 - \Gamma_t^{i,j}) \\ &\left[\sum_{t=1}^{M_T} (P_{\mathrm{BS},t}^{i,j} - P_{\mathrm{BS,s}}^{i,j}) \frac{T}{M_T} C_{\mathrm{e},t} + \Psi_{\mathrm{D},t}^{i,j} C_{\mathrm{RB},t} \right]. \end{aligned} \tag{4.12}$$

4.4.1 Optimisation Objective

The revenue maximisation objective function is the joint optimisation of the revenue[2] due to cell switching and spectrum leasing and can be expressed as:

$$\max_{\Gamma_t^{i,j}} \quad R_{\mathrm{T}}(\tau^{i,j}, \Gamma_t^{i,j}), \tag{4.13}$$

$$\text{s.t.} \quad \Upsilon^i = \hat{T}^i, \quad \forall i, j, \tag{4.14}$$

$$\hat{\tau}^{i,1} \leq \tau_{\mathrm{m}}^{i,1}, \quad \forall i, \tag{4.15}$$

$$\Gamma_t^{i,j} \in \{0, 1\}, \quad \forall i, j. \tag{4.16}$$

[2]Even though the optimisation function is about revenue, the optimisation parameter is the switching variable $\Gamma_t^{i,j}$, because the amount of revenue that can be generated from the cell switching and spectrum leasing operation is dependent on $\Gamma_t^{i,j}$, as can be seen in (4.12).

The constraints of (4.13) are explained in the following. The traffic demand, Υ^i, when all the BSs in the MC i are on (i.e., before traffic offloading) is computed as,

$$\Upsilon^i = \sum_{j=1}^{M_b} \tau^{i,j}, \quad \forall i. \tag{4.17}$$

To ensure that there is no coverage loss (i.e., the QoS of the network is maintained), the traffic load supported by the MC before and after the cell switching and spectrum leasing operation is performed must be the same (4.14), (assuming other factors, such as channel conditions, user location, etc., remain constant). For this to happen, the traffic load of any SBS that is switched off must be transferred to the MBS. Therefore, the actual traffic load of the MBS during the offloading process, denoted by $\hat{\tau}^{i,1}$ is equal to,

$$\hat{\tau}^{i,1} = \tau^{i,1} + \sum_{j=2}^{M_b} \tau^{i,j}(1 - \Gamma_t^{i,j}), \quad \forall i. \tag{4.18}$$

The traffic demand of the MC after traffic offloading, $\hat{T}^i$ can be expressed as,

$$\hat{T}^i = \hat{\tau}^{i,1} + \sum_{j=2}^{M_b} \tau^{i,j}\Gamma_t^{i,j}, \quad \forall i. \tag{4.19}$$

Therefore, (4.17) must be equal to (4.19) to satisfy the constraint in (4.14). However, for constraint (4.14) to be effective, another constraint needs to introduced, to ensure that there is sufficient radio resources or offloading capacity in the MBS before any cell switching and spectrum leasing operation can be performed. By so doing, the maximum offloading capacity of the MBS would never be exceeded, as this would result in the degradation of the QoS of the network. That is, let $\tau_{\mathrm{m}}^{i,1}$ denote the maximum traffic that MBS can serve in any time slot t. Then, the additional constraint is as obtained in (4.15).

The problem in (4.13) is a combinatorial problem which involves deciding the optimal set of SBSs to turn off out of all the possible combinations of SBSs, and then leasing their spectrum to the SN BSs in order to maximise the revenue of the PN. It is a NP hard problem, and as such, it is very difficult and time consuming to solve. In addition, its complexity increases exponentially with increasing numbers of SBSs, and it cannot easily be solved using standard methods [22]. Even though the optimal solution can be obtained using ES algorithm, however, due to the computational complexity involved in implementing ES, it cannot be used for cell switching and spectrum leasing in UDNs. Hence, a less complex heuristic is adopted which considers a lesser search space and can give a sub-optimal solution

with reduced computational complexity (lesser search spaces compared to ES).

4.5 Proposed Framework

The aim of this work is to determine the optimal cell switching and spectrum leasing strategy that would maximise the revenue of the PN without compromising the QoS of the network. Although ES always finds the optimal policy, it is computationally complex to implement because it has to sequentially search through all the possible cell switching and spectrum leasing combinations before deciding the optimal solution. As a result, in this research, the SA algorithm is employed which has lesser complexity since it involves lesser search spaces in finding the optimal solution. SA is preferred to other heuristic algorithms in this work because it is not easily trapped in the local minima [115] and it is also computationally efficient. In addition, it is easy to apply it to this problem and closely approximates the optimal solution. However, this algorithm is not always guaranteed to produce the optimal result as is the case with ES. In this regard, albeit being sub-optimal, through extensive simulations, it is proven that the developed SA algorithm based solution produces almost the same results as the ES algorithm—especially when the network sizes are reasonable—with much less computational complexity, providing a promising trade-off between the performance and complexity.

4.5.1 SA Algorithm for Cell Switching and Spectrum Leasing

To control the switching off/on of SBSs, it is necessary to determine the parameters of the algorithm in the first place. Then the objective function value of randomly generated initial solution s is calculated with (4.13). In this way, the revenues are obtained according to the energy saved from turning off some SBSs in the PN (4.7) and spectrum leased to the SN (4.9). During the search process, the algorithm attempts to transform the current solution s into one of its randomly selected new solution s'. However, in the developed algorithm, instead of randomly selecting a neighborhood structure, each neighborhood is applied in an order as in sequential variable neighborhood search (VNS) algorithm [121]. The search area is also expanded in each iteration due to the small number of neighborhood types.

Note that only feasible solutions which guarantee (4.14) and (4.15) are considered in the proposed SA algorithm. To ensure this, a feasibility check is per-

formed first in each of the neighborhood solution produced. With the applied neighborhood structure, several temporal solutions can be produced until a feasible solution is obtained. If the revenue of the obtained solution with the new neighborhood structure, s', is higher than the current solution s, the new solution is unconditionally accepted. If the revenue of the neighborhood solution is less than the existing solution, the probability of accepting the neighborhood solution is calculated as:

$$p = \exp\left(- \frac{R_{\mathrm{T}}(s') - R_{\mathrm{T}}(s)}{\mathcal{T}} \right). \tag{4.20}$$

After the local search process (after k iteration), the temperature is decreased according to the formula $\mathcal{T} = \mathcal{T} - \upsilon$, where υ is the temperature reduction parameter.

Feasibility Check

In order for a solution to be evaluated within the algorithm, a preliminary check is performed to determine whether it is feasible or not. For this reason, the transferred traffic loads of SBSs that are switched off in the s solution should not exceed the normalized capacity of the MBS (4.15). The pseudo code for feasibility check is shown in Algorithm 9.

Algorithm 8: Feasibility check

```
MBS traffic load = τ^{i,1};
for i in s' do
    if (s'(i) = 0) then
        calculate the transferred traffic load Σ_{j=2} τ^{i,j}(1 − Γ_t^{i,j});
        τ̂^{i,1} = τ^{i,1} + Σ_{j=2}^{M_b} τ^{i,j}(1 − Γ_t^{i,j});
        if τ̂^{i,1} ≤ 1 then
            s' is feasible
        else
            s' is not feasible
        end
    end
end
```

Solution Representation

The proposed SA algorithm has a representation scheme specially designed for the cell switching and spectrum leasing problem. It has a binary representation depending on whether the SBSs are off or on.

Initial Solution

In the SA algorithm, the initial solution, which is the first feasible solution at the beginning of the iterations in the SA algorithm, is generated randomly or with certain methodical approaches such as nearest neighbor heuristics [120]. Simple heuristic methods are considered to decrease the solution time and increase the quality of the solution in some NP-hard problems. However, in this work, the initial solution is generated randomly, and not with any constructive heuristic method, to prevent the initial solution from being trapped in a particular local optimum within the search space due to the inefficiency of the heuristic method applied.

Neighborhood Structures

The proposed SA algorithm has three different neighborhood structures, seeking for better results from different aspects in each iteration. The SA algorithm also has nested iterations. The primary iteration is associated with temperature drop. Each temperature level represents one iteration and performs a global search in the search space. In addition, there are local search iterations in which neighborhood structures are applied sequentially at each temperature level. Neighborhood structures are named as **1-reserve**, **2-reserve** and **swap**, and they are frequently used in applications such as vehicle routing problems, travelling salesman problems (TSP), and location problems [117, 118]. In the neighborhood of 1-reserve, a random cell is chosen from the solution state s and the selected cell's index is denoted by j. If the value of $s(j)$ is 1, this value is changed to 0 and vice versa for the case where the value of $s(j)$ is 0. In the 2-reserve neighborhood, this process is performed for two different cells, while in the swap neighborhood, the values of two randomly selected cells are replaced with each other.

In addition to the neighborhood structures, the shaking tool is also used for diversification before each temperature change in the algorithm. After the local search procedure at certain temperature, the bit representation (i.e., 0 and 1 values) are changed randomly to search in different spaces. This action is to prevent the algorithm from being stuck at a local optimum. The demonstration of the implementation of neighborhood structures is shown in the Fig. 4.3.

Parameter Settings

SA algorithm begins with five parameters: $\mathcal{T}$, $\mathcal{T}_F$, φ, υ_p and $\mathcal{K}$. $\mathcal{T}$ and $\mathcal{T}_F$ are the initial and final temperatures, respectively. The initial temperature must be high enough to allow the acceptance of any feasible solution. If the initial temperature

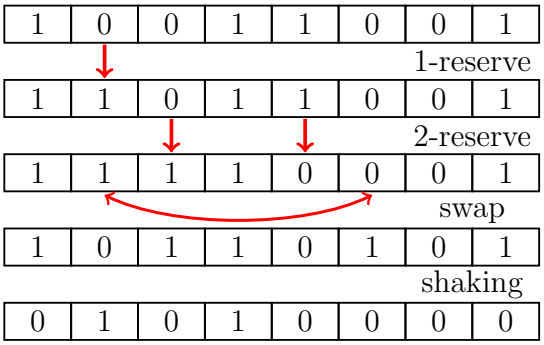

Figure 4.3: Illustration of the different types of neighborhood structures. The topmost bar shows the initial status of the SBSs, followed by the implementation of the three neighbourhood structures while the last bar represents the shaking operation.

is too high, the probability of generating random solutions among feasible solutions at the beginning of the algorithm is higher. On the other hand, if the initial temperature is too low, the probability of getting stuck at the local optimum of the algorithm increases. The final temperature of the algorithm is set to avoid spending too much time in reaching the optimum. φ is defined as the number of iterations of the local search procedure at each temperature, while υ_p is the temperature reduction parameter. It refers to the amount by which the temperature will be decayed at the end of each iteration. $\mathcal{K}$ is Boltzmann constant and is used in calculating the probability of accepting or rejecting worse solutions. If the new objective function value is worse than current best solution, it will generate u, which is a random variable between 0 and 1. Then, the obtained solution will be accepted if the criterion represented in (4.20) is satisfied. Except for this situation, an improved objective function value is always accepted. Different SA algorithm design parameters that are frequently used in the literature [117, 118] were considered and the ones that led to the best results during the preliminary tests were chosen. The best SA parameter combination is $\mathcal{T} = 1$, $\upsilon_p = 0.01$, $\mathcal{T}_F = 0.01$, $\varphi = 10M_b$, where M_b indicates the total number of SBSs in the PN. The pseudo code for the developed SA based cell switching and spectrum leasing framework is presented in Algorithm 9.

4.5.2 Complexity Comparison between SA and ES

An ES algorithm performs a complete space search of all the possible configurations until the optimum configuration is found. This may be suitable for functions of few variables, but considering the cell switching and spectrum leasing problem, it would result in exponential computational complexity of $\mathcal{O}(2^N)$. Due to

Algorithm 9: SA algorithm for cell switching and spectrum leasing

```
1  Randomly generate an initial solution: s_0 ∈ S
2  while s_0 is infeasible; do Randomly generate an initial solution: s_0 ∈ S;
3  Calculate revenue of s_0
4  Define an initial temperature 𝒯 > 0
5  Define temperature reduction function, υ_p and
6  s = s_0, s* = s_0, f(s) = f(s_0), f(s*) = f(s_0);
7  Define local search iteration number for each temperature (φ)
8  while 𝒯 > 0.01 do
9      n = φ;
10     while (n>0) do
11         generate (1-reserve) neighbor solution s'
12         while (s' is infeasible) do
13             generate (1-reserve) neighbor solution s'
14             ϑ = f(s') − f(s);
15             if (ϑ ≤ 0) then s = s';
16             else
17                 generate a random number from uniform distribution in the 0-1
                     range (u)
18                 if (u < exp(−ϑ/T)); then s = s';
19             if (f(s') < f(s*)); then s* = s';
20         end
21         generate (2-reserve) neighbor solution s'
22         while (s' is infeasible) do
23             generate (2-reserve) neighbor solution s'
24             ϑ = f(s') − f(s);
25             if τ^{i,1} ≤ 1 then s = s';
26             else
27                 generate a random number from uniform distribution in the 0-1
                     range (u)
28                 if (u < exp(−ϑ/T)); then s = s';
29             if (f(s') < f(s*)); then s* = s';
30         end
31         generate (swap) neighbor solution s'
32         while (s' is infeasible) do
33             generate (swap) neighbor solution s'
34             ϑ = f(s') − f(s);
35             if (ϑ ≤ 0); then s = s';
36             else
37                 generate a random number from uniform distribution in the 0-1
                     range (u) if (u < exp(−ϑ/T)); then s = s';
38             if (f(s') < f(s*)); then s* = s';
39         end
40         n = n − 1;
41     end
42     𝒯 = 𝒯 − υ_p
43     apply (shaking) procedures to s*, s = s*
44 end
45 s* is the heuristic solution of the problem
```

the computational complexity of problems like this and other NP-hard problems, many optimisation heuristics have been developed in order to obtain optimal or approximate optimal solutions. In addition, the solution times of heuristic ap-

proaches are incomparably low compared to algorithms that try all possible scenarios. Because, not all feasible solution combinations are considered in heuristic approaches. Heuristic approaches work with the best solution-oriented search and they focus on specific regions in the search space. Therefore, the computational cost of heuristic approaches are very low compared to ES, especially in large-scale cell switching problems. One widely used technique is the SA algorithm, which enables the introduction of a degree of stochasticity, potentially shifting from an optimal to a sub-optimal solution, in an attempt to reduce the complexity, escape local minima, and converge to a value closer to the global optimum.

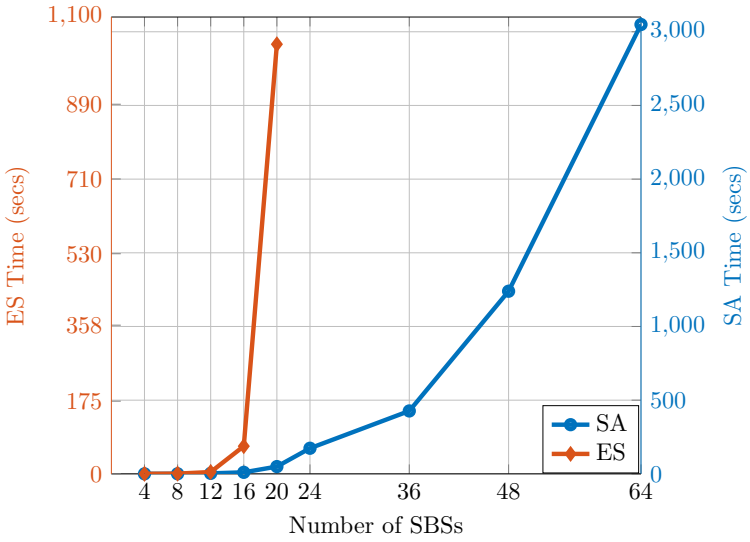

Figure 4.4: Time complexity comparison between ES and SA.

However, the time complexity of heuristic algorithms such as the SA algorithm[3] cannot be easily determined because such algorithms do not guarantee to find the global optimal solution within a certain time limit. Instead, determining the total simulation run time of the algorithm can give us an idea of the computational complexity of the algorithm.

Fig. 4.4 shows the simulation run time comparison between ES and the proposed SA algorithm. It can be clearly seen that the simulation run time of the ES algorithm is very small when the number of SBSs are less than 16. However, a huge leap is noticed in simulation time when the number of SBSs is increased from 16 to 20 because the number of search spaces of the ES increases exponentially with the number of SBSs. This accounts for the very wide difference in the simulation time that is observed when the number of SBSs are increased to 20 compared to when they were 16. It should be noted that the simulation is

[3]Since the convergence time of the SA algorithm increases with the number of BSs, the application of the proposed solution is limited by the amount of latency that can be tolerated by the network, so that the performance of the network is not negatively affected.

stopped at 20 SBSs for the ES algorithm because of the limitation of the computer, as it would take days to complete the simulation when the number of SBSs are increased to 24. The simulation time of the SA algorithm is also very low until about 20 SBS when it starts to increases with higher magnitudes. But this is much lesser than the magnitude of simulation time increase that is observed with the ES algorithm. The SA algorithm exhibits a polynomial order of computation complexity because it does not have to consider all the search spaces like the ES algorithm in order to determine the optimal cell switching and spectrum leasing strategy.

ES algorithm searches all the neighborhood solutions regardless of whether a solution vector yields worse results in terms of the objective function. This situation causes an unnecessary computational cost increase in the algorithm. However, SA does not check every solution in the entire solution space. While doing a local search in a solution space, it looks at the solution regions adjacent to the best solution. This is because the global optimum is likely to be close to the local best solutions. As a result, SA's superiority over ES algorithm in terms of computational complexity is due to its solution search strategy. Hence, the ES algorithm is only suitable for for small networks with few SBSs while the SA algorithm can be applied even when number of SBSs are very many.

4.6 Performance Evaluation

The proposed cell switching and spectrum leasing framework can be implemented in any network regardless of the network size in terms of the number of MBSs involved. Since the framework is implemented independently at each MBS, which is responsible for controlling all the SBSs under its coverage, the simulations are conducted for a single MBS with multiple SBSs for the sake of brevity. Hence, only one framework needs to be developed which can be implemented in all the other MBS-SBSs configuration throughout the network. The system configuration comprises the hardware, which is a HP-TXH0CCYBD0HV desktop computer and has the following specifications: The processor is Intel core i7-8700 @ 3.2 GHz, RAM of 16 GB, with Windows 10 Enterprise operating system and 475 GB hard disk capacity. The software employed is the Spyder version 4.0.1 which runs Python version 3.7. The development environment that is utilised is Anaconda because it has a complete suite for Python development as well as that of other high-level languages. The PN, SN, and SA algorithm parameters used in the simulations are presented in Table 4.1.

[4]Please note that every PN SBS has a SN BS of the same type associated with it.

Table 4.1: Simulation parameters for revenue maximisation in 5G HetNets

Parameter	**Value**
Bandwidth of MBS (MHz)	20
Bandwidth of SBSs, SN-BSs[4](RRH, micro, pico, femto)(MHz)	15, 10, 5, 3
Number of RBs per MBS	100
Number of RBs per SBSs, SN-BSs(RRH, micro, pico, femto)	75, 50, 25, 15
P_{tx} (MBS, RRH, micro, pico, femto) (W)	20, 20, 6.3, 0.13, 0.05
P_{o} (MBS, RRH, micro, pico, femto) (W)	130, 84, 56, 6.8, 4.8
η (MBS, RRH, micro, pico, femto)	4.7, 2.8, 2.6, 4.0, 8.0
$P_{\text{BS,s}}^{i,j}$ (RRH, micro, pico, femto) (W)	56, 39, 4.3, 2.9
Initial temperature, $\mathcal{T}$	1
Final temperature, $\mathcal{T}_{\text{F}}$	0.01
Fixed spectrum price (per RB) [5]	£0.13
Fixed electricity price (per kWhr)[6]	£0.1293
Number of PN MBS, SBSs	1, 12
Number of SN BSs	12

4.6.1 Dataset and Pre-processing

To compute the total revenue of the HetNet using (4.12), the traffic demand of each BS in the PN (τ) and SN (Ψ) is required. The call detail record (CDR) dataset of the city of Milan, Italy that was made available by Telecom Italia [272] is leveraged. In the dataset, Milan city was divided into 10,000 square grids with each having an area of 235×235 square meters. In addition, the call, short-message and Internet activities that were carried out in each grid was recorded every 10 minutes over a period of two months (November-December 2013). Although the activity levels contained in the dataset are without unit and no additional information was provided regarding how the dataset was processed, a decision was made to interpret the CDR of each grid as the traffic loads as they signify the amount of interaction between the users and the mobile network within the grid in each time slot. However, during the data processing stage of this work, only the Internet activity level was considered as the traffic load for the PN since it was the most significant part of the dataset and also considering the fact that 5G networks would be mainly Internet based. The Internet activity level of two grids were selected at random to represent the traffic load of the MBS while that of one grid was chosen for each SBS. Then, the traffic loads were normalized separately according to the capacity of each type of SBS. It is assumed that the traffic demand of each BS in the SN is a fraction of the traffic demand of the SBSs in the PN such that $\Psi = \beta\tau$ where β is a variable between 0 and 1 (β was chosen to be 0.7 in this work). The traffic demand of the SN is shifted so that its

[5]The fixed spectrum price is obtained from https://www.ofcom.org.uk/data/assets/pdffile/0021/130737/Annexes-5-18-supporting-information.pdf [accessed 10 Jan. 2021].

[6]The fixed price of electricity is acquired from https://www.businesselectricityprices.org.uk/corporate/ [accessed 10 Jan. 2021].

maximum traffic demand coincides with the period of the day when the spectrum leasing price is minimum in order to depict the DT case while for the NDT case, the traffic demand remains intact.

4.6.2 Benchmarks

The performance of the proposed method is compared with three benchmark methods namely: ES, A-type, and D-type algorithms, which are briefly described in the following paragraphs.

Exhaustive search (ES): This method sequentially considers all the possible cell switching and spectrum leasing combinations in order to determine the optimal off/on switching policy that would result in maximum revenue to the PN while ensuring that the QoS of the network is maintained. Therefore, this method is guaranteed to always find the optimal policy without violating the QoS of the network. However, the computational complexity involved in sequentially searching through all the possible combinations makes it unsuitable for online implementation. The goal of any other algorithm is to closely approximate the policy obtained from this approach, hence, it is suitable as a benchmark for this problem.

Sorting-based Algorithms Two additional benchmark algorithms are developed using the sorting approach which is named A-type and and D-type heuristic respectively. These benchmarks were derived from the work in [292]. In the D-type heuristic, a utility function, $\mathcal{N}$, which is the difference between the traffic demand of the SN BSs and that of the PN BSs, i.e., $\mathcal{N} = \Psi - \tau$ is first evaluated. This utility function $\mathcal{N}$ is important because the goal is not only to switch off the SBSs with low traffic demand, but also those whose associated SN BS has a high spectrum demand. It is necessary to satisfy both conditions if the revenue of the PN is maximised because both of them affects the total revenue (4.10) that can be generated by the PN. In addition, since the total revenue of the PN is dependent on the amount of revenue that can be obtained from energy savings and spectrum leasing, thus, higher values of $\mathcal{N}$ would result in greater revenue generation due to higher contributions from both components. On the other hand, lower values of $\mathcal{N}$ might result in lesser revenue generation due to smaller contribution either from the energy savings or spectrum leasing. After evaluating $\mathcal{N}$, the SBSs are arranged in descending order according to the value of $\mathcal{N}$. Then, the traffic load of the SBSs are sequential offloaded to the MBS until the capacity of the MBS is reached. The procedure for implementing A-type heuristic is similar to that of

D-type except that in A-type, the SBSs are sorted in ascending order according to $\mathcal{N}$.

4.6.3 Performance Metrics

The metrics that would be used in evaluating the performance of the proposed and benchmark methods are briefly discussed in this section.

Total Revenue: The goal of this work is to determine the maximum revenue that can be obtained by the PN over a given period of time, T. As described in Section IV, this is obtained by combining the revenue due to energy saving from cell switching and the revenue obtained from leasing the spectrum to the SN. The total revenue of the network can be obtained from (4.13).

$\mathcal{C}_L$: The effect of the proposed framework on the QoS of the network is evaluated using the coverage loss metric. Here, $\mathcal{C}_L$ is considered to be the percentage difference in total traffic demand that is served by the PN before and after cell switching and spectrum leasing is implemented. This can be expressed as in (3.24).

4.6.4 Results and Discussions

Fig. 4.5a shows the hourly total revenue obtained by the PN following the fixed electricity and spectrum pricing policy with NDT spectrum demand using the proposed and benchmark methods. In addition, the traffic load of the PN MBS, $\tau^{i,1}$, is also presented. The first thing that can be observed from Fig. 4.5a is that the revenue obtained from all methods follows a trend that is opposite of that of the traffic demanded of the PN. This is so because during the periods of the day where the PN traffic is low, more SBSs can be switched off which translates to more revenue generation from energy savings and spectrum leasing. The opposite is the case when the traffic of the PN is high. Second, the SA algorithm follows ES almost exactly, since it is able to employ its mechanisms such as feasibility check and neighbourhood structures to determine the optimal cell switching and spectrum leasing pattern, but with much lesser complexity.

Third, both the A-Type and D-type heuristic solutions never outperform ES and SA algorithms because they also respect the constraint of not exceeding the MBS capacity. Even though they both respect the MBS capacity in order to maintain the QoS of the network, they utility, $\mathcal{N}$, used in determining which BSs to switch off only considers the difference in traffic demand between the PN and SN, but is not able to distinguish between the various types of BSs present. In

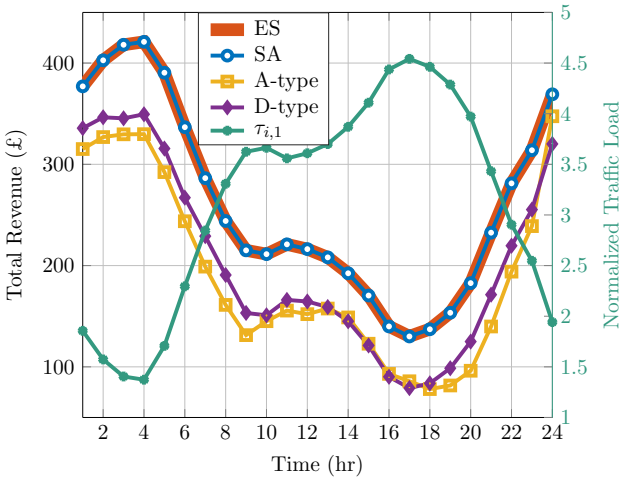

(a)

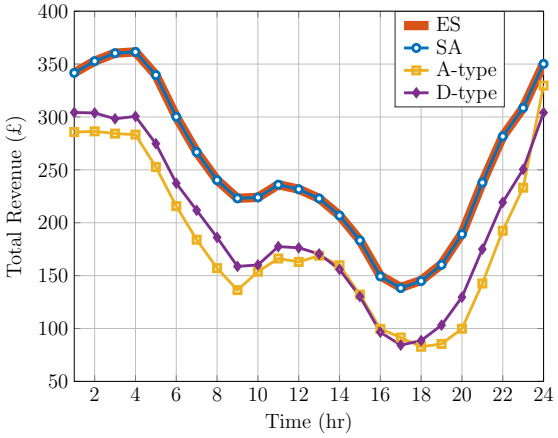

(b)

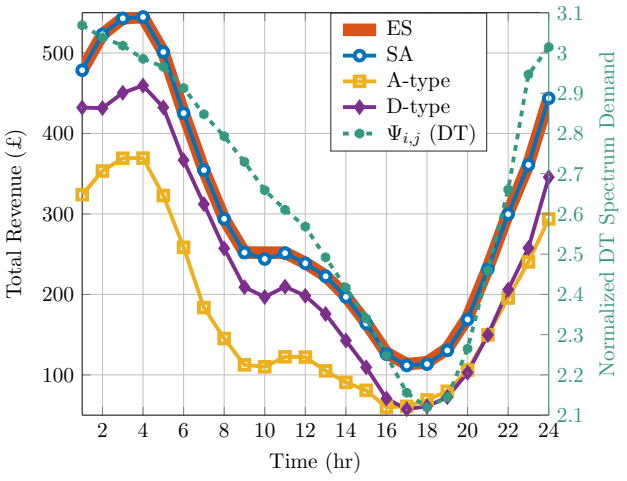

(c)

Figure 4.5: The revenue obtained from fixed, and dynamic pricing policy (DT and NDT spectrum demand) for 12 SBSs over a period of 24 hours. (a) The left y-axis is the total revenue obtained from fixed pricing policy with NDT while the right y-axis is the traffic load of the PN MBS. (b) Total revenue from dynamic pricing policy with NDT. (c) The left y-axis is the total revenue from dynamic pricing policy with DT while the right y-axis is the spectrum demand of the SN.

this work, the PN and SN BSs have different capacities and power consumption, as a result, switching off a SBS with higher capacity and power consumption and leasing its spectrum to the SN would result in higher revenue than switching off one with a lower capacity. This limitation accounts for the lesser revenue obtained from both the A-type and D-type heuristics.

Another interesting point to discuss about the observations in Fig. 4.5a is that the D-type heuristic mostly outperforms the A-type heuristic because it switches off the SBS with highest utility, $\mathcal{N}$, values first and this helps in the generation of more revenue compared to A-type which does the opposite. However, this performance difference is mostly observable during the times of low traffic as there are more options and the higher utility is able to find a better solution. For the time when the network traffic is high, they start performing alike, since the number of cell switching and spectrum leasing options becomes very low. Overall, the performance difference between the D-type and A-type solutions is not large, as the former outperforms the latter with a minimum of 1% and a maximum of 29%. The last observation worth discussing is that the SA solution mainly outperforms both A-type and D-type solutions (by about 90% and 65% respectively) during periods of high traffic. The reason for this is that the number of cell switching and spectrum leasing options becomes very few during this period, thereby making it very difficult for them to find the best solution while the SA solution is carefully designed to be able to perform excellently well even in such periods.

This is because the SA algorithm can search in different regions of the solution space. This is due to the diversification feature provided by the shaking procedure. SA performs a local search at each temperature level and arrives at the best solution (or approximate best) in a specified region of the solution space. Then the shaking procedure is applied with temperature drop. Thus, in the next iterations, it compares the local best solutions in different regions of the solution space with the current best solution and searches up to the termination criterion. However, heuristic methods such as A-type and D-type operate fixed (usually one or more feature-dependent utility functions) rules. This causes heuristic methods to get caught in the local best solution trap. In addition, the SA algorithm includes different neighborhood search strategies. These strategies provide more flexibility in local search and for this they determine the probabilistic acceptance criteria according to the temperature level.

Fig. 4.5b presents the total revenue obtained every hour by the PN when the dynamic pricing policy with NDT spectrum demand is considered using the proposed and benchmark methods. In the dynamic pricing policy, the prices of both electricity and spectrum vary at different times of the day depending on the

amount of spectrum or electricity demanded. Similar to what was observed in Fig. 4.5a, the pattern of the total revenue over the whole day is the inverse of the traffic profile of the PN. Moreover, the revenue is generally scaled down compared to Fig. 4.5a, and this is more noticeable during periods of low traffic. This is because a dynamic pricing policy is used, where the PN sometimes needs to lease the spectrum for less and at those times it also earns less from energy savings because the prices are lower. The D-type heuristic also slightly outperforms the A-type heuristics with almost the same percentage (1% to 29%) as in Fig. 4.5a, due to the fact that higher utility values are considered first during cell switching which helps in greater revenue generation in the former compared to the latter. The aforementioned confirms the previous argument on why the performance of the two benchmark algorithms are similar. The proposed SA algorithm also greatly outperforms the A-type and D-type algorithms with a similar percentage (90% and 65% respectively) as in Fig. 4.5a mostly during the period of high traffic in the PN because there are lesser cell switching and spectrum leasing options which make it difficult for the benchmark solutions to make the optimum decisions.

Another important point to note is that although the D-type solution offers better results than A-type, these two algorithms have similar working mechanisms as can be seen in Fig. 5a and Fig. 5b. The D-type sorts the SBSs in descending order of the value of the utility, $\mathcal{N}$, in order to determine the ones turn off and lease their spectrum to the SN while the D-type type does the opposite. Heuristic approaches such as A-Type and D-Type do not guarantee an optimal solution. However, the solutions found by such algorithms may converge to the optimal or approximate optimal. Heuristic algorithms have a probability of being optimal if the local search region is close to the global optimum in the solution space. This is also the case at 24hr. The results of the numerical experiments demonstrate that the proposed A-type and D-type benchmark methods obtain near optimal solutions at 24 hr. Another reason for this may be that there are not many feasible solution alternatives in the solution space at this period. In Fig. 5a, at the 24th hr, the results of the D-type, A-type, SA and ES algorithms are £320, £347, £369, and £369, respectively. Similarly, in Fig. 5b, the revenue values of £304, £329, £350, and £350 are obtained with D-type, A-type, SA and ES algorithms, respectively. However, it should be noted that benchmark methods still could not obtain the optimal solution. In cases where the problem size is small, it is natural for heuristic algorithms to reach optimal results. On the other hand, the larger the problem size, the less likely it is for them to converge to the optimal solution.

Fig. 4.5c presents the total revenue obtained by the PN when dynamic pricing

policy with DT spectrum demand is considered. In this case, the SN decides to delay its data transmission to periods when the spectrum price is low (which also coincides with period of low traffic demand in the PN) so that they can access more spectrum at a cheaper rate. It can be observed that there is an overall increase in the total revenue obtained by the PN in Fig. 4.5c, compared to Fig. 4.5a and Fig. 4.5b: the total revenue obtained from the proposed SA framework is about 19% and 16% higher than that obtained in the Fig. 4.5a and Fig. 4.5b, also it is evidenced by the peak value of the revenue of Fig. 4.5c being about £183 and £123 higher than that in Fig. 4.5a and Fig. 4.5b respectively. This is because in dynamic pricing policy with DT spectrum demand, the SN can lease more spectrum as the periods of low traffic in the PN matches the period of high spectrum demand by the SN although the prices are lower. This statement is validated by comparing the traffic demand of the PN in Fig. 4.5a with the DT spectrum demand in Fig. 4.5c; i.e., periods of lowest traffic demand in the PN (e.g., in the first quarter of the day where the traffic load is 14%) coincides with periods of highest spectrum demand from the SN (about 28%) so that even though the spectrum prices are lower at these times as seen in Fig. 4.2, the large amount of spectrum demanded by the SN causes the total revenue in this scenario to be highest.

The performance difference between the D-type and A-type heuristics is more significant in the dynamic pricing policy with DT spectrum demand scenario compared to both the fixed and dynamic pricing policy with NDT scenarios in Fig. 4.5a and Fig. 4.5b with values ranging from 5.3% to 86%. The reason for the wider performance gap is that the NDT spectrum demand is responsible for preventing the D-type heuristic from significantly outperforming A-type heuristic. This phenomenon originates from the fact that in the fixed and dynamic pricing policy with NDT spectrum demand, the trend of the SN traffic demand follows the PN traffic demand, hence the margin in the values of $\mathcal{N}$ is smaller in both cases compared to the dynamic pricing policy with DT spectrum demand, thus accounting for the lesser total revenue results of A-type and D-type heuristics in the previous scenarios. On the other hand, for the dynamic pricing policy with DT spectrum demand (Fig. 4.5c), since the traffic demand of the SN is the inverse of the traffic load of the PN, the difference in the values of $\mathcal{N}$ at different time slots is higher and since D-type gives preference to SBSs with higher $\mathcal{N}$ during cell switching and spectrum leasing, more revenue is generated by the D-type compared to A-type, hence the reason for the wider margin in the revenue generated in the former compared to the latter. In addition, the SA algorithm greatly outperforms the A-type and D-type benchmarks in terms of

revenue generation by a maximum of 124% and 95% respectively, during periods of high traffic demand in the PN. These values are 34% and 31% higher than its performance against the two benchmarks in both the fixed and dynamic pricing with NDT spectrum demand in Fig. 4.5a and Fig. 4.5b respectively. The reason is that the SA algorithm is able to take advantage of the available options to switch off SBSs during period of high traffic which coincides with low spectrum demand by the SN in order to generate much higher revenue than the A-type and D-type algorithms.

It can also be observed that the results of D-type and A-type methods are almost the same in a few instances with the A-type even slightly surpassing that of the D-type at some points. For the NDT cases (with both fixed and dynamic pricing policies), Fig. 4.5a and Fig. 4.5b, this occurs when both the data traffic of the PN and the spectrum demand of the SN are high. This is due to the fact that the difference in the values of the utility in this period is very small, thus, there is very little revenue from spectrum leasing as the SN is not able to access spectrum due to lack of dormant spectrum from the PN. Also, very little revenue can be obtained from energy saving since only very few SBSs can be turned off due to very high traffic load in the PN.

For the DT case with dynamic pricing policy, Fig. 4.5c, the similarity in the results of both the D-type and A-type heuristics occurs at 16hr-21hr, when the traffic demand of the PN is very high and the spectrum demand of the SN is very low. At these periods, both benchmarks begin to function alike because even though there is a large difference in the value of the utility function, there is very little opportunity to switch off the SBSs due to high traffic in the PN. Hence, there is an insignificant difference in the performance of both benchmarks as relatively less revenue can be obtained during this period. The traffic load of the PN is also high at 8hr-10hr, even though it is not as high as that of 16hr-21hr. However, the spectrum demand of the SN is quite high at 8hr-10hr but very low at 16hr-21hr. As a result, the D-type solution clearly outperforms the A-type solution at 8hr-10hr because it switches off SBSs with the highest utility first, which makes it able to take advantage of the available spectrum (due to not so high traffic in the PN) to generate higher revenue than the A-type solution which switches off the SBSs with lowest utility first.

Fig. 4.6a shows the total amount spent by the SN for spectrum purchase as well as the total quantity of spectrum obtained for a 24 hours period using the proposed SA-based framework and ES while Fig. 4.6b shows the unit cost of the spectrum (i.e., price per RB) for both DT and NDT spectrum demand using both algorithms. From Fig. 4.6a it can be seen that the total amount expended by

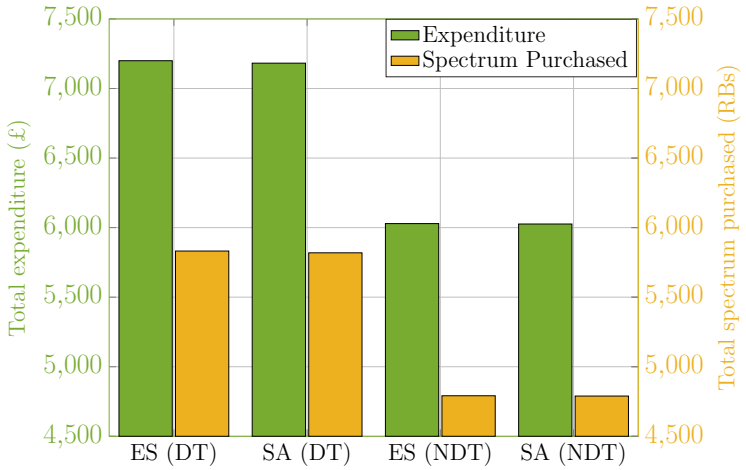

(a) Total amount spent on spectrum purchase and the quantity of spectrum obtained by SN.

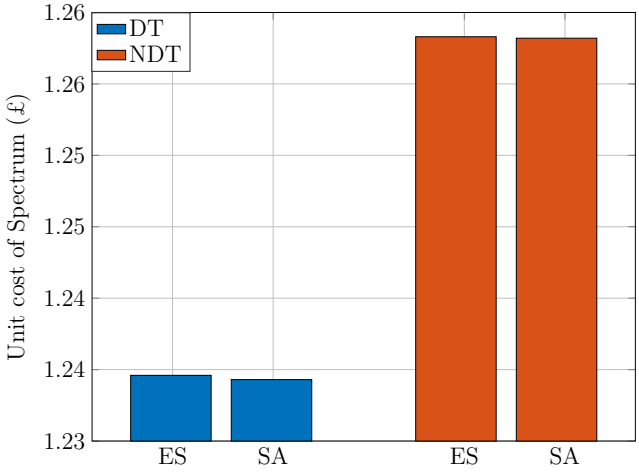

(b) Unit cost per RB.

Figure 4.6: Total expenditure and quantity of spectrum purchased by SN and the average unit cost of the spectrum for 12 SBSs.

the SN on spectrum purchase as well as the quantity of spectrum purchased are significantly higher in DT than in the NDT scenario with a percentage difference of 19% and 21% respectively. The rationale behind this is that most of the periods when the electricity and spectrum prices are low are also the periods when the traffic loads of the MBS and SBSs are low. As such, more SBSs can be turned off in order to ensure that more spectrum is available for SN to purchase during these periods. Although more spectrum is available to the SN for both DT and NDT spectrum leasing scenarios with the dynamic pricing polices during periods of low traffic load in the PN, the difference in the volume of spectrum demanded in both cases is what accounts for the difference in the amount expended on spectrum purchase in Fig. 4.6a.

In the DT case, the data to be transmitted is delayed until when the spectrum

and electricity prices are low, which means that the SN is able to take advantage of more spectrum available in order to offer more data services to it users. However, for the NDT case, even though more spectrum is available during periods of low prices, the spectrum demanded by the SN during this period is also low, so lesser revenue is generated and fewer data services can be offered in this scenario. For example, in the first quarter of the day where the traffic load of the PN is the lowest (about 14%), the revenue generated by the dynamic pricing policy with DT spectrum demand is 47% higher than that obtained from the dynamic spectrum demand with NDT spectrum demand because more spectrum is available for leasing as well as a corresponding high spectrum demand from the SN. However, the availability of more spectrum does not correspond with high spectrum demand in the NDT case thereby leading to a lesser revenue generation. Fig. 4.6a also reveals that the total expenditure and quantity of spectrum purchased using SA algorithm is almost the same as that of ES algorithm which validates the excellent performance of the SA algorithm earlier discussed under Fig. 4.5a, Fig. 4.5b and Fig. 4.5c.

The purchase of more spectrum by the SN in the DT case compared to the NDT case means that the SN incurs more expenses during DT data transmission compared to NDT data transmission. Therefore, the DT case is more beneficial to the PN because it results in more total revenue. It is also beneficial to the SN because it pays less for a unit of spectrum even though its total expenditures increase. Hence, where possible (for suitable applications), it can be concluded that the shift in the SN traffic demand would be recommended. However, the kind of shift in the data transmission time of the SN does not have to be implemented in exactly the same way as in this work, instead, depending on the type of application, the latency requirements are evaluated and the appropriate shift in the traffic is implemented accordingly, making the DT spectrum demand quite flexible and dynamic. Although this traffic shift may not always coincide with the cheapest time but to a cheaper time. In summary, DT spectrum demand will make the business of both PNs and SNs more sustainable because it is more profitable for both parties.

A major constraint in this work is to ensure that the QoS of the network is maintained (i.e., $\mathcal{C}_L = 0$) by ensuring that traffic served by the network remains constant even when some SBSs are switched off. The PN is supposed to respect the capacity constraints of the MBS before switching off any SBS. From the simulations, it can be observed that both the proposed and benchmark solutions are able to maintain the QoS of the PN by ensuring that the total traffic load of the network before and after cell switch and spectrum leasing is the same. The SA

algorithm uses the feasibility check in Algorithm 9 to ensure that only solutions that do not exceed the capacity of the MBS are considered. The ES algorithm follows similar procedure by guaranteeing that solutions that exceeds the MBS capacity are excluded when selecting the optimal cell switching and spectrum leasing strategy. Both the A-type and D-type algorithms are implemented in such a way that the traffic load of the SBSs are offloaded sequentially (in ascending and descending order respectively) and once the offloading capacity of the MBS is attained, no further SBS is turned off. By so doing, they both guarantee that $\mathcal{C}_L = 0$. It is also worthy of note that irrespective of the pricing model used for electricity and spectrum (fixed or dynamic) and the type of spectrum demanded by the SN (DT or NDT), the coverage loss of the PN remains the same. This is because both the proposed and benchmark algorithms take the constraint in (4.14) into consideration thereby ensuring that the QoS of the network is not violated.

In this study, SA, which is one of the meta-heuristic algorithms, is applied to solve the cell switching and spectrum leasing problem. Meta-heuristic algorithms such as SA may differ from each other in terms of various prominent features. In other words, these methods have various advantages and disadvantages. Although the SA algorithm is one of the most important meta-heuristic algorithms, it is insufficient when compared to modern meta-heuristic algorithms in terms of some features such as convergence speed and parallel computation. Thus, the SA algorithm can be hybridized with different meta-heuristics in order to perform parallel computation. In addition, the SA algorithm is a no memory class algorithm that offers a single solution. Memory-based meta-heuristic algorithms such as genetic algorithm, particle swarm optimisation can be applied to the current problem to present a comparative performance test study. As another option, an adaptive algorithmic structure can be presented to improve the performance of the SA algorithm.

4.7 Conclusion

In this Chapter, the problem of revenue Maximisation through cell switching and spectrum leasing was considered in order to optimise the revenue of the PN. An optimisation framework based on SA algorithm was proposed to determine the optimal cell switching and spectrum leasing strategy that would result in maximum revenue for the PN while ensuring that the QoS of the network is maintained. Both fixed and dynamic pricing policy were considered for electricity and spectrum leasing. Under the dynamic pricing policy, both DT and NDT

spectrum demand scenarios were considered in order to determine the effect of these policies on the revenue of the PN and the amount of service demands that can be met by the SN. The simulation results show that the PN can obtain more revenue using the dynamic pricing policy with DT spectrum demand. Moreover, in the DT spectrum demand scenario, the SN can lease more spectrum from the PN at a reduced average unit price which enables it to serve more data services. Thus making this scenario more profitable to the SN. Overall, the performance of the proposed method is almost the same as that of the ES algorithm with lesser time complexity.

Chapter 5

Energy-Efficient UAV Positioning

5.1 Introduction

UAV-BSs have been envisioned to play a significant role in 5G and beyond networks, including emergency communication [41], coverage and capacity enhancement, etc [293]. They have also been considered as a potential solution for enhancing energy savings in terrestrial cellular networks. This is because they can be easily deployed to provide additional traffic offloading capacity to the MBSs, during cell switching operation, as well as additional capacity for delay and rate sensitive users [64]. UAV-BSs can also be employed to enhance the offloading capacity of the PN, thereby making more spectrum available for SN to lease, during cell switching and spectrum leasing operation. This would result in increased revenue generation for the PN while enhancing the QoS of the SN. However, for UAV-BSs to be exploited for providing additional capacity, their application must not result in a significant increase in the total energy consumption of the network. There are already concerns about the energy consumption of UAV-BSs because, in addition to the energy consumed for signal processing and data transmission, there is also the energy consumption due to mobility, which is most significant component of their energy consumption [24]. Hence, there is a need to devise effective techniques to significantly reduce the energy consumption due to UAV mobility, else its application for improved energy savings, revenue generation, and other wireless network enhancement initiatives would be abortive.

To enhance the adoption of battery-powered UAVs, particularly miniature UAVs such as rotary-wing UAVs, in various domains of wireless communications, several charging mechanisms have been proposed, including battery swapping, solar charging, wireless power transfer, etc, [26]. In addition, techniques such as transmission scheduling, power allocation, trajectory design, etc., have been proposed to optimise the energy consumption of such systems [24]. Despite ad-

vancements in battery technology and energy consumption optimisation, it is still not realistic to make UAV-BSs hover or fly for the provisioning of wireless coverage over a long duration. This is because recharging the UAV's batteries is not very effective, as they have to be done very frequently due to their limited energy storage capacity, which would lead to huge running costs and might adversely affect the performance of the network [26]. Despite all the energy saving approaches, the overall energy consumption of the UAV-BS is still high due to the power required to fly or hover the UAV. In addition, the effect of the use of UAV-BSs on the the total energy consumption of the network due to its utilisation for cell switching and traffic offloading has not been taken into consideration in [64]. Hence, there is a need to come up with alternative solutions that would not only help to provide additional radio resources for traffic offloading during cell switching and spectrum leasing operations, but would also ensure that the overall energy consumption of the network is not greatly increased in the process.

A more suitable approach to achieving green wireless networks with UAV-BSs is to reconsider their planning and deployment strategies. In this regard, UAV-BSs can be made to land on some designated spots such as on top of tall buildings or specially designed platforms, also known as landing stations (LSs). It might be argued that this approach is similar to a fixed BS deployment, however this approach is quite different from installing a fixed BS at the LS because the flexibility of the UAV-BS is still maintained, as the UAV-BS only needs to stay at a LS to serve user demands for a specific time and can be redeployed to another location subsequently to meet varying network demands. This is not possible with fixed BSs, thus making the LS more robust and adaptable for wireless network applications.

Accordingly, the authors in [294] introduced a new design of wireless multihop network where they assumed that the BSs can be placed in their optimal locations using UAVs in order to maintain the mesh network. In [224], LSs were utilised to maximise the service time of a UAV-BS and sum-rate of the network. The authors in [225] performed a capacity comparison between hovering and landed mm-wave UAV-BSs in order to enable the selection of the preferred deployment option. However, in the previous works [224,225,294], the optimal locations of the LSs were assumed, while other works on optimal UAV placement without LS [24] consider the UAV-BSs to be constantly hovering to serve user demands, thereby consuming a huge amount of energy. To the best of my knowledge, there are no in-depth studies evaluating the LS positioning vis-a-vis various network performance metrics such as energy consumption, throughput and coverage probability, which makes this work timely and relevant.

Therefore, in this chapter, stochastic geometry tools are leveraged to analyse the trade-offs in terms of coverage probability and throughput that can be tolerated when LSs are exploited for UAV-BS deployment to achieve significant reduction in energy consumption. This would assist network operators in finding suitable locations within the network to position the LSs and facilitate the development of new use cases for UAVs in wireless networks. This work is the first attempt at investigating the LS concept from the perspective of determining the suitable locations where they can be positioned within the network to minimise the energy consumption of UAV-BSs while providing the required network performance.

The main focus of this work is on scenarios where the UAV-BS is deployed to provide back-up services such as ensuring service continuity during sudden breakdown of a fixed BS infrastructure or providing capacity enhancement during sudden surge in traffic demand. In such cases, installing a fixed BS at each LS is not necessary, as the UAV-BS only needs to stay temporarily at one LS before moving to another in response to changing network demand. It is assumed that it is not always possible to coincide an LS and the optimal hovering position (OHP) due to the unavailability of suitable LS at the OHP. By employing the LS concept, additional capacity can be provided for both cell switching and spectrum leasing operations, which would lead to enhanced energy saving and revenue generation, without the concern that the overall energy consumption of the network would be increased due to the adoption of UAV-BSs.

5.2 Related Works

Various approaches have been proposed in the literature for energy-efficient UAV positioning. The positioning strategies involve optimising the location, the altitude, and the radius of coverage of the UAV-BS to maximise EE while ensuring QoS of the ground users. Here, a review of the conventional and ML algorithms that have been used for optimal positioning or placement of the UAV-BSs in order to minimise their energy consumption is presented.

Regarding conventional methods, the authors in [295] considered the problem of energy efficient 3D-placement of a UAV-BS for coverage Maximisation. The problem was first modeled as a circle placement problem and a heuristic algorithm was used to determine the optimal 3D location that maximises the coverage area while minimizing the transmit power. The work in [296] investigated the cost and energy optimisation of a UAV-based communication network while considering both the communication and propulsion energy consumption.

In this regard, a multi-level circle parking (MCP) algorithm was developed to determine the optimal 3D-hovering positions of the UAVs that maximises both the uplink and downlink global EE of the network. In addition, the result of the optimal hovering positions obtained were used to determine the number of UAV-BSs and flight parameters required to minimise the total system cost. The authors in [297] proposed a deployment decision mechanism for optimising the number and locations of UAV-BSs in a UAV-assisted vehicular network to maximise the communication coverage and minimise the energy consumption of the UAV-BSs. The proposed mechanism employs circle packing theory to determine the optimal positions of the UAV-BSs while an energy optimisation model was developed to minimise the power consumption of the UAV-BSs.

The authors in [298] developed an analytic solution to determine the optimal altitude for a UAV-BS whereby the transmit power needed to provide coverage to a specific area is minimised. In [223], an EE Maximisation approach was proposed for a UAV-BS relay system to extend the battery life while maintaining network throughput. In the proposed approach, the hovering position, where the UAV-BS expends the least energy is considered to be the optimal UAV-BS location, is determined via mathematical analysis after which the power allocation was also optimised alongside. The work in [299] considered the optimal positioning of a UAV-BS in order to maximise its EE with the altitude and minimum user data rate being constraints. The EE problem was formulated as a monotonic fractional optimisation problem and solved using polyblock outer approximation algorithm. Two UAV location optimisation algorithms were proposed in [300] to minimise the transmit power of the UAV-BS. The first algorithm assumes equal power allocation while the second algorithm is based on successive convex approximation (SCA) and does not assume equal power allocation.

The authors in [301] proposed a UAV-BS positioning algorithm based on Coulomb's law to maximise the EE of the UAV-BSs while considering interference between UAV-BSs and user requirements. An energy-aware 3D deployment algorithm based on Lagrangian and sub-gradient projection for optimal placement of the UAV-BSs was proposed in [302]. In [303], the authors developed a framework for optimising the energy consumption of individual UAV-BSs in a multiple UAV-BSs network while carrying out location specific tasks. The proposed framework uses order-K Markov predictor to estimate the task locations to enable proactive deployment of UAV-BSs and minimise their energy consumption. In addition, a heuristic algorithm was developed to place the UAV-BSs in their right locations as well as assign their respective tasks to them. The authors in [304] investigated the optimal 3D-placement of a UAV-BS with tilting antenna to provide sufficient

coverage for ground users while utilizing minimum energy consumption. A gradient descent algorithm was then proposed to find the optimal altitude of the UAV-BSs.

The authors in [221] considered the importance of on-board circuit power consumption of the UAVs while addressing the problem of their optimal 3D placement in order to maximise the network lifetime. Then, using an analytical approach, the optimal hovering altitude of the UAV-BSs with respect to their coverage radius was derived to determine the coverage and on-board circuit power parameters that result in minimum power consumption. The work in [305] considered the energy efficient placement of UAV-BSs for data collection from ground users based on NOMA. A heuristic algorithm was proposed to determinate the optimal hovering height of the UAV-BS that maximises the EE of the network. The authors in [306] proposed a joint 3D location and transmit power optimisation scheme for UAV-based relay networks to maximise the sum-rate of users. A heuristic algorithm based on alternating descent and SCA was developed to solve the optimisation problem.

The authors in [307] proposed a joint optimisation scheme for both the 3D placement and pathloss factor with the aim of achieving maximum energy efficient coverage. A heuristic algorithm was developed to find the optimal UAV placement and compensation factor that maximises the energy efficient coverage. An optimal UAV placement framework that aims to find the optimal UAV locations required to minimise the total energy consumption of the network while providing a target coverage was introduced in [308]. Both centralized and localized heuristic algorithms were developed to determine the optimal UAV locations for both static and mobile users. The authors in [309] considered the joint optimisation of the transmission power and location of UAV-BS in a relay NOMA network to minimise the power consumption of the network. A double loop iterative algorithm was developed to solve the joint optimisation problem. In [310], the optimal 3D placement for UAVs serving as relays in IoT communications was considered in order to minimise the transmission power of the UAVs while considering the outage probability of the IoT devices. A 3D placement algorithm based on PSO was developed to minimise the transmitted power in both air-to-ground and ground-to-air links.

The case of energy efficient UAV placements in indoor environments for emergency wireless coverage was considered in [311]. Both iterative and ES algorithms were developed to determine the optimal position of the UAV in order to minimise the transmission power. Similarly, the authors in [312] investigated the optimal positioning of a UAV-BS for seamless IoT connectivity in an indoor environment

comprising multiple users at random locations in order to minimise the transmit power of the UAV-BS. An energy efficient low complexity heuristic algorithm was developed to solve the optimal UAV placement problem. The authors in [313] proposed a UAV-BS deployment and scheduling mechanism to ensure optimal placement and effective management of UAV-BS operations while minimizing the energy consumption and ensuring maximum coverage. To achieve these objectives, heuristic algorithms were proposed to ensure the UAVs are placed in the right locations as well as manage their battery recharging cycle.

The authors in [314] investigate EE Maximisation in UAV-assisted NOMA based network via joint optimisation of UAV placement and power allocation while considering QoS constraints. The joint optimisation problem was modeled as a non-linear fractional problem, then an alternating algorithm based on nested Dinkelbach structure was proposed to find the optimal solution. The work in [315] studied the joint optimisation of the UAV location and transmit power in a NOMA-based UAV network while considering the decoding order. The joint optimisation problem was first divided into two sub-problems after which an iterative algorithm was proposed to solve the optimisation problem alternately. The authors in [316] proposed an energy efficient transmission mechanism for UAV-enabled mmWave communication system with NOMA by jointly optimising the UAV position, power allocation, and precoding in order to maximise user coverage and minimise the energy consumption of the UAVs. Due to the complexity of the optimisation problem, it was first divided into three sub-problems and three heuristic algorithms were designed to solve each problem in an iterative manner.

With respect to ML methods, the authors in [317] proposed a proactive power control and positioning framework for UAV-BSs to minimise interference and enhance EE in multi-UAV systems. The proposed framework comprises both offline and online phases. In the former, a supervised learning algorithm (random forest) leverages historical data to build a mobility prediction model while in the latter, the predicted user positions are exploited to proactively determine the sleep/wake status of the UAV-BSs while an unsupervised ML algorithm (k-means) is employed to update UAV-BSs positions and regulate the power consumption. An energy efficient multi-UAV deployment framework was proposed in [318] in order to maximise user coverage probability. An ellipse clustering algorithm was developed to determine the optimal hovering altitude of the UAV that would result in minimal transmit power while maintaining QoS constraints.

A predictive on-demand ML-based UAV deployment for minimizing both the communication and propulsion energy consumption was introduced in [319]. In this regard, a ML framework was developed which uses Gaussian mixture

model (GMM) and weighted expectation Maximisation (WEM) algorithm to forecast the network traffic congestion areas. Then, k-means algorithm was used to partition the service area of each UAV after which a gradient based algorithm was developed to determine the optimal location of the UAVs that results in minimum energy consumption. The authors in [320] considered the problem of reducing the energy consumption required to provide coverage in a multiple UAV network. In pursuit of this objective, a coverage model based on actor-critic RL algorithm was developed to enhance the cooperation of the UAVs in order to provide the energy efficient coverage.

However, most of the energy-efficient UAV positioning techniques considered in the preceding paragraphs require the UAV to be in constant hovering position in order to serve user requests. This greatly limits the amount of energy savings that can be obtained as the UAV consumes a significant amount of energy during hovering [24, 25].

Hence, alternative UAV positioning approaches need to be developed which can reduce the hovering time of the UAV-BSs in order to further enhance the energy saving obtained from these energy optimisation techniques. To address this issue, the concept of LS was introduced in [224] such that the UAVs can land on some designated locations such as roof top of tall buildings, lamp post or some specially designed platforms which can also be equipped with charging pods, rather than having to hover continuously to serve user request and expend so much energy, which is a major challenge for battery limited UAVs. This also resulted in service time and sum-rate Maximisation.

In this regard, the authors in [225] performed a capacity comparison between landed and hovering UAV with the aim of determining which approach will be suitable for adoption. Their finding reveals that the choice of a suitable deployment option depends on certain factors including the number of UAVs deployed, the distance between the charging stations and service area, and capacity of the UAV battery. The work in [321] proposed a deep Q-learning approach for optimising UAV trajectories using the LS concept where the UAVs do not have to continuously fly along the trajectory but can land at some locations along its path in order to minimise energy consumption while meeting user demands. More research works need to be done in this direction to determine the optimal locations where UAVs can land along their trajectory and the optimal separation distances between the UAV OHP and the suitable LSs, in order to improve the amount of energy savings while respecting the QoS constraints.

Therefore, in this work, the feasibility of an alternative energy-efficient UAV positioning approach based on the LS concept is considered using stochastic ge-

ometry tools.

5.2.1 Contributions

This work investigates the impact of the separation distances between the LSs and the OHP on the coverage probability, throughput, and energy consumption of the UAV-BS. The following are the contributions of this work:

- Closed form expressions using stochastic geometry tools are derived to model the relationship between UAV power consumption, coverage probability, throughput and separation distance.
- The minimum transmit power required to maintain the same QoS at the LS as that of the OHP is derived, and the implication on the power consumption of the UAV-BS is analysed.
- A comparison of the UAV-BS battery lifetime using the LS approach with that of the OHP approach is performed to highlight the advantage of the LS method.
- The three categories of frequency bands employed in 5G; sub-1 GHz, mid-band, and mm-wave are considered to investigate the impact of the LS position on the coverage and throughput of the network.
- Numerical analysis are carried out using Monte Carlo simulations to validate the derived analytical models.

5.3 System Model

A 3D UAV network in cylindrical coordinate (r, θ, z) as shown in Fig 5.1 is considered. The UAV altitude is assumed to be constant (h), and the coverage area radius is denoted as R. The UEs are distributed following a homogeneous Poisson point process (PPP) Φ_u in a 2D plane with density, ϕ_u. The 2D UE distribution can be denoted by $S_u = \bigcup_{x \in \Phi_u} B(O, R)$, where $B(O, R)$ is a 2D circular area with the radius R centered at O. The distance between the optimal hovering position, O, and the LS is denoted by Δ, $f(v, \Delta)^2 = v^2 + \Delta^2 - 2v\Delta\cos\theta$. A single UAV deployment scenario is considered and it is assumed that the whole area is served by only the UAV, hence, the interference is assumed to be negligible.

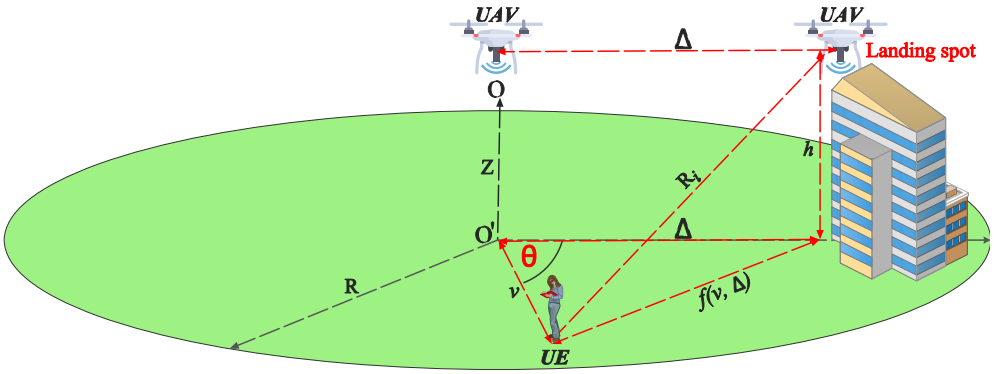

Figure 5.1: An illustration of the 3D UAV-BS network.

The channel model consists of the large-scale path loss and Rayleigh fading component[1]. For a typical UE, its received power from the UAV-BS is $PD_oH_iR_i^{-\alpha}$, where P is the transmit power, $H_i \sim \exp(\mu)$ is the channel gain and μ is the noise spectral density, $\alpha > 2$ is the path loss exponent, R_i is the distance between the LS and the i^{th} UE, and D_o is the path loss at reference distance. For simplicity and without loss of generality, it is assumed that the OHP for deploying UAV-BS is located at the origin $O \rightarrow (0, 0, h)$, and O' is the projection of O to 2D plane. However, one of the methods proposed in the literature [24] can be used to determine the OHP, but that is not the focus of this work. Δ is the distance between the OHP and the LS. The parameter v is the distance from O' to a typical UE, while θ is the angle formed by the projection of the LS to the 2D plane and the UE. Additionally, it is assumed that the UAV-BS is equipped with an omnidirectional antenna and that each UE can receive the UAV-BS's signal equally in all directions.

5.3.1 UAV-BS Power Consumption

The power consumption of the UAV-BS has two parts: hovering and communication.

- Power consumption due to hovering of the UAV is [76]:

$$P_{\text{hov}} = \frac{\delta_c}{8}\rho r_s A B_V^3 R_r^3 + (1+\kappa)\frac{W^{2/3}}{\sqrt{2\rho A}}. \tag{5.1}$$

- Power consumption due to communication is [72]:

[1]Rayleigh fading channel is mainly employed when there is a probability that there would be no dominant line of sight component. However, this channel is utilised in this proof of concept work because there is a possibility of having non-line of sight between the UAV-BS and the UE, even though the non-line of sight component has not been investigated in this initial work. Future work would consider both line of sight components, the presence of obstacles as well as the scenario where many UAV-BSs are deployed.

$$P_{\text{com}} = P_{\text{o}} + \tau_t \eta P. \tag{5.2}$$

The total power consumption of the UAV-BS, P_{total} can be expressed as the sum of the power consumption due to hovering and that due to communication and is given by:

$$P_{\text{total}} = P_{\text{hov}} + P_{\text{com}}. \tag{5.3}$$

The parameters in (5.1) and (5.2) are defined in Table 5.1.

5.4 Coverage Probability, Transmit Power, and Throughput Analysis

In this section, closed form expressions for finding the coverage probability, minimum transmit power required to maintain the same coverage probability at the OHP using the LS, and the throughput are derived using stochastic geometry. The results obtained from these closed form expressions are then compared with those obtained using simulations in section 5.5 in order to ascertain their validity.

5.4.1 Coverage Probability Analysis

It is assumed that the UAV network does not receive interference from other BSs. Thus, the coverage probability can be expressed as:

$$\mathrm{P_c} = \mathbb{P}(\mathrm{SNR} > \lambda), \tag{5.4}$$

where $\mathrm{P_c}$ is probability that $\mathrm{SNR}_i > \lambda$ over the entire circular area with radius R centered at the origin, O.

For a given distance R_i from the UAV position to UE, the SNR is given as

$$SNR_i = \frac{D_o \left(\frac{R_0}{R_i}\right)^{\alpha} \cdot (H_i)^2 \cdot P}{N}, \tag{5.5}$$

where $R_i = \sqrt{h^2 + \Delta^2 + v^2 - 2\Delta v \cos\theta}$ and N is the system noise.

Lemma 1. *The downlink coverage probability of the UAV network with the UAVs located at the LSs is given by*

$$\mathrm{P_c} = \frac{1}{2\pi R} \int_0^R \int_0^{2\pi} \exp\left(\frac{-\lambda N}{D_0 P} \times \left[\frac{\sqrt{h^2 + v^2 + \Delta^2 - 2\Delta v \cos\theta}}{R_0} \right]^{\alpha} \right) \mathrm{d}\theta \mathrm{d}v. \tag{5.6}$$

Proof. Inserting (5.5) into (5.4), $\mathrm{P_c}$ becomes

$$\begin{aligned}\mathrm{P_c} &= \mathbb{P}\left[\frac{D_o\left(\frac{R_0}{R_i}\right)^{\alpha}\cdot(H_i)^2\cdot P}{N} > \lambda\right] \\ &= \mathbb{P}\left[|H_i|^2 > \frac{\lambda N}{D_0 P}\left(\frac{R_i}{R_0}\right)^{\alpha}\right] \\ &= \mathbb{E}_{r_i}\left[\mathbb{P}\left[|H_i|^2 > \frac{\lambda N}{D_0 p}\left(\frac{R_i}{R_0}\right)^{\alpha}\right]\right] \\ &= \mathbb{E}_{r_i}\left[\exp\left[\frac{\lambda N}{D_0 p}\left(\frac{R_i}{R_0}\right)^{\alpha}\right]\right]\end{aligned} \tag{5.7}$$

The coverage probability is obtained over $B(O,R)$ that is defined over $0 \leq v \leq R$ and $0 \leq \theta \leq 2\pi$. Note that from Fig. 5.1 R_i can be expressed as $R_i = \sqrt{h^2+\Delta^2+v^2-2\Delta v\cos\theta}$. By substituting R_i into (5.7) and applying integral, the closed-form expression of coverage probability in (5.6) can be obtained. □

5.4.2 Transmit Power Analysis

As the value of Δ increases, the UAV-BS needs to adjust its transmit power in order to maintain the same coverage probability as that of the OHP. To achieve this target, $\mathbb{P}_c[R] = \mathbb{P}_c[R+\Delta]$.

Lemma 2. *The minimum transmit power, P_{ls}, required by the UAV-BS at the LS to maintain the same coverage reliability $\mathbb{P}_c$ at the cell edge as the OHP is given by*

$$P_{\mathrm{ls}} = P\left[1+\frac{\Delta}{R}\right]^{\alpha}. \tag{5.8}$$

Proof. See Appendix A. □

Substituting P_{ls} for P in (5.2), the total power consumption due to communication of the UAV-BS becomes:

$$P_{\mathrm{com}} = P_{\mathrm{o}} + \tau_t\eta P = P_{\mathrm{o}} + \tau_t\eta P\left[1+\frac{\Delta}{R}\right]^{\alpha}. \tag{5.9}$$

5.4.3 Throughput Analysis

The average throughput can be expressed as $\mathbb{T}_p = B\mathcal{R}/\log 2$ where B is the overall bandwidth of the channel and $\mathcal{R}$ is the average spectral efficiency in nats/sec/Hz.

Lemma 3. *Average spectral efficiency of a typical UE in the UAV network with the UAVs located at the LSs is given by*

$$\mathcal{R} = \frac{1}{2\pi R} \int_0^R \int_0^{2\pi} \int_0^{\infty} \exp\left(-\beta^{\alpha/2}\right) \times Q \times \left(e^t - 1\right) \mathrm{d}t\mathrm{d}\theta\mathrm{d}v \tag{5.10}$$

where $\beta = (h^2 + \Delta^2 + v^2 - 2v\Delta\cos\theta)$ and $Q = \frac{N}{D_0 P} \cdot R_0^{-\alpha}$.

Proof. See Appendix B. □

Table 5.1: UAV-BS power consumption parameters [72, 76]

Symbol	Meaning	Value
δ_c	Profile drag coefficient	0.012
ρ	Air density	1.225 kg/m^3
r_s	Rotor solidity	0.4255
R_r	Rotor radius	0.2286 m
A	Rotor disc area	0.1642 m^2
B_v	Blade angular velocity	942.5 rad/s
κ	Incremental correction factor for induced power	0.1
W	Aircraft weight	161.5 Newton
P_o	Circuit power	56 W
η	Amplifier efficiency	2.6
τ_t	Normalized traffic load	1
P	Transmit power	38 dBm

5.5 Results and Discussions

In this Section, the performance of the UAV-BS when deployed at OHP (i.e., $\Delta = 0$) is compared to when deployed at LS and the trade-offs in power consumption, coverage probability and throughput with variations in Δ values are quantified. The analytic formulations are validated in Section 5.4 using Monte Carlo simulations.

The simulations were carried out for the three categories of frequencies used in the 5G network, namely: sub-1 GHz (750 MHz) with 5 MHz bandwidth, mid-band (3.5 GHz) with 100 MHz bandwidth, and millimetre-wave (mm-wave) (28 GHz) with 1 GHz bandwidth in order to investigate the effect of the LS positioning on the coverage and throughput performance. The number of UEs is set to 300, $\alpha = 3$, h is assumed to be 20 m, $\mu = -174$ dBm/Hz, small-scale fading is taken into account, and an omnidirectional antenna is considered. The area of interest is considered to be a circle with radius $R = 3000$ m, while the UAV-BS is assumed to have maximum coverage radii of 200 m, 2000 m and 3000 m for mm-wave, mid-band and sub-1 GHz bands, respectively. The UAV considered in the simulation

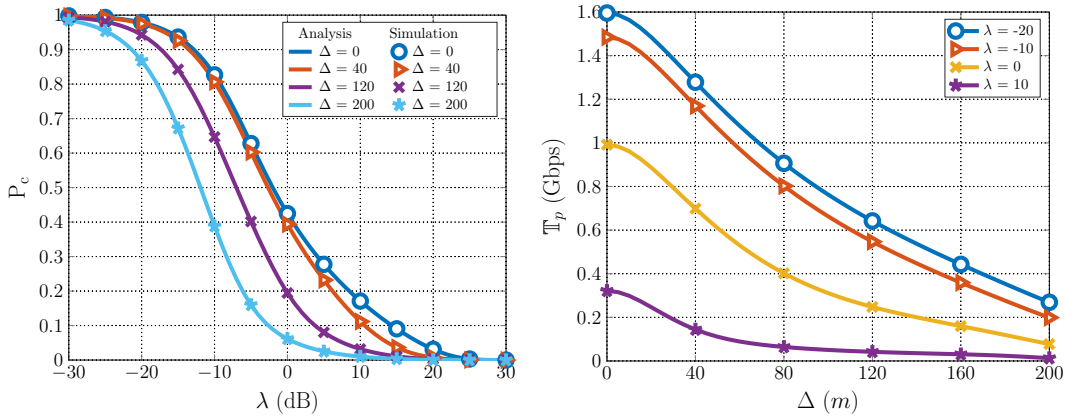

(a) Coverage probability at 28 GHz (b) Throughput at 28 GHz

Figure 5.2: The coverage probability and average throughput at 28 GHz, for different values of Δ (m) and λ (dB).

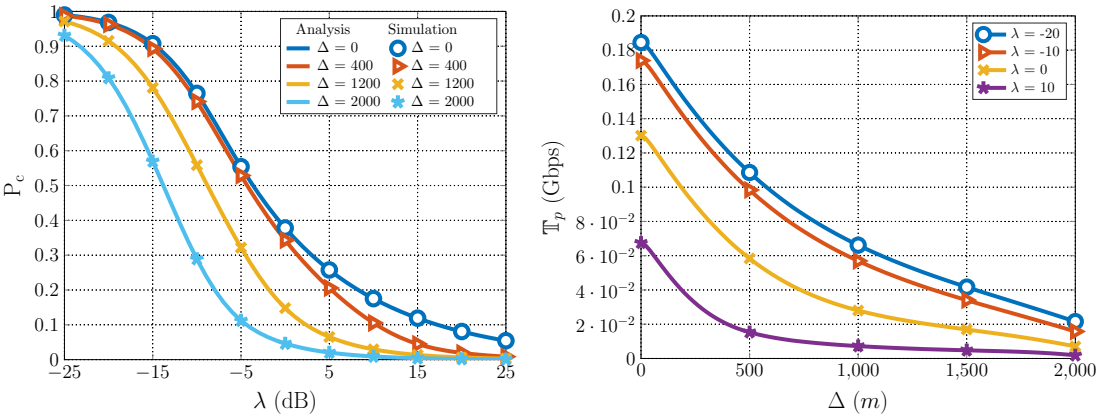

(a) Coverage probability at 3.5 GHz (b) Throughput at 3.5 GHz

Figure 5.3: The coverage probability and average throughput at 3.5 GHz, for different values of Δ (m) and λ (dB).

is the Aurelia X8 [322], with battery capacity and voltage of 24000 mAh and 22.2 V respectively. The parameters used for both OHP and LS are presented in Table 5.1.

Table 5.2: Power consumption comparison of the two types of UAV-BS deployments

Deployment Type	$P_{\mathbf{com}}$ **(W)**	$P_{\mathbf{hov}}$ **(W)**	$P_{\mathbf{total}}$ **(W)**	**Battery life time (mins)**
OHP	72.38	1335.50	1407.80	22.70
LS	72.38	0.00	72.38	445.65

The power consumption analysis of OHP and LS scenarios with fixed UAV-BS transmit power is shown in Table 5.2. Table 5.2 clearly indicates that LS can help

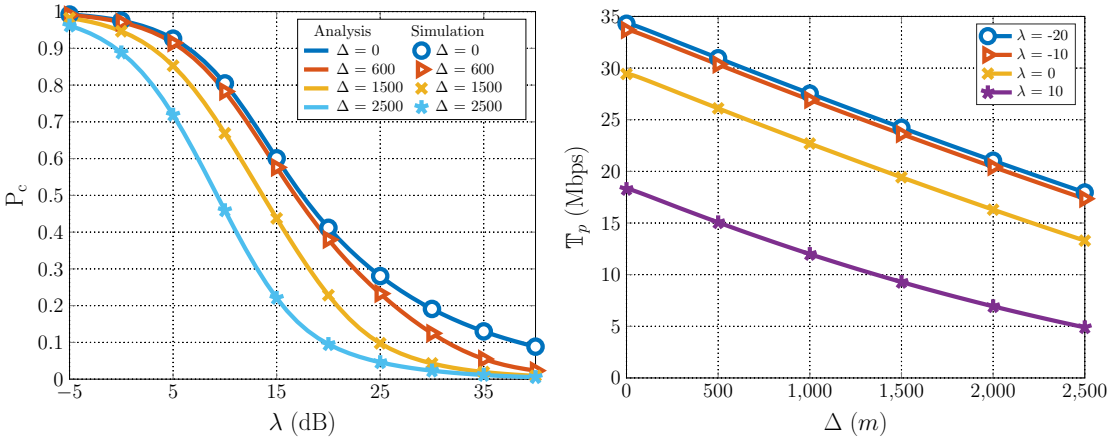

(a) Coverage probability at 750 MHz

(b) Throughput at 750 MHz

Figure 5.4: The coverage probability and average throughput at 750 MHz, for different values of Δ (m) and λ (dB).

increase the battery life time by about 20 times that of OHP. While exploiting LSs for UAV-BS deployment could be ideal for energy conservation, the LS might not be at the OHP which could affect network performance in terms of coverage probability and throughput.

The coverage probability at various frequency bands is obtained as shown in Fig. 5.2a, Fig. 5.3a, and Fig. 5.4a, with analytical and simulation results denoted by lines and markers, respectively. It can be seen that the simulation results closely match the analytical curves. Whereas, Fig. 5.2b, Fig. 5.3b, and Fig. 5.4b evaluate throughput as a function of Δ for different values of λ. In Fig. 5.2a, a very little difference in coverage probability can be observed when the value of Δ is less than 40 m for 28 GHz frequency. However, the difference in coverage probability becomes significant as Δ exceeds 40 m from the OHP. From the throughput perspective, Fig. 5.2b shows there is an exponential decay in the network throughput as the value of Δ increases. This means that moving the UAV-BS away from the OHP would significantly impact system throughput at 28 GHz frequency regardless of the distance of the LS from OHP.

The same analysis is conducted at 3.5 GHz, as shown in Figs. 5.3a and 5.3b for coverage probability and throughput, respectively. A similar trend in the coverage probability and throughput as in Figs. 5.2a and 5.2b is also observed here. However, the value of Δ where only a slight change in the coverage probability is observed increased from 40 m to 400 m while the throughput is less affected by the shift from the OHP at this frequency compared to the 28 GHz frequency. This means that at this frequency band, the LS can be located at a greater distance from the OHP. Figs. 5.4a and 5.4b illustrate the coverage probability and

throughput results for the 750 MHz frequency. Fig. 5.4a reveals that the coverage probability at this frequency is least affected by the movement of the UAV-BS away from the OHP. Hence, when the value of Δ is 600 m, the change in coverage probability is very little. The throughput is also least affected at this frequency as a linear decay in the slope of throughput curves is observed as the value of Δ increases for different SNR thresholds. This means that the UAV-BS can be moved farthest away from the OHP without much impact on the performance of the network at this band.

The difference in performance at these frequency bands can be traced to their propagation characteristics. Mm-wave frequency (28 GHz) have a small propagation distance as such are easily affected by slight movement from the OHP. The 3.5 GHz and 750 MHz frequencies have longer propagation distances, and hence they can tolerate larger values of Δ without much reduction in the network performance.

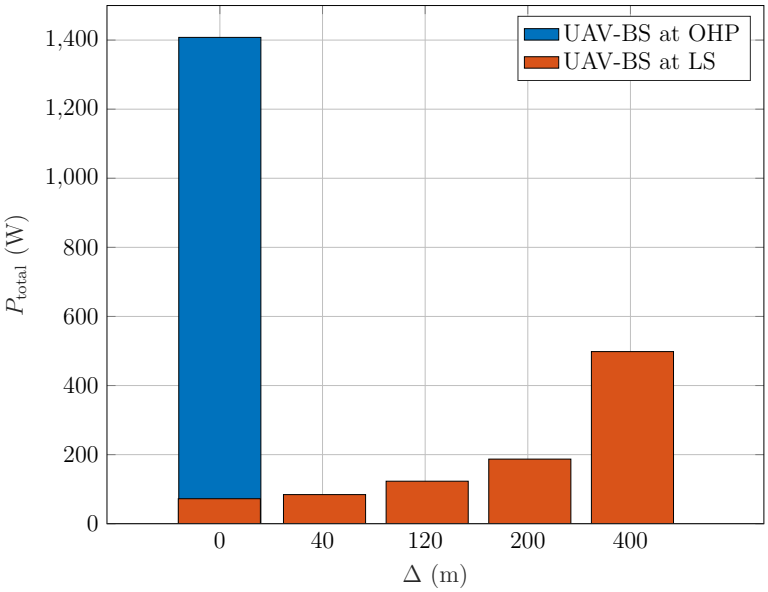

Figure 5.5: Total power consumption comparison of the UAV-BS at LS with different values of Δ and the total power consumption of the UAV-BS at OHP. Note that the QoS is maintained despite changes in Δ values for UAV-BS at LS.

Finally, as it may not always be possible to locate the LS at the OHP, a suitable position could be at a distance, Δ from the OHP. Hence, the impact on the total power consumption of the UAV-BS due to the increase in Δ is explored, while maintaining the same QoS as provided at the OHP. In this regard, the minimum transmit power (P_{ls}) that would be required to maintain the same coverage probability at the cell edge as that of OHP using the LS was first derived in (5.8). Eq. (5.8) clearly demonstrates that as Δ increases, the transmit power increases, and that would drive the increase in the total power consumption of

the UAV-BS. In Fig. 5.5, the impact of Δ on the total power consumption of the UAV-BS with LS in comparison to the total power consumption of the UAV-BS with OHP is illustrated. From Fig. 5.5, it can be clearly observed that the total power consumption of the UAV-BS with LS increases as Δ increases. This increase in the total power consumption is driven by the transmit power increase to maintain the QoS. However, with the increase in the value of Δ from 0 to 400 m, the total power consumption of the UAV-BS with LS at 400 m is still about one-third that of the UAV-BS with OHP.

However, it must be noted that even though it is possible to continue increasing the transmit power in order to maintain the QoS, the extent to which the transmit power can be increased is limited by restriction put in place by regulatory bodies and this ultimately limits the maximum distance that the LS can be situated from the OHP in real network deployments.

5.6 Conclusion

In this Chapter, the effect of utilising LSs on UAV energy consumption, coverage probability and throughput performance was investigated. A closed-form expression for each metric was first derived and validated using Monte Carlo simulations. Analytical and simulation results revealed that the distance between the LS and the OHP is inversely related to both the coverage probability and system throughput. However, the magnitude of performance reduction depends on the transmission frequency utilised. It was shown that the performance of the network can be maintained with the LS approach as in the OHP approach by adjusting the transmit power of the UAV-BS. Therefore, network providers can significantly reduce the energy consumption involved in exploiting UAVs for wireless communications by first examining the service requirements of users and the frequency band involved, then the analytical solutions developed in this work can be used to determine the best locations for the LSs as well as the transmit power offset required to maintain the QoS of the UEs.

Chapter 6

Conclusions and Future Research Directions

The contributions of this thesis are summarised in this chapter. In addition, the opportunities for the extension of this research work are also identified.

6.1 Thesis Summary

In this section, a chapter-by-chapter summary alongside major contributions and implications of the research work carried out in this thesis are presented.

In Chapter 1, an overview of the research works carried out in this thesis was presented. The major energy consumers in cellular networks, which are UDNs and UAV-BSs, were identified. In addition, the research motivations including:

- reduction in OPEX and CAPEX,
- reduction in greenhouse gas emissions,
- generation of additional revenue for MNOs,
- improvement in the QoS of the network,

were discussed. Furthermore, the main objectives and contributions of this thesis were also highlighted.

In Chapter 2, different BS deployments in the RAN, including homogeneous, heterogeneous, ultra-dense and UAV-based network were first highlighted. Afterwards, an overview of analytical, conventional and ML algorithms for energy optimisation in cellular networks was presented . Then, energy optimisation in both fixed and UAV-based cellular networks, and revenue Maximisation in cellular networks were considered including a review of the state-of-the-art on cell

switching, cell switching and spectrum leasing, and energy efficient UAV positioning while identifying and analysing the research gaps. The major take-away from Chapter 2 are itemised as follows:

- The RAN, which mainly comprises various types of BS deployments, is the major source of energy consumption in mobile cellular networks. Thus, minimising the energy consumption of the BSs would result in significant reductions in the total energy consumption of the mobile cellular networks.

- The cell switching approach is one of the most effective techniques for minimising energy consumption in cellular networks because it ensure that the total energy consumption is proportional to the total traffic load of the network, such that the network is only available when needed (or on-demand) rather than being always available (or always-on). This helps to prevent energy wastage during periods of under-utilisation or inactivity. In addition, it involves minimal changes to network configuration and it requires less monetary cost to implement.

- To preserve the QoS of the users originally connected to BSs that are switched off, both CDSA and traffic offloading are required. The functional separation of the control and data plane, as well as the duplication of coverage of the SBSs by the MBSs in the CDSA makes it easy to offload the traffic of SBSs to MBSs before switching them off. This in turn prevents coverage holes and degradation in the QoS of users originally associated with sleeping BSs.

- Although cell switching leads to energy savings, it also results in the under-utilisation of spectrum of BSs that are turned off in order to minimise the energy consumption of the network. Hence, spectrum leasing where the holders of spectrum license lease it for a fee has been considered to be a suitable approach for enhanced spectrum utilisation but most importantly, generating addition revenue for MNOs.

- Even though UAVs have found diverse applications in wireless communication networks, including emergency pop-up networks, backhauling, traffic offloading, etc., due to their flexibility, easy deployment and adaptability, the limited battery capacity seems to undermine the versatility of their application. Despite numerous attempts at developing various recharging mechanisms (e.g., swapping, laser charging, tethering, etc.) and energy optimisation techniques (e.g., optimal positioning, trajectory optimisation, etc.), they do not lead to significant energy reduction, as the energy spent on

flying or hovering the BS is very significant. Hence, an alternative energy-efficient deployment solution using the LS concept, where the UAVs can land in designated location within the network instead of flying or hovering continuously, could help prolong the battery lifetime and also maximise the UAV-BSs service time.

In the Chapter 3, the need to develop a scalable and computationally efficient cell switching framework for energy optimisation in UDNs was emphasised, due to the limitations of most state-of-the-art methods. Two energy optimisation frameworks based on Q-learning and ANN were first presented. The Q-learning algorithm has a limitation known as 'curse of dimensionality' [146]. This occurs because it uses tables to store the learnt state-action values, which means that a huge table needs to be learnt when the state or actions becomes very large, thereby leading to a huge computational overhead and large memory requirement. ANN models are very difficult and computationally demanding to train when the number of input variables becomes very large. As a result of the aforementioned limitations, the results obtained from both solutions revealed that they are only suitable for small to medium sized networks, as the would operate well with low complexity in such networks. However, they are infeasible for large scale networks such as UDNs, hence the need to develop a new energy optimisation framework.

In this regard, a hybrid cell switching framework known as THESIS, which combines the advantages of both ES (which is guaranteed to always produce the optimal cell switching strategy but with huge computation overhead) and k-means algorithm (which is very computationally efficient but very sub-optimal) was developed to produce a suitable trade-off between complexity and accuracy in order to enable its application in UDN. In addition, a MLC algorithm, which is purely based on k-means is also developed as a benchmark to represent the upper bound for computational complexity because of its high computational efficiency. Furthermore, ES algorithm was considered as another benchmark, to depict the upper bound for optimality because it always guarantees to find the optimal solution. The performance evaluation reveals that one hand, THESIS can find a good trade-off between ES and MLC as it is 30% less optimal than ES but has computational complexity that is significantly lesser than that of ES. On the other hand, its is about 31% more optimal than MLC but about 95% less computationally efficient.

With network densification been employed in 5G and beyond networks, rising energy prices and the need for environmental sustainability, the proposed cell switching and traffic offloading framework can be implemented in both existing and future networks to help MNOs scale their energy consumption with capacity

utilisation, irrespective of network size, thereby resulting in energy conservation, cost effectiveness, and achievement of net zero emission.

Seeing that MNOs need to continuously make profit in order to keep their business going, it is important that more creative avenues for generating income be developed in order to enhance the profitability of the business. As a result, in Chapter 4, the challenge of the spectrum under-utilisation due to the presence of dormant spectrum after cell switching operation was considered. To solve this problem, a revenue maximisation model was developed to take advantage of these dormant spectrum by leasing them to smaller network operators in order to generate additional revenue for MNOs. To achieve this goal, a cell switching and spectrum leasing framework based on SA algorithm was proposed to determine the optimal cell switching and spectrum leasing strategy that would result in maximum revenue to the MNO. Two spectrum and electricity pricing policies and two spectrum demand scenarios (DT and NDT spectrum demand) were considered. It was observed that the DT spectrum demand resulted in 19% more revenue for the PN, who are the spectrum license holders, than the NDT spectrum demand. In addition, it also enables the SN to access 21% more spectrum during periods of low traffic demand in the PN, since more BSs can be switched off at this time, thereby making more spectrum available for the accumulated data demands of the SN. Also, the unit cost of spectrum during DT spectrum demand is about 2% lesser than that of NDT spectrum demand as the spectrum cost is normally lesser during off peak periods due to the reduced real-time demand.

The additional revenue generated by the MNOs from cell switching and spectrum leasing can help offset part of the cost of the purchase of spectrum license. In addition, diverse IoT applications would also benefit from the proposed cell switching and spectrum leasing framework as small network operators that offer IoT services would be able to access the amount of spectrum needed for their non-delay tolerant data transmission, thereby facilitating massive IoT adoption.

In Chapter 5, the feasibility of an alternative energy-efficient UAV deployment solution using the LS concept was proposed since the comprehensive survey on energy consumption in UAV-based cellular network in Chapter II showed that most of the energy optimisation approaches proposed in literature do not lead to significant energy savings. This is due to the predominant energy consumption of the UAV due to hovering which greatly affects the battery life time of the UAV. Hence, leveraging stochastic geometry tools, mathematical expressions were derived to model the relationship between the separation distances and the OHP and LS positions, the power consumption, throughput, and coverage probability. These mathematical models were validated using simulations involving different

frequency bands utilised in 5G including sub 6 GHz, midband, and mm-wave frequencies. It was observed that the energy consumption with LS is 95% less than that of OHP and can help prolong the battery lifetime by up to 7 hours more than that of OHP. In addition, the simulations results also show that as the separation distance from the OHP increases, both the throughput and coverage probability decrease. However, the coverage probability and throughput with LS can still be maintained as that of OHP, though with some increase is the transmit power, which is still significantly lesser than the energy consumed by hovering the UAV-BS at the optimal position. However, this is depends on how much transmit power increase is allowable by telecommunication regulatory bodies.

Energy optimisation in UAVs would help reduce CAPEX and OPEX as lesser of UAV-BSs would need to be deployed, fewer cases of network interruptions would occur given that the need to replaced UAVs with depleted batteries would greatly reduce, thereby resulting in enhanced network performance. Hence, network engineers can make provision for incorporating LSs during their network planning stages, particularly in areas where sudden traffic surges may occur such as in stadia, concert centres, city centres, etc., to enable easy deployment of UAV,s to the locations where additional resources are required due to increased capacity demands. This is because the LS help reduce the energy consumption of the UAV-BS, thereby increasing the battery life and prolonging the period of service delivery.

6.2 Future Research Directions

In this section, the future research directions that could lead to improvement in the performance of the various optimisation frameworks proposed in this thesis are presented.

1. Energy optimisation in fixed cellular networks via cell switching and traffic offloading:

    - The amount of energy savings that can be achieved using cell switching approach is greatly affected by the amount of radio resources at the MBS, as this is required for traffic offloading in order to preserve the QoS of the users. The offloading capacity can be enhanced by replacing or augmenting the MBSs with UAV-BSs. Therefore, the effect of the UAV-BSs deployment in existing cellular networks alongside cell switching needs to be investigated to quantify its energy saving potential.

- There is also the possibility of adjusting the transmit power of the remaining BSs after cell switching is implemented to further enhance energy optimisation via optimal power allocation. Hence, the joint optimisation of cell switching and power allocation is another research area that can be exploited to improve the energy saving capabilities of cell switching technique.
- Recently, RIS have be exploited for cellular network optimisation because of their low energy consumption. This is possible because RIS are passive devices that do not have amplifiers, which is the major source of consumption in cellular BSs. An area of further research could be to consider a mixed deployment of RIS and SBSs is what can be know as RIS-assisted cell switching, such that the traffic of switched off SBSs can be redirected to RIS to further optimise energy consumption.
- Another area that needs to be considered is the holistic power consumption of the network involving the optimisation of both the power consumption of the BSs and user devices. As cell switching involves offloading users originally connected to switched off BSs to neighbouring or higher tier BSs, this is normally associated with increase in the transmission power of the users devices which negatively impacts their battery life. Therefore, a consideration of the power consumption of both BSs and user devices during cell switching in order to optimise the overall energy consumption of the network needs to be carried out.
- In order to improve the scalability, computational efficiency and privacy of users during cell switching implementation, federated ML can be exploited whereby the learning can be performed in a decentralized manner at each SBSs and only the trained model is shared with the MBS for final decision making to facilitate the cell switching decision making process.
- The effect of the power consumed during the switching on and off of the BSs in the UDHN on the amount of energy savings that can be obtained by the proposed solution should also be investigated.
- The effect of the users' channel condition, location, and mobility on their ability to access sufficient radio resources from the MBS in order to ensure that their QoS is maintained during cell switching and traffic offloading should also be considered.

2. Revenue maximisation in cellular networks via cell switching and spectrum

leasing:

- Even though the spectrum leasing scenario considered in this research involved a one-to-one mapping of the SN-BS to a PN-BS, however, there are scenarios where more than one SN operators would be competing for the spectrum of the PN in an area. In such a situation, there is a need to determine which SN operator to lease the spectrum or the possibility of sharing the spectrum among the SNs, in order to satisfy their spectrum demands.
- The proposed cell switching and spectrum leasing model may not be too applicable for NDT spectrum demand scenarios as the spectrum may be demanded for critical communication during periods where there is no dormant spectrum or insufficient spectrum. In such situations, UAVs can be deployed to provide not just additional offloading capacity, as previously discussed under cell switching, but additional spectrum for NDT spectrum demand as well as enhanced revenue for the PN. Thus, UAV-assisted cell switching and spectrum leasing need to be investigated.
- There is also the need for the development of more advanced algorithms for cell switching and spectrum leasing using other heuristics, such as matching theory, for cases where the available spectrum needs to be shared with multiple users. Also advanced ML and DL architectures can also be exploited to develop more efficient cell switching and spectrum leasing models.

3. Energy optimisation in UAV-based cellular networks via energy efficient UAV positioning:

   - A more detailed study of the LS concept by considering the presence of obstacles as well as multiple UAV deployments is required to fully appreciate the importance of the LS, as this would introduce some interference which would affect the power consumption of the network and other network performance metrics.
   - The combination of the LS concept and other energy optimisation techniques such as trajectory optimisation and transmission scheduling also needs to be investigated to ascertain the combined effect on the energy consumption of the network.
   - In addition, the LS concept can also be combined with cell switching and traffic offloading in fixed cellular networks, to improve the energy

saving potential of UAV-assisted cellular networks.

- In place of SBSs, RIS, which are low power consuming devices can also be mounted on UAVs to further reduce the energy consumption of the UAV, thereby increasing their battery life and service time of UAVs.
- The impact of THz frequency band on the position of the LSs also need to be investigated. This is because THz frequency presents a unique propagation characteristics that would affect the location of the LSs.
- The derivation of more tractable mathematical models to examine the throughput and coverage probability of the UAV-BS when the LS is utilised should be considered.

Appendix A

Proof of Lemma 2

The coverage probability at cell edge with the aim of meeting the minimum coverage probability of the hovering scenario is given by:

$$\bar{P}_c[R] = \exp\left[\frac{-\lambda N}{D_0 P}\left[\frac{R}{R_0}\right]^{\alpha}\right] \tag{6.1}$$

The minimum transmit power required in LS scenario to maintain the same coverage probability as the hovering scenario is $P_c[R] = \bar{P}_c(R+\Delta)$

$$\exp\left[\frac{-\lambda N}{D_0 P}\left[\frac{R}{R_0}\right]^{\alpha}\right] = \exp\left[\frac{-\lambda N}{D_0 P_{\text{ls}}}\left[\frac{R+\Delta}{R_0}\right]^{\alpha}\right] \tag{6.2}$$

let $K = \frac{\lambda \text{N}}{D_0 R_0^{\alpha}}$

$$\exp\left[-\frac{K}{P}R^{\alpha}\right] = \exp\left[-\frac{K}{P_{\text{ls}}}[R+\Delta]^{\alpha}\right] \tag{6.3}$$

Hence $P_{\text{ls}} = P\left[\frac{R+\Delta}{R}\right]^{\alpha} = P\left[1+\frac{\Delta}{R}\right]^{\alpha}$

Appendix B

Proof of Lemma 3

Following [98], the average spectral efficiency can be expressed in terms of the coverage probability as

$$\begin{aligned}\mathcal{R} &\triangleq E_x\left[E_{SNR}[\ln(1+SNR(x))]\right] \\ &= \int E_{SNR}[\ln(1+SNR(x))]f(x)\mathrm{d}x\end{aligned} \tag{6.4}$$

Given that $E[x] = \int_0^\infty P(x > x]dx$ for $x > 0$

$$\begin{aligned}E_{SNR}[\ln(1+SNR(x))) &= \int_0^\infty P\left[\ln\left(1+SNR\left(x\right) > t\right]\mathrm{d}t\right. \\ &= \int_0^\infty P\left[SNR(x) > e^t - 1\right]\mathrm{d}t\end{aligned} \tag{6.5}$$

where $SNR = \frac{D_0\left(\frac{R_0}{R_i}\right)^\alpha\left[H_\mathrm{i}\right]^2\cdot P}{N}$ from (5.5) and given $Q = \frac{N}{D_0 P}\cdot R_0^{-\alpha}$, $h_i = \left|H_\mathrm{i}\right|^2$ and $R_i = x$ then $SNR = \frac{h_k x^{-\alpha}}{Q}$. Note that x is expressed as $\sqrt{h^2+\Delta^2+v^2-2\Delta v\cos\theta}$

$$E_{SNR}[\ln(1+SNR(x))] = \int_0^\infty P\left[h_k > x^\alpha Q\left(e^t-1\right)\right]\mathrm{d}t \tag{6.6}$$

In addition the probability of random variable h_i can be presented as $P\left[h_k > x^\alpha Q\left(e^t-1\right)\right] = \exp\left[-x^\alpha Q\left(e^t-1\right)\right]$:

$$E_{SNR}[\ln(1+SNR(x))] = \int_0^\infty \exp\left(-x^\alpha Q\left(e^t-1\right)\right)\mathrm{d}t, \tag{6.7}$$

$$\mathcal{R} \triangleq E_x\left[E_{SNR}[\ln(1+SNR(x))]\right]. \tag{6.8}$$

By substituting (6.7) into (6.8) and integrating over the whole area we obtain the average spectral efficiency expression in (5.10).

Bibliography

[1] J. G. Andrews, S. Buzzi, W. Choi, S. V. Hanly, A. Lozano, A. C. K. Soong, and J. C. Zhang, "What Will 5G Be?" *IEEE Journal on Selected Areas in Communications*, vol. 32, no. 6, pp. 1065–1082, June 2014.

[2] Y. Li, Y. Zhang, K. Luo, T. Jiang, Z. Li, and W. Peng, "Ultra-dense HetNets meet big data: Green frameworks, techniques, and approaches," *IEEE Communications Magazine*, vol. 56, no. 6, pp. 56–63, Jun 2018.

[3] S. Gangakhedkar, H. Cao, A. R. Ali, K. Ganesan, M. Gharba, and J. Eichinger, "Use cases, requirements and challenges of 5G communication for industrial automation," in *2018 IEEE International Conference on Communications Workshops (ICC Workshops)*, July 2018, pp. 1–6.

[4] M. Agiwal, A. Roy, and N. Saxena, "Next generation 5G wireless networks: A comprehensive survey," *IEEE Communications Surveys & Tutorials*, vol. 18, no. 3, pp. 1617–1655, Feb 2016.

[5] W. Saad, M. Bennis, and M. Chen, "A vision of 6G wireless systems: Applications, trends, technologies, and open research problems," *IEEE Network*, vol. 34, no. 3, pp. 134–142, Jun 2020.

[6] M. Giordani, M. Polese, M. Mezzavilla, S. Rangan, and M. Zorzi, "Toward 6G networks: Use cases and technologies," *IEEE Communications Magazine*, vol. 58, no. 3, pp. 55–61, Mar 2020.

[7] Z. Zhang, Y. Xiao, Z. Ma, M. Xiao, Z. Ding, X. Lei, G. K. Karagiannidis, and P. Fan, "6G wireless networks: Vision, requirements, architecture, and key technologies," *IEEE Vehicular Technology Magazine*, vol. 14, no. 3, pp. 28–41, Sep 2019.

[8] H. Ishii, Y. Kishiyama, and H. Takahashi, "A novel architecture for LTE-B :C-plane/U-plane split and phantom cell concept," in *2012 IEEE Globecom Workshops*. IEEE, dec 2012.

[9] P. Demestichas, A. Georgakopoulos, D. Karvounas, K. Tsagkaris, V. Stavroulaki, J. Lu, C. Xiong, and J. Yao, "5G on the horizon: Key challenges for the radio-access network," *IEEE Vehicular Technology Magazine*, vol. 8, no. 3, pp. 47–53, sep 2013.

[10] N. Bhushan, J. Li, D. Malladi, R. Gilmore, D. Brenner, A. Damnjanovic, R. T. Sukhavasi, C. Patel, and S. Geirhofer, "Network densification: the dominant theme for wireless evolution into 5G," *IEEE Communications Magazine*, vol. 52, no. 2, pp. 82–89, feb 2014.

[11] B. Romanous, N. Bitar, A. Imran, and H. Refai, "Network densification: Challenges and opportunities in enabling 5G," in *2015 IEEE 20th International Workshop on Computer Aided Modelling and Design of Communication Links and Networks (CAMAD)*, Sep. 2015, pp. 129–134.

[12] J. Liu, M. Sheng, L. Liu, and J. Li, "Network Densification in 5G: From the Short-Range Communications Perspective," *IEEE Communications Magazine*, vol. 55, no. 12, pp. 96–102, dec 2017.

[13] M. Kamel, W. Hamouda, and A. Youssef, "Ultra-dense networks: A survey," *IEEE Communications Surveys & Tutorials*, vol. 18, no. 4, pp. 2522–2545, may 2016.

[14] S. Buzzi, C.-L. I, T. E. Klein, H. V. Poor, C. Yang, and A. Zappone, "A survey of energy-efficient techniques for 5G networks and challenges ahead," *IEEE Journal on Selected Areas in Communications*, vol. 34, no. 4, pp. 697–709, apr 2016.

[15] J. B. Rao and A. O. Fapojuwo, "A survey of energy efficient resource management techniques for multicell cellular networks," *IEEE Communications Surveys & Tutorials*, vol. 16, no. 1, pp. 154–180, may 2014.

[16] M. Ismail, W. Zhuang, E. Serpedin, and K. Qaraqe, "A survey on green mobile networking: From the perspectives of network operators and mobile users," *IEEE Communications Surveys Tutorials*, vol. 17, no. 3, pp. 1535–1556, nov 2015.

[17] F. Han, S. Zhao, L. Zhang, and J. Wu, "Survey of strategies for switching off base stations in heterogeneous networks for greener 5G systems," *IEEE Access*, vol. 4, pp. 4959–4973, aug 2016.

[18] J. Wu, J. Liu, Z. Huang, C. Du, H. Zhao, and Y. Bai, "Intelligent network selection for data offloading in 5G multi-radio heterogeneous networks," *China Communications*, vol. 12, no. Supplement, pp. 132–139, dec 2015.

[19] E. Oh, B. Krishnamachari, X. Liu, and Z. Niu, "Toward dynamic energy-efficient operation of cellular network infrastructure," *IEEE Communications Magazine*, vol. 49, no. 6, pp. 56–61, jun 2011.

[20] Z. Niu, "TANGO: traffic-aware network planning and green operation," *IEEE Wireless Communications*, vol. 18, no. 5, pp. 25–29, oct 2011.

[21] U. Paul, A. P. Subramanian, M. M. Buddhikot, and S. R. Das, "Understanding traffic dynamics in cellular data networks," in *2011 Proceedings IEEE INFOCOM*. IEEE, apr 2011.

[22] M. Feng, S. Mao, and T. Jiang, "Base station ON-OFF switching in 5G wireless networks: Approaches and challenges," *IEEE Wireless Communications*, vol. 24, no. 4, pp. 46–54, aug 2017.

[23] T. Huang, W. Yang, J. Wu, J. Ma, X. Zhang, and D. Zhang, "A survey on green 6G network: Architecture and technologies," *IEEE Access*, vol. 7, pp. 175 758–175 768, dec 2019.

[24] A. Fotouhi, H. Qiang, M. Ding, M. Hassan, L. G. Giordano, A. Garcia-Rodriguez, and J. Yuan, "Survey on UAV cellular communications: Practical aspects, standardization advancements, regulation, and security challenges," *IEEE Communications Surveys Tutorials*, vol. 21, no. 4, pp. 3417–3442, mar 2019.

[25] M. Mozaffari, W. Saad, M. Bennis, Y.-H. Nam, and M. Debbah, "A Tutorial on UAVs for Wireless Networks: Applications, Challenges, and Open Problems," *IEEE Communications Surveys Tutorials*, vol. 21, no. 3, pp. 2334–2360, mar 2019.

[26] M. N. Boukoberine, Z. Zhou, and M. Benbouzid, "A critical review on unmanned aerial vehicles power supply and energy management: Solutions, strategies, and prospects," *Applied Energy*, vol. 255, p. 113823, dec 2019.

[27] B. Mao, F. Tang, Y. Kawamoto, and N. Kato, "AI models for green communications towards 6G," *IEEE Communications Surveys Tutorials*, pp. 1–1, dec 2021.

[28] L. Belkhir and A. Elmeligi, "Assessing ICT global emissions footprint: Trends to 2040 and recommendations," *Journal of Cleaner Production*, vol. 177, pp. 448–463, mar 2018. [Online]. Available: https://www.sciencedirect.com/science/article/pii/S095965261733233X

[29] S. Vassaki, M. I. Poulakis, and A. D. Panagopoulos, "Spectrum leasing in cognitive radio networks: A matching theory approach," in *2015 IEEE 81st Vehicular Technology Conference (VTC Spring)*, jul 2015, pp. 1–5.

[30] M. C. Achtelik, J. Stumpf, D. Gurdan, and K.-M. Doth, "Design of a flexible high performance quadcopter platform breaking the mav endurance record with laser power beaming," in *2011 IEEE/RSJ International Conference on Intelligent Robots and Systems*, sep 2011, pp. 5166–5172.

[31] A. Damnjanovic, J. Montojo, Y. Wei, T. Ji, T. Luo, M. Vajapeyam, T. Yoo, O. Song, and D. Malladi, "A survey on 3GPP heterogeneous networks," *IEEE Wireless communications*, vol. 18, no. 3, pp. 10–21, jun 2011.

[32] M. Ali, S. Mumtaz, S. Qaisar, and M. Naeem, "Smart heterogeneous networks: a 5G paradigm," *Telecommunication Systems*, vol. 66, 02 2017.

[33] A. Hamed and R. Rao, "Spatial spectral and energy efficiencies of cellular networks limited by co-channel interference and path loss in Nakagami-m fading environment," *EURASIP Journal on Wireless Communications and Networking*, vol. 2018, 12 2018.

[34] A. Ghosh, N. Mangalvedhe, R. Ratasuk, B. Mondal, M. Cudak, E. Visotsky, T. A. Thomas, J. G. Andrews, P. Xia, H. S. Jo, H. S. Dhillon, and T. D. Novlan, "Heterogeneous cellular networks: From theory to practice," *IEEE Communications Magazine*, vol. 50, no. 6, pp. 54–64, jun 2012.

[35] X. Chu, D. Lopez-Perez, Y. Yang, and F. Gunnarsson, *Heterogeneous cellular networks: theory, simulation and deployment*. Cambridge University Press, 2013.

[36] J. G. Andrews, H. Claussen, M. Dohler, S. Rangan, and M. C. Reed, "Femtocells: Past, present, and future," *IEEE Journal on Selected Areas in Communications*, vol. 30, no. 3, pp. 497–508, mar 2012.

[37] W. Yu, H. Xu, H. Zhang, D. Griffith, and N. Golmie, "Ultra-dense networks: Survey of state of the art and future directions," in *2016 25th International Conference on Computer Communication and Networks (ICCCN)*, Aug 2016, pp. 1–10.

[38] K. Nonami, F. Kendoul, S. Suzuki, W. Wang, and D. Nakazawa, *Autonomous flying robots: unmanned aerial vehicles and micro aerial vehicles*. Springer Science & Business Media, 2010.

[39] A. S. Saeed, A. B. Younes, S. Islam, J. Dias, L. Seneviratne, and G. Cai, "A review on the platform design, dynamic modeling and control of hybrid UAVs," in *2015 International Conference on Unmanned Aircraft Systems (ICUAS)*. IEEE, jun 2015, pp. 806–815.

[40] G. J. Ducard and M. Allenspach, "Review of designs and flight control techniques of hybrid and convertible VTOL UAVs," *Aerospace Science and Technology*, vol. 118, p. 107035, nov 2021.

[41] D. G.C., A. Ladas, Y. A. Sambo, H. Pervaiz, C. Politis, and M. A. Imran, "An overview of post-disaster emergency communication systems in the future networks," *IEEE Wireless Communications*, vol. 26, no. 6, pp. 132–139, dec 2019.

[42] P. V. Klaine, J. P. B. Nadas, R. D. Souza, and M. A. Imran, "Distributed drone base station positioning for emergency cellular networks using reinforcement learning," *Cognitive Computation*, vol. 10, no. 5, pp. 790–804, may 2018. [Online]. Available: https://doi.org/10.1007%2Fs12559-018-9559-8

[43] J. Chakareski, S. Naqvi, N. Mastronarde, J. Xu, F. Afghah, and A. Razi, "An energy efficient framework for UAV-assisted millimeter wave 5G heterogeneous cellular networks," *IEEE Transactions on Green Communications and Networking*, vol. 3, no. 1, pp. 37–44, mar 2019.

[44] J. Ouyang, Y. Zhuang, M. Lin, and J. Liu, "Optimization of beamforming and path planning for UAV-assisted wireless relay networks," *Chinese Journal of Aeronautics*, vol. 27, no. 2, pp. 313–320, apr 2014.

[45] X. Chen, J. Tang, and S. Lao, "Review of unmanned aerial vehicle swarm communication architectures and routing protocols," *Applied Sciences*, vol. 10, no. 10, p. 3661, may 2020.

[46] A. I. Hentati and L. C. Fourati, "Comprehensive survey of UAVs communication networks," *Computer Standards & Interfaces*, vol. 72, p. 103451, oct 2020.

[47] A. Alsharoa, H. Ghazzai, A. Kadri, and A. E. Kamal, "Energy management in cellular HetNets assisted by solar powered drone small cells," in *2017*

IEEE Wireless Communications and Networking Conference (WCNC). IEEE, 2017, pp. 1–6.

[48] Y. Zeng, R. Zhang, and T. J. Lim, "Wireless communications with unmanned aerial vehicles: Opportunities and challenges," *IEEE Communications Magazine*, vol. 54, no. 5, pp. 36–42, may 2016.

[49] Y. Zhong, T. Q. Quek, and X. Ge, "Heterogeneous cellular networks with spatio-temporal traffic: Delay analysis and scheduling," *IEEE Journal on Selected Areas in Communications*, vol. 35, no. 6, pp. 1373–1386, mar 2017.

[50] Y. A. Sambo, P. V. Klaine, J. P. B. Nadas, and M. A. Imran, "Energy minimization UAV trajectory design for delay-tolerant emergency communication," in *2019 IEEE International Conference on Communications Workshops (ICC Workshops)*, may 2019, pp. 1–6.

[51] W. Jin, J. Yang, Y. Fang, and W. Feng, "Research on Application and Deployment of UAV in Emergency Response," in *2020 IEEE 10th International Conference on Electronics Information and Emergency Communication (ICEIEC)*. IEEE, jul 2020, pp. 277–280.

[52] S. Singh, A. Malik, R. Kumar, and P. K. Singh, "A proficient data gathering technique for unmanned aerial vehicle-enabled heterogeneous wireless sensor networks," *International Journal of Communication Systems*, vol. 34, no. 16, p. e4956, aug 2021.

[53] D. C. Tsouros, S. Bibi, and P. G. Sarigiannidis, "A review on UAV-based applications for precision agriculture," *Information*, vol. 10, no. 11, p. 349, nov 2019.

[54] D. Liu, B. Chen, C. Yang, and A. F. Molisch, "Caching at the wireless edge: design aspects, challenges, and future directions," *IEEE Communications Magazine*, vol. 54, no. 9, pp. 22–28, sep 2016.

[55] P. Mach and Z. Becvar, "Mobile edge computing: A survey on architecture and computation offloading," *IEEE Communications Surveys Tutorials*, vol. 19, no. 3, pp. 1628–1656, thirdquarter 2017.

[56] A. Sanike, A. Subramanyam, S. S. S. Reddy, and G. RaghuRam, "Load balancing technique to handle the congestion in the communication networks," in *2015 Conference on Power, Control, Communication and Computational Technologies for Sustainable Growth (PCCCTSG)*, dec 2015, pp. 289–293.

[57] J. Hu, H. Zhang, Y. Liu, X. Li, and H. Ji, "An Intelligent UAV Deployment Scheme for Load Balance in Small Cell Networks Using Machine Learning," in *2019 IEEE Wireless Communications and Networking Conference (WCNC)*, apr 2019, pp. 1–6.

[58] S. K. Zaidi, S. F. Hasan, X. Gui, N. Siddique, and S. Ahmad, "Exploiting UAV as NOMA based Relay for Coverage Extension," in *2019 2nd International Conference on Computer Applications Information Security (ICCAIS)*, may 2019, pp. 1–5.

[59] Y. Li, D. Yang, Y. Xu, L. Xiao, and H. Chen, "Throughput maximization for UAV-enabled relaying in wireless powered communication networks," *Sensors*, vol. 19, no. 13, p. 2989, apr 2019.

[60] V. Sharma, M. Bennis, and R. Kumar, "UAV-assisted heterogeneous networks for capacity enhancement," *IEEE Communications Letters*, vol. 20, no. 6, pp. 1207–1210, jun 2016.

[61] Q. Song, F.-C. Zheng, and S. Jin, "Multiple UAVs Enabled Data Offloading for Cellular Hotspots," in *2019 IEEE Wireless Communications and Networking Conference (WCNC)*, apr 2019, pp. 1–6.

[62] U. Challita and W. Saad, "Network formation in the sky: Unmanned aerial vehicles for multi-hop wireless backhauling," in *GLOBECOM 2017 - 2017 IEEE Global Communications Conference*, dec 2017, pp. 1–6.

[63] M. Gapeyenko, V. Petrov, D. Moltchanov, S. Andreev, N. Himayat, and Y. Koucheryavy, "Flexible and Reliable UAV-Assisted Backhaul Operation in 5G mmWave Cellular Networks," *IEEE Journal on Selected Areas in Communications*, vol. 36, no. 11, pp. 2486–2496, nov 2018.

[64] W. Chang, Z.-T. Meng, K.-C. Liu, and L.-C. Wang, "Energy-Efficient Sleep Strategy for the UBS-Assisted Small-Cell Network," *IEEE Transactions on Vehicular Technology*, vol. 70, no. 5, pp. 5178–5183, 2021.

[65] G. Auer, V. Giannini, C. Desset, I. Godor, P. Skillermark, M. Olsson, M. Imran, D. Sabella, M. Gonzalez, O. Blume, and A. Fehske, "How much energy is needed to run a wireless network?" *IEEE Wireless Communications*, vol. 18, no. 5, pp. 40–49, oct 2011.

[66] O. Arnold, F. Richter, G. Fettweis, and O. Blume, "Power consumption modeling of different base station types in heterogeneous cellular networks," in *2010 Future Network & Mobile Summit*. IEEE, mar 2010, pp. 1–8.

[67] A. K. Trehan, "Energy conservation solutions for mobile networks," in *Intelec 2012*, dec 2012, pp. 1–5.

[68] F. Richter, A. J. Fehske, and G. P. Fettweis, "Energy efficiency aspects of base station deployment strategies for cellular networks," in *2009 IEEE 70th Vehicular Technology Conference Fall.* IEEE, sep 2009.

[69] K. Son, H. Kim, Y. Yi, and B. Krishnamachari, "Base station operation and user association mechanisms for energy-delay tradeoffs in green cellular networks," *IEEE Journal on Selected Areas in Communications*, vol. 29, no. 8, pp. 1525–1536, sep 2011.

[70] C. Desset, B. Debaillie, V. Giannini, A. Fehske, G. Auer, H. Holtkamp, W. Wajda, D. Sabella, F. Richter, M. J. Gonzalez, H. Klessig, I. Godor, M. Olsson, M. A. Imran, A. Ambrosy, and O. Blume, "Flexible power modeling of LTE base stations," in *2012 IEEE Wireless Communications and Networking Conference (WCNC).* IEEE, apr 2012.

[71] H. Holtkamp, G. Auer, V. Giannini, and H. Haas, "A parameterized base station power model," *IEEE Communications Letters*, vol. 17, no. 11, pp. 2033–2035, nov 2013.

[72] B. Debaillie, C. Desset, and F. Louagie, "A flexible and future-proof power model for cellular base stations," in *2015 IEEE 81st Vehicular Technology Conference (VTC Spring).* IEEE, may 2015.

[73] G. Cai, J. Dias, and L. Seneviratne, "A survey of small-scale unmanned aerial vehicles: Recent advances and future development trends," *Unmanned Systems*, vol. 2, no. 02, pp. 175–199, apr 2014.

[74] A. Varshney, D. Gupta, and B. Dwivedi, "Speed response of brushless DC motor using fuzzy PID controller under varying load condition," *Journal of Electrical Systems and Information Technology*, vol. 4, no. 2, pp. 310–321, sep 2017.

[75] Y. Zeng and R. Zhang, "Energy-Efficient UAV Communication With Trajectory Optimization," *IEEE Transactions on Wireless Communications*, vol. 16, no. 6, pp. 3747–3760, jun 2017.

[76] Y. Zeng, J. Xu, and R. Zhang, "Energy minimization for wireless communication with rotary-wing UAV," *IEEE Transactions on Wireless Communications*, vol. 18, no. 4, pp. 2329–2345, mar 2019.

[77] H. V. Abeywickrama, B. A. Jayawickrama, Y. He, and E. Dutkiewicz, "Comprehensive energy consumption model for unmanned aerial vehicles, based on empirical studies of battery performance," *IEEE Access*, vol. 6, pp. 58 383–58 394, oct 2018.

[78] A. Thibbotuwawa, P. Nielsen, B. Zbigniew, and G. Bocewicz, "Energy consumption in unmanned aerial vehicles: A review of energy consumption models and their relation to the UAV routing," in *International Conference on Information Systems Architecture and Technology*. Springer, aug 2018, pp. 173–184.

[79] X. T. P. She, X. Lin, and H. Lang, "A data-driven power consumption model for electric UAVs," in *2020 American Control Conference (ACC)*. IEEE, jul 2020, pp. 4957–4962.

[80] N. A. Khofiyah, S. Maret, W. Sutopo, and B. D. A. Nugroho, "Goldsmith's commercialization model for feasibility study of technology lithium battery pack drone," in *2018 5th International Conference on Electric Vehicular Technology (ICEVT)*. IEEE, oct 2018, pp. 147–151.

[81] D. Verstraete, K. Lehmkuehler, and K. Wong, "Design of a fuel cell powered blended wing body UAV," in *ASME International Mechanical Engineering Congress and Exposition*, vol. 45172. American Society of Mechanical Engineers, nov 2012, pp. 621–629.

[82] M. A. Kishk, A. Bader, and M.-S. Alouini, "On the 3-D placement of airborne base stations using tethered UAVs," *IEEE Transactions on Communications*, vol. 68, no. 8, pp. 5202–5215, aug 2020.

[83] B. W. Gu, S. Y. Choi, Y. S. Choi, G. Cai, L. Seneviratne, and C. T. Rim, "Novel roaming and stationary tethered aerial robots for continuous mobile missions in nuclear power plants," *Nuclear Engineering and Technology*, vol. 48, no. 4, pp. 982–996, aug 2016.

[84] J.-J. Hwang, J.-K. Kuo, W. Wu, W.-R. Chang, C.-H. Lin, and S.-E. Wang, "Lifecycle performance assessment of fuel cell/battery electric vehicles," *International journal of hydrogen energy*, vol. 38, no. 8, pp. 3433–3446, mar 2013.

[85] Z. Pan, L. An, and C. Wen, "Recent advances in fuel cells based propulsion systems for unmanned aerial vehicles," *Applied Energy*, vol. 240, pp. 473–485, apr 2019.

[86] P. L. Richardson, "Upwind dynamic soaring of albatrosses and UAVs," *Progress in Oceanography*, vol. 130, pp. 146–156, jan 2015.

[87] P. Oettershagen, A. Melzer, T. Mantel, K. Rudin, R. Lotz, D. Siebenmann, S. Leutenegger, K. Alexis, and R. Siegwart, "A solar-powered hand-launchable UAV for low-altitude multi-day continuous flight," in *2015 IEEE International Conference on Robotics and Automation (ICRA)*. IEEE, may 2015, pp. 3986–3993.

[88] T. Donateo, A. Ficarella, L. Spedicato, A. Arista, and M. Ferraro, "A new approach to calculating endurance in electric flight and comparing fuel cells and batteries," *Applied energy*, vol. 187, pp. 807–819, feb 2017.

[89] N. Belmonte, S. Staulo, S. Fiorot, C. Luetto, P. Rizzi, and M. Baricco, "Fuel cell powered octocopter for inspection of mobile cranes: Design, cost analysis and environmental impacts," *Applied energy*, vol. 215, pp. 556–565, apr 2018.

[90] M. Lu, M. Bagheri, A. P. James, and T. Phung, "Wireless charging techniques for UAVs: A review, reconceptualization, and extension," *IEEE Access*, vol. 6, pp. 29 865–29 884, may 2018.

[91] J.-K. Shiau, D.-M. Ma, P.-Y. Yang, G.-F. Wang, and J. H. Gong, "Design of a solar power management system for an experimental UAV," *IEEE transactions on aerospace and electronic systems*, vol. 45, no. 4, pp. 1350–1360, oct 2009.

[92] B. Galkin, J. Kibilda, and L. A. DaSilva, "UAVs as mobile infrastructure: Addressing battery lifetime," *IEEE Communications Magazine*, vol. 57, no. 6, pp. 132–137, jun 2019.

[93] D. Lee, J. Zhou, and W. T. Lin, "Autonomous battery swapping system for quadcopter," in *2015 International Conference on Unmanned Aircraft Systems (ICUAS)*, jun 2015, pp. 118–124.

[94] M. N. Boukoberine, Z. Zhou, and M. Benbouzid, "Power supply architectures for drones-a review," in *IECON 2019-45th Annual Conference of the IEEE Industrial Electronics Society*, vol. 1. IEEE, oct 2019, pp. 5826–5831.

[95] M. Simic, C. Bil, and V. Vojisavljevic, "Investigation in wireless power transmission for UAV charging," *Procedia Computer Science*, vol. 60, pp. 1846–1855, 2015.

[96] J. Hassan, A. Bokani, and S. S. Kanhere, "Recharging of flying base stations using airborne RF energy sources," in *2019 IEEE Wireless Communications and Networking Conference Workshop (WCNCW)*, apr 2019, pp. 1–6.

[97] Y. Hmamouche, M. Benjillali, S. Saoudi, H. Yanikomeroglu, and M. D. Renzo, "New trends in stochastic geometry for wireless networks: A tutorial and survey," *Proceedings of the IEEE*, vol. 109, no. 7, pp. 1200–1252, jul 2021.

[98] H. ElSawy, A. Sultan-Salem, M.-S. Alouini, and M. Z. Win, "Modeling and analysis of cellular networks using stochastic geometry: A tutorial," *IEEE Communications Surveys & Tutorials*, vol. 19, no. 1, pp. 167–203, nov 2017.

[99] F. Rothlauf, "Optimization methods," in *Design of Modern Heuristics*. Springer, 2011, pp. 45–102.

[100] J. Nievergelt, "Exhaustive search, combinatorial optimization and enumeration: Exploring the potential of raw computing power," in *International Conference on Current Trends in Theory and Practice of Computer Science*. Springer, jan 2000, pp. 18–35.

[101] H. Y. Jeong, B. D. Song, and S. Lee, "Truck-drone hybrid delivery routing: Payload-energy dependency and No-Fly zones," *International Journal of Production Economics*, vol. 214, no. C, pp. 220–233, aug 2019. [Online]. Available: https://ideas.repec.org/a/eee/proeco/v214y2019icp220-233.html

[102] A. Gogna and A. Tayal, "Metaheuristics: review and application," *Journal of Experimental & Theoretical Artificial Intelligence*, vol. 25, no. 4, pp. 503–526, may 2013. [Online]. Available: https://doi.org/10.1080/0952813X.2013.782347

[103] A. Leach, "4.05 - ligand-based approaches: Core molecular modeling," in *Comprehensive Medicinal Chemistry II*, J. B. Taylor and D. J. Triggle, Eds. Oxford: Elsevier, 2007, pp. 87–118. [Online]. Available: https://www.sciencedirect.com/science/article/pii/B008045044X002467

[104] T. Bartz-Beielstein, J. Branke, J. Mehnen, and O. Mersmann, "Evolutionary algorithms," *Wiley Interdisciplinary Reviews: Data Mining and Knowledge Discovery*, vol. 4, no. 3, pp. 178–195, 2014.

[105] J. H. Holland, *Adaptation in natural and artificial systems: an introductory analysis with applications to biology, control, and artificial intelligence*. MIT press, 1992.

[106] S. Katoch, S. S. Chauhan, and V. Kumar, "A review on genetic algorithm: past, present, and future," *Multimedia Tools and Applications*, vol. 80, no. 5, pp. 8091–8126, oct 2020. [Online]. Available: https://doi.org/10.1007%2Fs11042-020-10139-6

[107] R. Shivgan and Z. Dong, "Energy-efficient drone coverage path planning using genetic algorithm," in *2020 IEEE 21st International Conference on High Performance Switching and Routing (HPSR)*, may 2020, pp. 1–6.

[108] B. M. Angadi, M. S. Kakkasageri, and S. S. Manvi, "Computational intelligence techniques for localization and clustering in wireless sensor networks," in *Recent Trends in Computational Intelligence Enabled Research*. Elsevier, july 2021, pp. 23–40.

[109] M. Sa'idi, N. Mostoufi, and R. Sotudeh-Gharebagh, "Application of bee colony algorithm for optimization of CCR reforming process," in *11th International Symposium on Process Systems Engineering*, ser. Computer Aided Chemical Engineering, I. A. Karimi and R. Srinivasan, Eds. Elsevier, 2012, vol. 31, pp. 620–624. [Online]. Available: https://www.sciencedirect.com/science/article/pii/B9780444595072501165

[110] J. Kennedy and R. Eberhart, "Particle swarm optimization," in *Proceedings of ICNN'95 - International Conference on Neural Networks*, vol. 4, 1995, pp. 1942–1948 vol.4.

[111] D. Wang, D. Tan, and L. Liu, "Particle swarm optimization algorithm: an overview," *Soft Computing*, vol. 22, no. 2, pp. 387–408, jan 2017. [Online]. Available: https://doi.org/10.1007%2Fs00500-016-2474-6

[112] Eberhart and Y. Shi, "Particle swarm optimization: developments, applications and resources," in *Proceedings of the 2001 Congress on Evolutionary Computation (IEEE Cat. No.01TH8546)*, vol. 1, 2001, pp. 81–86 vol. 1.

[113] M. Dorigo, V. Maniezzo, and A. Colorni, *IEEE Transactions on Systems, Man, and Cybernetics, Part B (Cybernetics)*, vol. 26, no. 1, pp. 29–41, Feb 1996.

[114] M. Dorigo and T. Stutzle, "Ant colony optimization: Overview and recent advances," in *Handbook of Metaheuristics*. Springer US, 2010, pp. 227–263. [Online]. Available: https://doi.org/10.1007%2F978-1-4419-1665-5-8

[115] S. Kirkpatrick, C. D. Gelatt, and M. P. Vecchi, "Optimization by simulated annealing," *Science*, vol. 220, no. 4598, pp. 671–680, may 1983. [Online]. Available: https://doi.org/10.1126%2Fscience.220.4598.671

[116] K. A. Dowsland and J. Thompson, "Simulated annealing," *Handbook of natural computing*, pp. 1623–1655, 2012.

[117] L. Wei, Z. Zhang, D. Zhang, and S. C. Leung, "A simulated annealing algorithm for the capacitated vehicle routing problem with two-dimensional loading constraints," *European Journal of Operational Research*, vol. 265, no. 3, pp. 843–859, mar 2018.

[118] A. Alvarez, P. Munari, and R. Morabito, "Iterated local search and simulated annealing algorithms for the inventory routing problem," *International Transactions in Operational Research*, vol. 25, no. 6, pp. 1785–1809, may 2018.

[119] Z. Lin, J. Wang, Z. Fang, M. Hu, C. Cai, and J. Zhang, "Accurate maximum power tracking of wireless power transfer system based on simulated annealing algorithm," *IEEE Access*, vol. 6, pp. 60 881–60 890, oct 2018.

[120] V. F. Yu, A. P. Redi, Y. A. Hidayat, and O. J. Wibowo, "A simulated annealing heuristic for the hybrid vehicle routing problem," *Appl. Soft Comput.*, vol. 53, no. C, p. 119–132, Apr. 2017.

[121] P. Hansen, N. Mladenović, and J. A. M. Pérez, "Variable neighbourhood search: methods and applications," *Annals of Operations Research*, vol. 175, no. 1, pp. 367–407, nov 2010.

[122] C. Zhang, P. Patras, and H. Haddadi, "Deep learning in mobile and wireless networking: A survey," *IEEE Communications Surveys Tutorials*, vol. 21, no. 3, pp. 2224–2287, mar 2019.

[123] F. Hussain, S. A. Hassan, R. Hussain, and E. Hossain, "Machine learning for resource management in cellular and IoT networks: Potentials, current solutions, and open challenges," *IEEE Communications Surveys Tutorials*, vol. 22, no. 2, pp. 1251–1275, jan 2020.

[124] N. Bui, M. Cesana, S. A. Hosseini, Q. Liao, I. Malanchini, and J. Widmer, "A survey of anticipatory mobile networking: Context-based classification, prediction methodologies, and optimization techniques," *IEEE Communications Surveys Tutorials*, vol. 19, no. 3, pp. 1790–1821, apr 2017.

[125] A. Imran, A. Zoha, and A. Abu-Dayya, "Challenges in 5G: how to empower SON with big data for enabling 5G," *IEEE Network*, vol. 28, no. 6, pp. 27–33, Nov 2014.

[126] A. Singh, N. Thakur, and A. Sharma, "A review of supervised machine learning algorithms," in *2016 3rd International Conference on Computing for Sustainable Global Development (INDIACom)*, mar 2016, pp. 1310–1315.

[127] S. B. Kotsiantis, I. Zaharakis, P. Pintelas *et al.*, "Supervised machine learning: A review of classification techniques," *Emerging artificial intelligence applications in computer engineering*, vol. 160, no. 1, pp. 3–24, jun 2007.

[128] S. Chen, Y.-J. J. Goo, and Z.-D. Shen, "A hybrid approach of stepwise regression, logistic regression, support vector machine, and decision tree for forecasting fraudulent financial statements," *The Scientific World Journal*, vol. 2014, pp. 1–9, sep 2014. [Online]. Available: https://doi.org/10.1155%2F2014%2F968712

[129] H. Fourati, R. Maaloul, and L. Chaari, "A survey of 5G network systems: challenges and machine learning approaches," *International Journal of Machine Learning and Cybernetics*, vol. 12, no. 2, pp. 385–431, feb 2021.

[130] P. V. Klaine, M. A. Imran, O. Onireti, and R. D. Souza, "A survey of machine learning techniques applied to self-organizing cellular networks," *IEEE Communications Surveys & Tutorials*, vol. 19, no. 4, pp. 2392–2431, july 2017.

[131] S. Haykin and R. Lippmann, "Neural networks, a comprehensive foundation," *International journal of neural systems*, vol. 5, no. 4, pp. 363–364, 1994.

[132] M. Öztürk, "Cognitive networking for next generation of cellular communication systems," Ph.D. dissertation, University of Glasgow, 2020.

[133] E. Alpaydin, "Introduction to machine learning. third edit," 2014.

[134] M. A. Nielsen, *Neural networks and deep learning*. Determination press San Francisco, CA, USA, 2015, vol. 25.

[135] N. Li, M. Shepperd, and Y. Guo, "A systematic review of unsupervised learning techniques for software defect prediction," *Information and Software Technology*, vol. 122, p. 106287, jun 2020. [Online]. Available: https://doi.org/10.1016%2Fj.infsof.2020.106287

[136] K. P. Sinaga and M.-S. Yang, "Unsupervised K-Means Clustering Algorithm," *IEEE Access*, vol. 8, pp. 80 716–80 727, Apr 2020.

[137] S. Ben-David, "A framework for statistical clustering with constant time approximation algorithms for K-median and K-means clustering," *Machine Learning*, vol. 66, no. 2-3, pp. 243–257, nov 2006. [Online]. Available: https://doi.org/10.1007%2Fs10994-006-0587-3

[138] N. Y. Yürüşen, B. Uzunoğlu, A. P. Talayero, and A. L. Estopiñán, "Apriori and K-Means algorithms of machine learning for spatio-temporal solar generation balancing," *Renewable Energy*, vol. 175, pp. 702–717, sep 2021. [Online]. Available: https://doi.org/10.1016%2Fj.renene.2021.04.098

[139] R. Zebari, A. Abdulazeez, D. Zeebaree, D. Zebari, and J. Saeed, "A comprehensive review of dimensionality reduction techniques for feature selection and feature extraction," *Journal of Applied Science and Technology Trends*, vol. 1, no. 2, pp. 56–70, may 2020. [Online]. Available: https://doi.org/10.38094%2Fjastt1224

[140] M. Kubat and Kubat, *An introduction to machine learning*. Springer, 2017, vol. 2.

[141] H. Xiong, J. Wu, and J. Chen, "K-means clustering versus validation measures: A data-distribution perspective," *IEEE Transactions on Systems, Man, and Cybernetics, Part B (Cybernetics)*, vol. 39, no. 2, pp. 318–331, Apr 2009.

[142] C. Yuan and H. Yang, "Research on K-Value Selection Method of K-Means Clustering Algorithm," *J*, vol. 2, no. 2, pp. 226–235, jun 2019. [Online]. Available: https://www.mdpi.com/2571-8800/2/2/16

[143] T. T. Nguyen, N. D. Nguyen, and S. Nahavandi, "Deep reinforcement learning for multiagent systems: A review of challenges, solutions, and applications," *IEEE Transactions on Cybernetics*, vol. 50, no. 9, pp. 3826–3839, Mar 2020.

[144] J. Kober, J. A. Bagnell, and J. Peters, "Reinforcement learning in robotics: A survey," *The International Journal of Robotics Research*, vol. 32, no. 11, pp. 1238–1274, aug 2013. [Online]. Available: https://doi.org/10.1177%2F0278364913495721

[145] Y. Sun, M. Peng, Y. Zhou, Y. Huang, and S. Mao, "Application of machine learning in wireless networks: Key techniques and open issues," *IEEE Communications Surveys Tutorials*, vol. 21, no. 4, pp. 3072–3108, 2019.

[146] R. S. Sutton and A. G. Barto, *Reinforcement learning: An introduction*. MIT press, 2018.

[147] J. R. Vázquez-Canteli and Z. Nagy, "Reinforcement learning for demand response: A review of algorithms and modeling techniques," *Applied Energy*, vol. 235, pp. 1072–1089, feb 2019. [Online]. Available: https://doi.org/10.1016%2Fj.apenergy.2018.11.002

[148] M. Littman and A. Moore, "Reinforcement learning: A survey, journal of artificial intelligence research 4," 1996.

[149] M. Ozturk, M. Jaber, and M. A. Imran, "Energy-aware smart connectivity for IoT networks: Enabling smart ports," *Wireless Communications and Mobile Computing*, vol. 2018, jun 2018.

[150] C. Mollén, J. Choi, E. G. Larsson, and R. W. Heath, "Uplink Performance of Wideband Massive MIMO With One-Bit ADCs," *IEEE Transactions on Wireless Communications*, vol. 16, no. 1, pp. 87–100, oct 2017.

[151] J. Zhang, L. Dai, Z. He, S. Jin, and X. Li, "Performance Analysis of Mixed-ADC Massive MIMO Systems Over Rician Fading Channels," *IEEE Journal on Selected Areas in Communications*, vol. 35, no. 6, pp. 1327–1338, jun 2017.

[152] J. Joung, C. K. Ho, K. Adachi, and S. Sun, "A survey on power-amplifier-centric techniques for spectrum- and energy-efficient wireless communications," *IEEE Communications Surveys Tutorials*, vol. 17, no. 1, pp. 315–333, aug 2015.

[153] B. M. Lee and Y. Kim, "Interference-aware PAPR reduction scheme to increase the energy efficiency of large-scale MIMO-OFDM systems," *Energies*, vol. 10, no. 8, p. 1184, aug 2017.

[154] N. N. Moghadam, G. Fodor, M. Bengtsson, and D. J. Love, "On the energy efficiency of MIMO hybrid beamforming for millimeter-wave systems with nonlinear power amplifiers," *IEEE Transactions on Wireless Communications*, vol. 17, no. 11, pp. 7208–7221, nov 2018.

[155] S. Ulukus, A. Yener, E. Erkip, O. Simeone, M. Zorzi, P. Grover, and K. Huang, "Energy harvesting wireless communications: A review of recent advances," *IEEE Journal on Selected Areas in Communications*, vol. 33, no. 3, pp. 360–381, mar 2015.

[156] X. Lu, P. Wang, D. Niyato, D. I. Kim, and Z. Han, "Wireless networks with RF energy harvesting: A contemporary survey," *IEEE Communications Surveys Tutorials*, vol. 17, no. 2, pp. 757–789, nov 2015.

[157] P. Frenger and K. W. Helmersson, "Massive MIMO muting using dual-polarized and array-size invariant beamforming," in *2021 IEEE 93rd Vehicular Technology Conference (VTC2021-Spring)*, apr 2021, pp. 1–6.

[158] X. Xu, C. Yuan, W. Chen, X. Tao, and Y. Sun, "Adaptive cell zooming and sleeping for green heterogeneous ultradense networks," *IEEE Transactions on Vehicular Technology*, vol. 67, no. 2, pp. 1612–1621, feb 2018.

[159] L. G. Hevizi and I. Gódor, "Power savings in mobile networks by dynamic base station sectorization," in *2011 IEEE 22nd International Symposium on Personal, Indoor and Mobile Radio Communications*, dec 2011, pp. 2415–2417.

[160] X. Gan, L. Wang, X. Feng, J. Liu, H. Yu, Z. Zhang, and H. Liu, "Energy efficient switch policy for small cells," *China Communications*, vol. 12, no. 1, pp. 78–88, jan 2015.

[161] A. D. Domenico, E. C. Strinati, and A. Capone, "Enabling green cellular networks: A survey and outlook," *Computer Communications*, vol. 37, pp. 5–24, jan 2014.

[162] A. Mohamed, O. Onireti, M. A. Imran, A. Imran, and R. Tafazolli, "Control-data separation architecture for cellular radio access networks: A survey and outlook," *IEEE Communications Surveys Tutorials*, vol. 18, no. 1, pp. 446–465, Firstquarter 2016.

[163] H. A. U. Mustafa, M. A. Imran, M. Z. Shakir, A. Imran, and R. Tafazolli, "Separation framework: An enabler for cooperative and D2D communica-

tion for future 5G networks," *IEEE Communications Surveys & Tutorials*, vol. 18, no. 1, pp. 419–445, jul 2016.

[164] H. Pervaiz, O. Onireti, A. Mohamed, M. Ali Imran, R. Tafazolli, and Q. Ni, "Energy-efficient and load-proportional eNodeB for 5G user-centric networks: A multilevel sleep strategy mechanism," *IEEE Vehicular Technology Magazine*, vol. 13, no. 4, pp. 51–59, oct 2018.

[165] L. Li, G. Zhao, and R. S. Blum, "A survey of caching techniques in cellular networks: Research issues and challenges in content placement and delivery strategies," *IEEE Communications Surveys Tutorials*, vol. 20, no. 3, pp. 1710–1732, mar 2018.

[166] A. Kabir, G. Rehman, S. M. Gilani, E. J. Kitindi, Z. Ul Abidin Jaffri, and K. M. Abbasi, "The role of caching in next generation cellular networks: A survey and research outlook," *Transactions on Emerging Telecommunications Technologies*, vol. 31, no. 2, p. e3702, aug 2020.

[167] R. Xie, Z. Li, T. Huang, and Y. Liu, "Energy-efficient joint content caching and small base station activation mechanism design in heterogeneous cellular networks," *China Communications*, vol. 14, no. 10, pp. 70–83, oct 2017.

[168] S. V. Hum and J. Perruisseau-Carrier, "Reconfigurable reflectarrays and array lenses for dynamic antenna beam control: A review," *IEEE Transactions on Antennas and Propagation*, vol. 62, no. 1, pp. 183–198, jan 2014.

[169] C. Huang, A. Zappone, G. C. Alexandropoulos, M. Debbah, and C. Yuen, "Reconfigurable intelligent surfaces for energy efficiency in wireless communication," *IEEE Transactions on Wireless Communications*, vol. 18, no. 8, pp. 4157–4170, oct 2019.

[170] Q. Wu, S. Zhang, B. Zheng, C. You, and R. Zhang, "Intelligent reflecting surface-aided wireless communications: A tutorial," *IEEE Transactions on Communications*, vol. 69, no. 5, pp. 3313–3351, may 2021.

[171] S. Gong, X. Lu, D. T. Hoang, D. Niyato, L. Shu, D. I. Kim, and Y.-C. Liang, "Toward smart wireless communications via intelligent reflecting surfaces: A contemporary survey," *IEEE Communications Surveys Tutorials*, vol. 22, no. 4, pp. 2283–2314, jun 2020.

[172] D. Feng, L. Lu, Y. Yuan-Wu, G. Y. Li, S. Li, and G. Feng, "Device-to-Device communications in cellular networks," *IEEE Communications Magazine*, vol. 52, no. 4, pp. 49–55, apr 2014.

[173] Y. Shen, C. Jiang, T. Q. S. Quek, and Y. Ren, "Device-to-Device-Assisted Communications in Cellular Networks: An Energy Efficient Approach in Downlink Video Sharing Scenario," *IEEE Transactions on Wireless Communications*, vol. 15, no. 2, pp. 1575–1587, feb 2016.

[174] J. Liu, Y. Kawamoto, H. Nishiyama, N. Kato, and N. Kadowaki, "Device-to-Device communications achieve efficient load balancing in LTE-advanced networks," *IEEE Wireless Communications*, vol. 21, no. 2, pp. 57–65, aug 2014.

[175] L. Xu, C. Jiang, Y. Shen, T. Q. S. Quek, Z. Han, and Y. Ren, "Energy Efficient D2D Communications: A Perspective of Mechanism Design," *IEEE Transactions on Wireless Communications*, vol. 15, no. 11, pp. 7272–7285, nov 2016.

[176] T. Wang, P. Li, X. Wang, Y. Wang, T. Guo, and Y. Cao, "A comprehensive survey on mobile data offloading in heterogeneous network," *Wireless Networks*, vol. 25, no. 2, pp. 573–584, aug 2019.

[177] X. Chen, J. Wu, Y. Cai, H. Zhang, and T. Chen, "Energy-efficiency oriented traffic offloading in wireless networks: A brief survey and a learning approach for heterogeneous cellular networks," *IEEE Journal on Selected Areas in Communications*, vol. 33, no. 4, pp. 627–640, apr 2015.

[178] H. Zhou, H. Wang, X. Li, and V. C. M. Leung, "A survey on mobile data offloading technologies," *IEEE Access*, vol. 6, pp. 5101–5111, jan 2018.

[179] A. Aijaz, H. Aghvami, and M. Amani, "A survey on mobile data offloading: technical and business perspectives," *IEEE Wireless Communications*, vol. 20, no. 2, pp. 104–112, apr 2013.

[180] F. Rebecchi, M. D. de Amorim, V. Conan, A. Passarella, R. Bruno, and M. Conti, "Data offloading techniques in cellular networks: A survey," *IEEE Communications Surveys & Tutorials*, vol. 17, no. 2, pp. 580–603, nov 2015.

[181] J. Wu, Y. Zhang, M. Zukerman, and E. K.-N. Yung, "Energy-efficient base-stations sleep-mode techniques in green cellular networks: A survey," *IEEE*

Communications Surveys Tutorials, vol. 17, no. 2, pp. 803–826, secondquarter 2015.

[182] Y. Chen, O. Blume, A. Gati, A. Capone, C.-E. Wu, U. Barth, T. Marzetta, H. Zhang, and S. Xu, in *2013 IEEE Wireless Communications and Networking Conference Workshops (WCNCW)*, apr 2013, pp. 12–17.

[183] O. Alamu, A. Gbenga-Ilori, M. Adelabu, A. Imoize, and O. Ladipo, "Energy efficiency techniques in ultra-dense wireless heterogeneous networks: An overview and outlook," *Engineering Science and Technology, an International Journal*, vol. 23, no. 6, pp. 1308 – 1326, dec 2020. [Online]. Available: http://www.sciencedirect.com/science/article/pii/S2215098619328745

[184] C. Luo and J. Liu, "Load based dynamic small cell on/off strategy in ultra-dense networks," in *2018 10th International Conference on Wireless Communications and Signal Processing (WCSP)*. IEEE, oct 2018.

[185] I. Donevski, G. Vallero, and M. A. Marsan, "Neural Networks for Cellular Base Station Switching," in *IEEE INFOCOM 2019 - IEEE Conference on Computer Communications Workshops (INFOCOM WKSHPS)*, April 2019, pp. 738–743.

[186] A. E. Amine, P. Dini, and L. Nuaymi, "Reinforcement learning for delay-constrained energy-aware small cells with multi-sleeping control," in *2020 IEEE International Conference on Communications Workshops (ICC Workshops)*, jul 2020, pp. 1–6.

[187] A. I. Abubakar, C. Ozturk, M. Ozturk, M. S. Mollel, S. M. Asad, N. U. Hassan, S. Hussain, and M. A. Imran, "Revenue maximization through cell switching and spectrum leasing in 5G hetnets," *IEEE Access*, vol. 10, pp. 48 301–48 317, may 2022.

[188] K. A. Yau, J. Qadir, C. Wu, M. A. Imran, and M. H. Ling, "Cognition-inspired 5G cellular networks: A review and the road ahead," *IEEE Access*, vol. 6, pp. 35 072–35 090, jul 2018.

[189] A. R. Syed and K.-L. A. Yau, "Spectrum leasing in cognitive radio networks: A survey," *International Journal of Distributed Sensor Networks*, vol. 10, no. 2, p. 329235, feb 2014. [Online]. Available: https://doi.org/10.1155/2014/329235

[190] X. Liu, L. Li, W. Liang, F. Yang, H. Xu, and Z. Han, "Joint optimization scheme for spectrum leasing in cognitive radio networks," in *2018 10th International Conference on Wireless Communications and Signal Processing (WCSP)*, dec 2018, pp. 1–6.

[191] M. Ozturk, A. I. Abubakar, N. U. Hassan, S. Hussain, M. A. Imran, and C. Yuen, "Spectrum cost optimization for cognitive radio transmission over TV white spaces using artificial neural networks," in *2019 UK/ China Emerging Technologies (UCET)*, aug 2019, pp. 1–4.

[192] N. U. Hassan, C. Yuen, and M. Bershgal Atique, "Tradeoff in delay, cost, and quality in data transmission over tv white spaces," in *2016 IEEE International Conference on Communications (ICC)*, may 2016, pp. 1–6.

[193] N. Sboui, H. Ghazzai, Z. Rezki, and M. Alouini, "Green collaboration in cognitive radio cellular networks with roaming and spectrum trading," in *2015 IEEE 26th Annual International Symposium on Personal, Indoor, and Mobile Radio Communications (PIMRC)*, sep 2015, pp. 1420–1425.

[194] L. Sboui, H. Ghazzai, Z. Rezki, and M. Alouini, "On green cognitive radio cellular networks: Dynamic spectrum and operation management," *IEEE Access*, vol. 4, pp. 4046–4057, jul 2016.

[195] F. Al-Turjman and H. Zahmatkesh, "A Comprehensive Review on the Use of AI in UAV Communications: Enabling Technologies, Applications, and Challenges," *Unmanned Aerial Vehicles in Smart Cities*, p. 1, apr 2020.

[196] K. Li, W. Ni, X. Wang, R. P. Liu, S. S. Kanhere, and S. Jha, "Energy-efficient cooperative relaying for unmanned aerial vehicles," *IEEE Transactions on Mobile Computing*, vol. 15, no. 6, pp. 1377–1386, june 2016.

[197] S. Koulali, E. Sabir, T. Taleb, and M. Azizi, "A green strategic activity scheduling for UAV networks: A sub-modular game perspective," *IEEE Communications Magazine*, vol. 54, no. 5, pp. 58–64, may 2016.

[198] M. Mozaffari, W. Saad, M. Bennis, and M. Debbah, "Optimal transport theory for power-efficient deployment of unmanned aerial vehicles," in *2016 IEEE International Conference on Communications (ICC)*, may 2016, pp. 1–6.

[199] D. Zorbas, L. D. P. Pugliese, T. Razafindralambo, and F. Guerriero, "Optimal drone placement and cost-efficient target coverage," *Journal of Network and Computer Applications*, vol. 75, pp. 16–31, nov 2016.

[200] L. D. P. Pugliese, F. Guerriero, D. Zorbas, and T. Razafindralambo, "Modelling the mobile target covering problem using flying drones," *Optimization Letters*, vol. 10, no. 5, pp. 1021–1052, aug 2016.

[201] E. Basar, M. Di Renzo, J. De Rosny, M. Debbah, M.-S. Alouini, and R. Zhang, "Wireless communications through reconfigurable intelligent surfaces," *IEEE Access*, vol. 7, pp. 116 753–116 773, aug 2019.

[202] C. Huang, A. Zappone, G. C. Alexandropoulos, M. Debbah, and C. Yuen, "Reconfigurable intelligent surfaces for energy efficiency in wireless communication," *IEEE Transactions on Wireless Communications*, vol. 18, no. 8, pp. 4157–4170, 2019.

[203] S. Li, B. Duo, X. Yuan, Y.-C. Liang, and M. Di Renzo, "Reconfigurable Intelligent Surface Assisted UAV Communication: Joint Trajectory Design and Passive Beamforming," *IEEE Wireless Communications Letters*, vol. 9, no. 5, pp. 716–720, may 2020.

[204] A. Ranjha and G. Kaddoum, "URLLC Facilitated by Mobile UAV Relay and RIS: A Joint Design of Passive Beamforming, Blocklength, and UAV Positioning," *IEEE Internet of Things Journal*, vol. 8, no. 6, pp. 4618–4627, mar 2021.

[205] X. Liu, Y. Liu, and Y. Chen, "Machine Learning Empowered Trajectory and Passive Beamforming Design in UAV-RIS Wireless Networks," *IEEE Journal on Selected Areas in Communications*, vol. 39, no. 7, pp. 2042–2055, dec 2021.

[206] E. T. Michailidis, N. I. Miridakis, A. Michalas, E. Skondras, and D. J. Vergados, "Energy optimization in dual-RIS UAV-aided MEC-enabled internet of vehicles," *Sensors*, vol. 21, no. 13, p. 4392, 2021.

[207] Z. Yang, C. Pan, K. Wang, and M. Shikh-Bahaei, "Energy Efficient Resource Allocation in UAV-Enabled Mobile Edge Computing Networks," *IEEE Transactions on Wireless Communications*, vol. 18, no. 9, pp. 4576–4589, sep 2019.

[208] M. Li, N. Cheng, J. Gao, Y. Wang, L. Zhao, and X. Shen, "Energy-Efficient UAV-Assisted Mobile Edge Computing: Resource Allocation and Trajectory Optimization," *IEEE Transactions on Vehicular Technology*, vol. 69, no. 3, pp. 3424–3438, mar 2020.

[209] G. Wu, Y. Miao, Y. Zhang, and A. Barnawi, "Energy efficient for UAV-enabled mobile edge computing networks: Intelligent task prediction and offloading," *Computer Communications*, vol. 150, pp. 556–562, jan 2020.

[210] L. Li, X. Wen, Z. Lu, Q. Pan, W. Jing, and Z. Hu, "Energy-efficient UAV-enabled MEC system: Bits allocation optimization and trajectory design," *Sensors*, vol. 19, no. 20, p. 4521, oct 2019.

[211] B. Yi, X. Wang, K. Li, M. Huang *et al.*, "A comprehensive survey of network function virtualization," *Computer Networks*, vol. 133, pp. 212–262, mar 2018.

[212] C. Tipantuña, X. Hesselbach, V. Sánchez-Aguero, F. Valera, I. Vidal, and B. Nogales, "An NFV-based energy scheduling algorithm for a 5G enabled fleet of programmable unmanned aerial vehicles," *Wireless Communications and Mobile Computing*, vol. 2019, feb 2019.

[213] Z. Xu, I. Petrunin, and A. Tsourdos, "Dynamic Spectrum Management with Network Function Virtualization for UAV Communication," *Journal of Intelligent & Robotic Systems*, vol. 101, no. 2, pp. 1–18, feb 2021.

[214] Y. Chen, W. Feng, and G. Zheng, "Optimum Placement of UAV as Relays," *IEEE Communications Letters*, vol. 22, no. 2, pp. 248–251, feb 2018.

[215] M. M. Azari, F. Rosas, K.-C. Chen, and S. Pollin, "Ultra Reliable UAV Communication Using Altitude and Cooperation Diversity," *IEEE Transactions on Communications*, vol. 66, no. 1, pp. 330–344, aug 2018.

[216] S. Yin, Y. Zhao, L. Li, and F. R. Yu, "UAV-Assisted Cooperative Communications With Time-Sharing Information and Power Transfer," *IEEE Transactions on Vehicular Technology*, vol. 69, no. 2, pp. 1554–1567, nov 2020.

[217] M. Thammawichai, S. P. Baliyarasimhuni, E. C. Kerrigan, and J. B. Sousa, "Optimizing Communication and Computation for Multi-UAV Information Gathering Applications," *IEEE Transactions on Aerospace and Electronic Systems*, vol. 54, no. 2, pp. 601–615, apr 2018.

[218] J. Huang, Y. Zhou, Z. Ning, and H. Gharavi, "Wireless power transfer and energy harvesting: Current status and future prospects," *IEEE Wireless Communications*, vol. 26, no. 4, pp. 163–169, apr 2019.

[219] T. V. Quyen, C. V. Nguyen, A. M. Le, and M. T. Nguyen, "Optimizing hybrid energy harvesting mechanisms for UAVs," *EAI Endorsed Transactions on Energy Web*, vol. 7, no. 30, p. e8, may 2020.

[220] S. Yin, Y. Zhao, L. Li, and F. R. Yu, "UAV-Assisted Cooperative Communications With Power-Splitting Information and Power Transfer," *IEEE Transactions on Green Communications and Networking*, vol. 3, no. 4, pp. 1044–1057, jul 2019.

[221] J. Lu, S. Wan, X. Chen, and P. Fan, "Energy-Efficient 3D UAV-BS Placement versus Mobile Users' Density and Circuit Power," in *2017 IEEE Globecom Workshops (GC Wkshps)*, dec 2017, pp. 1–6.

[222] X. Jiang, M. Sheng, N. Zhao, C. Xing, W. Lu, and X. Wang, "Green UAV communications for 6G: A survey," *Chinese Journal of Aeronautics*, may 2021. [Online]. Available: https://www.sciencedirect.com/science/article/pii/S1000936121001801

[223] M. I. Khalil, "Energy efficiency maximization of relay aerial robotic networks," *IEEE Transactions on Green Communications and Networking*, vol. 4, no. 4, pp. 1081–1090, july 2020.

[224] R. Gangula, D. Gesbert, D. F. Kuelzer, and J. M. Franceschi, "A landing spot approach for enhancing the performance of UAV-aided wireless networks," in *2018 IEEE International Conference on Communications Workshops (ICC Workshops)*, may 2018, pp. 1–6.

[225] V. Petrov, M. Gapeyenko, D. Moltchanov, S. Andreev, and R. W. Heath, "Hover or perch: Comparing capacity of airborne and landed millimeter-wave UAV cells," *IEEE Wireless Communications Letters*, vol. 9, no. 12, pp. 2059–2063, jul 2020.

[226] A. I. Abubakar, I. Ahmad, K. G. Omeke, M. Ozturk, C. Ozturk, A. Makine Abdel-Salam, M. S. Mollel, Q. H. Abbasi, S. Hussain, and M. A. Imran, "A Survey on Energy Optimization Techniques in UAV-Based Cellular Networks: From Conventional to Machine Learning Approaches," *arXiv e-prints*, p. arXiv:2204.07967, Apr. 2022.

[227] M. A. Adedoyin and O. E. Falowo, "Combination of ultra-dense networks and other 5G enabling technologies: A survey," *IEEE Access*, vol. 8, pp. 22 893–22 932, jan 2020.

[228] Y. Xu, G. Gui, H. Gacanin, and F. Adachi, "A survey on resource allocation for 5G heterogeneous networks: Current research, future trends, and challenges," *IEEE Communications Surveys Tutorials*, vol. 23, no. 2, pp. 668–695, feb 2021.

[229] Nidhi and A. Mihovska, "Small cell deployment challenges in ultradense networks: Architecture and resource management," in *2020 12th International Symposium on Communication Systems, Networks and Digital Signal Processing (CSNDSP)*, jul 2020, pp. 1–6.

[230] M. Usama and M. Erol-Kantarci, "A survey on recent trends and open issues in energy efficiency of 5G," *Sensors*, vol. 19, no. 14, p. 3126, jul 2019.

[231] L. Kaiser, M. Babaeizadeh, P. Milos, B. Osinski, R. H. Campbell, K. Czechowski, D. Erhan, C. Finn, P. Kozakowski, S. Levine *et al.*, "Model-based reinforcement learning for atari," *arXiv preprint arXiv:1903.00374*, 2019.

[232] P. Kormushev, S. Calinon, and D. G. Caldwell, "Reinforcement learning in robotics: Applications and real-world challenges," *Robotics*, vol. 2, no. 3, pp. 122–148, jul 2013.

[233] R. Li, Z. Zhao, X. Chen, J. Palicot, and H. Zhang, "TACT: A transfer actor-critic learning framework for energy saving in cellular radio access networks," *IEEE Transactions on Wireless Communications*, vol. 13, no. 4, pp. 2000–2011, apr 2014.

[234] A. Zappone, M. Di Renzo, and M. Debbah, "Wireless networks design in the era of deep learning: Model-based, ai-based, or both?" *IEEE Transactions on Communications*, vol. 67, no. 10, pp. 7331–7376, jun 2019.

[235] Ruhong Zeng, Shixiang Zhu, Hongwen Yang, and Jiaxin Zhu, "An artificial neural network based cell switch-off algorithm in cellular system," in *2016 2nd IEEE International Conference on Computer and Communications (ICCC)*, Oct 2016, pp. 1434–1439.

[236] L. Wang, S. Chen, and M. Pedram, "Context-driven power management in cache-enabled base stations using a Bayesian neural network," in *2017 Eighth International Green and Sustainable Computing Conference (IGSC)*, Oct 2017, pp. 1–8.

[237] M. Ozturk, A. I. Abubakar, J. P. B. Nadas, R. N. B. Rais, S. Hussain, and M. A. Imran, "Energy optimization in ultra-dense radio access networks via

traffic-aware cell switching," *IEEE Transactions on Green Communications and Networking*, pp. 1–1, feb 2021.

[238] S. Zhang, J. Gong, S. Zhou, and Z. Niu, "How many small cells can be turned off via vertical offloading under a separation architecture?" *IEEE Transactions on Wireless Communications*, vol. 14, no. 10, pp. 5440–5453, oct 2015.

[239] R. Tao, W. Liu, X. Chu, and J. Zhang, "An energy saving small cell sleeping mechanism with cell range expansion in heterogeneous networks," *IEEE Transactions on Wireless Communications*, pp. 1–1, feb 2019.

[240] Y. Luo, Z. Shi, F. Bu, and J. Xiong, "Joint optimization of area spectral efficiency and energy efficiency for two-tier heterogeneous ultra-dense networks," *IEEE Access*, vol. 7, pp. 12 073–12 086, jan 2019.

[241] Y. M. Abdelradi, A. A. El-Sherif, and L. H. Afify, "A queueing theory approach for maximized energy efficiency traffic offloading," in *2020 2nd Novel Intelligent and Leading Emerging Sciences Conference (NILES)*, oct 2020, pp. 549–554.

[242] S. Habibi, V. Solouk, and H. Kalbkhani, "Adaptive energy-efficient small cell sleeping and zooming in heterogeneous cellular networks," *Telecommunication Systems*, pp. 1–23, may 2021.

[243] Q. Alsafasfeh, O. A. Saraereh, A. Ali, L. Al-Tarawneh, I. Khan, and A. Silva, "Efficient power control framework for small-cell heterogeneous networks," *Sensors*, vol. 20, no. 5, mar 2020. [Online]. Available: https://www.mdpi.com/1424-8220/20/5/1467

[244] W. Yang, X. Bai, S. Guo, L. Wang, X. Luo, and M. Ji, "An adaptive base station management scheme based on particle swarm optimization," in *International Conference in Communications, Signal Processing, and Systems*. Springer, jun 2020, pp. 619–627.

[245] Y. E. Morabit, F. Mrabti, and E. H. Abarkan, "Small cell switch off using genetic algorithm," in *2017 International Conference on Advanced Technologies for Signal and Image Processing (ATSIP)*, may 2017, pp. 1–4.

[246] Y.-B. Lin, L.-C. Wang, and P. Lin, "SES: A novel yet simple energy saving scheme for small cells," *IEEE Transactions on Vehicular Technology*, vol. 66, no. 9, pp. 8347–8356, sep 2017.

[247] M. J. Daas, M. Jubran, and M. Hussein, "Energy management framework for 5G ultra-dense networks using graph theory," *IEEE Access*, vol. 7, pp. 175 313–175 323, dec 2019.

[248] S. H. Lee, M. Kim, H. Shin, and I. Lee, "Belief propagation for energy efficiency maximization in wireless heterogeneous networks," *IEEE Transactions on Wireless Communications*, vol. 20, no. 1, pp. 56–68, sep 2021.

[249] F. Dong, T. Wang, and S. Wang, "Power consumption minimization in cache-enabled mobile networks," *IEEE Transactions on Vehicular Technology*, vol. 68, no. 7, pp. 6917–6925, apr 2019.

[250] S. M. Asad, M. Ozturk, R. N. Bin Rais, A. Zoha, S. Hussain, Q. H. Abbasi, and M. A. Imran, "Reinforcement learning driven energy efficient mobile communication and applications," in *2019 IEEE International Symposium on Signal Processing and Information Technology (ISSPIT)*, dec 2019, pp. 1–7.

[251] S. M. Asad, S. Ansari, M. Ozturk, R. N. B. Rais, K. Dashtipour, S. Hussain, Q. H. Abbasi, and M. A. Imran, "Mobility management-based autonomous energy-aware framework using machine learning approach in dense mobile networks," *Signals*, vol. 1, no. 2, pp. 170–187, nov 2020. [Online]. Available: https://www.mdpi.com/2624-6120/1/2/10

[252] A. El-Amine, M. Iturralde, H. A. Haj Hassan, and L. Nuaymi, "A distributed q-learning approach for adaptive sleep modes in 5g networks," in *2019 IEEE Wireless Communications and Networking Conference (WCNC)*, oct 2019, pp. 1–6.

[253] F. E. Salem, Z. Altman, A. Gati, T. Chahed, and E. Altman, "Reinforcement learning approach for advanced sleep modes management in 5G networks," in *2018 IEEE 88th Vehicular Technology Conference (VTC-Fall)*. IEEE, aug 2018, pp. 1–5.

[254] A. El-Amine, H. A. Haj Hassan, M. Iturralde, and L. Nuaymi, "Location-aware sleep strategy for energy-delay tradeoffs in 5G with reinforcement learning," in *2019 IEEE 30th Annual International Symposium on Personal, Indoor and Mobile Radio Communications (PIMRC)*, sep 2019, pp. 1–6.

[255] F. H. Panahi, F. H. Panahi, G. Hattab, T. Ohtsuki, and D. Cabric, "Green heterogeneous networks via an intelligent sleep/wake-up mechanism and

D2D communications," *IEEE Transactions on Green Communications and Networking*, vol. 2, no. 4, pp. 915–931, jun 2018.

[256] Q. Zhang, X. Xu, J. Zhang, X. Tao, and C. Liu, "Dynamic load adjustments for small cells in heterogeneous ultra-dense networks," in *2020 IEEE Wireless Communications and Networking Conference (WCNC)*, may 2020, pp. 1–6.

[257] H. Wang, M. Huang, Z. Zhao, Z. Guo, Z. Wang, and M. Li, "Base station wake-up strategy in cellular networks with hybrid energy supplies for 6G networks in an IoT environment," *IEEE Internet of Things Journal*, vol. 8, no. 7, pp. 5230–5239, dec 2021.

[258] J. A. Ayala-Romero, J. J. Alcaraz, A. Zanella, and M. Zorzi, "Online learning for energy saving and interference coordination in HetNets," *IEEE Journal on Selected Areas in Communications*, vol. 37, no. 6, pp. 1374–1388, mar 2019.

[259] N. Modi, P. Mary, and C. Moy, "Transfer restless multi-armed bandit policy for energy-efficient heterogeneous cellular network," *EURASIP Journal on Advances in Signal Processing*, vol. 2019, no. 1, pp. 1–19, oct 2019.

[260] A. I. Abubakar, M. Ozturk, R. N. B. Rais, S. Hussain, and M. A. Imran, "Load-aware cell switching in ultra-dense networks: An artificial neural network approach," in *2020 International Conference on UK-China Emerging Technologies (UCET)*, aug 2020, pp. 1–4.

[261] L. Wang, S. Chen, and M. Pedram, "Context-driven power management in cache-enabled base stations using a bayesian neural network," in *2017 Eighth International Green and Sustainable Computing Conference (IGSC)*, oct 2017, pp. 1–8.

[262] Q. Wu, X. Chen, Z. Zhou, L. Chen, and J. Zhang, "Deep reinforcement learning with spatio-temporal traffic forecasting for data-driven base station sleep control," *IEEE/ACM Transactions on Networking*, vol. 29, no. 2, pp. 935–948, jan 2021.

[263] C. Huang and P. Chen, "Joint demand forecasting and DQN-based control for energy-aware mobile traffic offloading," *IEEE Access*, vol. 8, pp. 66 588–66 597, apr 2020.

[264] K. Zhang, X. Wen, Y. Chen, and Z. Lu, "Deep reinforcement learning for energy saving in radio access network," in *2020 IEEE/CIC International*

Conference on Communications in China (ICCC Workshops), aug 2020, pp. 35–40.

[265] J. Liu, B. Krishnamachari, S. Zhou, and Z. Niu, "DeepNap: Data-driven base station sleeping operations through deep reinforcement learning," *IEEE Internet of Things Journal*, vol. 5, no. 6, pp. 4273–4282, dec 2018.

[266] X. Huang, S. Tang, D. Zhang, and Q. Chen, "Cluster-based dynamic FBSs on/off scheme in heterogeneous cellular networks," in *International Conference on Communications and Networking in China*. Springer, jan 2018, pp. 325–335.

[267] C.-Q. Dai, B. Fu, and Q. Chen, "A cluster-based small cell on/off scheme for energy efficiency optimization in ultra-dense networks," in *International Conference on Communications and Networking in China*. Springer, feb 2019, pp. 385–401.

[268] J. Li, H. Wang, X. Wang, and Z. Li, "Optimized sleep strategy based on clustering in dense heterogeneous networks," *EURASIP Journal on Wireless Communications and Networking*, vol. 2018, no. 1, pp. 1–10, dec 2018.

[269] A. Prasad, A. Maeder, and C. Ng, "Energy efficient small cell activation mechanism for heterogeneous networks," in *2013 IEEE Globecom Workshops (GC Wkshps)*, Dec 2013, pp. 754–759.

[270] M. Ozturk, M. Akram, S. Hussain, and M. A. Imran, "Novel QoS-aware proactive spectrum access techniques for cognitive radio using machine learning," *IEEE Access*, vol. 7, pp. 70 811–70 827, may 2019.

[271] C. J. Watkins and P. Dayan, "Q-learning," *Machine learning*, vol. 8, no. 3-4, pp. 279–292, 1992.

[272] G. Barlacchi, M. De Nadai, R. Larcher, A. Casella, C. Chitic, G. Torrisi, F. Antonelli, A. Vespignani, A. Pentland, and B. Lepri, "A multi-source dataset of urban life in the city of milan and the province of trentino," *Scientific data*, vol. 2, p. 150055, oct 2015.

[273] A. D. Rasamoelina, F. Adjailia, and P. Sinčák, "A review of activation function for artificial neural network," in *2020 IEEE 18th World Symposium on Applied Machine Intelligence and Informatics (SAMI)*, jun 2020, pp. 281–286.

[274] D. P. Kingma and J. Ba, "Adam: A method for stochastic optimization," *CoRR*, vol. abs/1412.6980, 2014.

[275] J. Qin, W. Fu, H. Gao, and W. X. Zheng, "Distributed K-means algorithm and fuzzy C-means algorithm for sensor networks based on multiagent consensus theory," *IEEE Transactions on Cybernetics*, vol. 47, no. 3, pp. 772–783, mar 2017.

[276] A. K. Jain, "Data clustering: 50 years beyond K-means," *Pattern Recognition Letters*, vol. 31, no. 8, pp. 651 – 666, jun 2010.

[277] Y. Wei, Z. Zhang, F. R. Yu, and Z. Han, "Power allocation in HetNets with hybrid energy supply using actor-critic reinforcement learning," in *GLOBECOM 2017 - 2017 IEEE Global Communications Conference*. IEEE, dec 2017.

[278] M. Giordani, M. Mezzavilla, C. N. Barati, S. Rangan, and M. Zorzi, "Comparative analysis of initial access techniques in 5G mmWave cellular networks," in *2016 Annual Conference on Information Science and Systems (CISS)*, mar 2016, pp. 268–273.

[279] A. Mughees, M. Tahir, M. A. Sheikh, and A. Ahad, "Towards energy efficient 5G networks using machine learning: Taxonomy, research challenges, and future research directions," *IEEE Access*, vol. 8, pp. 187 498–187 522, oct 2020.

[280] Y. Liang, C. Sun, J. Jiang, X. Liu, H. He, and Y. Xie, "An Efficiency-Improved Clustering Algorithm Based on KNN Under Ultra-Dense Network," *IEEE Access*, vol. 8, pp. 43 796–43 805, mar 2020.

[281] A. Morgado, K. M. S. Huq, S. Mumtaz, and J. Rodriguez, "A survey of 5G technologies: regulatory, standardization and industrial perspectives," *Digital Communications and Networks*, vol. 4, no. 2, pp. 87 – 97, apr 2018. [Online]. Available: http://www.sciencedirect.com/science/article/pii/S2352864817302584

[282] G. A. Akpakwu, B. J. Silva, G. P. Hancke, and A. M. Abu-Mahfouz, "A survey on 5G networks for the internet of things: Communication technologies and challenges," *IEEE Access*, vol. 6, pp. 3619–3647, dec 2018.

[283] X. J. Tan and W. Zhan, "Traffic-adaptive spectrum leasing between primary and secondary networks," *IEEE Transactions on Vehicular Technology*, vol. 67, no. 7, pp. 6546–6560, feb 2018.

[284] C. Tsirakis, E. Lopez-Aguilera, P. Matzoros, G. Agapiou, and D. Varoutas, "Spectrum trading in virtualized multi-tenant 5G networks," in *2018 15th International Symposium on Wireless Communication Systems (ISWCS)*, may 2018, pp. 1–6.

[285] D. Bilibashi, E. M. Vitucci, V. Degli-Esposti, and A. Giorgetti, "An energy-efficient unselfish spectrum leasing scheme for cognitive radio networks," *Sensors*, vol. 20, no. 21, oct 2020. [Online]. Available: https://www.mdpi.com/1424-8220/20/21/6161

[286] Z. Liu, M. Zhao, K. Y. Chan, Y. Yuan, and X. Guan, "Approach of robust resource allocation in cognitive radio network with spectrum leasing," *IEEE Transactions on Green Communications and Networking*, vol. 4, no. 2, pp. 413–422, apr 2020.

[287] R. Fan, W. Chen, H. Jiang, J. An, K. Yang, and C. Xing, "Dynamic spectrum leasing with two sellers," *IEEE Transactions on Vehicular Technology*, vol. 67, no. 6, pp. 4852–4866, feb 2018.

[288] S. Handouf, E. Sabir, and M. Sadik, "A leasing-based spectrum sharing framework for cognitive radio networks," in *2018 6th International Conference on Wireless Networks and Mobile Communications (WINCOM)*, nov 2018, pp. 1–5.

[289] X. Xiao, F. Zeng, Z. Hu, and L. Jiao, "Dynamic flow-adaptive spectrum leasing with channel aggregation in cognitive radio networks," *Sensors*, vol. 20, no. 13, jul 2020. [Online]. Available: https://www.mdpi.com/1424-8220/20/13/3800

[290] C. Eid, E. Koliou, M. Valles, J. Reneses, and R. Hakvoort, "Time-based pricing and electricity demand response: Existing barriers and next steps," *Utilities Policy*, vol. 40, pp. 15–25, jun 2016.

[291] 3GPP, "Technical specification group radio access network; NR; physical channels and modulation (Release 15)," 2018.

[292] N. Saxena, A. Roy, and H. Kim, "Traffic-Aware Cloud RAN: A Key for Green 5G Networks," *IEEE Journal on Selected Areas in Communications*, vol. 34, no. 4, pp. 1010–1021, mar 2016.

[293] Y. Li, H. Zhang, J. Wang, B. Cao, Q. Liu, and M. Daneshmand, "Energy-efficient deployment and adaptive sleeping in heterogeneous cellular networks," *IEEE Access*, vol. 7, pp. 35 838–35 850, mar 2019.

[294] R. Shinkuma and Y. Goto, "Wireless multihop networks formed by unmanned aerial vehicles with separable access points and replaceable batteries," in *2016 IEEE 7th Annual Ubiquitous Computing, Electronics Mobile Communication Conference (UEMCON)*, oct 2016, pp. 1–6.

[295] M. Alzenad, A. El-Keyi, F. Lagum, and H. Yanikomeroglu, "3-D Placement of an Unmanned Aerial Vehicle Base Station (UAV-BS) for Energy-Efficient Maximal Coverage," *IEEE Wireless Communications Letters*, vol. 6, no. 4, pp. 434–437, aug 2017.

[296] N. Babu, M. Virgili, C. B. Papadias, P. Popovski, and A. J. Forsyth, "Cost- and energy-efficient aerial communication networks with interleaved hovering and flying," *IEEE Transactions on Vehicular Technology*, vol. 70, no. 9, pp. 9077–9087, jul 2021.

[297] F. Gao, Y. Zhou, X. Ma, T. Yang, N. Cheng, and N. Lu, "Coverage-maximization and energy-efficient drone small cell deployment in aerial-ground collaborative vehicular networks," in *2019 IEEE 4th International Conference on Computer and Communication Systems (ICCCS)*, feb 2019, pp. 559–564.

[298] M. Mozaffari, W. Saad, M. Bennis, and M. Debbah, "Drone small cells in the clouds: Design, deployment and performance analysis," in *2015 IEEE Global Communications Conference (GLOBECOM)*, dec 2015, pp. 1–6.

[299] N. Babu, K. Ntougias, C. B. Papadias, and P. Popovski, "Energy efficient altitude optimization of an aerial access point," in *2020 IEEE 31st Annual International Symposium on Personal, Indoor and Mobile Radio Communications*, oct 2020, pp. 1–7.

[300] L. Wang, B. Hu, and S. Chen, "Energy efficient placement of a drone base station for minimum required transmit power," *IEEE Wireless Communications Letters*, vol. 9, no. 12, pp. 2010–2014, dec 2020.

[301] J. Plachy and Z. Becvar, "Energy efficient positioning of flying base stations via coulomb's law," in *2020 IEEE Globecom Workshops (GC Wkshps)*, dec 2020, pp. 1–6.

[302] S.-F. Chou, A.-C. Pang, and Y.-J. Yu, "Energy-Aware 3D Unmanned Aerial Vehicle Deployment for Network Throughput Optimization," *IEEE Transactions on Wireless Communications*, vol. 19, no. 1, pp. 563–578, jan 2020.

[303] A. Bera, S. Misra, and C. Chatterjee, "Energy-Aware Multi-UAV Networks for On-Demand Task Execution," in *2020 IEEE International Conference on Communications Workshops (ICC Workshops)*, jun 2020, pp. 1–6.

[304] J. You, S. Jung, J. Seo, and J. Kang, "Energy-Efficient 3-D Placement of an Unmanned Aerial Vehicle Base Station With Antenna Tilting," *IEEE Communications Letters*, vol. 24, no. 6, pp. 1323–1327, jun 2020.

[305] N. Babu, C. B. Papadias, and P. Popovski, "Energy-efficient deployment of a non-orthogonal multiple access unmanned aerial system," in *2021 IEEE International Conference on Communications Workshops (ICC Workshops)*, jun 2021, pp. 1–6.

[306] Z. Xue, J. Wang, G. Ding, and Q. Wu, "Joint 3D Location and Power Optimization for UAV-Enabled Relaying Systems," *IEEE Access*, vol. 6, pp. 43 113–43 124, aug 2018.

[307] S. Shakoor, Z. Kaleem, D.-T. Do, O. A. Dobre, and A. Jamalipour, "Joint Optimization of UAV 3-D Placement and Path-Loss Factor for Energy-Efficient Maximal Coverage," *IEEE Internet of Things Journal*, vol. 8, no. 12, pp. 9776–9786, jun 2021.

[308] D. Zorbas, L. D. P. Pugliese, T. Razafindralambo, and F. Guerriero, "Optimal drone placement and cost-efficient target coverage," *Journal of Network and Computer Applications*, vol. 75, pp. 16–31, nov 2016.

[309] X. Jiang, Z. Wu, Z. Yin, Z. Yang, and N. Zhao, "Power Consumption Minimization of UAV Relay in NOMA Networks," *IEEE Wireless Communications Letters*, vol. 9, no. 5, pp. 666–670, may 2020.

[310] A. Bahr, M. A. Mehaseb, S. A. Doliel, S. El-Rabaie, and F. E. Abd El-Samie, "Power-Aware 3D UAV Placement for IoT Emergency Communications," in *2020 8th International Japan-Africa Conference on Electronics, Communications, and Computations (JAC-ECC)*, dec 2020, pp. 18–23.

[311] J. Cui, H. Shakhatreh, B. Hu, S. Chen, and C. Wang, "Power-Efficient Deployment of a UAV for Emergency Indoor Wireless Coverage," *IEEE Access*, vol. 6, pp. 73 200–73 209, nov 2018.

[312] A. Pandey, D. Kushwaha, and S. Kumar, "Energy Efficient UAV Placement for Multiple Users in IoT Networks," in *2019 IEEE Global Communications Conference (GLOBECOM)*, dec 2019, pp. 1–6.

[313] E. Bozkaya, K.-T. Foerster, S. Schmid, and B. Canberk, "Airnet: Energy-aware deployment and scheduling of aerial networks," *IEEE Transactions on Vehicular Technology*, vol. 69, no. 10, pp. 12 252–12 263, oct 2020.

[314] M. F. Sohail, C. Y. Leow, and S. Won, "Energy-Efficient Non-Orthogonal Multiple Access for UAV Communication System," *IEEE Transactions on Vehicular Technology*, vol. 68, no. 11, pp. 10 834–10 845, nov 2019.

[315] R. Zhang, X. Pang, J. Tang, Y. Chen, N. Zhao, and X. Wang, "Joint Location and Transmit Power Optimization for NOMA-UAV Networks via Updating Decoding Order," *IEEE Wireless Communications Letters*, vol. 10, no. 1, pp. 136–140, jan 2021.

[316] X. Pang, J. Tang, N. Zhao, X. Zhang, and Y. Qian, "Energy-efficient design for mmWave-enabled NOMA-UAV networks," *Science China Information Sciences*, vol. 64, no. 4, pp. 1–14, jan 2021.

[317] S.-H. Cheng, Y.-T. Shih, and K.-C. Chang, "Proactive power control and position deployment for drone small cells: Joint supervised and unsupervised learning," *IEEE Access*, vol. 9, pp. 126 735–126 747, sep 2021.

[318] S.-C. Noh, H.-B. Jeon, and C.-B. Chae, "Energy-Efficient Deployment of Multiple UAVs Using Ellipse Clustering to Establish Base Stations," *IEEE Wireless Communications Letters*, vol. 9, no. 8, pp. 1155–1159, aug 2020.

[319] Q. Zhang, M. Mozaffari, W. Saad, M. Bennis, and M. Debbah, "Machine Learning for Predictive On-Demand Deployment of Uavs for Wireless Communications," in *2018 IEEE Global Communications Conference (GLOBECOM)*, dec 2018, pp. 1–6.

[320] B. Liu, Y. Zhang, S. Fu, and X. Liu, "Reduce UAV Coverage Energy Consumption through Actor-Critic Algorithm," in *2019 15th International Conference on Mobile Ad-Hoc and Sensor Networks (MSN)*, dec 2019, pp. 332–337.

[321] H. Bayerlein, R. Gangula, and D. Gesbert, "Learning to rest: A Q-learning approach to flying base station trajectory design with landing spots," in *2018 52nd Asilomar Conference on Signals, Systems, and Computers*, oct 2018, pp. 724–728.

[322] "Aurelia X8," https://uavsystemsinternational.com/products/aurelia-x8-standard, accessed: 2021-07-10.